

ESA-ESTEC

Keplerlaan 1
2201 AZ Noordwijk
The Netherlands

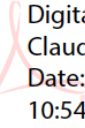
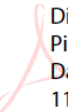
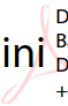
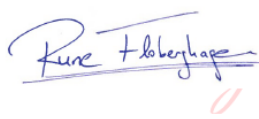
www.esa.int

Copernicus Imaging Microwave Radiometer (CIMR) Mission Requirements Document

Prepared by	Earth and Mission Science Division
Document type	Mission Requirements Document (MRD)
Reference	ESA-EOPSM-CIMR-MRD-3236
Issue/Revision	5.0
Date of Issue	11 February 2023
Status	ISSUED

Approval

Title: Copernicus Imaging Microwave Radiometer (CIMR) Mission Requirements Document

Issue Number: 5	Revision: 0	
Author: Craig Donlon (EOP-SME)	Date: 11 February 2023	
Approved By	Signature	Date of Approval
Mark Drinkwater (EOP-SM) Head/Earth and Mission Science Division		Digitally signed by Mark Drinkwater Location: EOP-SM Date: 2023.02.12 20:08:58 +01'00'
Claudio Galeazzi (EOP-PZP) CIMR Project Manager		Digitally signed by Claudio Galeazzi Date: 2023.02.20 10:54:42 +01'00'
Betlem Rosich Tell (EOP-GC) Head/Copernicus Ground Segment and Data Management Division		Digitally signed by Betlem Rosich Date: 2023.02.22 10:57:45 +01'00'
Pierre Potin (EOP-FC) Head/Copernicus Space Office		Digitally signed by Pierre Potin Date: 2023.02.22 11:56:49 +01'00'
Pier Bargellini (EOP-PZ) Copernicus Space Segment Programme Manager		Digitally signed by Pier Bargellini Date: 2023.02.26 11:46:03 +01'00'
Authorised By	Signature	Date of Authorisation
Rune Floberghagen (EOP-S) Head/Science, Applications and Climate Department		Digitally signed by Rune Floberghagen Date: 2023.02.27 09:02:19 +01'00'

Change Log

Title: Copernicus Imaging Microwave Radiometer (CIMR) Mission Requirements Document

Reason for change	Issue.	Revision	Date
Version 3 for Phase B2/C/D/E	3	0	30/09/2019
Version 3.1 updates following MAG 08 and MAG 09	3	1	20/02/2020
Version 3.2 updates to secondary products based on MAG discussions	3	2	21/02/2020
Version 3.3 updates based on discussions with CIMR study team.	3	3	27/02/2020
Updated with comments from further comments from ESA and CIMR-MAG	3	4	29/02/2020
Updated based on end-to-end review and text editorial	3	5	20/03/2020
Harmonisation with SSRD/SRD and inputs from EOP-G	3	6	27/03/2020
Inputs from ESA Copernicus GS and EUMETSAT	3	7	15/04/2020
Clarifications on v3.7 (added to the change record that also includes v3.7 items)	3	8	05/06/2020
Updates to reflect changes in SSRD	3	9	29/06/2020
Updates following MAG #10	3	10	09/07/2020
V 4.0 for issue at KO of CIMR Phase B2	4	0	13/07/2020
V5.0 consolidation of issues raised in Phase B2 prior to PDR based on Project, Industry and MAG discussions and conclusions. Reviewed by M. Drinkwater and B. Rosich. Final editorial update.	5	0	11/02/2023

Change Record

Issue: 5	Revision: 0		
Reason for change	Date	Pages	Paragraph(s)
Definition of 'adjacent Seas clarified as follows: Adjacent Seas: encompass all Seas and water bodies adjacent to the Arctic that are <u>influenced by sea ice</u> including Gulf of Bothnia, Gulf of Finland, Baltic Sea, Caspian Sea, Sea of Azov (Black Sea), Bering Sea, Sea of Okhotsk, <u>northern</u> Yellow Sea, Bohai Sea, Baikal Lake, Labrador Sea, Gulf of St Lawrence, American Great Lakes, Gulf of Alaska.	21/07/21	Appendix 1	Sec. 9
Added Non Time Critical (NTC) delivery and timeliness of all products in new requirement MRD-1105 after discussion with IPF manager. This had been erroneously deleted.	29/11/21		Sec. 4.3.7
Updated definition of Non Time Critical (NTC) timeliness.	29/11/21		Appendix 9
Added definition of coastal zone and revised definitions of coastal region. Coastal boundary is specified in MRD-852.	18/06/22		Appendix 9 and Table 6.3-1
MRD-750 updated to focus on the L1b samples only. L1c is designed to provide a simple 'one-size-fits-all' gridded Tb product similar to Remote Sensing Systems approach.	15/12/21		Sec. 4.3.4
Revised L1b definitions at MAG #14 based on discussions related to geolocation tie-points and content of L1b samples. Removed L1b measurement quantities as these are redundant since all CIMR samples	15/12/21	Table 4.3.4-1	Sec 4.3.4

are included in the product: L1b measurements will be constructed by ground segment processing.			
Added MRD-330 to ensure CIMR channel spectral response functions are available to users based on lessons learned from MetOp MWI.	15/12/21		Sec. 4.2.6
MRD-770. Example L1b elements revised and updated based on MAG #14 discussions and MetOp MWI L1b format specification.	15/12/21		Sec 4.3.4
Added MRD-778 to ensure data acquired during manoeuvres is collected and available to users.	15/12/21		Sec 4.3.4
Based on discussions with MAG and EUMETSAT, a definition of CIMR Product Families added in MRD-865 linked to Table 6.3-1.	22/03/22		Sec. 4.3.6
MRD-1000 and MRD-1010 updated to use Hydrology Target Mask. Note 4 added to clarify relationship to LST products.	22/03/22 07/09/22		Sec. 4.3.6
Updated Table 4.3.6-1 to remove elements related to gridded products based on CIMR- MAG #15 inputs. L2 products will be in swath instrument geometry but could be in gridded containers depending on the variable and application. The emphasis is toward instrument geometry allowing Users to grid the product in the best manner for their specific application.	22/03/22		Sec. 4.3.6
MRD-860 updated to clarify that production of L2 products does not require a gridded product. Notes are now used to indicate that gridded projected products can be provided if deemed appropriate depending on the variable and application.	22/03/22		Sec. 4.3.6
MRD-180 revised and notes updated for L-band based on discussions and advice at CIMR MAG #15.	22/03/22		Sec. 4.1.3
Clarification on production of BUFR (as notes). Note 4 for MRD-760 (L1b) removed and Note 4 in MRD-810 (L1c) added. MRD-765 added requesting BUFR products at L1b for selected operational users. Note 5 of MRD-860 (related to BUFR) removed.	30/03/22		Sec. 4.3.4
Figure MRD-6.3.1.2 updated			
Revised Table 4.3.4-1 in terms of how L1b products could be provided.	30/03/22		Sec. 4.3.4
MRD-1110 clarified NRT1H production to include only (SIC), Sea Ice Edge (SIED), Sea Ice Drift (SID), and Ocean Wind Speed (OWS). Pre-amble text also revised based on MAG#16 discussion.	14/06/22		Sec. 4.3.7
MRD-770 and MRD-800 added notes on how to deal with cosmetic fill and orphaned pixels in L1C data files. The approach is to maintain all data as part of the Level-1b file if a gridded approach is used.	30/03/22		Sec. 4.3.5
MRD-810 added Note 5 on selection of grid kernel for gridded L1c products. Revised at MAG #17 to clarify Note 5.	30/02/22 07/09/22		Sec. 4.3.5
Figure 4.3.1-1 updated L2 products as either instrument geometry or gridded fields depending on the applications.	17/06/22		Sec. 4.3.1
MRD-1300 updated to include L1c ATBD.	30/03/22		Sec. 4.6
Added definition of Global Ocean from EUMETSAT	01/04/22		App. 1.
MRD-985 Note 8 and Note 9 added Update text based on N. Reul contributions for Sec. 2.4.9	01/04/22 07/09/22		Sec. 4.3.6
MRD-990 and MRD-995 notes updated to refer to non-precipitating conditions and need to resolve ambiguities in wind direction retrievals.	07/04/22		Sec. 4.3.6
Note 4 added to MRD-510 noting moon calibration approach.	07/04/22		Sec. 4.2.11
MRD-370 updated to permit gaps in Ka-band of <1.3 km in the along-track direction	17/06/22		Sec. 4.2.6

Figure MRD-6.3.1.2 updated.	31/05/22		Sec. 6.3.1
Sec. 6.3.17 freeze-thaw algorithm section fully revised	31/05/22		Sec 6.3.18
MRD-440, MRD-450 and MRD-460 updated for consistency with MRD-580, MRD-590, MRD-600, MRD-610 and MRD-620 (Table MRD-2 ID-080-1-7)	12/06/22		Sec. 4.2.10
MRD-380 notes updated to include options for larger bandwidths at L-band facilitating compliance with NEΔT specifications. Also clarifying that management of RFI is important.	03/06/22		Sec. 4.2.7
MRD-240 Notes clarified and Note 12 added regarding use of extended bandwidth.	03/06/22		Sec. 4.2.2
MRD-250 and MRD-260 notes clarified to ensure adequate protection is in place for RFI should larger bandwidths be employed.	08/06/22		Sec. 4.2.2
MRD-300 notes clarified.	08/06/22		Sec. 4.2.5
MRD-270 updated to manage different OZA for L-band in Table MRD-2. Note 11 added to explain the approach.	08/06/22		Sec. 4.2.3
Added Figure MRD-2.4.9-1 to highlight the importance of sea surface temperature sensitivity to L-band Tb in the context of salinity retrievals.	08/06/22		Sec. 2.4.9
Revised MRD-900 based on MAG feedback to ensure consistency with masks defined by revised MRD-852 and MRD-854 (new notes added).	12/06/22		Sec 4.3.6
Following CIMR MAG recommendations, a simplified CIMR coastline boundary is defined in MRD-852.	17/06/22		Sec. 4.3.6
Following CIMR MAG recommendations, a simplified CIMR Hydrology Target Mask is defined in MRD-854.	12/06/22		Sec. 4.3.6
MRD-586 added defining sea ice edge mask.	17/06/22		Sec. 4.3.6
Section 4.3.4.1 added to emphasise the importance of correcting for galactic radiation in CIMR L1b retrievals.	18/06/22		Sec. 4.3.4.1
MRD-732 added: The impact of galactic radiation on CIMR L-band Tb shall be compensated at Level-1b.			
Section 4.3.4.2 added to emphasise the importance of correcting for Faraday rotation on CIMR Tb.	18/06/22		Sec. 4.3.4.2
MRD-734 added: The impact of Faraday rotation on CIMR Tb shall be compensated at Level-1b.			
MRD-1210 updated to include goal of reprocessing every 2 years	18/06/22		Sec. 4.4.2
Definitions of Global Ocean, sea ice and snow parameters updated.	18/06/22		Appendix 9
MRD-895 updated to clarify that it is calculated at a resolution of ≤5 km with a note explaining that this quantity is to be generated from CIMR SIC products that may require processing beyond L2 (since SIE is a single number for a given area).	18/06/22		Sec. 4.3.6
MRD-920 notes updated to clarify that the Sea Ice Drift product is a vector based product.	23/06/22		Sec. 4.3.6
MRD-1060 updated to clarify SWF is over land	23/06/22		Sec. 4.3.6
Updated Section 7 to include AMSR-3 details	23/06/22		Sec. 7
MRD-900 and MRD-905 updated to include notes highlighting the importance of adhering to the GHRSST SST product standards for CIMR SST products.	23/06/22		Sec. 4.3.6

Revised Table 6.3-1 to clarify that NRT1H products are for limited areas of the Arctic Polar Region.	29/06/22		Sec. 6.3
Differences between MRD-1110 and Table 6.3-1 regarding SIED and OWS/OWV reconciled.	10/07/22		Sec. 6.3
Following detailed discussions with ESTEC frequency management team, MRD-655 MRD-657 added to monitor RFI detections and determine if the OBP configuration remains valid (i.e., if an update to the RFI algorithm coefficients is required due to incorrect flagging of RFI or missed RFI events).	17/07/22		Sec. 4.2.15
Update of RFI section based on detailed discussion with ESA Frequency Management Team with new REQ MRD-655 and MRD-657 to ensure correct reporting via ITU SIRRS following example in place for SMOS.	31/08/22		Sec. 4.2.15
Added MRD-845 as a catch all relevant to the calculation of in-flight performance metrics for L2 surface products.	07/09/22		Sec. 4.3.6
Added science background text/correction updates to multiple sections and corrected spelling and formatting.	12/09/22		All
Updated text with inputs from M. Berdahl (DG.DEFIS)	16/10/22		Sec. 1.
MRD-390 revised to reflect the user need and ITU user need for RFI detection	16/10/2022		Sec. 4.2.7
Note 3 added to MRD-490 clarifying that calibration knowledge is required for the duration of the CIMR mission and in Level-1b products	16/10/2022		Sec. 4.2.10
Note 4 of MRD-500 updated to reflect the need to monitor the reflector temperature using either direct measurements or a model correlated to on-board parameters)	16/10/2022		Sec. 4.2.11
Final traceability with CIMR Project SRD/SSRD	12/10/2022		All
Resolved conflict between MRD-220 and MRD-778. MRD-220 text changed and Note 2 added to refer to MRD-778. Added Note 4 to MRD-778 pointing back to MRD-220.	21/10/2022		Sec. 4.3.4.3
Based on feedback from ESA GS, MRD-765 deleted and merged as note 4 in MRD-760 since this is an implementation choice.	8/11/2022		Sec. 4.3.4.3
Definition of Copernicus Ground Segment (Copernicus GS) added and the term PDGS has been removed from the MRD.	8/11/2022		
Added MRD-885 that requires geophysical consistency across CIMR Level-2 products	8/11/2022		Sec. 4.3.6
Update of MRD-1310 to change from MAAW to CEM-PAL.	8/11/2022		Sec. 4.6
Notes for MRD-040, MRD-050 updated (since MRD-040 sets the across track separation). MRD-060 simplified to request knowledge of the relative along-track separation of satellites in tandem. MRD-090 clarified	8/11/2022		Sec. 4.1.1
MRD-770 clarified to focus on L1b information necessary to generate L2 products.	8/11/2022		Sec. 4.3.4.3
Revision to MRD-854 to complement Hydrology Target Mask with Lehner and Doll (2004) 1 km data set	8/11/2022		Sec. 4.3.6
Following CIMR MAG #18, clarified notes in MRD-660 (geolocation) which is about performance measures. To ensure all L1b samples are geolocated notes have been reorganised and a new note added to stress that samples must be geolocated.	9/12/2022		Sec. 4.2.16
MRD-856 clarified as sea ice mask for sizing purposes only (since CIMR will provide a sea ice mask)	11/02/2023		Sec. 4.3.6

Corrected typos in MRD-760 and MRD-810 (L1a → L1) based on review by B. Rosich	11/02/2023		Sec. 4.3.4.3
MRD-765 added “L1b data products shall be produced and made available to users.”	11/02/2023		Sec. 4.3.4.3
Updated definitions of Footprint and Footprint Centre with R. Midthassel and B. Fiorelli	11/02/2023		Appendix 1

Distribution

Name/Organisational Unit		
ESTEC:	ESRIN:	European Commission:
T. Tolker-Nielsen (EOP-P)	R. Floberghagen (EOP-S)	M. Facchini (DG-DEFIS)
P. Bargellini (EOP-PZ)	Y-L. Desnos (EOP-SD)	M. Berdahl (DG-DEFIS)
C. Galeazzi (EOP-P2)	N. Hanowski (EOP-G)	
M. Sallusti (EOP-P2O)	B. Rosich Tell (EOP-GC)	
R. Midthassel (EOP-P2P)	B. Tsonevska (EOP-GCS)	
M. Triggianese (EOP-P2S)	K. Scipal (EOP-GM)	
B. Fiorelli (TEC-EFA)	P. Goryl (EOP-GMQ)	
G. de Paris (EOP-P2)	P. Féménias (EOP-GMQ)	Members of the CIMR-MAG
N. Hadala (EOP-P5)	M. Scagliola (EOP-GMQ)	
R. Volpini (EOP-BC)	R. Sabia (EOP-GMQ)	
C. Sancho (EOP-B)	R. Crappolichio (EOP-GMQ)	
A. Kornienko (EOP-P2S)	P. Potin (EOP-E)	
M. Drinkwater (EOP-SM)		
T. Casal (EOP-SMS)		
P. Martimort (EOP-FM)	ESOC:	
B. Duesmann, (EOP-PES)	A. Pris-Nino (OPS-OSA)	
M. Pinot-Sole (EOP-PES)	J. Morales (OPS-OE)	
A. Ipsilonanti (CIP-PEO)	E. Zornoza (OPS-OEL)	
I. Khlystova (EOP-P2O)	F. Zurletti (OPS-OEL)	

Members of the CIMR Mission Advisory Group (MAG) 2017-2025

Dr. C. Donlon	(Chair) ESA/ESTEC, Noordwijk, The Netherlands.
Dr. C. Prigent,	Observatoire de Paris (LERMA), France.
Prof. C. Merchant,	University of Reading, United Kingdom.
T. Lavergne,	Norwegian Meteorological Institute, Oslo, Norway.
Dr. G. Heygster,	University of Bremen, Germany.
Dr. J. Høyer,	Danish Meteorological Institute, Copenhagen, Denmark.
Prof. J. Johannessen,	Nansen Centre (NERSC), Bergen, Norway.
Dr. K. Luojus	Finnish Meteorological Institute, Helsinki, Finland.
Dr. M. Piles,	University of Valencia, Valencia, Spain.
Dr. P. de Rosnay,	ECMWF, Reading, United Kingdom.
Dr. N. Reul,	IFREMER, Toulon, France.
Dr. R. Santolieri,	CNR-ISAC, Rome, Italy.
Dr. D. Smith	Rutherford Appleton Laboratory, Oxford, United Kingdom.
Dr. G. Spreen,	University of Bremen, Germany.
Dr. R. Tonboe,	Danish Meteorological Institute, Copenhagen, Denmark.
Dr. C. Accadia,	EUMETSAT, Darmstadt, Germany.
Dr. S. Yueh,	NASA/JPL, Pasadena, USA.
Dr. T. Meissner,	Remote Sensing Systems, USA
Dr. V. Toumazou,	DG GROW, European Commission, Brussels, Belgium (until Jan 2019).
O. Nordbeck,	DG GROW, European Commission, Brussels, Belgium (until June 2021).
M. Berdahl.	DG GROW, European Commission, Brussels, Belgium.

TABLE OF CONTENTS

Table of contents.....	10
1 Introduction.....	13
1.1 Document and Requirement Conventions	13
1.1.1 Terms.....	13
1.1.2 Requirement Numbering and Approach	14
1.1.3 Requirements and Guidelines	14
2 Background and Justification	15
2.1 Copernicus Evolution	17
2.2 The Integrated European Union Policy for the Arctic	19
2.3 A High-Priority Copernicus Mission to support the Integrated EU Policy for the Arctic: The Copernicus Imaging Microwave Radiometer (CIMR)	22
2.4 Established Copernicus user needs for the CIMR mission	25
2.4.1 Sea Ice Concentration (Sea Ice Fraction).....	27
2.4.2 Sea Surface Temperature (SST).....	35
2.4.3 Sea Ice Thickness (SIT)	39
2.4.4 Sea Ice Drift	42
2.4.5 Snow Depth on Sea Ice.....	43
2.4.6 Ice type/Ice stage of development	45
2.4.7 Sea Ice Surface Temperature (SIST)	46
2.4.8 Terrestrial Snow Cover: Snow Area and Snow Water Equivalent	47
2.4.9 Sea Surface Salinity (SSS).....	49
2.4.10 Wind speed over the ocean and extreme winds in Polar regions	52
2.4.11 Other parameters that can be derived from CIMR.....	54
3 CIMR Mission Aim and Objectives	63
3.1 CIMR Mission Aim.....	63
3.2 CIMR Mission Objectives	63
4 Mission Requirements	65
4.1 General Mission Requirements.....	65
4.1.1 CIMR Tandem flight.....	65
4.1.2 Orbit Requirements.....	70
4.1.3 Coverage Requirements.....	73
4.1.4 Temporal Resolution (Revisit) Requirements	75
4.2 Level-1 Observation Requirements.....	76
4.2.1 General Requirements.....	76
4.2.2 Frequency Band Requirements	76
4.2.3 Observation Zenith Angle Requirements	83
4.2.4 CIMR Scanning Requirements	85
4.2.5 Spatial Resolution Requirements	87
4.2.6 Sampling Requirements	91

4.2.7	CIMR Spectral Performance Requirements	96
4.2.8	Radiometric resolution (NEAT) Requirements.....	98
4.2.9	Dynamic Range Requirements.....	98
4.2.10	Radiometric Uncertainty and Stability Requirements.	98
4.2.11	Calibration System Requirements	102
4.2.12	Inter-channel calibration.	103
4.2.13	Polarisation Requirements.....	104
4.2.14	Antenna main beam requirements.....	108
4.2.15	Radio Frequency Interference (RFI) Mitigation Requirements.	116
4.2.16	Geo-location Requirements.	119
4.3	Product Requirements.	123
4.3.1	CIMR Product types.....	123
4.3.2	L0 Products.....	126
4.3.3	L1a Un-gridded Products	126
4.3.4	L1b Un-gridded Products	128
4.3.5	L1c Gridded Products	138
	European ice services for SIC and SIE products.....	142
4.3.6	L2 Products.....	142
4.3.7	Product Delivery Latency	160
4.4	User Service Requirements	162
4.4.1	Routine Processing Requirements	162
4.4.2	Reprocessing Requirements	163
4.5	Calibration and Validation Requirements.....	165
4.6	Software Requirements.....	166
5	Preliminary System Concept(s) and Characteristics	169
5.1	CIMR mission preliminary system characteristics.....	169
5.2	CIMR mission preliminary system concept	170
6	Data Products and Usage	172
6.1	Level-0 data products.....	172
6.2	Level-1 data products.....	172
6.3	Level-2 data products.....	174
6.3.1	Polar Sea Ice Concentration algorithm	178
6.3.2	Global and Polar Sea Surface Temperature algorithm	182
6.3.3	Polar Thin Sea Ice Thickness algorithm	184
6.3.4	Polar Sea Ice Type / Stage of Development algorithm	185
6.3.5	Polar Sea Ice Edge algorithm	186
6.3.6	Polar Sea Ice Drift algorithm	186
6.3.7	Polar Snow Depth on Sea Ice algorithm	187
6.3.8	Polar Sea Ice Surface Temperature algorithm	188
6.3.9	Global Terrestrial Snow Area algorithm.....	188

6.3.10	Global Terrestrial Snow Water Equivalent algorithm	189
6.3.11	Global Sea Surface Salinity algorithm	191
6.3.12	Global Soil Moisture algorithm.....	191
6.3.13	Global Precipitation (rain rate) algorithm	192
6.3.14	Global Ocean Surface Wind Vector/Speed algorithm.....	192
6.3.15	Global Water Vapor, Cloud Liquid Water, and Precipitation algorithms	194
6.3.16	Global Land Surface Temperature algorithm.....	194
6.3.17	Landscape freeze/thaw state (FT) algorithm	195
6.3.18	Multi-frequency Microwave Vegetation Indicators (MMVI) algorithm.....	196
6.4	Example European Operational Users.....	198
6.4.1	EUMETSAT OSI-SAF:.....	198
6.4.2	FMI – Finnish Meteorological Institute	198
6.4.3	DMI- Denmark Meteorological Institute	199
6.4.4	MET Norway – Norwegian Meteorological Institute	199
6.4.5	SMHI – Swedish Meteorological and Hydrological Institute	200
6.4.6	MetOffice – United Kingdom Meteorological Office	200
6.4.7	ECMWF – European Centre for Medium Range Weather Forecasting.....	200
6.4.8	Vandersat (NL)	201
7	Synergies and International Context	202
8	References	209
8.1	Applicable Documents	209
8.2	Reference Documents	209
9	Appendix I. Definition of Terms	233
10	Appendix II Major Policies anD EO applications supported by the CIMR mission	246
11	Appendix III CIMR Requirements Traceability Matrix.....	249
11.1.1	Sea Ice Concentration (Sea Ice Fraction).....	251
11.1.2	Sea Surface Temperature (SST)	253
11.1.3	Sea Ice Thickness (SIT)	254
11.1.4	Snow Depth on Sea Ice	254
11.1.5	Ice type/Ice stage of development.....	255
11.1.6	Ice Surface Temperature (IST)	256
11.1.7	Snow Melt and Total Snow Area (dry) on Ice Sheets and Glaciers.....	257
11.1.8	Sea Surface Salinity (SSS).....	258
12	Appendix IV Acronyms	266

1 INTRODUCTION

This document is the formal Mission Requirements Document (MRD) for the *Copernicus Imaging Microwave Radiometry* (CIMR) Mission.

The CIMR Copernicus Expansion Mission considers the inclusion of global multi-frequency imaging microwave radiometry, with a focus on high-latitude regions in support of the Integrated European Union (EU) Policy for the Arctic (see https://eeas.europa.eu/arctic-policy/eu-arctic-policy_en). It is part of the evolution of the current Copernicus Space Component (CSC) capabilities described in the CSC Long Term Scenario (LTS, ESA, 2022 and subsequent updates) to address the User Requirements expressed by the European Commission (EC).

The CIMR Mission Requirements Document (MRD) provides guidance and serves as an input to the European Space Agency (ESA) preparatory phase (Phase A/B1) study activities started in 2018, and for the implementation phase (Phase B2/C/D/E) initiated in 2020. It is managed by the CIMR Mission Scientist according to the ESA Quality Management System (QMS) procedure for Mission Requirements Management (QMS-PR-MMAN-2050-EOP) and Mission Implementation and Operations (ESA-EOP-QMS-PR-2100).

1.1 Document and Requirement Conventions

1.1.1 Terms

The term “**To Be Confirmed**” (TBC) will be used in combination with the numerical definition of some performance parameters, the final value of which may be changed by the Agency because of Definition Study engineering work.

The term “**To Be Determined**” (TBD) will be used for the numerical definition of a parameter at a later stage. Engineering assumptions shall be made in consultation with the Agency for interim numerical definitions.

Requirements marked as To be Defined (TBD) or To Be Confirmed (TBC) indicate open issues and will be confirmed by the Mission Advisory Group (MAG) or by ESA in the course of Phase A/B1 or future Mission Phases B2/C/D/E1.

The terms “**shall**” and “**will**” denote mandatory requirements.

The term “**goal**” denotes a desirable extension to a requirement even though a commitment to such performance cannot be confirmed or verified.

The terms “**should**” and “**may**” denote requirements whose implementation shall be discussed between the Contractor and the Agency.

The term “**Note**” denotes additional information providing useful background information to a requirement.

Within this MRD, Mission Objectives are split into:

Primary Objectives (PRI-OBJ-XX) that are mandatory for the success of the mission and

Secondary Objectives (SEC-OBJ-XX) that shall not drive the system design.

1.1.2 Requirement Numbering and Approach

Within this MRD, requirements are identified by a unique alphanumeric code with the following format:

MRD-DDD

The digits DDDD are requirements numbers. The sequence of these numbers may contain gaps and is independent for each combination of MRD-DDDD. Some requirements are supported by explanatory comments, which are in a different style.

Requirements are supported by explanatory comments, which are reported in a different style. Paragraphs without such annotation provide information.

All requirements **shall** have one value that guarantees a successful mission fulfilling its aim and objectives.

'**≥**' **shall** be used to set the requirement equal to a quantity that is the minimum value compulsory for the mission to achieve its aim and objectives, but enhanced performance can be attained if the quantity is greater than the required number. E.g., $X \geq 1.5$ means that the baseline requirement is equal to 1.5 but enhanced performance would be attained at $X=2.5$. $X \geq 1.5$ (g:3.5) qualifies that the requirement goal is 3.5.

'**≤**' **shall** be used to set the requirement equal to a quantity that is the minimum value compulsory for the mission to achieve its aim and objectives, but enhanced performance can be attained if the quantity is smaller than the required number. E.g., $Y \leq 0.03$ means that the baseline requirement is equal to 0.03 but enhanced performance would be attained at $Y=0.01$. $Y \leq 0.03$ (g:0.005) qualifies that the requirement goal is 0.005.

1.1.3 Requirements and Guidelines

Compliance with all the requirements specified within this document is necessary for complete success of the mission. Harmonisation of the definition of these requirements and the technical design of the mission is necessary to ensure that the mission, as eventually implemented, will be capable of full compliance with the requirements.

All the requirements specified in the MRD shall be verified and traceability provided.

Similarly, comments may indicate some guidance or limitation.

2 BACKGROUND AND JUSTIFICATION

Copernicus [<http://www.copernicus.eu/>] is a European system for monitoring the Earth in support of European policy. It includes Earth Observation satellites (notably the Sentinel series developed by ESA), ground-based measurements and, services to process data to provide users with reliable and up-to-date information through a set of Copernicus operational services related to environmental and security issues. Copernicus services provide critical information to support a wide range of applications, including environment protection, management of urban areas, regional and local planning, agriculture, forestry, fisheries, health, transport, climate change, sustainable development, civil protection and tourism. Copernicus satellite missions are designed to provide ‘upstream’ inputs to all Copernicus Services as systematic measurements of Earth’s oceans, land, ice and atmosphere to monitor and understand large-scale global dynamics. The core users and consumers of Copernicus services are policymakers and public authorities that need information to develop environmental legislation and policies or to take critical decisions in the event of an emergency, such as a natural disaster or a humanitarian crisis. The Copernicus programme is coordinated and managed by the European Commission. The development of the observation infrastructure is performed under the aegis of the European Space Agency (ESA) for the space component and of the European Environment Agency (EEA) and the Member States for a separate, but important, in-situ measurement component.

The Copernicus services transform this wealth of satellite and in situ data into value-added information by processing and analysing the data together with numerical forecasting and prediction models. Datasets stretching back for decades are made comparable and searchable, thus ensuring the monitoring of changes; patterns are examined and used to create better forecasts, for example, of the ocean and the atmosphere. Maps are created from imagery, features and anomalies are identified and statistical information is extracted. These value-adding activities are streamlined through six thematic streams of Copernicus services:



The Copernicus Marine Service (CMEMS <http://marine.copernicus.eu>) is the marine component of the Copernicus Programme of the European Union. It provides free, regular, and systematic authoritative information on the state of the Blue (physical), White (sea ice) and Green (biogeochemical) ocean, on a global and regional scale. It is funded by the European Commission (EC) and implemented by Mercator Ocean International. It is designed to serve EU policies and International legal Commitments related to Ocean Governance, to cater for the needs of society at large for global ocean knowledge and to boost the Blue Economy across all maritime sectors by providing free-of-charge state-of-the-art ocean data and information. The application of satellite data on sea surface temperature, sea surface salinity, sea ice concentration, sea ice thickness, wind and waves over the ocean, sea surface height, sea level rise, ocean circulation, derived from satellite missions are all fundamental inputs to CMEMS activities. Mercator Ocean International (MOI) was selected by the European Commission (EC) to implement the Copernicus Marine Service in 2014.



Copernicus Global Land Monitoring component of the Land Service (CGLMS, <http://land.copernicus.eu>) leads activities in this domain. It provides geographical information on land cover to a broad range of users in the field of environmental terrestrial applications. This includes land use, land cover characteristics and changes, vegetation state, water cycle and earth surface energy variables and the terrestrial cryosphere. The Copernicus Land Monitoring Service has been jointly implemented by the European Environment Agency (EEA) and the Joint Research Centre (JRC) since 2011.



The Copernicus Climate Change Service (C3S, <http://climate.copernicus.eu>) leads activities in the domain of climate change. It supports society by providing authoritative information about the past, present, and future climate in Europe and the rest of the World. The C3S mission is to support adaptation and mitigation policies of the European Union by providing consistent and authoritative information about climate change. C3S users include scientists, consultants, planners and policy makers, the media, and the public. C3S offers free and open access to climate data and tools based on the best available science. It maintains an active dialog with users and endeavours to help them meet their goals in dealing with the impacts of climate change. C3S relies on climate research carried out within the World Climate Research Programme (WCRP) and responds to user requirements defined by the Global Climate Observing System (GCOS). It provides an important resource to the Global Framework for Climate Services (GFCS).



The Copernicus service for Security (<https://www.copernicus.eu/en/copernicus-services/security>) leads activities in this domain. The European Boarder and coast Guard Agency (FRONTEX, <https://frontex.europa.eu/>) provides the border surveillance component of the Copernicus Security Service to support the EU's external border surveillance information exchange framework (EUROSUR) by providing near real time data over land and at sea around the EU's borders. In the area of maritime surveillance, the European Maritime Safety Agency (EMSA, <http://www.emsa.europa.eu/copernicus.html>) operates the maritime surveillance component of the Copernicus Security Service. Copernicus Sentinel 1, 2 and 3 together with additional satellite data are combined with other sources of maritime information to monitor maritime areas of interest. The European Satellite Centre ([EU SatCen](#)) provides Support to External Action ([SEA](#)) within the Copernicus Security Service. SEA assists the EU in its operations, providing decision makers with geo-information on remote, difficult to access areas, where security issues are at stake.



Copernicus Emergency Management Service (CEMS, <http://emergency.copernicus.eu/>) leads activities in this Domain. It provides all actors involved in the management of natural disasters, man-made emergency situations, and humanitarian crises with timely and accurate geo-spatial information derived from satellite remote sensing and completed by available in situ or open data sources. The Copernicus EMS consists of a mapping component and an early warning component. The mapping component of the service (Copernicus EMS - Mapping) has a worldwide coverage based on satellite imagery implemented by the European Commission DG Joint Research Centre (JRC). Copernicus EMS - Mapping can support all phases of the emergency management cycle: preparedness, prevention, disaster risk reduction, emergency response and recovery. The early warning component of the Copernicus EMS includes the European Flood Awareness System (EFAS, which provides overviews on ongoing and forecasted floods in Europe up to 10 days in advance) and the European Drought Observatory (EDO, which provides drought-relevant information and early-warnings for Europe). Global Flood Awareness System (GloFAS), Global Wildfire Information System (GWIS) and Global Drought Observatory (GDO) are used at global level.



The Copernicus Atmospheric Monitoring Service (CAMS, <https://atmosphere.copernicus.eu/>) leads activities in this domain. It provides consistent and quality-controlled information related to air pollution and health, solar energy, greenhouse gases and climate forcing, everywhere in the world. CAMS is implemented by the European Centre for Medium-Range Weather Forecasts (ECMWF).

2.1 Copernicus Evolution

As set out in the ESA Program Board for Earth Observation (PB-EO) paper (ESA/PB-EO(2017)31 Paris, 5 September 2017), the Copernicus Space Component (CSC) has been established as the largest and most proficient Earth Observation infrastructure in the world. With seven high-performance satellites in orbit and more than 200,000 registered Sentinel data users on the ESA/EC Copernicus data portal as well as numerous sophisticated operational services, the system has evolved at a rapid pace. To preserve the momentum in fulfilling the growth in user needs, the future evolution of the CSC needs to be initiated now in close cooperation with all stakeholders.

According to the Copernicus Regulation (EU Regulation No. 377/2014 dated 3 April 2014), ESA is mandated by the EU Council and European Parliament to define “*the overall system architecture for the Copernicus space component and its evolution on the basis of user requirements, coordinated by the Commission*”. Following this rationale, ESA in close interaction with the EC, EUMETSAT and Member States, has identified key components of a Long-Term Scenario which captures the essential elements of the space infrastructure in relation to the Copernicus users, as well as its evolution.

The intense use and increased awareness for the potential of Copernicus have generated great expectations for an evolved Copernicus system. There is now a large set of concrete needs and requirements for the future configuration of the CSC. User and observation requirements have been identified, structured and prioritized in a continuous reflection process led by the EC. Results from EU policy analyses, consultation of Services and Member States, as well as various workshops, gap analyses, studies and task forces now provide the rationale for the LTS. Clearly, a resolute approach is needed to achieve the time-critical objectives of new policies, such as the Integrated European Union Policy for the Arctic, Climate Change, the Sustainable Development Goals of the UN, or European EO Data Commercialization and Democratization.

Two distinct sets of expectations have emerged from the user consultation process:

1. Stability and continuity, while increasing the quantity and quality of CSC products and services, lead to one set of requirements. These requirements are addressed by a **Next Generation** of the current series of Sentinel 1 to 6 satellite capability by providing enhanced continuity of baseline Copernicus observations.
2. Emerging and urgent needs for new types of observations constitute a second distinct set of requirements. They are addressed by a timely **Expansion** of the current Sentinel satellite fleet. Both sets of expectations have been systematically reflected and integrated by ESA (as the CSC System Evolution Architect) in response to formal documented EC requirements.

The ‘Extension’ and the ‘Expansion’ components are organised around broad observation domains. The distinction between ‘Expansion’ and ‘Next Generation’ components is not schedule-based. The ‘Expansion’ component corresponds to the enlargement of the present measurements through the introduction of new missions to answer emerging and urgent user requirements. The ‘Next Generation’ component corresponds to a more progressive improvement of the current measurement capabilities, by delivering enhanced continuity compared to the series of Copernicus Sentinel missions currently deployed.

The “CSC Expansion” includes new **Copernicus Expansion Missions** that have been identified by the European Commission (EC) as priorities for implementation in the coming years by providing new capabilities in support of current emerging user needs. Three priorities have been identified:

- **Priority 1:** Greenhouse gas monitoring, specifically on anthropogenic CO₂ emissions for which currently no European satellite observations are available.
- **Priority 2:** Monitoring Polar regions, specifically concerning polar/Arctic observations, namely sea ice/floating ice concentration and surface elevation; Monitoring Agriculture, specifically on parameters which potentially could be addressed through thermal infrared and hyperspectral observations
- **Priority 3:** Mining, biodiversity, soil moisture and other parameters, requiring observations in additional bands, currently not available

The following missions have been identified to address these prioritised needs:

- **Copernicus Anthropogenic CO₂ Monitoring (CO2M) mission:** this mission employs imaging spectrometry to monitor man-made CO₂ emissions and overall CO₂ budget at country and regional/megacity scales and assess the effectiveness of the relevant emissions reduction commitments. This requires a capability to provide accurate and consistent quantification of anthropogenic CO₂ emission and their trends.
- **Copernicus Imaging Microwave Radiometer (CIMR) mission:** this mission employs Multi-frequency Imaging Microwave Radiometers to provide day and night observations of sea ice concentration and a wide range of other floating sea ice parameters, to support operational systems in non-precipitating atmosphere conditions. This mission will provide improved continuity of missions monitoring floating sea ice parameters, notably in terms of spatial resolution (~5 km), temporal resolution (sub-daily) and geophysical accuracy. Additional global measurements of Sea Surface Temperature and other parameters will also be included but with a primary focus on the polar regions.
- **Copernicus Polar Ice and Snow Topography Altimeter (CRISTAL) mission:** this mission shall provide enhanced measurements of land ice elevation and sea ice thickness implementing higher spatial resolution for improved lead detection and additional capability to determine snow loading on sea ice.
- **Copernicus Land Surface Temperature Monitoring (LSTM) mission:** this mission shall be able to complement the current visible (VIS) and near-infrared (NIR) Copernicus observations with high spatio-temporal resolution Thermal Infrared observations over land and coastal zones in support of agriculture management services and possibly a range of additional services.
- **Copernicus Hyperspectral Imaging Mission for the Environment (CHIME):** this mission aims to augment the Copernicus space component with precise spectroscopic measurements to derive quantitative surface characteristics supporting the monitoring, implementation, and improvement of a range of policies in the domain of raw materials, agriculture, soils, food security, biodiversity, environmental degradation and hazards, inland and coastal waters, snow, forestry and the urban environment
- **Copernicus L-band Synthetic Aperture Radar (ROSE-L) mission:** this mission is responding to the requirements expressed by both the Land Monitoring and the Emergency Management services. Its target applications are soil moisture, crop type discrimination, forest type/forest cover (in support to biomass estimation), food security and precision farming. In addition, the mission will contribute to the monitoring of ice extent in the polar region. Other emerging applications will be possible by the synergetic and complementary observations with C band and X band SAR systems.

While the long-term consolidation of current CSC capabilities is the utmost priority, no hierarchy is established at this point among the proposed missions, which are all backed by strong priority user needs and must all be considered an integral part of the evolving Copernicus system.

2.2 The Integrated European Union Policy for the Arctic.

The Arctic Ocean is changing dramatically responding to significant global atmospheric warming by pan-Arctic sea-ice retreat and thinning (e.g., *Meier et al.*, 2014; *Werner et al.*, 2016). The rise in Arctic near-surface air temperatures has been almost twice as large as the global average in recent decade (e.g., *Serreze and Francis*, 2006) that is called ‘Arctic amplification’ (*Kellogg*, 1975) although the underlying causes of Arctic amplification remain uncertain (e.g., *Screen and Simmonds*, 2010). Arctic amplification is the outcome of many complex and interrelated feedback mechanisms (e.g., ice retreat/albedo, surface/lower troposphere air temperatures, synoptic weather patterns, ocean-atmosphere fluxes, cloud, amongst others) and is poorly reproduced in climate models: other feedback mechanisms may emerge in the future complicating the situation even further.

Measurements of geophysical and societal change provide the evidence to underpin the establishment, implementation and monitoring of policy, policy decisions and their impact, not just in Europe, but across the world. In the Arctic region, several extreme concerns have been recently raised by the International Panel for Climate Change (*IPCC*, 2018):

- Warming greater than the global annual average is being experienced in many land regions and seasons, including two to three times higher in the Arctic with warming generally higher over land than over the ocean.
- Climate related risks for natural and human systems are higher for global warming of 1.5°C than at present. These risks depend on the magnitude and rate of warming, geographic location, levels of development and vulnerability, and on the choices and implementation of adaptation and mitigation options.
- There is high confidence that the probability of a sea-ice-free Arctic Ocean during summer is substantially lower at global warming of 1.5°C when compared to 2°C. With 1.5°C of global warming, one sea ice-free Arctic summer is projected per century. This likelihood is increased to at least one per decade with 2°C global warming. Effects of a temperature overshoot are reversible for Arctic sea ice cover on decadal time scales.
- Populations at disproportionately higher risk of adverse consequences of global warming of 1.5°C and beyond include disadvantaged and vulnerable populations, some indigenous peoples, and local communities’ dependent on agricultural or coastal livelihoods. Regions at disproportionately higher risk include Arctic ecosystems, dryland regions, small-island developing states, and least developed countries. Poverty and disadvantages are expected to increase in some populations as global warming increases; limiting global warming to 1.5°C, compared with 2°C, could reduce the number of people both exposed to climate-related risks and susceptible to poverty by up to several hundred million by 2050.
- Limiting global warming to 1.5°C compared to 2°C is projected to reduce increases in ocean temperature as well as associated increases in ocean acidity and decreases in ocean oxygen levels. Consequently, limiting global warming to 1.5°C is projected to reduce risks to marine biodiversity, fisheries, and ecosystems, and their functions and services to humans, as illustrated by recent changes to Arctic sea ice and warm water coral reef ecosystems.

These changes may lead to dramatic consequences as discussed by *Stephen* (2018) who describes the societal impacts of a rapidly changing Arctic. Climate change and globalisation are

the dominant drivers of societal impacts in the Arctic. As the climate changes access to the Arctic is improving and, through globalisation and new economic development, a rapid transformation of the environmental and geo-political environment of the region is in progress. While there is a strong desire for sustainable development of the fragile Arctic environment at both the national and international level, significant societal impacts are inevitable. Oil and gas industries prospect for potentially lucrative deposits in the Arctic Ocean. The north-east/north-west polar ocean shipping routes are gaining popularity. Tourism is rapidly expanding with new very large cruise ships dedicated to more adventurous activities reaching deep into the Arctic environment. Consequently, the demands on highly specialised - but limited - international search and rescue service capacity are growing enormously. As the Arctic climate changes, uncertainty surrounds fisheries that are under pressure in terms of ecological change (i.e. species composition, invasive species, changes in ocean temperature and salinity) with large potential impact on fish stocks. Furthermore, as new prospectors increase activities in the Arctic region using modern techniques, the sustainability of fisheries is a critical question for the indigenous population that rely on the ocean as the major source of protein. Permafrost change is leading to loss of land and unpredictable infrastructure stability – a remarkable observation in a time when investment and further development are increasing.

Arctic climate change can also lead to *decreasing* access, movement, and living options across the region. Permafrost thaw, extreme weather events, flooding, diminishing sea and land ice, and coastal erosion (exacerbated by sea level rise) result in unreliable ice roads, damage to houses, pipelines, railroads, airports, ports and harbours, unreliable energy, and water supply. These may conspire in some regions leading to such a burden that relocation of entire communities may be required. This in turn, may result in the abandonment of lifestyles and cultural traditions that have been established over thousands of years (Stephen, 2018). The often-cited concept of a 'Global Arctic' highlights the inextricable linkages between Arctic and global processes and systems and the entangled fate of the Arctic region and the world as a whole (*ibid*). In this evolving complex setting, while increasingly engaged in rights-holder issues and as active participants in governance, law, politics, and research, Arctic indigenous peoples remain vulnerable. As an increasing number of national and international stakeholders place increasing demands on the Arctic region, political tensions, and insecurity across the region, as a whole, are increasing.

The societal impacts of a rapidly changing Arctic are thus complex, uncertain, and ambiguous. In response, the European Commission and the High Representative of the Union for Foreign Affairs and Security Policy issued to the European Parliament and the Council, on 27 April 2016, a joint communication that proposed "*An integrated European Union policy for the Arctic*". The communication highlights the strategic, environmental, and socio-economic importance of the Arctic region, including the Arctic Ocean and adjacent seas. The Arctic's fragile environment is also a direct and key indicator of the climate change, which requires specific mitigation and adaptation actions, as agreed at the COP-21 held in Paris in December 2015. Continuously monitoring the vast and harsh Arctic environment in such a changing world with Earth observation, navigation, and communication satellites (considering the sparse population and the lack of transport links) is considered essential to the successful implementation and effective management of the Integrated EU Arctic Policy.

To this end, the "*integrated EU Arctic policy*" has identified and is addressing three priority areas:

1. Climate Change and Safeguarding the Arctic Environment (livelihoods of indigenous peoples, Arctic environment).
2. Sustainable Development in and around the Arctic (exploitation of natural resources e.g., fish, minerals, oil and gas), "Blue economy", safe and reliable navigation (e.g., the Arctic Northern Sea Route).

3. International Cooperation on Arctic Issues (scientific research, EU and bilateral cooperation projects, fisheries management/ecosystems protection, commercial fishing).

The Policy was recently revisited (see https://eeas.europa.eu/sites/default/files/2_en_act_part1_v7.pdf) where a stronger EU engagement for a peaceful, sustainable and prosperous Arctic is emphasised. In particular, the EU will strengthen its Arctic engagement through:

- contributing to maintaining peaceful and constructive dialogue and cooperation in a changing geopolitical landscape, to keep the Arctic safe and stable, by raising Arctic matters in its external contacts, intensifying regional cooperation, and developing strategic foresight on emerging security challenges.
- addressing the ecological, social, economic, and political challenges arising as a consequence of climate change and taking strong action to tackle climate change and environmental degradation, making the Arctic more resilient, through environmental legislation, concerted action on black carbon and permafrost thaw, and by pushing for oil, coal and gas to stay in the ground, including in Arctic regions.
- supporting the inclusive and sustainable development of the Arctic regions to the benefit of its inhabitants and future generations, focusing on the needs of Indigenous Peoples, women and the young, and investing in future-orientated jobs and the blue economy.

The existing Copernicus programme already offers operational thematic services in the fields of atmosphere monitoring, marine environment monitoring, land monitoring, climate change, emergency management and security. For example, the CMEMS Arctic – Monitoring Forecasting Centre (ARC MFC) provides accurate forecast and reanalysis products for sea ice, ocean, biology, and surface waves in the whole Arctic. The system is based on a numerical ocean model assimilating in situ and satellite data. The Copernicus Atmospheric Service provides information products about atmospheric composition and solar radiation. Several products are of interest for the Arctic region including monitoring and assessing the impact of emissions from fires at high latitudes (Canada, Siberia) and transport of the corresponding plumes of gases and aerosol affecting atmospheric composition in the Arctic region and monitoring and forecasting of the ozone layer, including Arctic “mini-holes” events. The Copernicus Climate Service is developing new approaches to provide high-resolution regional climate-quality reanalysis over the Arctic and production of sea-ice Essential Climate Variables. In addition, Economic Sectoral analyses of Arctic shipping addresses the impact of climate change on ship routing issues.

These aspects were strongly reiterated by the European Commission Council Conclusions on Copernicus adopted by the Council at its 3877th meeting held on 10 June 2022 (EC, 2022). Notably (emphasis for MRD purposes):

- NOTES the Council conclusions on ‘Space solutions for a sustainable Arctic’ of 29 November 2019, recognise Europe’s remarkable capabilities in **Earth observation and their importance for monitoring and combatting the effects of climate change in the Arctic environment; noting, however, [there are] some remaining gaps in the monitoring capacities and services.**
- HIGHLIGHTS the **need to ensure the calibration and validation of satellite data** and information products, using reliable high quality in situ data, with documented quality, access to analysis ready data, the fusion of data from all sources and different resolutions, as well as the **rapid availability of high-quality data** in order to maximise their use.
- CALLS FOR the **long-term enhanced continuity** of current space and in situ observations and Services.
- URGES the **implementation** of priorities for Copernicus that have not yet been implemented, including the Sentinels Next Generation **and the six Copernicus Expansion**

missions and the dedicated support to policy areas such as Arctic, coastal areas, cultural heritage, environmental compliance, taking into account the security of the space and ground segment and the integrity of the data; **HIGHLIGHTS** the need to address new services such as agriculture, food and water security; and **RECOMMENDS** preparing the long term evolution of the Sentinel family, based on updated user requirements.

- **HIGHLIGHTS the need to ensure the calibration and validation of satellite data and information products, using reliable high quality in situ data**, with documented quality, access to analysis ready data, the fusion of data from all sources and different resolutions, as well as the rapid availability of high-quality data in order to maximise their use.

These important conclusions are fully addressed in the requirements set out in this MRD that are designed to guide the implementation of the CIMR mission.

2.3 A High-Priority Copernicus Mission to support the Integrated EU Policy for the Arctic: The Copernicus Imaging Microwave Radiometer (CIMR).

New High-Priority requirements from key Arctic users' communities have recently emerged within Copernicus that highlight the need for new satellite measurements not available as part of the current Copernicus satellite fleet. The new requirements were reviewed at a Polar Ice and Snow workshop held in June 2016, organised by DG GROW involving relevant European Commission (EC) Directorate General (DGs). The workshop gathered inputs from 70 attendees across EU Member States working in various domains. A strong interest for a *Polar Ice and Snow Mission* was further reinforced when discussed in a wider international context that considered UN Conventions and pan-Arctic cooperation activities. This situation led DG GROW to set up a new group of European Polar Experts Group (PEG) in spring 2017. The mandate of PEG was to update and/or complete the review and analysis of the Users' needs, thus allowing the Commission to assess the relevance of the development of a "Copernicus expansion mission" dedicated to Polar and Snow monitoring.

The EC Polar Expert Group process concluded with two dedicated reports: "*Polar Expert Group User Requirements for a Copernicus Polar Mission Phase-I report*" (Duchossois et al, 2018a) and "*Polar expert group, Phase 2 report on Users' requirements*" (Duchossois et al, 2018b). A Phase-III report was released in 2021 (Nordbeck et al, 2021) that focussed on Operational Products and Services.

The Phase-I report provided a detailed inventory of user requirements that were consolidated and prioritised in the Phase-II report. This report highlighted the fragile future continuity of low-frequency satellite microwave radiometers and the need for high spatial resolution. Notably, at the end of the JAXA GCOM-2 mission (e.g., Kasahara et al. 2012) in 2017 there was a definite gap in capability as shown in Figure MRD-2.3.1-1. Based on an assessment of Users needs and the likely gap in capability, the PEG recommended, **as first priority** [AD-2], an Imaging Microwave Radiometry Mission that meets the Joint EC Communication high priorities, in particular the provision of operational sea-ice services that are of prime importance for navigation safety in the Arctic and adjacent seas **with at least daily revisit in Polar regions** [AD-2].

Passive Microwave Satellites for Sea Ice Concentration / Type / Drift Monitoring

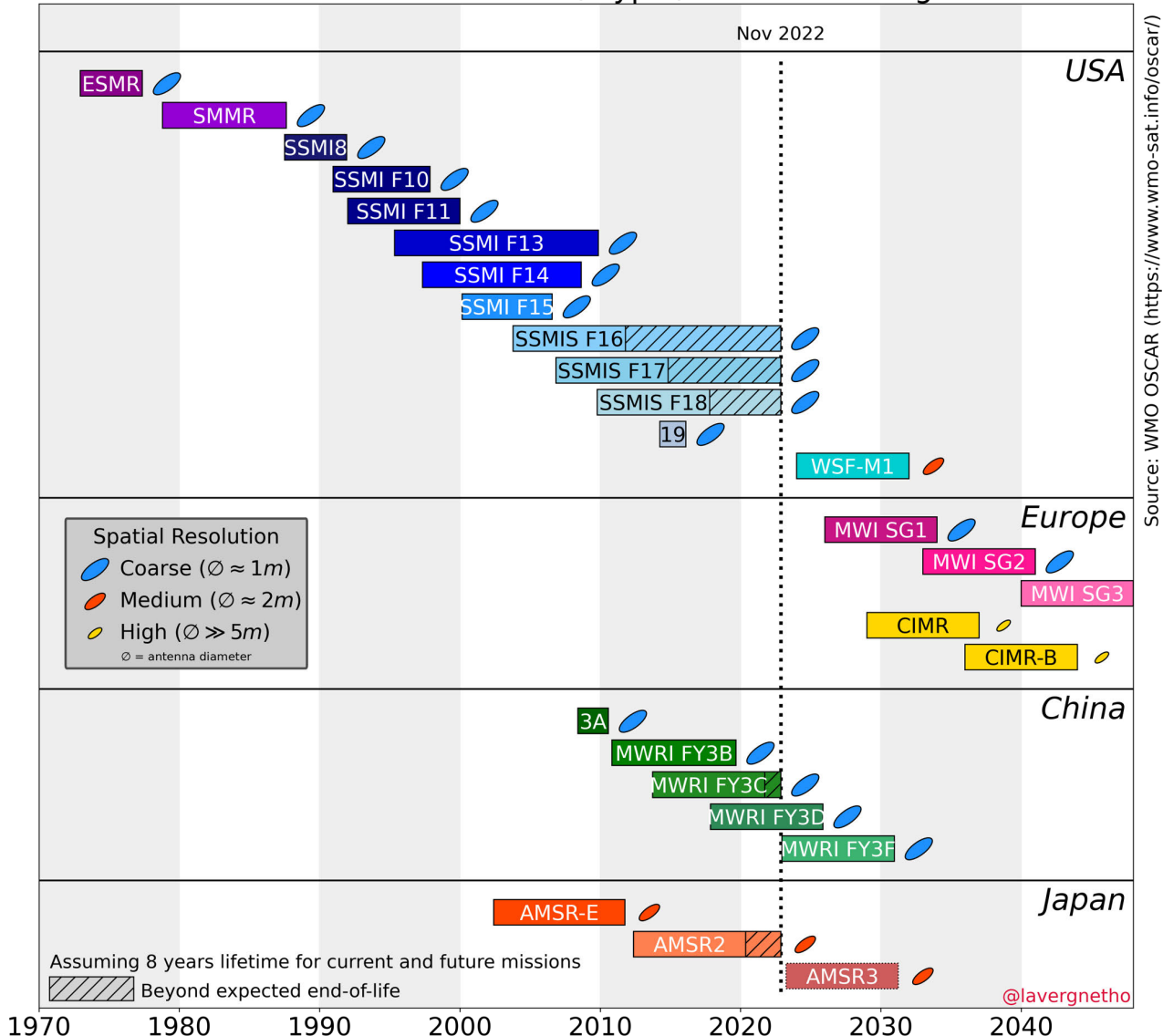


Figure MRD-2.3.1. Timeline of past, present, and future microwave satellite radiometer missions relevant for sea ice concentration mapping for the period 1980s to 2030s highlighting a gap in capability and the use of Chinese missions to bridge the gap. However, these missions do not include the low-frequency channels or high-spatial resolution offered by CIMR. Directly responding to the Integrated European Policy for the Arctic, CIMR will be a unique mission providing low frequency and high-spatial resolution measurements: a game changer for Arctic monitoring. (After T. Lavergne)

On 30th March 2020 the Japan Aerospace Exploration Agency (JAXA) announced (<https://www.mitsubishi-electric.com/sites/news/2020/pdf/0330.pdf>) the development of Global Observing SATellite for Greenhouse gases and Water cycle (GOSAT-GW), the third in the GOSAT series. GOSAT-GW will have two missions: greenhouse gases observation for Japan's Ministry of the Environment and the National Institute for Environmental Studies (NIES), and water-cycle observation for JAXA. GOSAT-GW will also be equipped with the newly developed Advanced Microwave Scanning Radiometer 3 (AMSR3, JAXA, 2020), which will estimate geophysical quantity of earth's water on land, sea-surface and in the atmosphere. The mission is designed to

provide measurements of water vapour, cloud liquid water, precipitation including snowfall, winds, sea surface temperature, sea ice concentration, snow cover, soil moisture. AMSR3 will use an increased number of frequency bands compared to its predecessors for more accurate estimation of hydro-geophysical conditions, such as precipitation, water vapor, sea ice and sea-surface temperatures (JAXA, 2020). AMSR-3 will include channels centred at 6.925 GHz, 7.3 GHz, 10.65 GHz, 18.7 GHz, 23.8 GHz, 36.5 GHz, 89.0 GHz, 165.5 GHz, 183.3 GHz. AMSR-3 will include new channels centred at 10.25 GHz V/H-pol (wider bandwidth to mitigate random noise), 165.5 GHz V-pol, 183±3GHz V-pol, and 183±7 GHz V-pol. The mission is designed for a 7-year duration with a planned launch in 2023 into sun synchronous orbit (98.06° inclination) at 666 km altitude with a revisit time of 3 days and a local time of ascending node at 13:30. AMSR-3 will ‘bridge the gap’ to the CIMR mission that is expected in 2027+.

In addition, and in an independent manner, the Copernicus Marine Environment Monitoring Service (CMEMS, <http://marine.copernicus.eu>) has reviewed its own requirements for the evolution of the CSC. The service is targeted around four main areas of benefits: Maritime Safety, Coastal and Marine Environment, Marine Resources, and Weather, Seasonal Forecasting and Climate activities. CMEMS provides regular and systematic core reference information on the state of the global ocean and regional seas – including the Global Ocean (including all Antarctic/Arctic sea ice), the Arctic Ocean and the Baltic Sea. The analyses and forecasts produced by the service support any user requesting generic information on the state of the ocean and sea ice, and especially downstream service providers who use the information as an input to their own value-added services to end-users. CMEMS operates the Sea Ice Thematic Assembly Centre (SI-TAC) providing Sea Ice products for Arctic Ocean and Southern Ocean based on microwaves, infrared and SAR satellite observations. The “Sea Surface Temperature Thematic Assembly Centre” (SST-TAC) provides SST observation products for the global ocean and European regional based on multi-sensors Infrared and microwave SST satellite data. These data are regularly distributed to the more than 200,000¹ registered users for data download directly at the EU/ESA Sentinel Data Hubs and assimilated to the CMEMS modelling components which provides regular forecasts of the Arctic Ocean, Baltic Sea regions as well as the global ocean and all the other European Seas.

CMEMS requires a sustainable European operational provision of medium-resolution (5-10 km) multi-frequency and multi-polarization microwave radiometer observations delivering Sea Ice Concentration (SIC), Sea Ice Edge (SIED), Sea Ice Drift (SID), Sea Ice Thickness (SIT) snow parameters on sea ice, Sea Ice Surface Temperature (SIST), Sea Surface Salinity (SSS), Ocean Vector Winds (OVW) and Sea Surface Temperature (SST) [AD-3] overlapping with the requirements of PEG [AD-2]. The need to make measurements in cloudy conditions (where infrared measurements are precluded) was noted.

Beyond the provision of key polar ice and snow parameters, the microwave radiometer mission, through the selection of well stable, well-calibrated and validated set of channels will also be of high interest for the observation of non-polar regions in particular for the oceans (SST, ocean vector wind, Ovw), continuity of current ocean surface salinity (SSS) capability and, for land applications such as hydrology, snow-cover extent, snow water equivalent, large scale soil characteristics (moisture), large scale vegetation extent monitoring and biomass, land surface temperature, flooding extent, amongst others [AD-2], depending on the final mission configuration.

Climate requirements are set out in other documents notably those developed by the EC for climate [AD-4] which notes that monitoring of salinity and sea ice parameters are important variables required to leverage the continuity of existing Copernicus satellite measurements.

¹ As of February 2019

The development of an advanced microwave radiometer mission in Europe will offer many advantages/benefits including:

- Security in the availability of microwave radiometer data for scientific and operational applications in polar and non-polar regions.
- European autonomy and independence from non-European sources (USA, Japan, China, Russia) for the provision of satellite microwave radiometer data meeting Copernicus and EC Arctic Policy objectives.
- Evolution of European space industry technical capacity and skill, complementing the existing experience acquired for the development of active microwave (Synthetic Aperture Radar (SAR), Altimeter, Scatterometer) and optical imagers (Visible (VIS), Infrared (IR), Hyper-spectral etc.).
- It is well understood that the CIMR mission will not address the full set of requirements set out by [AD-1], [AD-2] and [AD-3]. It is also understood that the Next Generation Copernicus missions will result in a sustained monitoring architecture with operational continuity that will consider any remaining requirements [AD-2].

2.4 Established Copernicus user needs for the CIMR mission

The EC has built up a repository of prioritized requirements and needs based on the following independent considerations and interactions:

- EU policies priorities,
- Member States input,
- Needs of the existing Services,
- Needs identified in thematic Workshops,
- Climate Change (11 March 2016),
- Polar and Snow Cover Applications (23 June 2016),
- Raw Materials (5 September 2016),
- Security – Support to External Action and applications for EEA (5 April 2017),
- Cultural Heritage (24 April 2017),
- European Environmental Protection Agencies (7 June 2017),
- Coastal Areas (29 June 2017),
- Energy Sector (12 Oct 2017),
- User Requirements Studies,
- Task Forces and Expert Groups focusing on the four domains of EU policy priority,
- Polar Regions Industry Workshop (7 Nov 2018).

EC consultations also included various exchanges in the Copernicus Committee and User Forum. On 9th of June 2017, an extraordinary joint meeting of the Copernicus Committee and ESA PB-EO delegates took place to present the status of the requirements process and thoughts on the CSC evolution. The feedback was subsequently included in further discussions in the frame of a Joint Working Group (EC, ESA and EUMETSAT), which met regularly to reflect on the emerging requirements and to consolidate the LTS. Feedback from the four Task Forces/Expert Groups to the Joint Working Group (EC, ESA and EUMETSAT), held on 27th of July, confirmed a high degree of correspondence in terms of overall observation priorities for the expansion of the CSC. The User needs for the CIMR mission are set out in reports from EC-led Polar Expert Group (PEG) user consultation processes, which are supplemented by a document expressing CMEMS recommendations and a document expressing Climate User requirements. They are:

1. Polar Expert Group User Requirements for a Copernicus Polar Mission Phase-I report (12 June 2017) [AD-1].
2. Polar expert group, Phase 2 report on Users' requirements (31 July 2017) [AD-2],
3. The Copernicus Marine Environmental Monitoring System (CMEMS) requirements for the Evolution of the Copernicus Satellite Component (21 February 2017) [AD-3].
4. Climate Change User Requirements Document Nextspace-SC3 Final v4 (31st July 2017) [AD-4].
5. Polar expert group, Phase 3 report on operational products and services (2021) [AD-5],

CMEMS has responsibility for monitoring the Global Ocean and European regional seas including sea ice parameters in the Antarctic, Arctic Ocean and Baltic Sea which is why [AD-3] is also an applicable document for a Polar Ice and Snow satellite mission. While today many “polar parameters/products” already exist (e.g. CMEMS Arctic products: <http://marine.copernicus.eu>) and are available on an operational or quasi-operational basis, users often look for improved performances and quality (e.g., spatial and temporal resolution, accuracies, timeliness etc.) [AD-1].

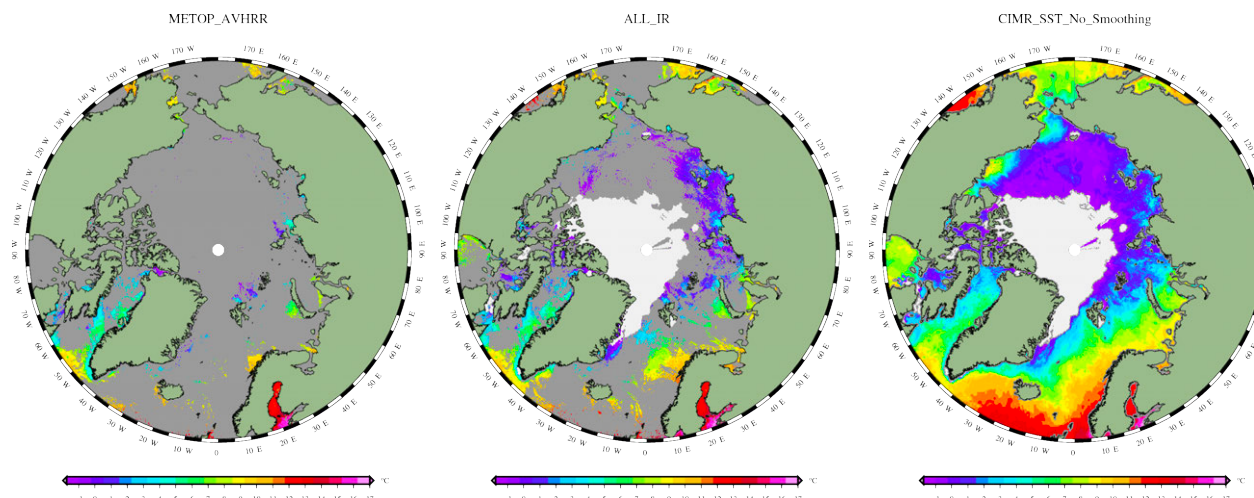


Figure MRD-2.4.1. comparison of Thermal Infrared satellite measurements ((taken from Copernicus Marine Environmental Services (CMEMS) data production) and microwave radiometer SST coverage in the Arctic, September 2012. (left) Data coverage of one (MetOp-A) satellite, (centre) all available infrared satellites and (right) simulated Copernicus Microwave Imaging Radiometer (CIMR) coverage during the sea ice minimum in September 2012. It is clear that IR satellites have severe limitations in the cloud covered Arctic and that CIMR is needed to deliver pan-Arctic coverage.

Moreover, these products rely on non-European research satellite missions delivering microwave radiometer data sets (e.g., from JAXA AMSR-2) and are therefore not secure in the long-term operational context of Copernicus. Furthermore, such data sets do not address the high spatial resolution, dedicated low-frequency channels and radiometric fidelity requirements requested by Copernicus services.

Floating ice parameters (including concentration / sea ice extent / thickness / type / drift, thin sea ice distribution, iceberg detection/volume change and drift, ice shelf thickness and extent) are key to operational services in the Polar-regions (i.e. for navigation, marine operations, safety of life at sea) as well as for climate monitoring and modelling [AD-1]. However, high-resolution (~1 km) optical satellite measurements of the earth surface, including the thermal infrared region, are confounded by the presence of clouds (see Figure MRD-2.4.1 and MRD-2.4.2) and the polar night so they cannot provide the necessary coverage (e.g., Drue and Heinemann, 2004). There are

significant gaps in coverage and revisit particularly in areas with persistent cloud cover including the polar-regions [AD-2], [AD-3].

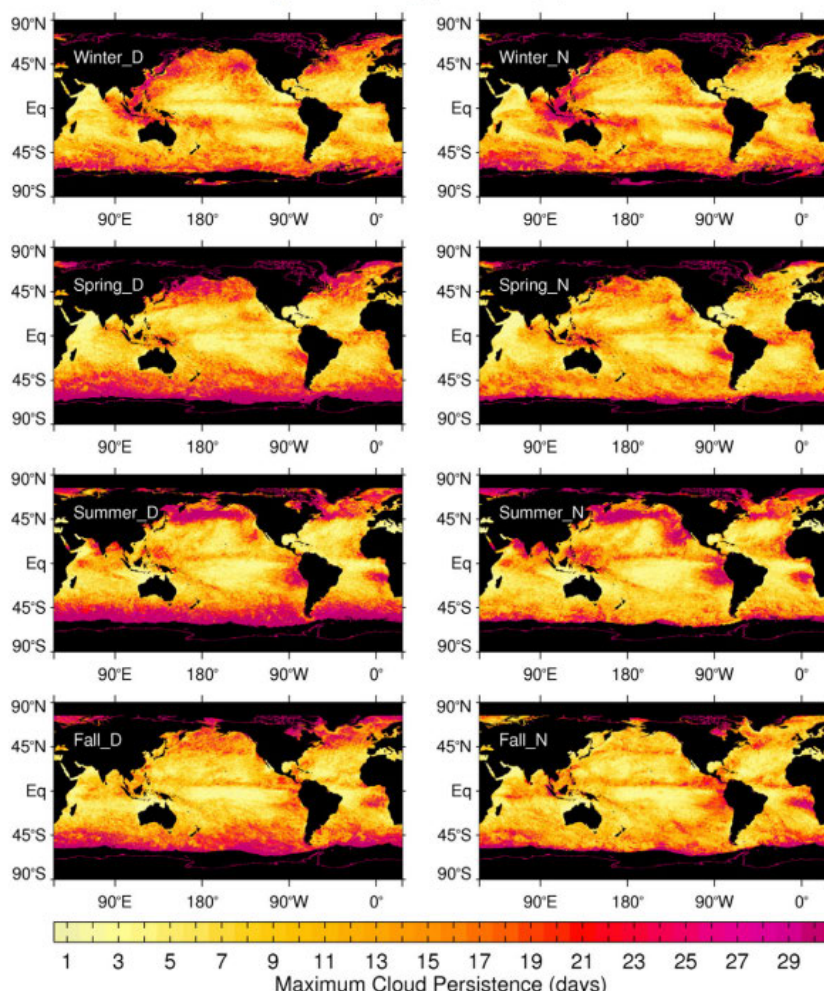


Figure MRD-2.4.2.
Maximum cloud persistence (days) from MODIS v6 daytime cloud mask data (seasons relate to Northern Hemisphere; D indicates daytime part of each orbit, N indicates night-time (alternative retrieval)). This figure clearly highlights regions where infrared SST retrievals are prevented due to persistent cloud cover. Regions where 11GHz channel SST retrievals are not accurate and infrared retrievals are not possible due to cloud are highly correlated. This figure emphasizes need for 6-7GHz channels flown on future microwave radiometer satellite instruments (From Liu and Minnett 2016).

Microwave Synthetic Aperture Radar (SAR) including Sentinel-1 operating with varied polarisation and C-band frequency provide coverage at a high spatial resolution except in precipitating atmospheres and with ice discrimination capability although the accuracy of SAR sea ice concentration is still an active field of research and ice-water discrimination still can be challenging under certain conditions (e.g., Karvonen, 2014). However, due to the characteristics of the Sentinel-1 missions with limited swath coverage, sub-daily revisit and coverage is not presently available. In contrast, wide-swath microwave imaging multi-spectral radiometers uniquely observe a wide range of parameters, including Sea Ice Concentration and Sea Surface Temperature that serve operational systems in non-precipitating atmospheric conditions, day, and night [AD-2], with excellent revisit and coverage characteristics.

2.4.1 Sea Ice Concentration (Sea Ice Fraction)

Sea Ice Concentration (SIC, or sea ice surface fraction) is the most important parameter for operational navigation in sea-ice infested waters and for climate services [AD-2]. SIC describes the relative amount of area covered by ice, compared to a reference area. For example, SIC could describe how large a fraction of a 25.0 x 25.0 km area is covered by sea ice (typically expressed in %). Sea ice area (SIA) of a region, e.g., the complete Arctic, is calculated by multiplying SIC with the grid cell areas and integrating over the region.

Sea Ice Extent (SIE) and Sea Ice Area (SIA) are integrated quantities counting the total area covered by sea ice. SIE and SIA are computed from daily composited maps of SIC and have the unit km². SIE is typically mapped by taking any grid cell with a SIC of ≥15 % and labelling that cell as ice (typically expressed in km²). Compared to SIA, SIE is much less affected by systematic sea ice algorithm biases caused by sea ice emissivity anomalies during summer and winter. The uncertainty (systematic or random) at high SICs (due to uncertainty in sea-ice and snow emissivity and melt-ponds) ranges from 2-3% SIC in winter to, ~10-15% SIC in summer. This noise has little influence on SIE since the threshold for SIE is low (15%). It is common that datasets that compare well in terms of SIE, do less so in terms of SIA and SIC (because the thresholding of SIE removes a large part of the noise). However, SIE is affected by atmospheric noise and spatial resolution issues along the ice edge. SIE is more easily comparable to other sea ice information datasets (ice charts, SAR imagery...) because the measure is not linked to a specific SIC algorithm. On the other hand, SIE is grid cell size dependent (coarser grid resolutions will result in larger SIE because of the 15% SIC criterion for SIE), which can complicate comparisons. During summer a microwave radiometer will measure the sea ice surface fraction meaning that open melt ponds and leads in between the floes are measured as open water - even if melt ponds are located on top of the ice floe. This is an important consideration when using the data for computing the fluxes between the ocean and the atmosphere in ice covered waters during summer.

Microwave radiometer data are available at coarse resolution and are used to derive SIC, e.g., as available from CMEMs' catalogue (e.g., see <http://marine.copernicus.eu/>). The expected increase in operational model resolution and time availability of products from operational systems will require sub-daily observations and resolution < 10 km in the future. Synergy with Sentinel-1 SAR data would be useful particularly in the Marginal Ice Zone (MIZ). However, radar backscattering of sea ice is a highly non-linear process where surface features and roughness elements can totally dominate the total backscatter magnitude. Furthermore, SAR ice and water backscatter signatures are not unique which means that it is not possible to determine an unambiguous surface classification - especially at sub-pixel level.

[AD-1] states the requirement for SIC as follows:

THM	DOM	Parameter	AOI	Resolution	TOY	Frequency	Leadtime	TL	Unit	Range	Accuracy	I	S	C	P
SI	OC	Sea ice Fraction	0	T: 5km	0	6hr	n/a	2	0: [%]	[0,100]	5%	0	0	3	2
	CL		1	T: 10 km G: 1km	0	1dy	n/a	0	0: [%]	[0,100]	1%	0	2	2	2
	TR		0	T: 20m G: 2m	0	T: 1dy G: 12hr	24h	1	0: [%]	[0,100]	5%	1	2	2	2

Note the stringent delivery timeliness requirement of '2' (Nera Real Time 1-hour NRT1H defined as ≤1 hour of sensing. (0=non-time critical, 1=Near Real Time 6 hours (NRT6H) within 6 hours of sensing – which is different to the Near Real Time 3-hours (NRT3H) definition used by Copernicus).

[AD-2] states the prioritised operational requirement as:

Sea ice concentration	<p>Sea ice concentration is the most important variable for operational oceanography.</p> <ul style="list-style-type: none"> Passive Microwave products are currently assimilated in CMEM's operational systems. High resolution concentration from the manually derived ice charts. These products are mainly based on Sentinel-1 in Extra Wide Swath Dual polarisation but also on corresponding data from Copernicus Contributing Missions. 	<ul style="list-style-type: none"> The future availability of multifrequency microwave radiometry (AMSR-2) is uncertain and reason for concern. The future MWI in MetOp SG will eventually secure continuation of the SSMI(S) series of coarse resolution radiometry for climate monitoring, but will not fulfil the requirements for medium resolution (< 10 km). Reliable automated sea ice chart-like products that can be delivered in NRT for navigational aid and for high-resolution input to numerical forecasting models are needed. Such product will probably need a multisensor approach where SAR will be the core input in combination with PMW. 	<ul style="list-style-type: none"> Actual PMW data from CMEM's catalogue are available at coarse resolution. It will be likely that increase in resolution and time availability of products from operational systems will require sub-daily and resolution less than 10km in the future with at least a continuation of observations with a spatial resolution no less than those provided by the AMSR-2 instrument (threshold). Area: pan-Arctic, frequency: at least daily, threshold resolution < 10km. SAR requirements: Area: Pan Arctic; Frequency: At least daily or 2-4 times in key areas. Resolution: 20m or at least no less than those provided by Sentinel-1
-----------------------	--	---	---

[AD-2] states the prioritised climate requirement as:

Sea ice concentration	<p>Core resolution ~25km Resolution of 6km (12 km) are provided by AMSR (SSMI) products in case they use radiometric measurements in the 89 GHz (85 GHz) channels</p> <p>Sea ice concentration is the most important sea ice variable for climate studies as it provides the longest satellite time series available to assess the sea ice variability. It is also the parameter now predicted by all climate models and routinely assimilated in ocean and atmosphere reanalyses</p>	<p>MWI on MetOp SG will eventually secure continuation of the SSMI(S) serie, but will not fulfil a requirement for medium resolution (<10km) as currently available on AMSR-2. A continuation of AMSR-2 like sensor is highly uncertain.</p> <p>Accuracy in the small concentration range (MIZ and near the ice edge) should be improved by an order of magnitude. This will require in-situ infrastructure as well as space infrastructure.</p> <p>A PMW with <10km resolution could have been an important contribution for an high resolution concentration product for operational navigation. (See separate table for operational needs)</p>	<p>Area: Pan Arctic Frequency: At least daily Resolution: 25km with a goal of < 5km (depending on the channel used).</p>
-----------------------	---	---	---

[AD-4] states the climate requirement for SIC as:

Requirement	Type of requirement (observation/product)	Spatial resolution	Vertical resolution	Temporal resolution	Accuracy
Sea Ice Concentration	Observation	10 - 15 km	N/A	weekly	5%

SIC in sea ice charts is typically determined manually using either synthetic aperture radar (SAR) instruments providing high resolution estimates of SIC (e.g., *Grenfell et al.*, 1992) and/or polarised multi-spectral microwave radiometer measurements including different combinations of 6, 19, 37, 89 GHz frequencies depending on the algorithm used (e.g., *Comiso et al.*, 2003; *Spreen et al.*, 2008; *Ivanova et al.*, 2015). A critical aspect is to ensure spectral diversity with sensitivity to sea ice and open water (see Figure MRD-2.4.1.1) and high spatial resolution to determine the presence of sea ice.

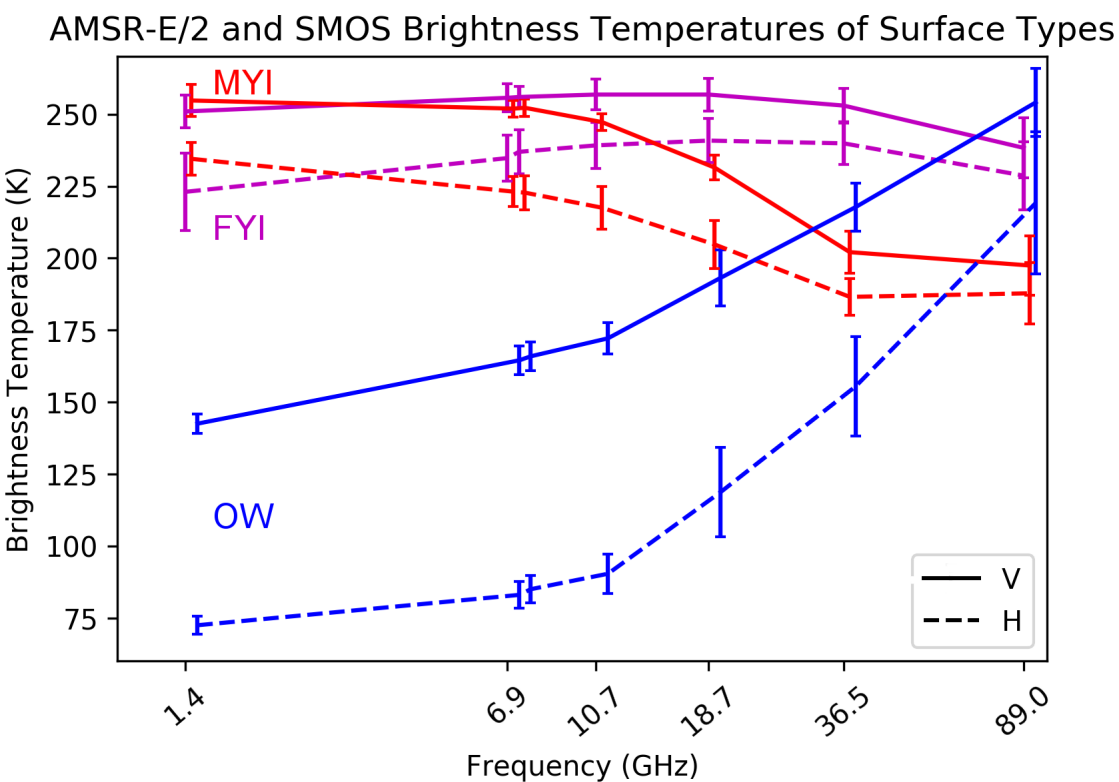


Figure MRD-2.4.1.1. Average top of atmosphere brightness temperatures (Tb) and standard deviations of Arctic open water, first-year and multiyear sea ice at typical imaging frequencies between L-band (1.4 GHz) and W-band (89 GHz). Data highlight the spectral separation of sea ice signatures in the 1.4-36.5 GHz region of the spectrum compared to 89 GHz. FYI= First Year Ice, MYI=Multi-year Ice, OW=Open Water. Solid lines indicate vertical polarisation, dashed lines indicate horizontal polarization. 1.4 GHz data from SMOS 40°-50° incidence angle averaged. Data based on Round Robin Data Package of ESA Sea Ice CCI project (Pedersen et al., 2018). See also Spreen et al. (2008) and Eppler et al. (1992) for a similar plot. (Lu, Junshen; Heygster, Georg (2018): AMSR-E/2 and SMOS Brightness Temperatures of Surface Types. figshare. Figure. <https://doi.org/10.6084/m9.figshare.7370261.v2>)

For climate data record (CDR) applications, channels near 19 and 37 GHz are used by the most widespread algorithms for SIC retrievals (e.g., Andersen et al., 2006; Lavergne et al., 2019) providing spectral diversity but at relatively poor spatial resolution. 19 and 37 GHz channels have been available from an unbroken series of satellites since the 1970's and they are therefore attractive for Climate Data Records (CDR). Some algorithms utilise 89 GHz frequency measurements (e.g., Spreen et al, 2008, see Figure MRD-2.4.1.1). While this channel provides a very attractive high spatial resolution (e.g., 3 x 5 km Instantaneous Field of View (IFOV) for AMSR-2) that reduces the sensitivity of algorithms to surface inhomogeneity, data are more sensitive to atmospheric emission and scattering effects. Consequently, a radiative transfer model and meteorological forecast model are required to compensate for these effects (e.g., Lu et al., 2018; Meier et al., 2017) significantly complicating the use of this channel. For example, the EUMETSAT OSISAF is using atmospheric correction both operationally and for CDR generation. This approach requires algorithm tie-points that are calibrated after the correction step and before the computation of the SIC (Tonboe et al., 2016; Lavergne et al., 2019). In general, while offering a high spatial resolution, the use of 89 GHz channels is considered more complex (it also requires accurate NWP data to compensate for atmospheric scattering). Should high spatial resolution channels at lower frequencies be available, a more robust approach would be possible.

Ivanova *et al.* (2015) present a review of SIC algorithms and performance noting that the best performing algorithm uses 6.9 GHz data of all available channels from historical and contemporary sensors (Figure MRD-2.4.1.2). At this frequency, the atmosphere has little impact (except in precipitating conditions) and there is a large diversity of spectral signature between ice and water (e.g., Eppler *et al.*, 1992 and shown in Figure MRD-2.4.1.1) which is a significant asset for SIC algorithms. However, this channel is severely limited in performance due to the large spatial resolution (e.g., AMSR-2 has a 64 x 32 km field of view at 6.9 GHz) that has been offered by all sensors to date (and those currently planned in the future). **Improving the spatial resolution of 6 GHz measurements could provide a significant improvement in SIC retrievals.** For tactical applications (e.g., ice breaking, navigation, maritime operations in the Arctic etc.) high-resolution microwave radiometry can be used in synergy with other data characterised by very high spatial resolution e.g., C-band SAR measurements (e.g., Karvonen, 2014; 2017) or satellite altimetry estimates of Sea Ice thickness if those missions have sufficient revisit and coverage.

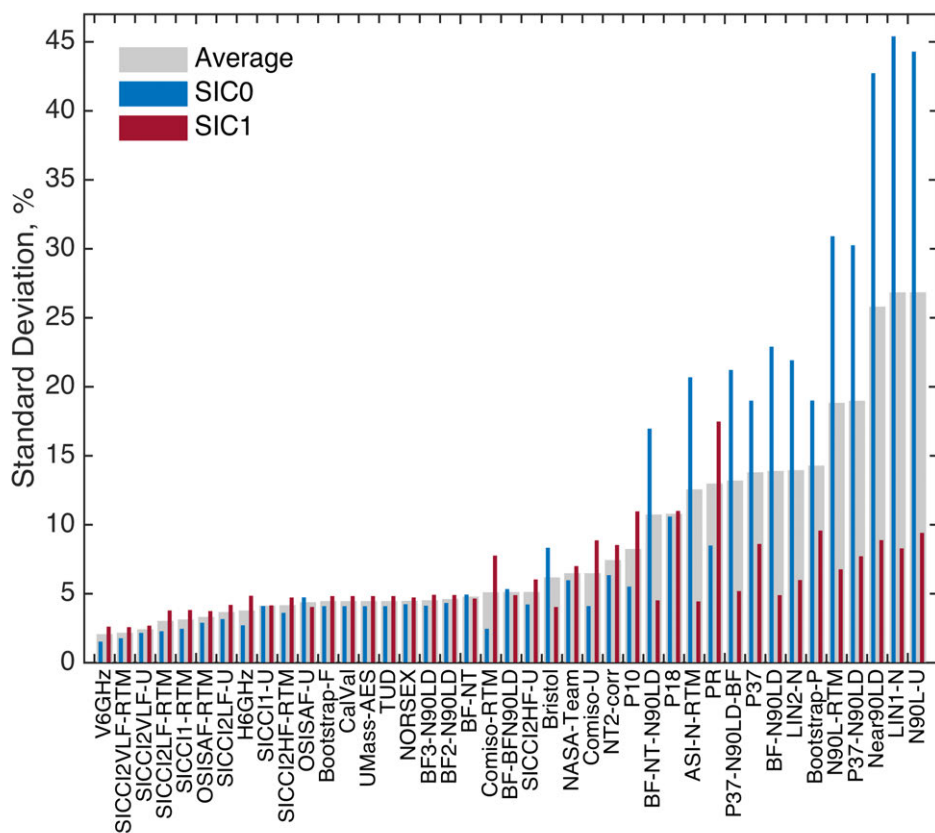


Figure MRD-2.4.1.2. Evaluation of 40+ Sea Ice Concentration algorithms against independent ground truth: ice charts for 0% ice (SIC0) and SAR-drift convergence areas for 100% ice (SIC1). The algorithms with best skills are to the left (low standard deviation, thus high accuracy). The best algorithms use 6GHz and/or optimized combinations of Ku and Ka-band. Results from the ESA CCI Sea Ice projects.

Importantly, current estimates of SIC that use 6-11 GHz channels within ~100 km of any shoreline or the marginal ice zone are not possible with the present and future microwave radiometer satellite mission's due to the large field of view being contaminated by land or ice. **This is a second important driver to significantly improve the spatial resolution of these channels.**

Radio Frequency Interference (RFI) must be detected and mitigated when using low frequency (i.e. L-, C- and X-band) channels in geophysical retrieval algorithms (e.g., *Maeda et al.*, 2011; *Soldo et al.*, 2017). However, this needs to be managed with care as it is known that mitigation will impact the NEΔT of each channel since spectral RFI filtering (where specific sub-bands are flagged as RFI contaminated and removed from the signal) results in a reduction in the available channel bandwidth. Other implications include discarding excessively polluted data or incorrectly flagged data. In the absence of atmospheric precipitation, microwave radiometer retrievals of SIC suffer from two discrepancies that are not resolved: (1) uncertainties in retrievals of the summer period caused by higher variability in sea ice emissivity due to the increase in surface wetness (snow melt) and presence of melt ponds of water (e.g., *Comiso and Kwok*, 1996). Virtually all SIC algorithms based on microwave radiometer channels are very sensitive to presence of melt water on the ice. Melt ponds may exhibit a diurnal cycle with interchanging periods of open water and thin ice. This further complicates SIC retrieval using satellite microwave radiometry during summer and increases the level of uncertainty (e.g., *Ivanova et al.*, 2015; *Kern et al.*, 2016). (2) There will most likely be some underestimation of the concentration of smooth thin ice because such a surface has lower emissivity at all frequencies. Thus, retrieved ice concentration is influenced by the thickness of thin sea ice (e.g., *Heygster et al.*, 2014).

Table MRD-1. MetOp-SG (B) MWI bands and AMSR-2 bands (shown in grey boxes) for comparison.
Application (SIC = Sea Ice Concentration, SST = Sea Surface Temperature, SIT = Sea Ice thickness, SSS= Sea Surface Salinity, WS = Wind speed, SD = Snow Depth, SM = Soil Moisture, SWE = Snow Water Equivalent, SID = Sea Ice Drift, PCP=precipitation, TCWV = Total Column Water Vapour, LWP = Liquid Water Path)

	MWI	AMSR-2	MWI	AMSR-2	MWI	AMSR-2	MWI	AMSR-2
Frequency [GHz]	18.7	18.7	23.8	23.8	31.4	36.5	89	89
Polarisation	Vertical and Horizontal							
Bandwidth [MHz]	200	200	400	400	200	1000	4000	3000
Swath width [km]	≥ 1400							
Footprint corresponding to -3dB beam width [km]	35 x 65	14 x 22	35 x 65	14 x 22	23 x 37	7 x 12	8 x 12	3 x 5
Observation Zenith Angle [deg]	53.0 [55.0 for AMSR-2]							
Radiometric resolution (NEΔT). Tref is: MWI 1σ at 280 K [K] AMSR-2 1σ at 150 K [K]	0.7	≤ 0.7	0.6	≤ 0.6	0.8	≤ 0.7	0.8	≤ 1.2
Applications	TCWV, LWP, PCP, SIC, SD, SM, SID		TCWV, LWP, PCP, SST, SIC, WS, SD, SM, SID		TCWV, LWP, PCP, SST, SIC, WS, SD, SM, SID		PCP, SIC, SD, SID, SM	

Additional co-located and near-contemporaneous measurements of thin sea ice thickness (e.g., from L-band radiometer measurements), thermal/visible optical, C/L-band SAR imagers, and scatterometer measurements can resolve melt water ponds to some extent and would help resolve these two issues. The combination of both active-microwave Sentinel-1 C-band SAR sea ice texture measurements (especially using vertical, horizontal and cross-polarisation) in synergy with microwave radiometry from AMSR-2 delivers a more reliable and accurate estimate of SIC (e.g., *Karvonen*, 2017). The resulting combined SIC estimates are “sharpened” and include many details not visible in the lower spatial resolution AMSR-2 products alone including much more detail at challenging boundaries such as the marginal ice zone.

SIC is required for the “Polar Regions” (encompassing the pan-Arctic domain ($>55^{\circ}\text{N}$, $0\text{-}360^{\circ}$ longitude), all adjacent Seas ($>55^{\circ}$ North latitude), and Antarctica ($>58^{\circ}\text{S}$, $0\text{-}360^{\circ}$ longitude)) with at least a daily revisit and an effective spatial resolution of 25 km (addressing climate aspects) with a goal resolution of ≤ 5 km and every 6 hours [AD-1] that is prioritised at “sub-daily” coverage in [AD-2] (addressing operational sea ice monitoring aspects) depending on the channels used [AD-2]. Accuracy in the small ice concentration range (Marginal Ice Zone and near the ice edge) should be improved by an order of magnitude [AD-2].

While the Microwave Imager (MWI) on the MetOp-SG(B) satellite will eventually secure continuation of the Special Sensor Microwave Imager (SSM/I) series, it **will not fulfil** the requirement for medium resolution (<10 km) measurements as currently available on AMSR-2 [AD-2] – see Table MRD-1. **A continuation of multi-spectral microwave radiometer measurements with a high spatial resolution (no less than those provided by the AMSR-2 instrument) is requested in [AD-2].**

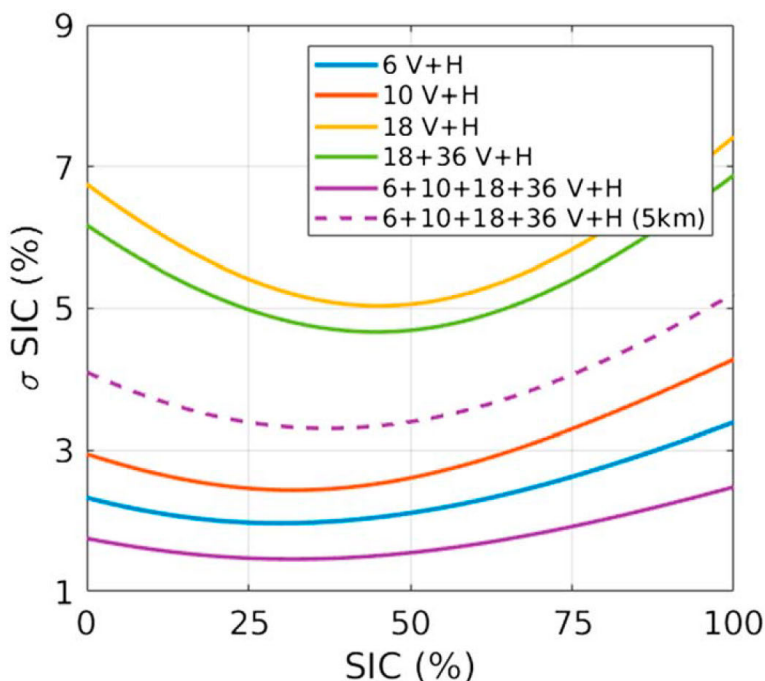


Figure MRD-2.4.1.3. Theoretical retrieval error standard deviation on SIC from the information content analysis with different combinations of Copernicus Imaging Microwave Radiometer channels. SIC = sea ice concentration (Kilic et al., 2018).

Kilic et al. (2018) estimate the SIC performance for a CIMR radiometer using the same specifications as set out in this MRD. An information content analysis approach was used to estimate theoretical retrieval uncertainties for SIC. Figure MRD-2.4.1.3 shows the SIC retrieval error standard deviation as a function of SIC, first for each frequency, using both vertical and horizontal polarizations. The calculations use the winter part of the ESA Sea Ice Climate Change Project Round Robin data set, as is usually done for model developments. The combined use of the 6.9-, 10.65-, 18.7-, and 36.5-GHz channels together improves the retrieval, with a SIC theoretical retrieval error standard deviation between 2% and 3%. A 5 km multi-channel retrieval is shown which will be refined in the future.

The CIMR Mission Requirement Consolidation (CIMR MRC) team studied a prototype L2 SIC algorithm baseline, and looked at the effect of using low-frequency channels (C- and X-band) on the accuracy and spatial resolution of a future L2 SIC product (Figure MRD-2.4.1.4). Algorithms

combining only Ku- and Ka-band Tb channels with explicit correction of atmospheric correction with a Radiative Transfer Model (RTM) where found to provide the best compromise between uncertainty and spatial resolution. See *Lavergne et al.* (2020) for a full description. Figure MRD-2.4.1.5 shows a simulation of the sea-ice edge/extent (SIC = 15%) obtained for CIMR.

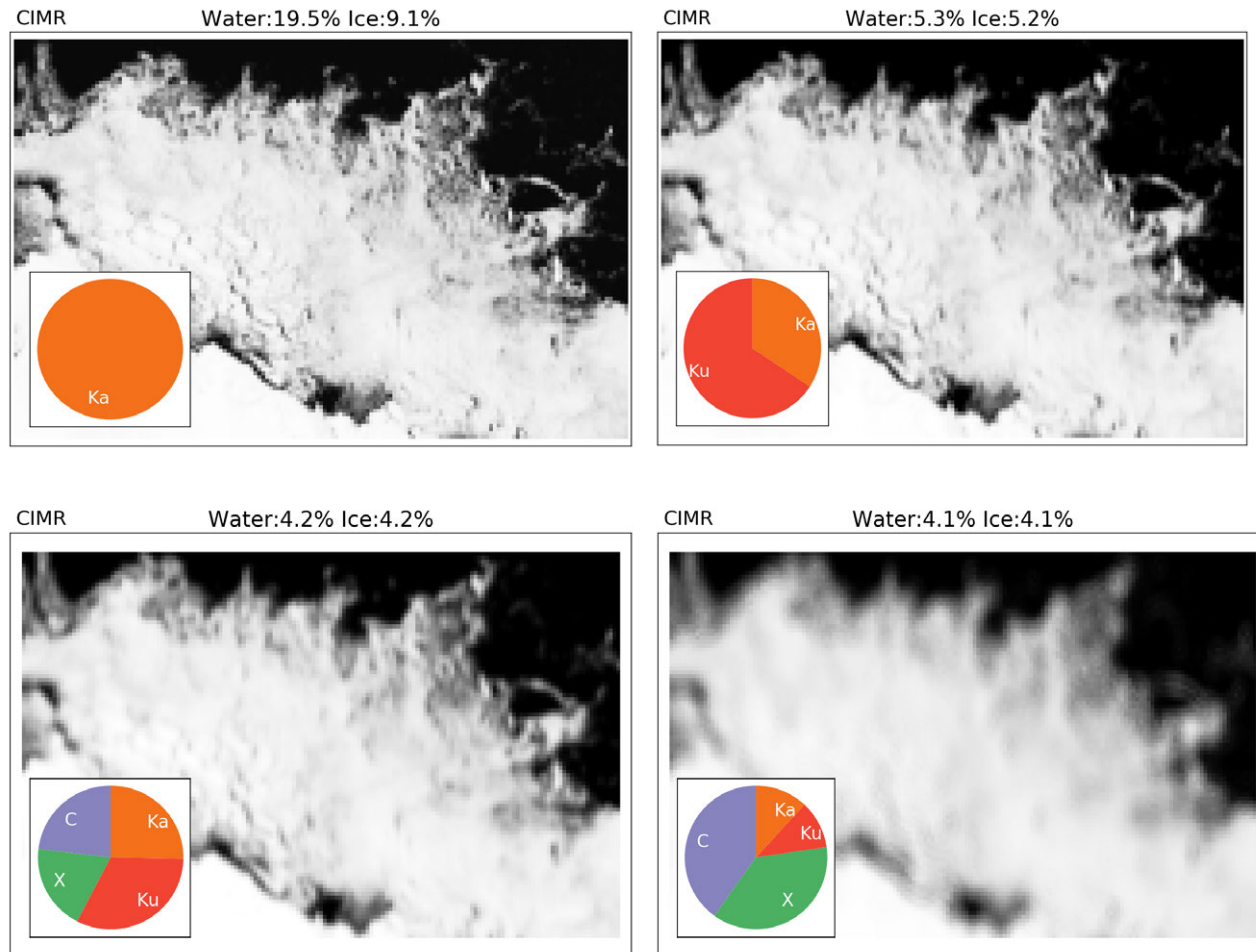


Figure MRD-2.4.1.4: Simulation of four SIC algorithms: top-row two algorithms using only Ku- and Ka-bands, bottom row two algorithms using all CIMR bands (but L-band). The inlet pie-chart represents the relative weight of each channel into the algorithm. The percent values are simulated standard deviation of algorithm uncertainty over 0% SIC (Water) and 100% SIC (Ice) without explicit atmospheric correction. Note that many more algorithms using the C-, X-, Ku-, and Ka-band channels can be devised that achieve lower uncertainties (often at the cost of coarser spatial resolution).

Another study proposed a new SIC algorithm called Ice Concentration REtrieval from the Analysis of Microwaves (IceCREAM) (*Kilic et al.*, 2020; *Prigent et al.*, 2020), specifically designed to exploit the multi-frequency capability of CIMR, from 6 to 36 GHz. It is based on an optimal estimation and a scheme to benefit from the low errors of the low frequencies and the high spatial resolutions of the high frequencies. It is globally applicable, without fine-tuning or further weather filtering, with a systematic use of all channels from 6 to 36 GHz making it robust to changes in ice surface conditions and to weather interactions.

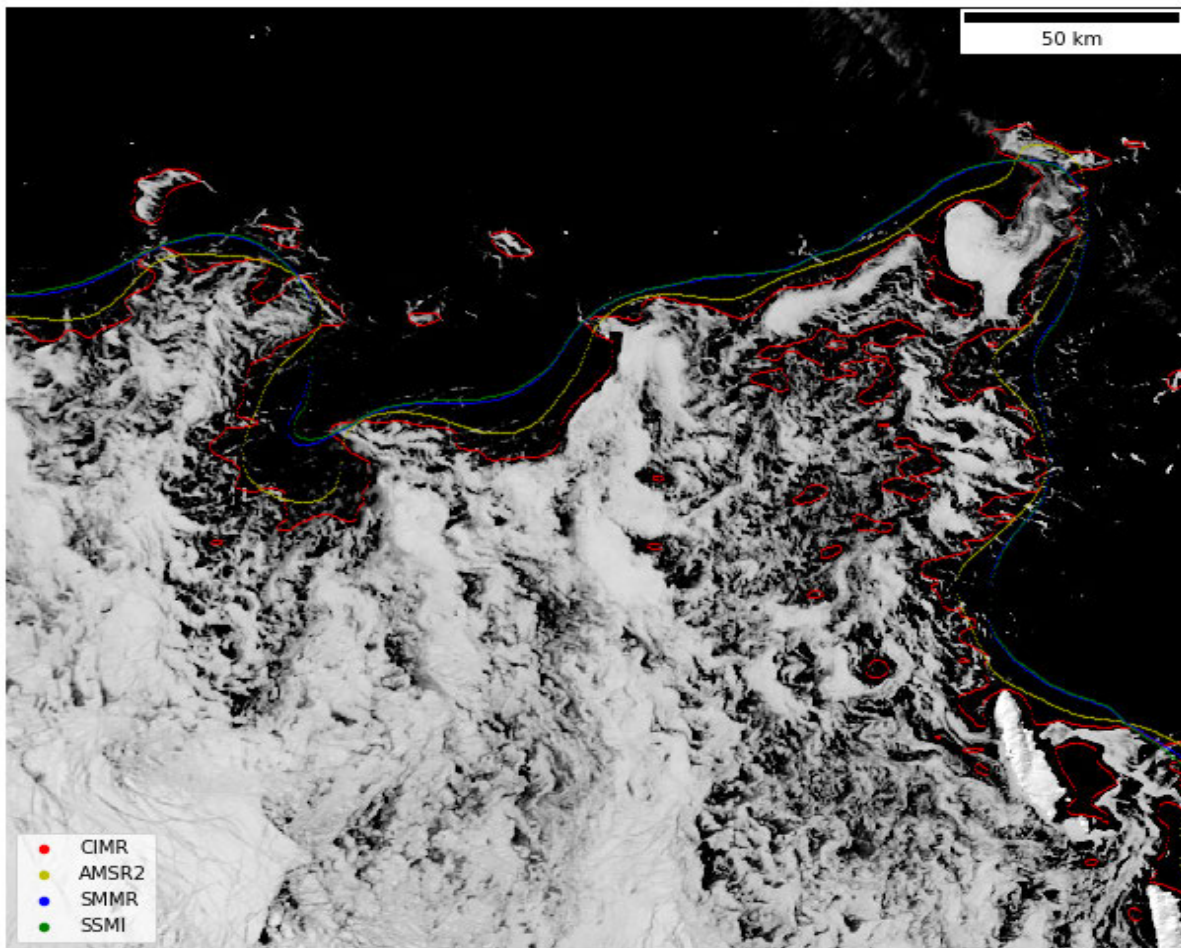


Figure MRD-2.4.1.5. Simulation of the sea-ice edge/extent (SIC = 15%) obtained for CIMR, AMSR2, SMMR, and SSM/I missions using a typical algorithm combining Ku- and Ka-band channels. CIMR offers many more details and follows the “true ice edge” (here based on a MODIS image) more closely. Credit: R. Tonboe (DMI).

2.4.2 Sea Surface Temperature (SST)

SST in non-precipitating atmospheric conditions (e.g., *Chelton et al.*, 2005; *Donlon et al.*, 2012) is **one of the top priorities in [AD-1] and the fourth priority in [AD-2]**. SST in non-precipitating atmospheric conditions is required [AD-2] for climate modelling, mesoscale analysis, oceanic predictions and as climate change indicator [AD-1]. Sub-daily sampling to sample diurnal cycle (e.g., *Donlon et al.*, 2009) is requested [AD-2]. Microwave radiometer SST observations are very important in the global ocean as well as in polar-regions [AD-3] and these data are assimilated in oceanic and meteorological forecast systems [AD-2]. From the merging of Sea Surface Temperature and altimetry data improved global surface currents can be derived. It has been shown that the level of accuracy obtained by combining altimeter velocities based on a two-satellite configuration and microwave SST data is equivalent or higher to the one from a four-altimeter constellation in western boundary currents (*Rio et al.* 2018).

[AD-1] states the requirement as follows:

THM	DOM	Parameter	AOI	Resolution	TOY	Frequency	Leadtime	TL	Unit	Range	Accuracy	I	S	C	P
OC	CL	SST		T: 10km G: 1km	0		n/a	0	0 : [°K]	[271,283]	0.1K	1		2	
OC	OC			0	T: 5km	0	6hr	n/a	1	0 : [°K]		0	2	1	

SST accuracy of 0.1 K at a spatial resolution of 1 km is an extremely demanding target even for the best available mercury cadmium telluride (HgCdTe) cryo-cooled detectors in the infrared. To reach an SST accuracy of 0.1 K using a microwave radiometer at 1 km spatial resolution with current (2019) technology (even using an extremely large antenna) and the best on-board calibration systems available today is considered unfeasible.

[AD-2] states the prioritised operational requirement as:

All weather SST	SST is a key variable for short term forecasts but also seasonal forecast applications. These data also are likely the oldest variables being assimilated in oceanic systems. Global daily ocean SST (L4) from Pathfinder AVHRR and (A)ASTR instrument is a CMEMS' product given at 1/20° horizontal resolution (~5km) in NRT and presently assimilated. Ice surface temperature (IST) is a CMEMS' product .	MWI also lack the necessary frequencies to measure all weather SST. A potential future C-band microwave radiometer (EE-10 suggestion) could fulfil the SST requirements, but resolution better than 5km at frequencies below 40 GHz is not foreseen and still will be needed. Other Status of Pathfinder instruments ? There is a gap in operational Sentinel-3 products where no SLSTR IST product is foreseen over sea ice.	A continuity is at least required. Infrared ice surface temperature is also required. Area : Pan-Arctic Frequency: At least daily; Sub-daily sampling shall be monitored to sample diurnal cycle. Resolution: for gridded data : < 5km
-----------------	--	---	---

[AD-2] states the prioritised climate requirement as:

All weather SST/IST	All weather SST/IST are available at low resolution based on PMW . High resolution, weather dependent IR products are available at 1 km resolution	High resolution (1 km) IST are useful to estimate heat transfer through sea ice and sea ice growth rates but are hardly available in cloudy high latitudes.	Continuity of the PMW retrieved SST/IST is required together with high resolution weather dependent SST/IST as this parameter is crucial for climate studies and model validation
---------------------	--	---	---

[AD-4] states the climate requirement as:

Requirement	Type of requirement (observation/product)	Spatial resolution	Vertical resolution	Temporal resolution	Accuracy
Sea Surface Temperature	Observation	1-10 km	N/A	24 h	0.1 K over 100 km scale

The subskin temperature of the sea surface (SSTsubskin) represents the temperature at the base of the thermally conductive laminar sub-layer of the ocean surface (see *Donlon et al.*, 2009). For practical purposes, SSTsubskin can be well approximated to the measurement of surface temperature by a microwave radiometer operating in the 6-11 GHz frequency range (see *Wentz*, 1997; *Wentz and Meissner*, 2000; 2006; 2016) but the relationship is indirect and is not invariant to changing physical conditions or to the specific geometry of the microwave measurements.

However, 6.9-10.6 GHz channels are severely limited in performance due to the large spatial resolution that has been offered by all sensors to date (and those currently planned in the future). Improving the spatial resolution of polarised measurements at 6-10 GHz could provide a significant improvement in SST retrievals and their information content for global SST and regional analysis systems. An improvement in real-aperture spatial resolution is important because this means that CIMR data could be included in the SST analyses of semi-enclosed seas (e.g., Mediterranean, Baltic) and monitor the coastal regions – which is currently not possible using existing microwave imagers.

An accurate SST retrieval (e.g., *Gentemann et al.*, 2010) requires an estimate of sea surface emissivity that depends on wind-induced surface ocean roughness (e.g., *Meissner and Wentz*,

2002; 2012) that can be derived from microwave radiometer observations at 10 to 36 GHz (*Prigent et al.*, 2013, *Kilic et al.*, 2018) or scatterometer measurement of sigma-zero (e.g., from MetOp-SG B). A second order correction for a weak SST dependency on C-band and X-band Tb used in sea surface salinity (SSS) and a second order SST dependence in the wind emissivity needs to be included (e.g., *Meissner and Wentz*, 2002; 2012). When rain is not present, attenuation by the atmosphere is very small at 6-11 GHz, with 97% of the radiation emitted at the sea surface reaching the top of the atmosphere. Using channels at 6.9 to 37 GHz, the *Wentz et al.* (2000) SST retrieval algorithm precisely estimates the 3% attenuation due to oxygen, water vapour, and clouds. A full radiative transfer model can be used with microwave radiometer observations to estimate the surface roughness. In addition, the polarization ratio (horizontal versus vertical) of the measurements can be used to estimate sea surface roughness to first order (a better solution would utilise more direct surface roughness measurements such as those from scatterometry). The spatial resolution of the SST retrieval is limited by the ratio of the radiation wavelength to the antenna diameter and by the satellite altitude (*Wentz et al.*, 2000) and hence a large antenna is required to have a high spatial resolution: for a resolution of ~10 km at X-band an antenna of >6m is required).

Recently a detailed analysis of optimal channels for SST retrievals using AMSR-2 data has been performed (*Pearson et al.*, 2018). This suggests that an optimal combination of five channels (6.9V, 6.9H, 7.3V, 10.7V and 36.5H) yields the best SST retrieval using their optimal estimation retrieval framework. The 36.5 H measurements provide information on the total column water vapour content while the others account for SST, and the effect of surface roughness and SSS within the retrieval framework. However, the *Wentz et al.* (2000) forward model shows significantly different Tb/emissivity dependencies with respect to salinity and wind speed. In addition, regression models show larger retrieval errors, using these channels only, compared to using all channels and further optimisation studies are required.

Currently, estimates of SST within 100 km of any shoreline or the marginal ice zone are not possible with the present and future microwave radiometer satellite mission's due to the large field of view (e.g., AMSR-2 has a 64 x 32 km field of view at 6.925 GHz) being contaminated by land or ice. **Significant improvement in the spatial resolution of these channels is required to obtain SST to within ~15 km of these transitions.**

Radio Frequency Interference (RFI) must be mitigated when using low frequency (i.e. L-, C- and X-band) channels in geophysical retrieval algorithms (e.g., *Maeda et al.*, 2011; *Soldo et al.*, 2017). *Nielsen et al.* (2018), show that an Optimal Estimation retrieval is very efficient to filter out RFI effects in C and X band channels.

MetOp-SG(A) METimage is a multi-spectral (visible and IR) imaging passive radiometer which will provide detailed information on clouds, wind, aerosols and surface properties which are essential for meteorological and climate applications. METimage will provide continuity to the AVHRR (Advanced Very High-Resolution Radiometer) series on board the MetOp and NOAA satellites, and VIIRS on board NOAA satellites. METimage is expected to have a great improvement with respect to AVHRR and comparable performance with respect to VIIRS. The primary objective of the mission is to provide high quality imagery data for global and regional Numerical Weather Prediction, nowcasting, and climate monitoring through the provision of:

- High horizontal resolution cloud products including microphysical analysis
- Sea surface temperature
- Vegetation, snow coverage, and fire monitoring products
- Aerosol products
- Polar atmospheric motion vectors

Compared to its predecessor AVHRR, METimage will have many more channels for the benefit of measuring far more geophysical variables. This combined with on-board radiometric calibration of

solar channels and the enhanced spatial sampling (500 m compared to 1 km at nadir) will provide a breakthrough in several application areas: numerical weather forecast, very short-range forecast and now-casting, oceanography, hydrology, land-surface applications, and climate monitoring. The imaging radiometer measures the thermal radiance emitted by the earth and solar backscattered radiation. It, thus, covers a broad spectral range in 20 spectral bands from 443 to 13.345 μm . Due to the presence of clouds preventing measurements of the Earth surface using these bands, MetImage alone cannot meet the needs of CMEMS.

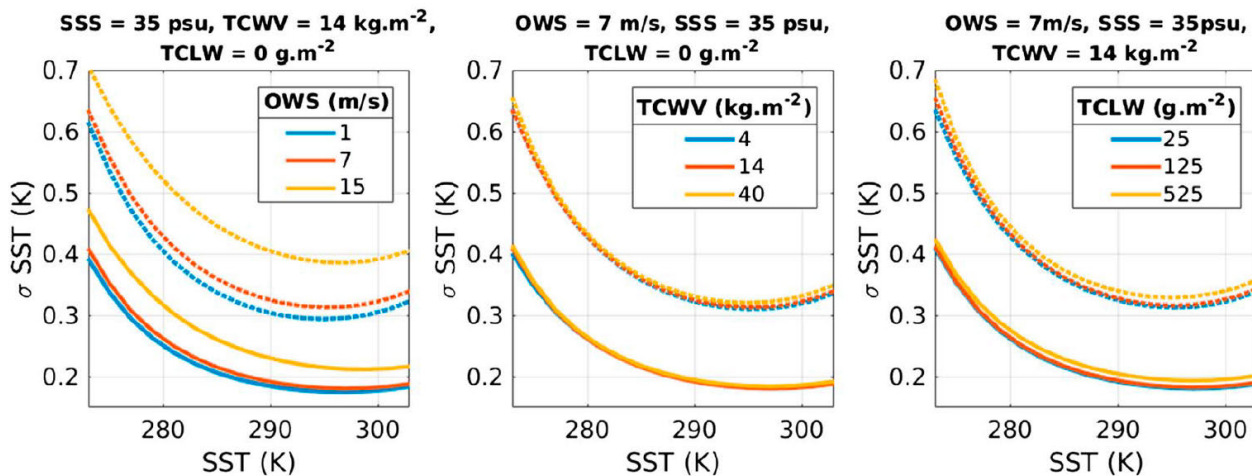


Figure MRD-2.4.2.1. The SST theoretical retrieval error standard deviation estimated with the Copernicus Imaging Microwave Radiometer specifications (solid lines) and the Advanced Microwave Scanning Radiometer 2 specifications (dotted lines) for different OWSs (left), TCWVs (middle), and TCLWs (right). SST = sea surface temperature; OWS = ocean wind speed; SSS = sea surface salinity; TCWV = Total Column Water Vapor; TCLW = Total Column Liquid Water (from Kilic et al., 2019).

The MWI on the MetOp-SG(B) satellite will not fulfil the requirement for medium resolution (<10 km) SST measurements as currently available on AMSR-2 [AD-2] because the low-frequency 6.9–10 GHz channels required for SST retrieval are not included in the instrument design – see Table MRD-1. Furthermore, a significant gap exists in continuity of 6–7 GHz channels beyond 2021/22 (see Section 5.1.1). Continuity of SST in non-precipitating atmospheric conditions is at least required (i.e. that derived from AMSR-2) [AD-1] with at least a daily revisit and a spatial resolution of 10 km [AD-2]. Ideally to address emerging CMEMS needs, a spatial resolution of ~5 km is required.

Building on the previous work of Prigent et al. (2013) and as part of CIMR science support studies based on information content analysis, Kilic et al. (2018) derive a mean global SST uncertainty of ~0.2 K (the retrieval uncertainty varies between 0.15 and 0.45 K with higher uncertainty in cold waters) using the CIMR channel specifications set out in this MRD. Figure MRD-2.4.2.1 shows a comparison for theoretically retrieved SST using the CIMR channel specifications set out in this MRD compared to those of AMSR2. The impact of CIMR on SST performance is obvious. While very challenging it is clear that an uncertainty of ~0.2 K is considered feasible² for a spatial resolution of ~15 km in warmer waters and ~0.3 K in colder waters. The same SST retrieval has been tested, within the CIMR End-to-End simulator and showed that CIMR can provide SST (as well as SSS, and OWS) with precisions and spatial resolutions conforming with the mission requirements (Jimenez et al., 2021). See Figure 2.4.2.2.

² Calculated for a theoretical retrieval as the mode value of daily global ocean average discrepancies assuming no uncertainty in the validation data set.

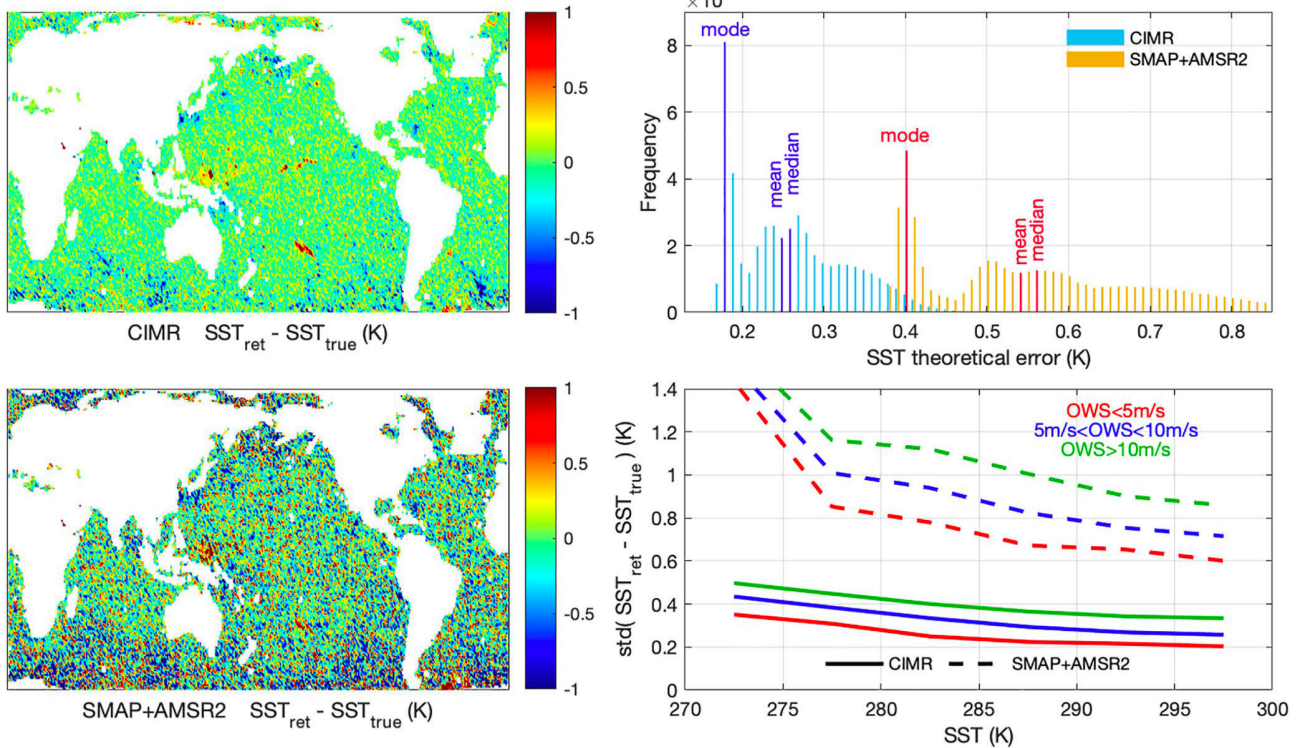


Figure 2.4.2.2 : SST retrieval performance from CIMR and an imaginary instrument simulated by adopting SMAP and AMSR2 main technical characteristics. Plotted the differences between the retrieved and true SST (SST_{true}) for the simulated scene (top-left for CIMR, top-bottom for SMAP + AMSR2), histograms of the theoretical error associated with the retrievals (top-right), and standard deviation of the retrieved and true SST differences for several SST and ocean wind speed conditions (bottom-right). From Jimenez et al. (2021).

2.4.3 Sea Ice Thickness (SIT)

Sea Ice Thickness (units of meters) is the thickness of a sea ice layer measured from sea ice surface to the underside of a specified sea ice extent. For ice $>\sim 1$ m thick, SIT is typically and successfully measured using satellite altimeters (e.g., Guerreiro et al., 2017; Laxon et al., 2013). For thin SIT, microwave radiometry provides a useful complement (e.g., Heygster et al., 2014; Kaleschke et al., 2010, 2016). **Sea ice modellers** (e.g., Sakov et al., 2012) and **operational ice services** (WMO, 2017) **consistently rank improved measurement of sea ice thickness distribution as their top priority [AD-1]**.

Assimilation of thin (<0.5 m) sea ice thickness data derived from L-band (1.4 GHz) satellite missions into dynamic sea ice models results in more accurate forecasts (e.g., Xie et al., 2016; Richter et al., 2018; Tietsche et al., 2017) [AD-2]. However, a high spatial resolution thin sea ice thickness product for navigation purposes does not exist for the Arctic Ocean [AD-2]. The complete daily coverage and the near real-time availability of thin sea ice thickness data are crucial for operational applications [AD-1]. Following the highly successful suite of measurements from the ESA Soil Moisture and Ocean Salinity (SMOS) and United States Soil Moisture Active/Passive (SMAP) missions from which thin sea ice thickness is currently derived (see Patilea et al. (2017) for combined SMAP/SMOS SIT retrievals) it is important to secure continuity of L-band measurements in an operational context. Techniques exist that use thermal optical imager data (e.g., Maekynen et al., 2013) although this is confounded by the presence of clouds.

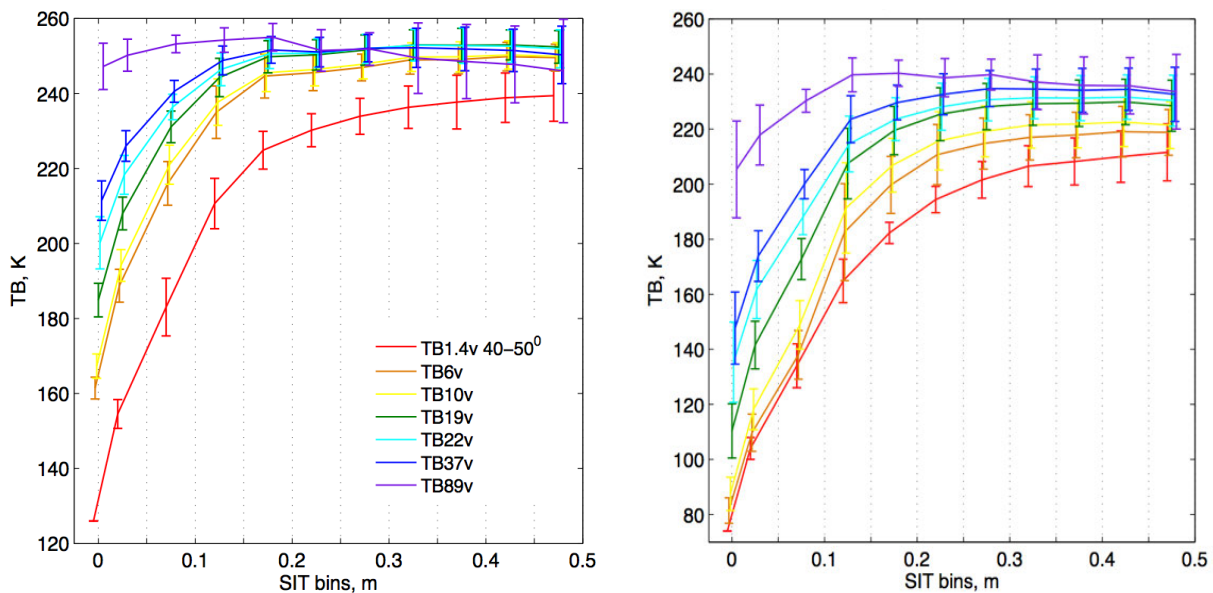


Figure MRD-2.4.3.1. Vertically (left), horizontally (right) polarized brightness temperatures as function of sea ice thickness for various frequencies (from Heygster et al., 2014). The best performing frequency for thin sea ice determination is 1.4 GHz.

The CMEMS position paper presented at the “Polar and Snow Cover Applications – User Requirements Workshop” for future Sentinels (23 June 2016, Brussels) states [AD-1]: “Sea ice thickness is a very important indicator of climate change in the Arctic. In view of the uncertainty in the freeboard to sea ice thickness inversion, a CryoSat type mission is an attractive option, preferably in combination with a laser altimeter. However, for operational sea ice monitoring, input to sea ice models and sea ice charting, satellite measurements of the thin sea ice below 0.5 m (i.e. L-band microwave radiometry) is also required.” [AD-1].

For thin sea ice (<0.5 m thick) microwave radiometry operating at 1.4 GHz frequencies provides a viable solution as shown in Figure MRD-2.4.3.1 (e.g., Grenfell et al. (1992, 1998); Heygster et al. 2014; Naoki et al. 2008; Kaleschke et al. 2010, Kaleschke et al. 2016). In addition, Johnson et al. (2021) and Andrews et al. (2022) recently explored the 500-2000 MHz RFI environment and potential of wideband radiometry using airborne instruments, concluding that wideband radiometry from 500 to 2000 MHz is viable for a broad range of science applications in the majority of the regions surveyed. Additional channels within this bandwidth may improve tSIT retrieval performance. Note that 6.9 GHz vertically polarised measurements can determine SIT up to a thickness of ~20 cm whereas 1.4 GHz measurements are able to determine thin SIT up to a depth of ~0.5 m (e.g., Naoki et al. 2008).

[AD-1] states the requirement as follows:

THM	DOM	Parameter	AOI	Resolution	TOY	Frequency	Leadtime	TL	Unit	Range	Accuracy	I	S	C	P
SI	CL	Thin sea ice	1	T: 10km G: 1km	0	1dy	n/a	0	0: [m]	[0, 0.5]	5%	1	2		2
SI	OC		0	T: 5km	0	T: 6hr	n/a	2	0: [%]	[0,100]	5%	0	0	2	2
SI	TR		0	T: 20m G: 2m	0	T: 2d G: 1d	24h	1	0: [m]	[0, 0.3]	T: 0.03 G: 0.01	0	1		1

The spatial resolution requirement of 10 km cannot be met for thin SIT above ~20 cm thick using available L-band microwave radiometer technologies. Note the stringent delivery timeliness requirement of ‘2’ NRT1H.

[AD-2] states the operational requirement as:

Sea ice thickness (freeboard) (including summer ice and thin ice)	Pan-Arctic data does not exist presently in the CMEM's catalogue. Assimilation of sea ice thickness data (SMOS-like one) is underway in operational systems. High resolution product for navigation purposes does not exist for the Arctic Ocean.	A need to solve the knowledge gap in snow depth estimation over sea ice. For operational navigation purposes it is difficult to utilize Cryosat data due to its temporal and spatial resolution and too large uncertainty. It is noted that the spatial and temporal resolution requirements needed may not be achievable with today's technology. However, some studies have shown a potential of using ice type as a proxy to derive ice thickness. This will need to be investigated further. Requirements related to ice type are included below.	Area: Pan Arctic Temporal resolution: 1 day (G), 2 days (T) Coverage: pan-arctic Spatial resolution: 20m (G), 80m (T)
---	--	---	--

[AD-2] states the climate requirement as:

ice thickness (freeboard) (including summer ice and thin ice)	Cryosat-2 for thick ice (medium resolution, 25 km ?) and SMOS estimates of thin (<0.5 -1 m) sea ice	Cryosat estimates are too uncertain in the melt season (due to melt pond effects). Complete coverage of the Arctic is only available at the expense of the time resolution (monthly means). SMOS estimates are limited to small thickness ranges (< 1 m). Revisit and resolution should be similar as described by the climate community. Uncertainty due to snow cover in CS2 ice thickness estimates must be reduced	The threshold requirements in terms of revisit, coverage and precision are the same as those specified for Cryosat-2. The goal requirements would also include to extend temporal coverage over the melt season, to reduce uncertainties due to snow loading and ice density by a TBC amount, and to be able to measure over the entire range of ice thicknesses.
---	---	---	---

[AD-4] states the climate requirement as:

Requirement	Type of requirement (observation/product)	Spatial resolution	Vertical resolution	Temporal resolution	Accuracy
Sea Ice Thickness	Observation	25 km	N/A	monthly	0.1 m

Note that in [AD-2] Table 2 notes that a secondary mission objective for the microwave radiometer is “Topography”. Clearly a microwave radiometer cannot make “Sea ice topography” measurements and this entry is considered a direct reference to “thin sea ice thickness” typically derived from a 1.4135 GHz channel. Such a capability complements the proposed topography SARIn altimeter mission measurements of sea ice freeboard because an altimeter is unable to provide meaningful ice thickness measurements much below 1 m. Furthermore, the CIMR mission will provide complementary information on snow loading (“snow depth on sea ice”) to assist the topography mission measurement of sea ice thickness derived from sea ice freeboard estimates. In this sense CIMR and the proposed Topography mission are highly complementary. **Continuity of thin (<0.5 m depth) sea ice measurements using L-band microwave radiometry with daily coverage of the Marginal Ice Zone in the pan-Arctic and adjacent Seas (>55° North latitude), and Antarctica regions is requested [AD-1][AD-2][AD-3].** Kaleschke et al (2016) note that an uncertainty of <30% is possible based on SMOS tSIT measurements although validation remains a challenge using aircraft and in situ data sets. Figure 2.4.3.2 highlights the significant decreasing trend of tSIT in the Arctic Ocean based on ESA SMOS L-band measurements highlighting the importance of maintaining a long time series of measurements at L-band. CIMR is the currently the only satellite mission that proposes L-band microwave radiometer measurements in an operational context.

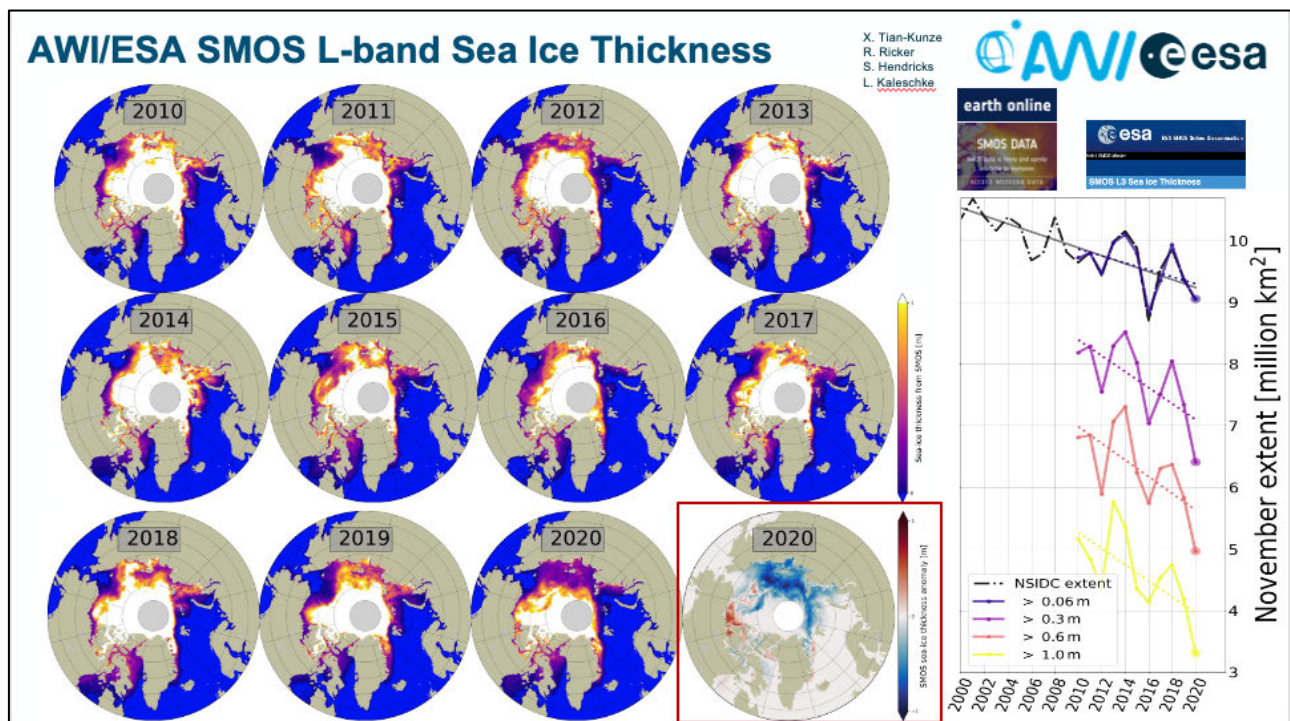


Figure MRD-2.4.3.2. (Left) maps of Thin Sea Ice Thickness (tSIT) in the Arctic 2010–2020 derived from the SMOS mission. The last panel shows the tSIT anomaly for 2022. (Right) comparison of SMOS data at different tSIT with NSIDC reference sea ice extent. (Credit: L. Kaleschke, AWI). CIMR will provide baseline continuity to L-band measurements but with the additional benefit of multi-frequency measurements (particularly in C-band) that could enhance tSIT monitoring).

2.4.4 Sea Ice Drift

Sea ice drift measures the displacement of sea ice for a given location and time period. It does not describe the trajectory of ice within the measurement period. Sea ice drift has been derived from optical imagery, synthetic aperture radar imagers, hi-resolution multi-frequency microwave radiometry and scatterometry based on feature recognition and maximum cross-correlation techniques (e.g., *Emery et al.*, 1997; *Girard-Ardhuin et al.*, 2012; *Heil et al.*, 2006; *Kwok et al.*, 1998). Sea ice drift products are available from CMEMS catalogue (<http://marine.copernicus.eu>) and from the EUMETSAT Ocean and Sea Ice Satellite Applications Facility (OSI-SAF) at coarse resolution and currently use a number of dedicated channels including AMSR-2 36.5 GHz and SSMI/S at 91.0 GHz (e.g., *Lavergne et al.*, 2010; 2016a; 2016b). Note that other channels (e.g., 6.9–18.7 GHz) provide better spectral diversity and could potentially provide a better SID result if the spatial resolution is significantly improved. 18.7 GHz AMSR-2 (14 x 22 km spatial resolution) data are being used to provide 2-day global sea ice drift estimates during summer, but much better spatial resolution / spectral feature resolution is required (≤ 5 km). The CMEMS Arctic Modelling and Forecast Centre (MFC) is assimilating sea ice drift and products are available from CMEMS catalogue at coarse resolution. Summer sea ice drift is also derived from Sentinel-1 SAR data, but daily full coverage in the Polar Regions cannot be reached using this approach alone: an optimal combination is the use of SAR and microwave radiometry in synergy.

The resolution of gridded sea ice drift products is currently poor, and products deteriorate near the ice edge or in summer [AD-2]. To better constrain the high sea ice drift variability and better understand its response to high frequency forcing (tides, wind), an increase of the spatial resolution and frequency of the currently available data is required [AD-1]. Results from a recent ESA CCI Sea Ice algorithm study indicate that the accuracy of sea ice drift products from

microwave radiometer imagery are mainly influenced by 1) the resolution of the instrument, 2) the presence of stable sea ice emissivity patterns to be tracked between images, 3) the geo-location accuracy, and 4) a see-through atmosphere. Accuracy targets of sea ice drift products put additional requirement on the spatial resolution, but also geo-location accuracy. The lower frequencies (C and X) might not have stable enough emissivity patterns to be tracked compared to those at Ku and Ka band. Near-90 GHz channels suffers from the complicating effect of atmospheric absorption and scattering that must be corrected.

Sea ice drift products are required with daily coverage in the pan-Arctic and adjacent Seas (>58° North latitude), and Antarctica regions and a spatial resolution of 10 km [AD-2].

[AD-2] states the prioritised operational requirement as:

Sea Ice drift	<p>CMEMS' operational systems assimilate pan-Arctic coarse resolution (60km) and 3 day-lag datasets.</p> <p>Currently CMEMS provide a pan Arctic high resolution ice drift product based on Sentinel-1 data in HH polarisation that meets the current high-priority requirements.</p>	<p>It will be likely that increase in resolution and time availability of products from operational systems will require higher resolution and frequency.</p> <p>Higher resolution could be used to increase the drift resolution.</p> <p>For planning of a next generation of S1 this should be taken into consideration.</p>	<p>Coverage: Pan Arctic</p> <p>Temporal resolution: At least daily</p> <p>Spatial resolution: Corresponding to Sentinel-1</p>
---------------	---	--	---

[AD-2] states the prioritised climate requirement as:

Sea Ice drift	<p>Pan-Arctic coarse resolution (25-60 km) (combination of active and passive sensors) gridded datasets. High resolution lagrangian products deduced from processed SAR images (ex : RADARSAT GPS) are also extremely useful for process studies on sea ice mechanics as well as validation of drift/deformation fields produced by sea ice models</p>	<p>Resolution of gridded products is too low. Products deteriorate near the ice edge or in summer. SAR data do not provide global coverage : improve on the use of these data.</p>	<p>Area: Pan Arctic</p> <p>Frequency: daily</p> <p>Resolution: 10 km, as for SIC</p>
---------------	--	--	--

[AD-4] states the climate requirement as:

Requirement	Type of requirement (observation/product)	Spatial resolution	Vertical resolution	Temporal resolution	Accuracy
Sea Ice Drift	Observation	5 km	N/A	weekly	1 km/day

2.4.5 Snow Depth on Sea Ice.

Snow is a critically important and rapidly changing feature of the Arctic. However, snow-cover and snowpack conditions change through time and pose challenges for measuring and prediction of snow. Plausible scenarios of how Arctic snow cover will respond to changing Arctic climate are important for impact assessments and adaptation strategies (*Bokhorst et al., 2016*). *Merkouriadi et al. (2017)* discuss the critical role of snow on sea ice growth in the Atlantic sector of the Arctic Ocean. Snow lying on top of sea ice modulates the growth and decay of sea ice (*Maykut, 1978; Sturm and Massom, 2010*). Snow has a high albedo (*Perovich et al., 2017*) and even when limited snowfall occurs on sea ice in spring conditions (high insolation) it may reduce significantly surface melt. In winter conditions, when high Arctic sea ice grows in the absence of solar insolation snow has two roles: (1) it insulates the sea ice surface from cold air temperatures, hindering

thermodynamic growth of sea ice (*Ledley, 1991; Maykut, 1978*) thus reduces the heat transfer from ocean to atmosphere, influences the sea ice growth below and thereby the sea ice mass balance. (2) snow contribute to the sea ice mass balance through the formation of snow-ice (e.g., *Leppäranta, 1983*). Snow-ice forms when seawater floods and refreezes at the ice/snow interface, due to excessive snow load that pushes the ice surface below sea level. Snow-ice is a common process in seasonally ice-covered seas but has not been prevalent in the Arctic, where thick perennial sea ice has dominated (*Sturm and Massom, 2010*). Due to its high friction, information about snow depth is also important for shipping operations (e.g., *Huang et al, 2018*) in the ice-infested regions such as the northern polar route.

The main limitation of using microwave radiometers is the coarse resolution (i.e. tens of kilometres), whereas radars lack the appropriate frequencies (*Bokhorst et al., 2016*). Monitoring of snow depth on sea ice is clearly a significant parameter to monitor by CIMR due to the relatively high spatial resolution of this mission. Snow cover on sea ice influences the Earth's climate and biology in the ocean. The only current snow-depth-on-sea ice algorithm that uses satellite data is based on microwave radiometer observations (*Cavalieri et al. 2012; Brucker and Markus 2013*).

Snow depth measurements (e.g., *Warren et al., 1999; Maass et al., 2015; Zheng et al., 2017*) over sea ice are needed for an accurate determination of the sea ice freeboard when used together with satellite altimeter measurements (e.g., *Kern et al., 2015; Kurtz et al., 2013*) [AD-2]. Snow depth can be estimated from microwave radiometry using a combination of AMSR-E or AMSR-2 brightness temperatures (e.g., 18.7 and 36.5, GHz) using a spectral gradient approach (e.g., *Markus et al., 2006; Comiso et al., 2003*). Although the method is confounded in the presence of snow melt water and sensitive to the ice roughness below, potentially this can allow direct snow measurements to replace the Warren snow climatology. Recently, the use of neural network approaches has shown promising improvements (e.g., *Brackmann-Folkmann and Donlon, 2019*) although more work is required to develop this approach further.

[AD-1] states the requirement as follows:

THM	DOM	Parameter	AOI	Resolution	TOY	Frequency	Leadtime	TL	Unit	Range	Accuracy	I	S	C	P
SI	OC	snow depth and density	0	<5km	0	1dy	n/a	1	0: [m]	[0,10]		0	0		1
SI	CL		1	1-10 km	0	1dy	n/a	0	0: [m]	[0,1]	0,01 m	1	1		2
SI	TR		0	25m	0	T: 1dy G: 12hr	n/a	2	0: [m]	[0,10]	0,1m	0		2	2
SI	OC, ME		0	T: 3 km G: 1 km	0	T: 12hr G: 6hr	n/a	2	0: [m]	[0,10]	horizontal: T: 10 % , G: 5% vertical: T: 0.1m	0	1	2	2
SI	OC		0	T: 10km G: 1km	0	30dy	n/a	0	0: [m]	[0,0,5]	T: 0.05m , G: 0.02m	1	1	2	2
SN	ME EM TR OI		0	T: 1km G: 5m	snow covered period	T: 1dy G: 1hr	n/a	1	0: [m]	[0,4]	vertical: T: 0.1m G: 0.01m	3	1	2	2

[AD-2] states the prioritised operational requirement as: “*Snow depth measurements are needed to best measure sea ice freeboard. The specification should follow the ice thickness specifications in terms of resolution and time sampling*”. Note the stringent delivery timeliness requirement of ‘2’ (NRT1H).

[AD-2] states the prioritised climate requirement as:

Snow depth and density on sea ice	Empirical method exist based on PMW brightness temperatures measured at different frequencies for SSM/I or AMSR-E.	The current estimates of snow over ice are empirical and medium resolution. They do not work for thick snow cover	Snow depth measurements are needed to better assess snow loading and altimeter freeboard measurements, as well as the role of snow in the evolution of the sea ice cover. The specification should follow the ice thickness specifications in terms of resolution and time sampling.
-----------------------------------	--	---	--

[AD-2] notes that snow depth on sea ice measurements are needed to best measure sea ice freeboard. The specification should follow the ice thickness specifications in terms of resolution and time sampling.

2.4.6 Ice type/Ice stage of development

Sea ice includes any form of ice found at sea which has originated from the freezing of seawater (e.g., *Eppler et al.*, 1992). It can be broadly described in terms of Ice Type/Stage of Development using the following classification: new ice, young ice, first/second-year ice and multi-year ice (e.g., *Walker et al.*, 2006). These categories broadly reflect the age of the ice and include different forms and thicknesses of ice at various stages of development. [AD-2] states that sea ice type is key to operational services (navigation, marine operations) as well as to climate modelling. At present, sea ice type information is needed for converting sea ice freeboard (from satellite radar altimeter measurements) to sea ice thickness;

Ice-type is typically derived from scatterometers (e.g., MetOp ASCAT) in combination with AMSR-2 or SSMI microwave radiometry measurements, e.g., as in the current operational OSI-SAF and CMEMS catalogue. Historically, ice type from microwave radiometry alone has used Ka-band (31 or 36 GHz), but some sensitivity also exists at lower frequencies (e.g., *Lee et al.*, 2017). Because of the many types of sea ice and its dynamic nature, scattering from sea ice is very complex. The general approach is to create feature vectors with either fixed reference vectors, dynamically-selected reference vectors, or automated clustering techniques to classify the observed scattering characteristics for each pixel to a particular ice type (e.g., *Long*, 2017, *Ye et al.* 2015, 2016). The combination of microwave radiometry and scatterometry (and optical data when available) to provide sea ice type in non-precipitating atmospheric conditions offers a powerful synergy for sea ice parameters including ice classification.

[AD-1] states the requirement as follows:

THM	DOM	Parameter	AOI	Resolution	TOY	Frequency	Leadtime	TL	Unit	Range	Accuracy	I	S	C	P
SI	TR	Ice Type	0	T: 20m G: 2m	0	T: 2d G: 1d	24h	1	1	[New ice, Nilas/Level ice, Rafed ice, Ridged ice, Hummocked ice, Brash ice]	T: 85%, G: 95%	1	0	2	2
SI	TR		0	T: 40m G: 25m	0	T: 1dy G: 6hr	n/a	2	1	FY/MY/ New Ice	T: 85%, G: 95%	0	2	0	
SI	ME, OC		0	T: 3 km G: 1 km	0	T: 1dy G: 12hr	1	0	1	FY/MY	T: 85%, G: 95%				

Note the stringent delivery timeliness requirement of '2' (NRT1H).

[AD-2] states the prioritised operational requirement as:

Stage of development / Ice type	<p>Ice services are making a visual interpretation based on the SAR backscatter values.</p>	<p>Automatic products should be available.</p> <p>Fully polarimetric SAR observations are required in order to enable automation of product generation.</p> <p>Dynamic topography products are required at high spatial and temporal resolutions. These can be provided by single pass interferometric SAR (bistatic SAR).</p>	<p>Accuracy: Fractions of deformed ice has to be measured with an accuracy of 10%.</p> <p>Coverage: pan-arctic (G), areas near shipping routes and marginal ice zone (T)</p> <p>Frequency: 1 day(G), 2 days (T)</p> <p>Spatial resolution: 20m(G), 80m (T)</p>
---------------------------------	---	--	--

[AD-2] states the prioritised climate requirement as:

Ice type	Multiyear ice concentration are available from PMW. Distinction of deformed/leveled ice is available via scatterometer data.	Continuity of the temperature at different polarizations.	Accuracy: Fractions of deformed ice has to be measured with an accuracy of 10%. Coverage: pan-arctic Frequency: daily (for monitoring of ice kinematics) Spatial resolution: same as for ice drift (order 10 km), ultimate goal would be 1 km.
----------	--	---	---

Continuity of ice-type in non-precipitating atmospheric conditions is at least required [AD-1] with at least a daily revisit and an effective (gridded) resolution of <5 km [AD-2].

2.4.7 Sea Ice Surface Temperature (SIST)

Ice Surface Temperature (IST) is a general term that refers to all ice surfaces. Sea Ice Surface Temperature (SIST) is a more specific term in the context of CIMR. IST and SIST will be considered equivalent in this document. SIST is typically retrieved using thermal infrared (TIR) measurements that are confounded by the presence of clouds (e.g., Scott *et al.*, 2014).

Microwave radiometry has potential to retrieve the ice surface temperature using 6.9 GHz AMSR-E and AMSR-2 data (e.g., Comiso *et al.*, 2003) in combination with other microwave channels and thermal infrared satellite data when available (cloud cover remains a challenge in the Polar Regions). At ~6 GHz an effective temperature (T_{eff}) of the emitting layer due to the finite emission depth at this frequency is retrieved. T_{eff} is more representative of the snow-ice interface temperature rather than the SIST derived by TIR measurements. Figure 5 provides an example of the differences between IST (derived from a TIR radiometer) and the temperature at different depths in the snow-pack and at the ice/snow interface.

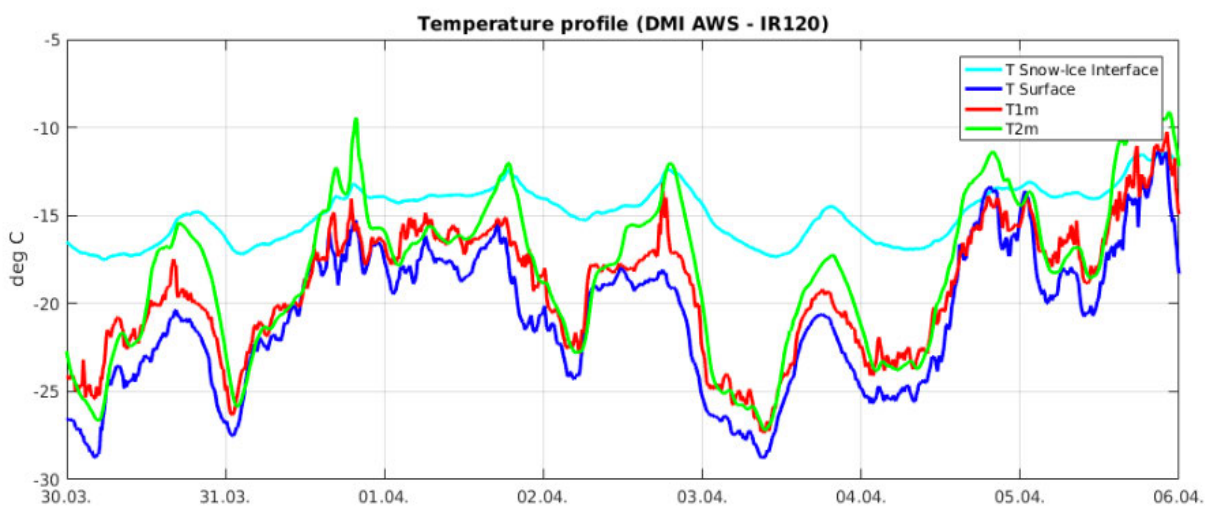


Figure MRD-2.4.7.1. (S)IST temperatures at DMI Automatic Weather Station IR120 highlighting the significant differences between the temperature at the snow/ice interface (bottom of the snow layer) and the skin IST as measured by an infrared radiometer. (credit: Kilic *et al.*, 2018b).

Recent developments using satellite microwave radiometer data at 6.9, 18.6 and 35.5 GHz with empirical algorithms (*Kilic et al., 2018b*, shown in Figure MRD-2.4.7.1) suggest that the snow-ice interface temperature, the effective temperature, and the snow depth in terms of brightness temperature can be retrieved (*OS/ISAF, 2017*). SIST is potentially as important as SST in terms of assimilation for vertical heat diffusion. SIST is a CMEMS product derived from MetOp AVHRR and provided daily with 5 km resolution for the Arctic domain (> 58°N) [AD-1].

[AD-1] states the requirement as:

THM	DOM	Parameter	AOI	Resolution	TOY	Frequency	Leadtime	TL	Unit	Range	Accuracy	I	S	C	P
SI	OC	IST	0	T: 5km	0	6hr	n/a	2	0 : [°K]	[210,290]	0,5K	0	2	2	1
SI	TR		0	T: 150m G: 50m	0	T: 2dy G: 1dy	24h	1	0 : [°K]	[173,278]	T: 1K G: 0.25K	1	2		0
IS	CL ME HY		2 Antarctica Greenland	10 km	0	T: 1 yr G: 1 mo	n/a	0	0 : [°K]	[178-278]	1K	1	1		0

Note the stringent delivery timeliness requirement of '2' (NRT1H).

[AD-2] states the prioritised climate requirement as:

All weather SST/IST	All weather SST/IST are available at low resolution based on PMW. High resolution, weather dependent IR products are available at 1 km resolution	High resolution (1 km) IST are useful to estimate heat transfer through sea ice and sea ice growth rates but are hardly available in cloudy high latitudes.	Continuity of the PMW retrieved SST/IST is required together with high resolution weather dependent SST/IST as this parameter is crucial for climate studies and model validation
---------------------	---	---	---

Continuity of SIST in non-precipitating atmospheric conditions is required (i.e. that derived from AMSR-2) [AD-1] with at least a daily revisit [AD-2].

2.4.8 Terrestrial Snow Cover: Snow Area and Snow Water Equivalent.

[AD-1] notes that seasonal snow is a main element of the global water cycle and climate system. Due to its strong influence on the radiation and energy balance, changes in snow extent tend to amplify climate fluctuations. Terrestrial snow covers up to 50 million km² of the Northern Hemisphere in winter and is characterized by high spatial and temporal variability. Seasonal snow is an important resource, supplying major parts of Europe but also many other regions in the world with water for human consumption, agriculture, hydropower generation, support of geotechnical and construction planning activities, management of water supply for agricultural industry, and other economic activities. Seasonal snow is also important for hydrological forecasting in the context of flood prevention [AD-1].

High priority parameters needed to monitor the seasonal snow are snow water equivalent (snow mass: SWE), snow extent / fraction, and the snow melt extent (presence of liquid water in the snow pack). **Among those parameters SWE is the most needed parameter of the seasonal snow [AD-1].** For many applications (e.g., in hydrology, climate, meteorology, water resource management, etc.) high resolution SWE is required with improved accuracy and appropriate spatial resolution for complex terrains and forests. Seasonal snow is a main element of the global water cycle and climate system. SWE is an emerging product of the Copernicus Land Monitoring Service (<http://land.copernicus.eu/global/products/swe>) based on SSM/I and optical satellite data.

Snow Water Equivalent (SWE) is one of the most useful parameters to monitor seasonal snow and [AD-1] states the requirement as follows:

THM	DO M	Parameter	AOI	Resolution	TOY	Frequency	Leadtime	TL	Unit	Range	Accuracy	I	S	C	P
SN	GEN CL ME	Snow Water Equivalent	T: Northern Hemisphere G: Global	T: 10km G: 1km	0	T: 5dy G: 1dy	n/a	1	[mm (kg/m ²)]	[0,500]	For SWE < 200 mm: T: 40 mm, G: 20 mm For SWE > 200 mm: T: 20%, G: 10%		2	2	2
SN	GEN HY EN ME		2: T: North. Hemis. G: Global;	T: 1km G: 200m	0	T: 5dy G: 1dy	n/a	1	[mm (kg/m ²)]	[0,500]	For SWE < 200 mm: T: 40 mm, G: 20 mm For SWE > 200 mm: T: 20%, G: 10%		1	2	2
SN	GEN PF		2: G: Mountain regions, permafrost regions;	T: 50m G: 10m	1 snow covered period	T: 5dy G: 1dy	n/a		[mm (kg/m ²)]	[0,500]		0	1	3	2

It is feasible to measure SWE from space (e.g., *Pulliainen et al.*, 2001) using empirical spectral and polarization difference algorithms that are driven by microwave radiometer brightness temperatures. Empirical methods exist based on SMMR and SSM/I microwave radiometer brightness temperatures (e.g., 37 GHz and either 18 or 10.7 GHz, e.g., *Hallikainen and Joma*, 1992; *Tsutsui and Maeda*, 2017). Both AMSR-E and AMSR-2 have SWE algorithms based on 18.7 and 36.5 GHz channels (e.g., *Cho et al.*, 2017) [AD-2]. Snow water equivalent (SWE) SWE is observed by current satellite microwave radiometer systems on-board of Defence Meteorological Satellite Program (DMSP) SSM/I satellites at coarse spatial resolution (a few tens of km), but retrieval algorithms are saturated for deep snow and are not capable of measuring SWE in complex terrain. The availability of microwave radiometer sensors on-board of DSMP satellites is uncertain. Observations by MetOp-SG MWI will not improve spatial resolution or retrieval skill [AD-1].

[AD-2] requests the following:

SEASONAL SNOW	Status	Gaps
Total Snow Area	VIS, NIR & TIR imager, some problems with cloud / snow discrimination; available products show significant differences.	Higher resolution required for complex terrain (mountains); cloudiness / polar night; in some products filled with coarse IMWR.
Snow Mass (SWE) on land	Low spatial resolution SWE maps available from IMWR, but at comparatively large uncertainty. Operational products available (GlobSnow, etc.), continuity of PMW on METOP.	IMWR SWE: accuracy needs to be improved; problems with spatial resolution in complex terrain, forests, saturation over deep snow. High resolution product needed, not covered by current sensors.
Snow Melt Extent	C Band SAR (S1, ERS, ENVISAT) provide snapshot, algorithms mature for mountain regions.	Problems in forests. Melt extent depends on acquisition time;

Snow Extent is an important parameter for climate change assessment, but also important for water management, hydrology and meteorology. Snow extent (binary and fractional) is monitored by means of multi-spectral, medium resolution optical sensors like AVHRR, MODIS, ATSR-2/AATSR, and monitoring is continued by Sentinel-3 SLSTR and OLCI, providing improved spectral properties and spatial resolution. Long time series of satellite data are available since the beginning of 1980s [AD-1] although only for cloud-free conditions.

The extent of the Snow Melt is important for hydrology, water management, and snow melt flood forecasting. At coarse resolution, microwave radiometer and scatterometer measurements are used that are continued by sensors on-board MetOp-SG. Sentinel-1 Interferometric Wide Swath (IWS) and the Extended Wide Swath (EWS) modes are suitable to map the melt snow extent, but this approach requires a suitable acquisition planning [AD-1].

[AD-4] states the climate requirement as:

Requirement	Type of requirement (observation/product)	Spatial resolution	Vertical resolution	Temporal resolution	Accuracy
Snow Area Extent	Observation	1 km; 100 m in	N/A	24h	5% (max error of omission and commission in snow area); location accuracy: better than 1/3 IFOV with target IFOV 100 m in complex terrain; 1km elsewhere
		complex terrain			
Snow Water Equivalent	Observation	1 km	N/A	24h	10 mm

2.4.9 Sea Surface Salinity (SSS)

Salinity refers to the mass of dissolved salts in a kilogram of seawater. It is a dimensionless ratio (quantity of conductivity), expressed according to the Practical Salinity Scale. While a challenging measurement to make from space (e.g., Yueh *et al.*, 2001), for warmer waters great progress has been made using 1.4135 GHz measurements from the ESA SMOS (e.g., Reul *et al.*, 2012a) and NASA Aquarius (e.g., Meissner *et al.* 2018; Yueh *et al.*, 2014) and SMAP missions (e.g., Meissner and Wentz, 2016).

Garcia-Eidell (2017) highlight the relatively low sensitivity of SSS at low temperature waters complicate the ability to obtain accurate salinity in the cold waters of the polar regions. Figure MRD-2.4.9-1 (b) and (c) highlight how at a given temperature, TB decreases as SSS increases with a wider SSS spread in the vertical component than in the horizontal component (thus vertical polarization is slightly more sensitive to SSS changes). In addition, Tb is highly sensitive to the presence of sea ice due to the differences in emissivity, which can be erroneously interpreted as a decrease of SSS or freshening if not managed properly in the retrieval. This is a constraint on the L-band channel that is primarily used for SSS retrieval which must be of the order ~0.3K or better since a 0.1K uncertainty in Tb manifests as 0.3 psu. salinity error at L2 in the Arctic.

New algorithms, recently developed at the Barcelona Expert Centre (BEC) to improve the quality of L-band measurements show that for the first time cold-water SSS maps from SMOS data can be derived (Olmedo *et al.*, 2017; Garcia-Eidell *et al.*, 2017) to observe the variability of the SSS in the higher north Atlantic and the Arctic Ocean. Also, BEC has proposed a methodology to mitigate systematic errors produced by the contamination of the land over the sea that allows obtaining SMOS SSS fields over enclosed seas such as the Mediterranean (Olmedo *et al.*, 2018).

Buongiorno Nardelli *et al.*, 2012 and 2016 demonstrated that SST can be used together with SSS data to produce L4 SSS products with higher resolution and improved accuracy and to directly estimates the sea surface density (SSD) fields. This method is now adopted by CMEMS to produce global reanalysis of SSS and SSD (1993-2016) at $\frac{1}{4}^\circ$ spatial resolution available from the CMEMS catalogue since April 2018 (Droghei *et al.* 2016, Droghei *et al.* 2018). The NRT3H SSS and SSD production is planned for end of 2018.

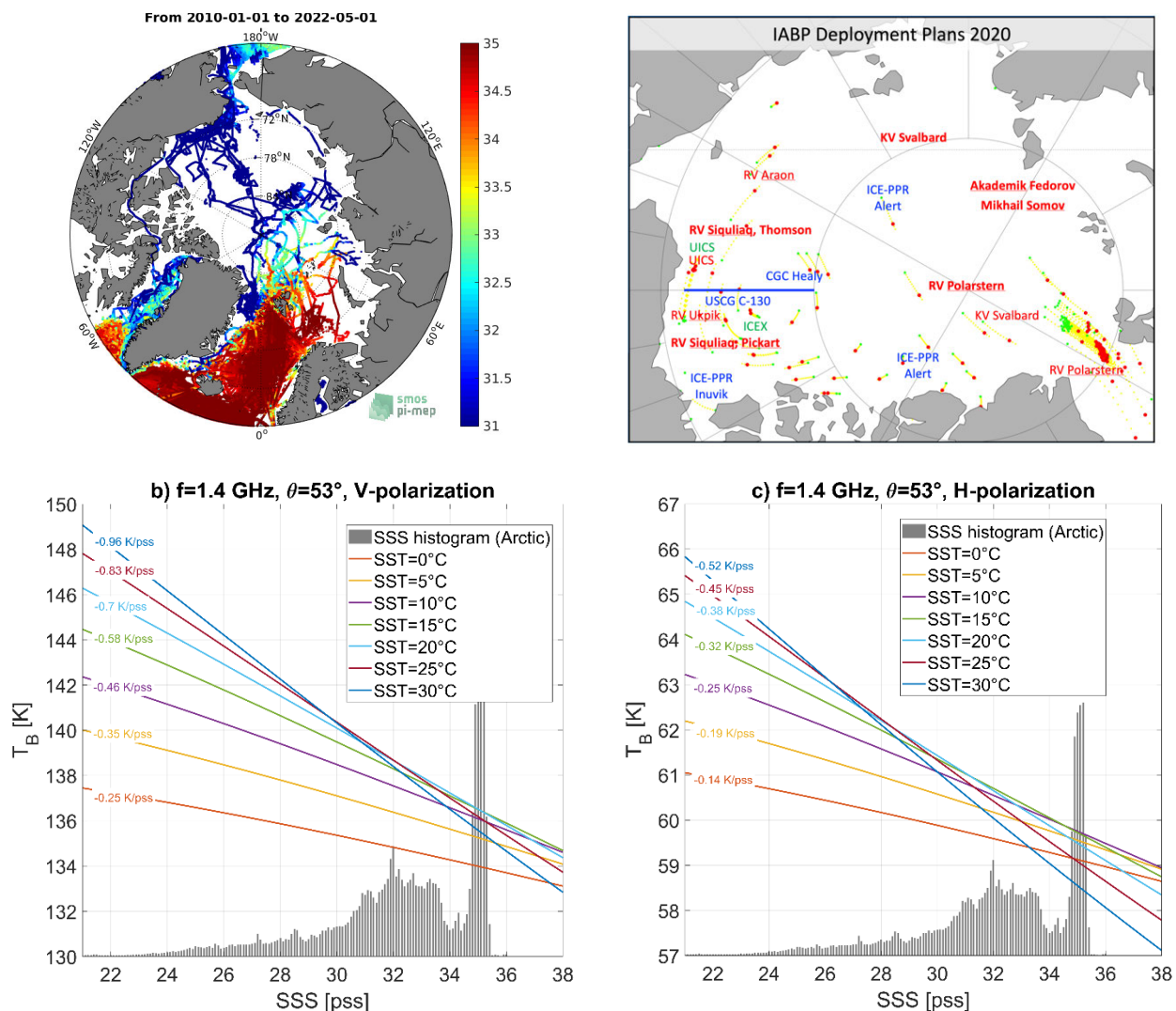


Figure MRD-2.4.9-1. (top left) Ensemble of in situ SSS data collected in the Pi-MEP salinity platform (<https://www.salinity-pimep.org/>) from January 2010 to April 2022. The data include upper measurements from Argo floats, TSG (LEGOS, GOSUD, SAMOS, Polarstern), marine mammals and surface drifters. (top-right) Deployment Plan: The map on the right shows a broad overview of IABP deployment plans. The yellow tracks show the expected drift of buoys reporting on the Arctic Ocean in May 2020. The IABP and Collaborators planned to deploy over 100 buoys at over 70 different locations during the Spring (green), and Summer (red) of 2020. The deployments shown in blue were cancelled due to COVID-19. Deployments in shown in bold, red text are planned for September – November 2020 (Ignatius Rigor, IABP Coordinator). b) Modelled perfectly flat ocean brightness temperature T_B at 1.4 GHz (L-band) and EIA=53° as a function of SSS (x-axis) and SST (colour, see legend) for b) V-polarization and c) H-polarization. The dielectric constant model of Meissner and Wentz (Meissner and Wentz, 2004; Meissner et al., 2018) is used. The linear sensitivity of T_B to SSS [K/pss] is indicated by coloured numbers for each SST values. The normalized histograms of in situ SSS encountered in the Arctic in a) is shown by the grey bars.

Radio Frequency Interference (RFI) must be mitigated when using low-frequency L-X band channels, in geophysical retrieval algorithms (e.g., Soldo et al., 2017; Mohammed et al., 2016). However, Johnson et al. (2021) and Andrews et al. (2022) recently explored the 500-2000 MHz RFI environment using airborne techniques concluding that wideband radiometry from 500 to 2000 MHz is viable for science applications in the majority of the regions surveyed. Additional channels

in this spectral bandwidth could help improve SSS retrievals since the sensitivity of Tb to SSS increases to a maximum at around 600 MHz.

SSS is a very important variable for CMEMS [AD-3] and first results of assimilating SMOS SSS indicate positive skill (ESA SMOS-NINO15 Project). New Global L4 SSS and SSD datasets including satellite SSS from multiple satellite sensors (SMOS, Aquarius, SMAP) will be developed and produced in the future. However, there are no planned missions to secure continuity of L-band measurements following SMOS or SMAP missions from which sea surface salinity is best derived. Actions should be developed to advance our capabilities to observe SSS from space [AD-3].

Table-MRD-SSS. Requirements for future SSS observations from Space as function of oceanographic processes. S=Spatial resolution, T=Temporal resolution, U=uncertainty, SRL: Scientific Readiness Level, ARL: Application Readiness Level, y=year, m=month, w=week, d=day, hr=hour. N.B. Uncertainties are given in psu and correspond to the accuracies of the SSS at the corresponding temporal and spatial scales

Oceanographic Processes	Useful ³			Required			Optimal			SRL	ARL
	S	T	U	S	T	U	S	T	U		
SSS long-term change (>10years)	10°	1 y	0.01	5°	1 y	0.005	5°	1 m	0.01	4	3
Barrier layer and vertical compensated layers	1.5°	1m	0.1	0.5°	1 w	0.1	0.25°	1 w	0.02	4	3
Density compensation on horizontal	0.5°	1m	0.3	0.25°	8d	0.15	0.01°	1d	0.05	4	3
ENSO/IOD SSS anomalies	10°	1m	0.2	1°	8d	0.2	0.25°	4d	0.1	7	6
Mesoscale/eddy propagation	1°	1m	0.2	0.5°	1w	0.1	0.25°	1w	0.05	5	3
Tropical Instability Waves	1°	8d	0.2	0.5°	8d	0.1	0.25°	4d	0.1	4	3
AMOC	1°	2w	0.2	1°	1m	0.05	1°	2w	0.02	3	3
River plumes	1°	1m	1	0.5°	8d	0.2	0.1°	1d	1	7	6
Rain-induced SSS freshening	0.5°	<1hr	1	0.1°	<1hr	1	0.1°	<1hr	0.2	5	3
Ice melting	0.5°	8d	1	0.5°	4d	0.5	0.25°	4d	0.2	1	1
Carbon Cycle and biogeochemistry: air-sea CO ₂ fluxes	1.5°	1 m	0.2	0.5°	1m	0.1	0.25°	1w	0.1	4	3
Carbon Cycle and biogeochemistry: alkalinity	1.5°	1m	0.2	0.5°	1m	0.1	0.25°	1w	0.1	7	6

[AD-4] states the climate requirement as:

Requirement	Type of requirement (observation/product)	Spatial resolution	Vertical resolution	Temporal resolution	Accuracy
Sea surface Salinity	Observation	50-100 km; 1-10 km	N/A	24h - 1 week	0.01 psu

³ Indicates Spatial, Temporal and Accuracy Required. Useful, Required and Optimal Requirements respectively (useful means that below this threshold data is of very little impact, required is the value which people want, optimal is the day dreaming value)

[AD-3] requests that there is a further advance in Copernicus capabilities to observe sea surface salinity over the global ocean from space. During recent workshops (Cesbio, Nov 2017; ECMWF, Dec 2017, LOCEAN, 2018) the need for L-band radiometer continuity was discussed. It was identified that any future sensor should provide L2 measurements with the same spatial resolution as currently orbiting systems SMOS mission. The following requirements for future SSS observations from Space as function of oceanographic processes were determined as shown in Table-MRD-SSS.

2.4.10 Wind speed over the ocean and extreme winds in Polar regions

Multi-channel microwave radiometers have been used to measure ocean surface winds for several decades. As discussed by Wentz (1992), wind induced roughness of the sea surface reduces the polarisation of sea surface emissions at microwave frequencies (except at incidence angles above 60° for which the vertically polarized emission decreases). Surface waves having wavelengths long compared to the radiation wavelength mix the horizontal and vertical polarization states and change the local incidence angle. Foam at the sea surface (a mixture of air and water) increases in the emissivity for both polarizations. Sea surface emissivity depends on wind-induced surface ocean roughness (e.g., Meissner and Wentz, 2002; 2012) that can be derived from microwave radiometer observations at 10 to 36 GHz (Prigent et al., 2013, Kilic et al., 2018). These estimates are then used to derive an estimate of the surface wind over the ocean. The technique is mature and validated data sets are available from SSM/I, AMSR/E/2 amongst others. CIMR will derive wind speed and direction estimates by combining, X- with C- and L-band channels and the use of full Stokes parameters.

[AD-4] states the climate requirement as:

Requirement	Type of requirement (observation/product)	Spatial resolution	Vertical resolution	Temporal resolution	Accuracy
Surface Wind	Observation	10 km	N/A	3 h	0.5 m/s

The first fully polarimetric satellite microwave radiometer, CORIOLIS WindSat (Gaiser et al., 2004), was launched in January 2003. The mission was developed to evaluate the potential of polarimetric microwave radiometry to retrieve ocean surface wind vectors. The polarization properties of an electromagnetic wave can be fully characterized by measuring the modified Stokes vector. The modified Stokes vector includes the vertical and horizontal polarizations and the third and fourth Stokes parameters that provides sufficient information to retrieve an estimate of the ocean surface wind vector. Because the wind direction dependence differs for the 4 Stokes parameters it is possible to resolve the vector wind ambiguities without the use of an ancillary numerical weather prediction field. Nonlinear iterative retrieval algorithms for wind vector retrievals from WindSat data have been developed (e.g., Bettenhausen et al., 2006). Bourassa et al (2019) review the current capability of ocean wind measurements from space. At wind speeds below 6m s⁻¹, the wind direction signal from microwave radiometry is small in all polarizations leading to noisy wind direction estimates. At 6m s⁻¹, the uncertainty of WindSat wind direction is 20° (Hilburn et al., 2016). Above 8m s⁻¹, the uncertainty is 10°-15° and is similar to that derived from scatterometers (Ricciardulli et al., 2012; Hilburn et al., 2016). At high winds (above 10m s⁻¹) the wind direction signal derived from microwave radiometry is strong in all 4 Stokes parameters.

The combined use of both CIMR full Stokes measurements and MetOp-SG(B) active microwave sea surface wind estimates will provide an unprecedented wind speed/vector data set at high spatial and temporal resolution, in rain free conditions, for application in Copernicus.

[AD-4] states the climate requirement for wind speed as:

OBSERVATION	Spatial resolution	Vertical resolution	Temporal resolution	Accuracy
Surface wind speed and direction	10 km	N/A	3 h	0.5 m/s

CIMR also provides L-band measurements that have been recently used to determine extreme wind speeds over the ocean. The application of L-band measurements to measure extreme wind speed over the ocean has been pioneered by *Reul et al.* (2017). Estimates of storm intensity and sizes are being produced in near-real time from SMOS (www.smosstorm.org) and SMAP (www.remss.com) for operational applications at the US Navy and the Joint Typhoon Warning Center have started to ingest this information into their Automated Tropical Cyclone Forecasting Systems (*Sampson and Schrader*, 2000; *Bender et al.* 2017, *Knaff et al.* 2018). Considering the Arctic, Polar Lows (PL) are intense mesoscale cyclones that are associated with cold air outbreaks and form pole ward of the main baroclinic zone. Sometimes referred to as Arctic hurricanes, polar lows are short-lived (the mean lifetime is ~15 h) and small-scale cyclones (diameters ranging from 200 to 600 km), unlike their tropical counterparts (*Smirnova et al.*, 2015). What they do have in common is strong surface winds: at least gale force is required for a polar low (*Rasmussen and Turner* 2003).

Early detection and evaluation of PL parameters are extremely important to ensure the safety of navigation, fishing and oil industry, and expanding construction on the Arctic shelf. This a timeliness of NRT1H is required. These extreme storms, characterized by strong and rapidly changing winds, are known to enhance vertical mixing processes. This can affect the cold halocline layer, possibly leading to positive feedback that impacts sea-ice formation. Because of the sparse network of weather stations and irregular meteorological observations at the sea, fast movement and short life cycle of PLs, the phenomena are not always identified in the pressure fields on the surface weather maps. That is why satellite data remain the basic source of information on PLs.

Polar lows can be identified in integrated Water Vapor Content (WVC) fields (*Sminova et al.*, 2016), but in some regions (Chukchi Sea, Laptev Sea and the East Siberian), they are associated with extremely low WVC values which make their detection from high-frequency radiometers (e.g., SSM/I) difficult (*Zabolotskikh et al.*, 2016). Efficient masking of the areas over the oceans, where geophysical parameter retrievals are objectively impossible due to non-transparent atmosphere, is still an important issue for satellite radiometer measurements working at frequency higher or equal than C-band. As demonstrated for Tropical cyclones (*Reul et al.*, 2012b, 2016, 2017, *Meissner et al.*, 2017) L-band radiometer data can provide a direct way to probe surface wind speed in extreme weather events, being almost transparent to the atmosphere. In addition, *Andrews et al.* (2022) recently explored the 500-2000 MHz RFI environment using airborne techniques concluding that wideband radiometry from 500 to 2000 MHz is viable for science applications in the majority of the regions surveyed. Additional channels in this bandwidth could improve measurements of wind speed. Estimation of the total atmospheric absorption can be also done from the ~10 GHz channel with high accuracy due to the weak influence of liquid water and especially water vapour (*Zabolotskikh et al.*, 2013). This helps to refine a new filter to considerably reduce masking ocean areas in e.g., AMSR2 radiometer data for severe weather systems such as PL, characterized by high wind speeds and moderate atmospheric absorption. Combining, X- with C- and L-band channels, a methodology can be proposed to jointly retrieve sea surface wind speed and sea surface temperature in PL.

The combined usage of both CIMR passive and MetOp-SG(B) SCA active microwave sea surface wind estimates will demonstrate the potential of the highest spatial and temporal resolution in the investigation of PL intensity. The ability to better measure warm SST PLs wakes thanks to X/C

band combination for SST and L-band wind retrievals will also help in better characterizing feedbacks of PLs to impact sea-ice formation.

2.4.11 Other parameters that can be derived from CIMR

Land is an integrated part of the Polar regions. Globally, understanding changes on continental land helps to understand changes in the Arctic (e.g., soil moisture, permafrost, vegetation dynamics, snow, etc.). Arctic changes today are driven by a combination of local and global change and CIMR will provide a global view of these changes using a variety of products.

CIMR observations at L-, C- and X-bands enable derivation of vegetation information that is critical for answering important ecological, eco-hydrological and hydrologic science questions (Baur *et al.*, 2019). Multi-frequency soil and vegetation water information enables major advances in understanding the plant water content variations across the soil-plant-atmosphere continuum, and the ecosystem responses to water stress, particularly if linked with synergistic canopy structural information from other satellites. In this regard, CIMR can complement the soil moisture and vegetation products that are now provided through Copernicus Global Land Monitoring Service (GLMS), and serve a wide range of applications.

Microwave radiometer-based products of bio-geophysical properties of snow (SCE, Terrestrial SWE), inland waters (LSWT, LIC) and continental surface (LST and SM) are recognized as Essential Climate Variables by GCOS and included in the Copernicus Climate Service (3CS). The envisaged long-term commitment of the CIMR mission will allow to extend these climate data records up to more than half a century in length, which are crucial for monitoring the impact of climate change and anthropogenic forcing on natural and agricultural ecosystems.

2.4.11.1 Soil Moisture (SM)

Soil moisture is a primary state variable of hydrology and the water cycle over land either as an initial condition or a boundary condition of relevant hydrologic models (NASA, 2014). Applications that require accurate maps of high-resolution soil moisture and its spatial and temporal evolution include: weather forecasting, modelling and prediction of climate variability and change, agricultural productivity, water resource management, drought prediction, flood area mapping, and ecosystem health monitoring all require information on the status of soil moisture. See Dorigo *et al.* (2017) for a full review. Satellite surface soil moisture, up to 5cm soil depth, is recognized as an Essential Climate Variable by the Global Climate Observing System (GCOS), alongside subsidiary variables freeze/thaw state, vegetation optical depth, surface inundation and root-zone soil moisture.

[AD-4] states the climate requirement as:

Requirement	Type of requirement (observation/product)	Spatial resolution	Vertical resolution	Temporal resolution	Accuracy
Soil Moisture at the surface	Observation	1-25 km	N/A	24 h	0.04 m ³ /m ³

The Copernicus Land service provides estimates of Soil Moisture (in development) and a Soil Water Index (Albergel *et al.*, 2008; Wagner *et al.*, 1999) that quantifies the moisture condition at various depths in the soil. It is mainly driven by the precipitation via the process of infiltration. Soil moisture is a very heterogeneous variable and varies on small scales with soil properties and drainage patterns. Satellite measurements integrate over relative large-scale areas, with the presence of vegetation adding complexity to the interpretation.

ECMWF has been monitoring SMOS data for soil moisture applications for almost 10 years (*de Rosnay et al.* 2020, *Muñoz-Sabater et al.*, 2012). The SMOS neural network soil moisture data was implemented for operational NWP assimilation in June 2019 (*de Rosnay et al.*, 2019).

Microwave observations are sensitive to soil moisture because moisture affects the dielectric constant of the surface and thus the emissivity of soil surfaces. Vegetation and surface roughness reduce the microwave sensitivity to soil moisture and are more pronounced as microwave frequency increases. At L-band frequencies the soil moisture emission originates from deeper in the soil (a few centimetres) than higher frequencies, giving a more representative measurement of conditions below the surface crust or skin layer.

The Copernicus GLMS provides estimates of Soil Moisture and a Soil Water Index (SWI) that quantifies the moisture condition at various depths in the soil over Europe at a 1 km spatial resolution. They are based on Sentinel 1 C-band data. There is also a global SWI product at 15 km spatial resolution based on C-band ASCAT. Measurements at C-band range are sensitive to soil moisture, but primarily in regions of low vegetation but the attenuation by vegetation and the shallow sensing depth of ~1 cm for bare soil imposes limitations on the retrieval of soil moisture. The CIMR L-band channel at 1.4315 GHz is ideally suited to soil moisture measurements, since soil emissivity at L-band originates from the top 5 cm of the soil and is only partially attenuated under moderate to vegetation canopy covers. In addition, *Johnson et al. (2021)* and *Andrews et al. (2022)* have recently explored the 500-2000 MHz RFI environment using airborne techniques concluding that wideband radiometry from 500 to 2000 MHz is viable for science applications in the majority of the regions surveyed. Additional channels in this bandwidth may improve estimates of soil moisture and vegetation parameters. Retrieval algorithms that estimate both soil moisture and the degree of attenuation through vegetation can improve the soil moisture retrieval at C- and X-bands (see *Owe et al., 2001,2008*, *de Jeu et al., 2003*, *Karthik et al., 2019*) and L-band (*Konings et al., 2016; Fernández-Moran et al., 2017; Konings et al., 2017*). CIMR can adopt a new Microwave Multichannel Vegetation Indicators (MMVI) that exploits the benefits of all CIMR channels to derive a number of different vegetation indicators. Also, CIMR high revisit frequency is adequate to capture rapid dynamic SM processes such as preconditions, wettings and dry-downs from storm events which are now unattainable. These are key variables affecting soil water capacity and flood risk.

2.4.11.2 Land Surface Temperature (LST)

The Copernicus Land Service provides estimates of LST defined as the radiative skin temperature of the land surface, as measured in the direction of the remote sensor. It is estimated from Top-of-Atmosphere brightness temperatures from the infrared spectral channels of a constellation of geostationary satellites (Meteosat Second Generation, GOES, MTSAT/Himawari) in cloud free conditions. Its estimation further depends on the albedo, the vegetation cover and the soil moisture. LST is a mixture of vegetation and bare soil temperatures. Because both respond rapidly to changes in incoming solar radiation due to cloud cover and aerosol load modifications and diurnal variation of illumination, the LST displays quick variations too. In turn, the LST influences the partition of energy between ground and vegetation and determines the surface air temperature. The Global Land Service provides the following LST-based products (see *Freitas et al., 2013*):

- LST: hourly LST from instantaneous observations
- LST10-DC: 10-day Land Surface Temperature with Daily Cycle
- LST10-TCI: Thermal Condition Index with a 10-day composite of Land Surface Temperature

[AD-4] states the climate requirement as:

Requirement	Type of requirement (observation/product)	Spatial resolution	Vertical resolution	Temporal resolution	Accuracy
Land-surface Temperature	Observation	1 km	N/A	1 h	1 K

A significant challenge for LST when retrieved from TIR measurements is the presence of clouds that preclude the retrieval. Microwave observations between 18 and 36 GHz can overcome this primary difficulty and have been successfully used to retrieve LST (e.g., Aires *et al.*, 2001, Holmes *et al.*, 2009, Prigent *et al.*, 2016, Jimenez *et al.*, 2017, Ermida *et al.*, 2017). The errors on these LSTs are slightly larger than for their infrared counter parts, but the estimates are available ~90% of the time (compared to less than ~40% of the time with the infrared estimates). Note that the microwave derived LSTs are not part of the Copernicus Land Service yet but are part of the ESA LST Climate Change Initiative (CCI). However, it is part of the ESA LST Climate Change Initiative (CCI), and Prigent *et al.* (2016) algorithm is applied over SSM/I and SSMIS times series to produce ‘all weather’ LST from 1996 to 2020. See <https://climate.esa.int/en/odp/#/project/land-surface-temperature> for more information and Figure 2.4.11.2 for a comparison of the microwave LST anomalies over two regions, as compared to the ERA5 LST anomalies.

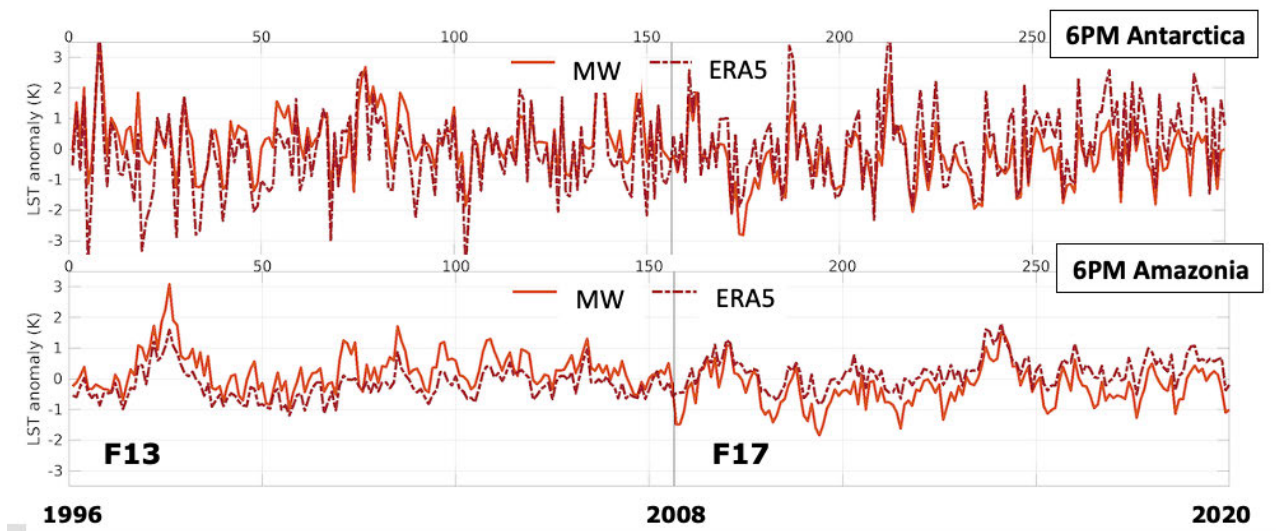


Figure 2.4.11.2. Antarctica (top) and Amazonia (bottom) area-averaged microwave LST (solid) and ERA5 (dashed) 6pm monthly anomalies. The anomalies are calculated by removing the annual cycle LST from the original LST. Credit: C. Jimenez.

2.4.11.3 Global Lake Surface water Temperature (LSWT).

Monitoring of Lakes is an important aspect of the climate system (GCOS. 2016) for the following applications:

- Observing lake freeze-up and ice break-up dates is an important indicator for climate change in boreal and polar regions.
- Presence and development of new lakes, through melting of land ice, as a key indicator of warming in boreal and polar regions.
- Assessment of changes in regional climate and better knowledge of the regional water balance, which is an important issue for sustainable development.
- The volume of the lake water body is an integrator variable reflecting both atmospheric (precipitation, evaporation-energy) and hydrological (surface-water recharge, discharge and ground-water) conditions.
- Improving the reporting and dissemination of hydrological data (rivers, lakes and groundwater) and its free exchange is vital for climate uses. Observational data on hydrological ECVs need to be reported internationally.

- GCOS Essential Climate Variable (ECV) products under Lakes that are amenable to satellite retrieval include Lake Surface Water Temperature and Lake Ice Coverage.

The Copernicus Land Service is divided into four main components: Global, Pan-European, Local and Reference Data. The Global component includes a water bodies product which detects the areas covered by inland water through the year providing the maximum and the minimum extent of the water surface as well as the seasonal dynamics as a contribution to GCOS.

[AD-4] states the climate requirement as:

Requirement	Type of requirement (observation/product)	Spatial resolution	Vertical resolution	Temporal resolution	Accuracy
Lake surface water temperature	Observation	300 m	N/A	1 week	1 K

[AD-4] states the climate requirement for lake ice cover and lake ice thickness as:

Requirement	Type of requirement (observation/product)	Spatial resolution	Vertical resolution	Temporal resolution	Accuracy
Lake ice cover	Observation	300 m	N/A	24 h	10%
Lake ice thickness	Observation	100 m	N/A	1 month	1-2 cm

2.4.11.4 Irrigation applications.

Low frequency (< 10 GHz) microwave radiometer systems like CIMR are very well suited to monitor soil moisture (e.g., *Enthekabi et al.*, 2010; *Kerr et al.*, 2012;) which makes them an attractive resource for several agricultural applications. For example, a farmer can use soil moisture information to optimize its irrigation practices which could lead to an improvement in water use efficiency. Remotely sensed soil moisture has proved a valuable resource for estimating irrigation water use at the continental scale (*Brocca et al.*, 2018, *Zaussinger et al.*, 2019) and as such can be used to estimate and optimise water use efficiency globally.

However, the coarse gridded resolution of ~25 km from current missions (e.g., SMOS/SMAP) providing soil moisture products limits the applicability for this sector. With the recent advances in downscaling, this situation has improved, and it is now able to capture local variability caused by irrigation. For example, in 2016, *Gevaert et al.* (2016) revealed a clear irrigation signal in Australia when C-band soil moisture retrievals from AMSR-E were enhanced with Ka-band observations. *Escorihuela and Quintana Sequi* (2016) showed an irrigation signal in Spain when the SMOS signal was downscaled with LST observations.

These irrigation signals were all derived from existing microwave radiometer systems. With the proposed improvement in spatial resolution and continuity of historical capability by CIMR, it is expected that the possibilities within the agriculture sector will further expand.

2.4.11.5 Vegetation Water Content and Biomass

Vegetation Optical Depth (VOD) describes the attenuation of microwave radiation by the vegetation canopy layer and, hence, is closely related to vegetation water content and biomass. VOD is simultaneously derived with soil moisture from microwave radiometer observations at low to mid-frequencies (1 -20 GHz; *Owe et al.*, 2001), where each frequency shows a unique sensitivity to different parts of the canopy: while lower frequencies are more strongly related to stems and branches (*Rodriguez-Fernandez et al.*, 2018), the higher frequencies appear to be more sensitive to leaf material and crops and therefore a powerful indicator of plant production (*Teubner et al.*, 2018; *Andela et al.*, 2014) complementary to traditional indicators from optical remote sensing like Normalised Difference Vegetation Index (NDVI) and leaf area index.

The multi-frequency capability of CMIR will, for the first time, allow for a complete characterisation from a single platform of the water contained in the vegetation, including stems, branches, leaves, and buds as a set of Microwave Multichannel Vegetation Indicators (MMVI). Indicators would be collected in a single MMVI product rather than provided as separate products. Furthermore, the proposed improvement in spatial resolution of CIMR will allow for a purer characterisation of vegetation types, which is crucial for agricultural applications.

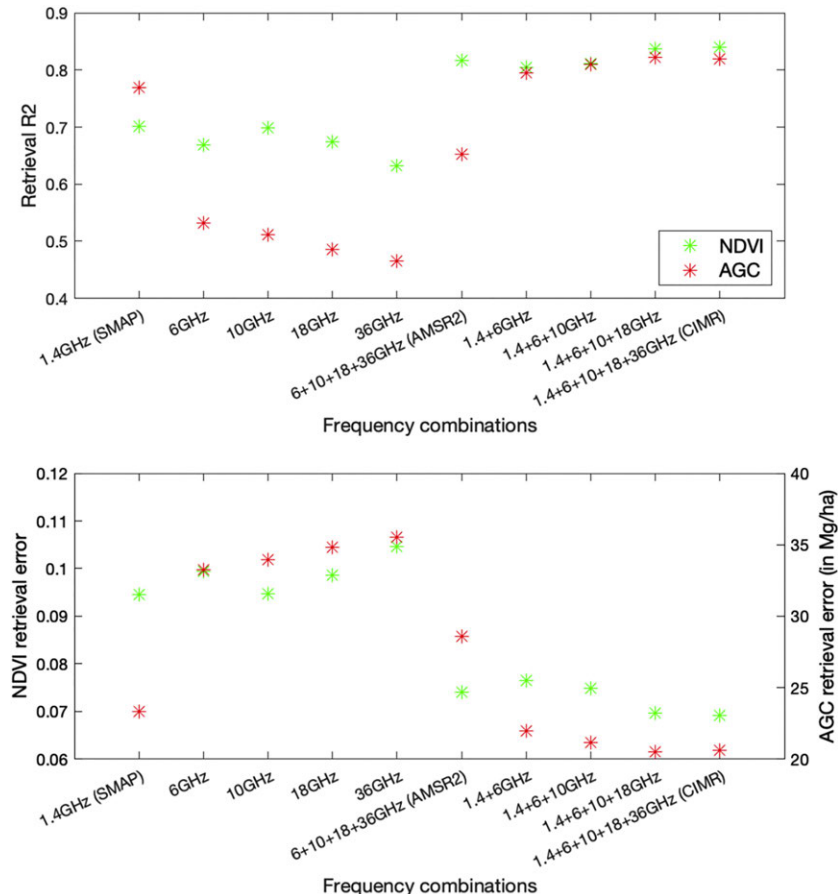


Figure 2.4.11.5-1. Performance of NDVI and AGC retrievals with different passive microwave combinations. True NDVI and AGC are respectively from MODIS and from Saatchi et al. (2011). Top: the coefficient of determination R^2 between the retrieval and the truth for NDVI (left axis) and AGC (right axis). Bottom: the retrieval error (RMSE) for NDVI (left axis) and AGC (right axis).

VOD observations from various radiometer missions have been combined into climate data records up to 30 years in length (*Liu et al.*, 2015; *Moesinger et al.*, 2019). These Climate Data Records (CDR) allow studying the variability and trends in vegetation activity and biomass, both due to climate forcing and human intervention (e.g., deforestation, grazing; *Liu et al.*, 2013). The envisaged long-term commitment of the CIMR mission will allow to extend these CDRs (and their development as a MMVI) up to more than half a century in length, which are crucial for monitoring the impact of climate change and anthropogenic forcing on natural and agricultural ecosystems. This long data coverage will complement more dedicated vegetation microwave missions like ESA Biomass.

The VOD are calculated at individual window frequencies and are usually used separately. Recently, the synergy of the CIMR frequency range has been tested for vegetation characterization, through the estimation of two vegetation parameters, its foliage and its

photosynthesis activity as described by NDVI, and its woody components and carbon stock (Above Ground Carbon, AGC), using different combinations of CIMR-like channels. The analysis showed the expected potential of the CIMR instrument for the monitoring of vegetation parameters, as compared to current microwave instruments (*Prigent and Jimenez, 2021*) (Figure 2.4.11.5-1).

2.4.11.6 Continental Surface water fraction

Surface water fraction (also called surface water extent) and dynamics have been estimated with passive microwaves, using essentially at 18 and 36 GHz. Monthly mean estimates have been calculated since 1992, at a spatial resolution of ~25 km, including the surface water under dense vegetation (*Prigent et al., 2001, 2012, 2019*). These estimates have been widely used to model Earth hydrological and biochemical cycles. They complement the optical estimates (Landsat or MODIS) that can only detect open waters in cloud free conditions. The inter-annual variability of the surface water extent derived from passive microwaves partly explain the variability of the atmospheric methane emission. So far, the inland water bodies considered by the Copernicus Land Services are limited to open water bodies, i.e., surface water areas that are not covered by vegetation (or only by sparse vegetation). The surface water fraction that can be estimated by microwave radiometry and especially by CIMR include vegetated areas that play a key role in the hydrological and biogeochemical cycles. The surface water extent estimated from microwave radiometers can be related to natural methane emission, and consequently can contribute to the Copernicus Climate Services that provide atmospheric methane information.

Recent works using L-band observations are reported in *Parrens et al. (2017)* and *Du et al. (2018)*. In addition, *Andrews et al. (2022)* explored the 500-2000 MHz RFI environment using airborne techniques concluding that wideband radiometry from 500 to 2000 MHz is viable for science applications in the majority of the regions surveyed.

[AD-4] states the climate requirement as:

Requirement	Type of requirement (observation/product)	Spatial resolution	Vertical resolution	Temporal resolution	Accuracy
Water Extent	Observation	20 m	N/A	24 h	10 % (relative) 5% (for 70 largest lakes)

2.4.11.7 Soil freeze/thaw

The soil freeze/thaw monitoring can be carried out using the low frequency bands of CIMR. The observations of the soil freeze state from L-band (*Derksen et al. 2017; Rautiainen et al. 2016*) bring the advantage of higher emission depth and lower sensitivity to vegetation and snow cover compared to observations from higher frequencies (*Kim et al. 2011*). The L-band is a superior channel to higher frequency channels for obtaining direct observations from the soil layer simply due to a longer wavelength used. At 1.4 GHz frequency, direct observations of soil properties beneath the immediate soil surface can be acquired. In addition, *Johnson et al. (2021)* recently explored the potential of wideband radiometry using the UWBRAD airborne instrument, concluding that wideband radiometry from 500 to 1400 MHz is viable for a broad range of science applications in the majority of the regions surveyed. Additional channels in this bandwidth may improve retrievals of soil freeze/thaw supporting permafrost applications.

The current F/T algorithms use a threshold detection approach to determine the average soil state of each observation grid cell. The algorithms rely on empirically defined reference signatures for frozen and thawed states. Soil categorization to either frozen or thaw state is based on comparing

the current observations to these empirical references (*Derkzen et al. 2017; Rautiainen et al. 2016*).

2.4.11.8 Cloud Liquid Water over Ocean

Atmospheric water vapour is a major greenhouse gas. In its vapour and liquid states, it is a key parameter in the global hydrological cycle, a component of climate change and ocean–atmosphere energy exchange studies. Water vapour changes in the Arctic are poorly described because of a lack of direct observations and large sea ice cover over which atmospheric water retrievals are either complicated or impossible (e.g., *Vihma, 2014*). Regular long-term observations of water vapour over the open seawater are provided by satellite microwave radiometer instruments. Both atmospheric total column water vapour (TCWV) and total liquid water path (LWP) have been successfully retrieved from AMSR-E measurements (e.g., *Kazumori, 2012*) and more recently from AMSR2 (e.g., *Zabolotskikh and Chapron, 2017*). CIMR does not have a water vapor channel centred at ~22 GHz and it is likely that CIMR will not provide any additional information with respect to the a priori information from ECMWF and other instruments.

However, cloud liquid water content can be retrieved from CIMR (e.g., *Greenwald et al., 2018*) typically at the same time as precipitation estimates are made (to reduce the risk of inconsistency).

[AD-4] states the climate requirement as:

Requirement	Type of requirement (observation/product)	Spatial resolution	Vertical resolution	Temporal resolution	Accuracy
Cloud Water Path liquid and ice (CWP)	Observation	50 km	N/A	3 h	25%

2.4.11.9 Precipitation Rate Over Ocean

Precipitation is a key hydrological and climate variable and includes both the liquid (rain) and solid (snow and ice) forms. Precipitation occurs when a particle formed by the condensation of water vapour becomes heavy enough to fall under the force of gravity. Precipitation rate estimates are a fundamental component of the water cycle characterization. The physical basis for retrieving precipitation from microwave radiometer measurements depends on distinguishing the radiation from Earth's surface from the radiation emitted from precipitation (e.g., *Hilburton and Wentz, 2008*). Microwave emission from the ocean surface is strongly polarized, while the emission from raindrops is un-polarized. Thus, precipitation can be accurately distinguished from the underlying ocean surface using measurements of the vertically and horizontally polarized radiation (see examples at <http://www.remss.com/measurements/rain-rate/>). CIMR will be able to provide estimates of precipitation rate, although further algorithm development is required, in particular to exploit forward and backwards views together.

2.4.11.10 Other applications

A Joint Cryosphere-Ocean-Land-Ecosystems CIMR Science Workshop was held in Arcadia, California from August 13-15, 2019. The objective of the workshop was to document the potential utility of the CIMR mission for NASA Earth science programs. Four panels, Cryosphere, Oceanography, Terrestrial Hydrology, and Terrestrial Ecology reviewed the CIMR mission and its potential in each application domain. Based on the discussions at this meeting, notable additions to the previous paragraphs include:

- CIMR measurements will significantly enhance the understanding of air-sea interaction processes in the Polar regions and global ocean.
- The higher temporal resolution of SSS and SST together with simultaneous measurements of SST, SSS, and wind improves studies of ocean response to synoptic weather and can

better constrain coupled modelling for hurricanes as well as tropical/extratropical cyclones, including forecast and impact studies.

- CIMR's ability to extend the satellite SSS record to cover multiple ENSO events can thus improve ENSO forecast capabilities in climate prediction centres.
- Daily simultaneous measurements of SSS and winds from the CIMR will also enhance the research on processes associated with the dispersal of river-plume induced freshwater as well as the associated redistributions of nutrients and contaminants.
- Simultaneous measurements of soil moisture, surface inundation, SSS will also improve the assessment of flooding impacts across the land-sea interface.
- The simultaneous measurements of SST and SSS will also improve the tracking of horizontal surface density fronts and the related studies of ocean dynamics on mesoscales. Ocean circulation at horizontal density fronts on scales of tens of kilometres is considered to be responsible for transporting much of the heat and carbon from the ocean surface to deeper layers.
- CIMR's higher resolution and lower noise SST estimates (compared to past C-band MW radiometers), combined with the dense temporal sampling at high latitudes, should allow a new capability to estimate daily gridded upper ocean vector currents.
- CIMR will enable estimation of a number of confounding factors that are essential to accurate soil moisture retrieval from space. These factors include land surface temperature, fractional surface water inundation extent, and vegetation contributions (microwave scattering, absorption, and emission). The availability of these coincident estimates reduces the dependence, latency, and uncertainty of external static and dynamic ancillary data, leading to a faster and more robust operational delivery of soil moisture data to the end users.
- The boost in revisit frequency compared with SMAP or SMOS will allow CIMR adequate temporal resolution to capture rapid dynamic soil moisture processes previously unattainable by existing L-band sensors. The corresponding CIMR soil moisture retrievals will allow assessments of rapid dry-downs from storm events when much of the drainage and runoff occurs. The daily fidelity of CIMR observations will improve the characterization of soil moisture preconditions and wetting from severe rainfall events, which are key variables affecting soil water storage capacity and flood risk.
- The CIMR observations at L-, C- and X-bands enable derivation of vegetation information that 1) can be used for improving the CIMR soil moisture retrieval, and 2) is critical for answering important ecological, eco-hydrological and hydrologic science questions.
- CIMR dual polarized L-band measurements, and C- and X-band measurements, can be used to retrieve vegetation opacity. Vegetation opacity information obtained simultaneously with the soil moisture retrieval can improve the soil moisture retrieval. The microwave vegetation opacity can be related to other important vegetation characteristics such as vegetation water content (VWC) and above-ground biomass.
- The CIMR mission will potentially provide enabling observations to improve process understanding, monitoring and model predictions of environmental change. CIMR's multi-frequency observations are sensitive to variations in water content across multiple layers of the vegetation canopy, and in the surface soil. Since different plant components take up and lose water at different rates, they differ in water status at any given time. CIMR's simultaneous, single-platform measurements would potentially for the first time enable mapping of plant water content variations along the entire soil-plant-atmosphere continuum.

- The Multi-layer soil and plant water content retrievals from CIMR would enable major advances in understanding ecosystem responses to water stress, particularly if linked with synergistic canopy structural information from other satellites including Lidar or Radar and foliar chemistry and trait information from hyperspectral optical sensors.
- CIMR's multifrequency capabilities will improve the delineation of freeze-thaw conditions in soil and vegetation, which are key environmental constraints to water mobility and energy and carbon exchange in seasonally frozen environments.

3 CIMR MISSION AIM AND OBJECTIVES

3.1 CIMR Mission Aim

Considering the User needs expressed in [AD-1], [AD-2], [AD-3], [AD-4] and [AD-5] and concisely articulated in the previous sections, the **aim** of a Copernicus Imaging Microwave Radiometry (CIMR) Mission is to:

Provide high-spatial resolution microwave imaging radiometry measurements and derived products with global coverage and sub-daily revisit in the polar regions and adjacent seas to address Copernicus user needs.

3.2 CIMR Mission Objectives

Objectives are split into:

- **Primary Objectives (PRI-OBJ-XX)** that are mandatory for the success of the mission and
- **Secondary Objectives (SEC-OBJ-XX)** that shall not drive the system design.

Mission requirements are then derived from Mission Objectives. In this context, the primary objectives of the CIMR mission are to:

PRI-OBJ-1. Measure **Sea Ice Concentration** (SIC) and **Sea Ice Extent⁴** (SIE) in non-precipitating atmospheres at a spatial resolution of $\leq 5^5$ km (goal: 4 km), with a total standard uncertainty of $\leq 5\%^{6,7}$, and **sub-daily coverage** of the Polar Regions⁷ and daily coverage of Adjacent Seas⁸ [AD-1], [AD-2], [AD-3], [AD-4] and [AD-5].

PRI-OBJ-2. Measure **Sea Surface Temperature** (SST) in non-precipitating atmospheres at an effective spatial resolution of ≤ 15 km, with a total standard uncertainty of $\leq 0.3^9$ K with a focus on **sub-daily coverage** of Polar Regions and daily coverage of Adjacent Seas [AD-1], [AD-2], [AD-3], [AD-4] and [AD-5].

PRI-OBJ-3. Ensure European operational continuity of **L-band** (e.g., SMOS/SMAP) and **enhanced AMSR type measurement capability** in synergy with other missions [AD-2] (e.g., MetOp-SG(B)) to enhance monitoring of the Polar Regions and Adjacent Seas.

⁴ SIE is an integrated quantity computed from daily composited maps of CIMR SIC. It has units of km². See definition of Sea Ice Extent.

⁵ ≤ 5 km (goal 4 km) spatial resolution is a critical specification for the CIMR mission.

⁶ Averaged over all seasons.

⁷ See definition of Polar Regions.

⁸ See definition of Adjacent Seas.

⁹ Calculated for a theoretical retrieval as the mode value of daily ocean average discrepancies noting anticipated theoretical discrepancies varying between 0.15 K (warm waters) to 0.45 K for (cold <280K waters). A standard total uncertainty of ≤ 0.2 K for $\geq 95\%$ global coverage and standard total uncertainty of ≤ 0.3 K in the Polar Regions and Adjacent Seas is requested for L2 products.

The **secondary objectives**¹⁰ of the CIMR mission are to:

SEC-OBJ-1. Measure **Sea Surface Temperature (SST)** in non-precipitating atmospheres at an effective **spatial resolution of <15 km**, with a total standard uncertainty of $\leq 0.2^{11}$ K with daily coverage of the **global ocean and inland seas** [AD-1], [AD-2], [AD-3], [AD-4] and [AD-5].

SEC-OBJ-2. Measure **Thin Sea Ice (<0.5 m depth)** in non-precipitating atmospheres and freezing conditions at an effective spatial resolution of <60 km, with a total standard **uncertainty of <20%¹²** (goal: <10%) with **daily coverage** of the marginal ice zone in the Polar Regions and Adjacent Seas [AD-1], [AD-2], [AD-3], [AD-4] and [AD-5].

SEC-OBJ-3. Measure **Sea Ice Drift Vectors** in non-precipitating atmospheres at an effective spatial resolution of ≤ 25 km with a standard uncertainty of $\leq 3^{13}$ cm s $^{-1}$ [AD-1], [AD-2] with daily coverage in the Polar Regions and Adjacent [AD-1], [AD-2], [AD-3], [AD-4] and [AD-5].

SEC-OBJ-4. Measure **Ice type/Stage of development** in non-precipitating atmospheres and freezing conditions [AD-1], [AD-2] in combination with other satellite data including scatterometer and SAR measurements with daily coverage in the Polar Regions and Adjacent Seas [AD-1], [AD-2], [AD-3] and [AD-5].

SEC-OBJ-5. Measure **Snow depth on sea ice** in non-precipitating atmospheres and freezing conditions with an effective spatial resolution of ≤ 15 km and standard uncertainty of ≤ 10 cm [AD-1], [AD-2] with daily coverage in the Polar Regions and Adjacent Seas [AD-1], [AD-2], [AD-3] and [AD-5].

SEC-OBJ-6. Measure terrestrial **Total Snow Area** with an effective spatial resolution of ≤ 15 km and standard uncertainty of ≤ 10 % with daily coverage in the Polar Regions [AD-1], [AD-2], [AD-3] and [AD-4].

SEC-OBJ-7. Measure terrestrial **Snow Water Equivalent (SWE)** with an effective spatial resolution of ≤ 15 km and standard uncertainty of ≤ 40 mm with daily coverage in the Polar Regions [AD-1], [AD-2], [AD-3], [AD-4] and [AD-5].

SEC-OBJ-8. Measure **Sea Ice Surface Temperature (SIST)** in freezing conditions with an effective spatial resolution of ≤ 15 km standard uncertainty of ≤ 1.0 K [AD-1], [AD-2] and [AD-3] in combination with other satellite data including thermal infrared imagery in the Polar Regions and Adjacent Seas [AD-1], [AD-2], [AD-3] and [AD-5].

SEC-OBJ-9. Measure **Sea Surface Salinity (SSS)** over the global ice-free ocean from space [AD-3], [AD-4] with a target gridded spatial resolution of 40 km and uncertainty ≤ 0.3 pss¹⁴ over monthly time-scales [AD-3 and [AD-5].

SEC-OBJ-10. Measure **wind speed over ocean** [AD-4], **soil moisture** [AD-4], **land surface temperature** [AD-4], **cloud liquid water over ocean** [AD-4], **precipitation over ocean**, **terrestrial surface water extent** [AD-4] and **vegetation indices**.

¹⁰ Secondary objectives should be accommodated in the payload design if possible.

¹¹ Calculated for a theoretical retrieval as the mode value of daily global ocean average discrepancies assuming no uncertainty in the validation data set and varying between 0.15 K to 0.45 K for cold waters.

¹² Assuming uniform, level ice within the footprint. If a mixture of ice types and open water prevail in the footprint the uncertainty is expected to be higher. *Kaleschke et al.* (2016) note that an uncertainty of <30% is possible based on SMOS tSIT measurements although validation remains a challenge using aircraft and in situ data sets.

¹³ 3 cm/s is the required uncertainty for each gridded components (dx and dy) of the drift vector, separately. This is furthermore the uncertainty for a reference 24 hours drift duration, equivalent to 2.6 km for a 24h drift vector. Drift vectors for shorter drift duration might perform better, drift vectors for longer drift duration might perform worse, see Fig. 5 in Lavergne et al. (2021). OSI-SAF product <http://osisaf.met.no/p/ice/index.html#lrdrift>. CMEMS also has an all-year Sentinel-1 SAR based sea ice drift product at 10 km resolution, produced by DTU (<http://www.seaice.dk>). This product has gaps in daily polar coverage due to limited Sentinel-1 duty-cycle and swath acquisitions in some parts of the polar regions. The microwave radiometer product has a 62.5 km resolution but complete coverage of 2-day sea-ice drift. The 62.5 km could potentially be improved to 25 km with CIMR.

¹⁴ See definition of sea surface salinity

4 MISSION REQUIREMENTS

Mission requirements are derived from the CIMR mission Objectives. Definitions are presented in Appendix-I. Traceability to documented user needs is provided in Appendix-II (Major Policies) and Appendix-III (Requirements Traceability Matrix).

4.1 General Mission Requirements

- MRD-010 The CIMR mission shall embark a conically scanning multi-frequency imaging microwave radiometer payload to measure the brightness temperature of the upwelling microwave radiation at different frequencies.

Note 1: This is the fundamental CIMR mission payload.

Note 2: A conically-scanning microwave radiometer is assumed based on [AD-2] conclusions.

Note 3: The payload should be supported by adequate infrastructure to address orbital knowledge requirements.

- MRD-020 Mission requirements specified in this document shall be met using a single satellite.

Note 1: Multiple CIMR satellites may be on-orbit at the same time to provide continuity of the mission beyond the lifetime of a single satellite. Dedicated requirements are provided to ensure follow-on spacecraft are inter-calibrated with existing spacecraft during a dedicated tandem flight in Sec. 4.1.1.

4.1.1 CIMR Tandem flight

A key commitment in the United Nations Framework Convention on Climate Change (UNFCCC) concerns systematic observation and development of data archives related to the climate system. The Global Climate Observing System (GCOS, established 1992) has on behalf of UNFCCC, established a list of ‘Essential Climate Variables’ (ECVs) that have high impact. In 2006 it identified specific requirements for satellite data products related to these ECVs. The Intergovernmental Panel on Climate Change (IPCC) Fifth Assessment Report (IPCC, 2014) states that “human influence on the climate system is clear, and recent anthropogenic emissions of greenhouse gases are the highest in history. Warming of the climate system is unequivocal, and since the 1950s, many of the observed changes are unprecedented”. The importance of climate change has been recognised by Copernicus and the Copernicus Climate Change Service (C3S) will provide key indicators on climate change drivers to support European adaptation and mitigation policies in a number of sectors (see <https://climate.copernicus.eu/about-c3s>). Other Copernicus services will conduct their own reanalysis activities to provide the best Climate Data Records (CDR under their domains).

As noted by the National Research Council (NRC) of the USA (NRC, 2004) “Validation and overlap of successive satellite missions is critical for developing consistent CDRs over time. Satellite

measurements are by their very nature “remote” and thus in situ observations are needed to validate remotely sensed data and monitor sensor degradation, while overlap is needed to reduce satellite biases”.

As stated by the Global Climate Observing System (GCOS, 2016) “*Observations remain crucial for monitoring, understanding and predicting the variations and changes of the climate system. They need to be collected over substantial timescales with a high degree of accuracy and consistency to observe directly long-term trends in climate. Informed decisions can only be made on prevention, mitigation, and adaptation strategies based on sustained, local and comparable observations*”.

GCOS has established a set of Climate Monitoring Principles (GCMP, GCOS, 2003) that include dedicated principles for satellite operators and systems. The need to fully understand biases between satellite missions is firmly highlighted in the GCMP most notably:

“Take steps to make radiance calibration, calibration-monitoring and satellite-to-satellite cross-calibration of the full operational constellation a part of the operational satellite system”

and

“A suitable period of overlap for new and old satellite systems should be ensured for a period adequate to determine inter-satellite biases and maintain the homogeneity and consistency of time-series observations”

ESA established its own Climate Change Initiative (CCI) programme in 2006 as a response to the UNFCCC. The aim is to realise the full potential of the long-term global Earth Observation archives that ESA together with its Member states have established over the last thirty years, as a significant and timely contribution to the ECV databases required by the UNFCCC. The ESA CCI has been a significant challenge demanding a significant investment to produce a long-term data record, involving a series of satellites from different Space Agencies, different sensors, each with different performance characteristics, most notably, different spatial and temporal sampling, different time extents, and different stability, but with overlaps and calibrations sufficient to allow the generation of homogeneous and well characterised global products that are accurate and stable enough for climate monitoring.

Finally, EUMETSAT operates a Climate Satellite Application Facility (CM-SAF, http://www.cmsaf.eu/EN/Home/home_node.html). The CM-SAF contributes relevant data sets for climate monitoring and research, improves understanding of the climate system by supporting process studies, climate trend and variability analysis and contributes to the improvement of climate models by providing data sets for validation purposes.

Properly characterising differences between a number of CIMR satellite instruments is critical to the success of GCOS ECV activities and in turn the activities of the Copernicus Climate change Service.

Recognising that, even though CIMR satellites would be identical in design, it is expected that differences in performance of payload instruments will exist due to subtle tolerances of materials, manufacture and pre-flight characterisation. Furthermore, as demonstrated by the very successful Copernicus Sentinel-3 Tandem flight there are enormous benefits to conducting a Tandem flight in terms of in-flight calibrations, calibration and validation activities that will significantly enhance the early application of data from new CIMR satellites and the overall mission robustness. Noting the discussion above, it is essential that relative discrepancies between CIMR satellites are properly characterised for CDR construction and the success of the entire CIMR mission.

The main challenge is to reduce uncertainties when comparing data from different CIMR satellite missions that form a time series. When data are obtained from two satellites at different times but at the same location, there is significant correlated uncertainty:

- Uncertainty due to ocean geophysical space and time variability that complicates inter-comparison, especially in regions dominated by mesoscale structure (1-10 days, <10-50 km), which are particularly lucrative to understand inter-satellite bias;
- Uncertainty due to atmospheric space and time variability.

Both issues introduce uncertainty to the direct inter-calibration of CIMR instruments.

However, if a new satellite is added to the CIMR mission resulting in more than one satellite on-orbit at the same time, by flying CIMR satellites in tandem separated by ~30-60s seconds on the same ground track, the correlation between these uncertainties is maximized so that for all practical purposes they can be ignored: the difference between two satellite measurements is solely due to instrumental aspects. Thus, when appropriate, information learned from the commissioning and calibration of one satellite may be transferred to a second satellite with confidence. In addition, End Of Life (EOL) estimates can be established by comparing the performance of the ‘new’ satellite with the ‘old’ satellite.

MRD-030	If a new satellite is added to the CIMR mission resulting in more than one satellite on-orbit at the same time, a tandem flight shall be flown as soon as practically possible, composed of a drift phase towards a tandem configuration, followed by a tandem phase and completed by a last drift phase towards a nominal operational position.
---------	--

Note 1: The user needs of the Copernicus Climate Change Service is for a stable time series of measurements that comply with the Climate Monitoring Principles (GCMP, GCOS, 2003). This implies that the tandem phase is flown entirely during the Phase E1 commissioning phase (i.e. tandem flight to be completed at IOCR and drift to nominal orbit position started).

Note 2: For example, Sentinel-3 has implemented a highly successful Tandem phase during Phase E1. Sentinel-6 will conduct a 12-month Tandem phase building on the previous heritage of the Jason missions.

Note 3: the duration of a CIMR tandem flight (excluding drift phases) is foreseen to be 6 months as specified in MRD-070 implying a tandem phase of 9 months to allow sufficient time for satellite and payload commissioning activities.

MRD-040	The relative along-track separation of CIMR satellites, if configured in a tandem phase, shall be nominally 30 seconds in time apart. The maximum separation between satellites that can be tolerated is 60 seconds.
---------	--

Note 1: The shortest possible separation along-track mitigates the uncertainty due to ocean geophysical space and time variability that complicates inter-comparison and inter-satellite bias; and uncertainty due to atmospheric space and time variability.

Note 2: Sentinel-3A and Sentinel-3B flew a tandem phase separated by 30s in time. The Jason-3 and Sentinel-6 Tandem flight will also separate spacecraft by 30 seconds in time.

Note 3: A separation distance of up to 60s in time was used by the Sentinel-3A/B tandem flight.

Note 4: See MRD-060 regarding tolerance for drift separation.

Note 5: The achieved along-track separation between satellites depends on the launch injection that it is only known after launch.

Note 6: During tandem, the relative across track separation distance must be managed so that differences associated with each satellite payload measurement geometry are minimal. 5 seconds along-track relative separation corresponds to ~2 km relative across track distance - if the orbital planes remain identical. Note that the tandem performed after the launch of Sentinel-3B used sub second relative along track separation distances.

Note 7: MRD-050 defines the tolerance for along-track drift separation.

MRD-050

The relative cross-track separation of CIMR satellites, if configured in a tandem phase, shall be $\leq \pm 1$ km.

Note 1: During tandem, the relative across track separation distance must be managed so that measurement differences associated with conical scan geometry are minimal. This is important for the analysis of tandem data.

Note 2: See MRD-040. During tandem, the relative across track separation distance must be managed so that differences associated with each satellite payload measurement geometry are minimal. 5 seconds along-track relative separation corresponds to ~2 km relative across track distance - if the orbital planes remain identical. Note that the tandem performed after the launch of Sentinel-3B used sub second relative along track separation distances.

Note 3: See also MRD-040. 5 seconds relative along-track relative separation corresponds to ~2 km relative across track distance - if the orbital planes remain identical.

Note 4: This requirement should be met over all surfaces/latitudes if possible since larger across track separation complicated interpretation of river and lake stage heights, data over ice sheet margins and transponder/corner reflectors used for validation activities.

MRD-060

If configured in a tandem phase, knowledge of the relative along-track separation between satellites is required.

Note 1: Knowledge of along-track satellite separation is important for the analysis of tandem data.

Note 2: The nominal along-track separation of spacecraft is 30 s as requested by MRD-040.

Note 3: The achieved along-track separation between satellites depends on the launch injection that it is only known after launch.

An optimal duration for a tandem flight is 12 months as requested by GCOS (2016) and required by the European Integrated Policy for the Arctic (climate pillar). However, for a satellite system

observing both the north and south hemisphere (and therefore a holistic view of seasonal aspects) a 6-month duration is the minimum duration. This excludes the additional time required for the satellite to drift towards the tandem position and towards a nominal phasing position ($\sim 180^\circ$) after a tandem phase.

MRD-070	The duration of a CIMR tandem flight phase shall be a minimum of 6 months from the point at which a Tandem flight configuration is reached.
---------	---

Note 1: Ideally a 12-month tandem phase would allow a full analysis of seasonal uncertainties at a global level as requested by GCOS(2016) and the Integrated European Policy for the arctic (climate pillar). This is the basis for the 12-month tandem flight flown by Jason-3 and Copernicus Sentinel-6.

Note 2: A 6-month tandem phase is considered a minimum duration based on the assumption that uncertainties can be identified over a full seasonal cycle by using coverage of both north and south hemisphere measurements.

Note 3: A tandem flight of 6 months excludes the additional time required to commission the satellite and payload and for the satellite to drift towards the tandem position and towards a nominal orbit position after a tandem phase.

Note 4: The completion of a 6-month tandem flight is likely to include satellite commissioning activities related to the update of the new Satellite Characterisation and Calibration Data Base (SSCDB).

Note 5: A 6-month tandem phase is considered sufficient to detect and quantify regional and seasonal differences between CIMR satellites. The objective is to fully characterise such differences in support of the Copernicus Climate Change Service (3CS).

MRD-080	Deleted
---------	---------

MRD-085	If configured in a tandem phase, data shall be made available to commissioning teams from both satellites operating in Tandem.
---------	--

Note 1: Data from the operational satellite already in orbit will be made nominally available as part the routine operations.

Note 2: Data is required by CIMR validation teams from the new satellite to compare with the old satellite during Phase E1.

MRD-090	If configured in a tandem calibration/validation phase, there shall be no impact on the ground segment operation of the existing in-orbit operational satellite, which shall take precedence.
---------	---

Note 1: Normal operations are required by operational satellites during the Tandem phase.

MRD-095 If configured in a tandem phase, CIMR satellite commissioning activities and on-orbit CIMR manoeuvres shall take precedence over Tandem operations.

Note 1: It is anticipated that commissioning activities may be required during the Tandem flight period.

MRD-100 If configured in a tandem phase and excluding satellite commissioning activities, data shall be acquired in nominal acquisition mode from the satellite to be commissioned throughout the Tandem flight phase.

Note 1: The principle is to assemble a dataset for analysis and establish differences between CIMR instruments that can be used to inter-calibrate CIMR measurements. This is best achieved by maintaining normal operations.

Note 2: The data collected will be used to transfer calibration and characterisation data collected by operational satellite(s) and using that information to understand any differences with respect to new satellites. This may accelerate the uptake and application of CIMR mission data.

4.1.2 Orbit Requirements

The orbit of CIMR is to be placed in a dawn-dusk orbit. This orbit will minimise daily eclipse periods to mitigate the impact of thermoelastic distortion, maximise power generation and minimise the complexity and size of the solar array. Bearing in mind the strong desire to fly in synergy with MetOp-SG(B) and MetOp-SG(A) take full advantage the SCA, MWI, ICI, 3MI and MetImage instruments, the orbit characteristics of CIMR are chosen to maximise the colocation between CIMR measurements and MetOp-SG(B) within ± 10 minutes in the polar regions. In this configuration:

- SST measurements will return an estimate the Sea Surface Foundation Temperature (pre-dawn) for a large portion of the Earth ocean surface. This is preferred by Numerical Weather and Ocean Prediction centres. Should a JAXA AMSR3 instrument fly (potentially in a ~13:00 orbit), CIMR and AMSR3 would be highly complementary in terms of sampling the Diurnal Cycle of SST although the reduced spatial resolution of AMSR would limit its utility in the proximity of coastal regions and inland Seas.
- L-band measurements from SMOS and SMAP are made in a dawn-dusk 06:00/18:00 orbit when Total Electron Content (TEC) is minimal. CIMR will provide continuity of this orbit. In addition, sun-glint over the ocean would also be minimized for better SSS retrieval and would also satisfy some tertiary soil moisture applications (e.g., aid in determining the presence of dew on crop canopy).
- Over 25 years, a large range of geophysical products are derived from the SSMI / SSMIS collection using frequencies that are also available on CIMR. These instruments have a 06:00 / 18:00 orbit. CIMR will provide continuity of this orbit.

MRD-110 The CIMR reference orbit shall be:

CIMR reference orbit definition	
Repeat cycle	29 days
Cycle Length	412 Orbits
Inclination	Sun-synchronous
MLST at descending node	6 h 00 min ±10 min
Eccentricity vector	Frozen
Longitude of 1st Ascending node	Same as MetOp-SG(B) see note 2

CIMR Mean Keplerian Parameters (ToD)	
Semi-major axis	7195.605 km
Eccentricity	0.0011441
Inclination	98.702°
Arg. Of Perigee	90°
MLST at descending node	6h 00 min ±10 min
Longitude of 1st Ascending node	Same as MetOp-SG(B) see note 2

Note 1: For information, the corresponding mean Keplerian parameters in the True of Date reference system are provided. The calculation of these parameters depends on the model used to derive the orbit that fulfils the orbit definition stated above. However, these differences should not exceed a few (tens) meters.

Note 2: The current MetOp-SG(B) longitude of the ascending node of the first ground track at equator is 0°E.

MRD-120 If more than one CIMR satellite is on-orbit at the same time the relative phase between satellites shall be configurable.

Note 1: This requirement allows CIMR to use any phase position in the orbit to accommodate the final configuration of the MetOp-SG(B) satellite constellation.

Note 2: MRD-130 places a single CIMR satellite in a loose formation with MetOp-SG(B). Two MetOp-SG(B) satellites are foreseen and appropriate phasing of CIMR satellites with MetOp-SG(B) satellites is required based on the final flight configuration of MetOp-SG(B).

Note 3: This requirement excludes a tandem flight configuration that have specific phase requirements.

MRD-130 The separation in time between the ascending node crossing of MetOp-SG(B) and the ascending node crossing of CIMR shall be between 1 and 7 minutes.

Note 1: This requirement is used to set the timeliness of crossovers between CIMR and MetOp-SG(B) in the polar regions within ±10 minutes (CIMR orbit control ‘box’ parameter). The impact of a time separation of ±10 minutes between many geophysical products can be, in general, ignored because at a scale of 5-10 km the surface target scene properties of the ocean surface, sea ice and ice sheets will not have changed sufficiently to introduce significant uncertainty into the final products.

Note 2: However, ±10 minutes is significant with respect to atmospheric state: for example (e.g., onset, variation in intensity and vertical position of precipitation; movement of atmospheric field/clouds/rain-bands at 14 m/s corresponds to ~5 km and is possible in that time). But (i) the implications for primary products are small, (ii) background knowledge of atmospheric flow can inform algorithms to help mitigate impact on products, and (iii) potentially contaminated data for which mitigation algorithms are inadequate must be flagged.

Note 3: By flying in synergy with MetOp-SG (B) co-located and near-contemporaneous measurements from MWI channels at frequencies >10.65 GHz MetOp MWI data provide a means to satisfy an AMSR-2-like capability and augment CIMR data products. This implies that implementation of similar bands and channels on CIMR may not be required except for improved spatial resolution and/or redundancy. Relevant MWI bands for the CIMR “mission” are summarised in Table MRD-1 that together with the proposed CIMR “instrument” bands specified in Table MRD-2.

Note 4: There is no obligation to manage detailed spacecraft operations that maintain a strict separation or follow all maneuverers of either spacecraft if properly defined orbit control boxes are specified.

Note 5: MetOp-SG(1B) SCA scatterometer data are extremely valuable to independently verify the ocean surface roughness from CIMR data, for sea ice type classification and SIC melt pond detection amongst other applications in synergy with CIMR.

Note 6: The instrument suite of MetOp-SG (1A) provides a powerful means to validate SIC, SST and other products in cloud free conditions using independent data as well as input to geophysical retrieval algorithms e.g., SIST.

MRD-140 The CIMR ground track shall be maintained to be within ±2.0 km of the reference ground track at the pole defined at the sub-satellite point at nadir.

Note 1: This requirement is used to ensure MRD-180 “no hole at the Pole” is always met.

Note 2: The reference ground track of CIMR is the same as MetOp-SG(B).

Note 3: The meaning is that CIMR will remain within a corridor of 2.0 km either side of the nominal ground track of MetOp-SG(B).

Note 4: See also MRD-180.

MRD-150 The CIMR ground track shall be maintained to be within ± 5.0 km of the reference ground track at the equator defined at the sub-satellite point at nadir.

Note 1: This requirement is used to minimise the differences view geometry between MetOp-SG(B) and CIMR.

Note 2: MetOp-SG(B) has a requirement of ± 5.0 km over the whole orbit which means that the maximum across track distance between geometries (with respect to the sub-satellite point) can be up to 10 km.

Note 3: This requirement controls the along track variation of CIMR with respect to the reference orbit that is relevant to the implementation of MRD-130.

MRD-160 Orbital manoeuvres shall be performed in a manner that minimises data loss of SIC and SST coverage.

Note 1: As the CIMR mission is focused on ocean and sea ice applications, where feasible, all orbital manoeuvres should ideally take place over land surfaces.

Note 2: Large lakes where the largest distance to land exceeds 25 km are an exception to this requirement and include the following Lakes: Caspian Sea, lake Victoria, lake Superior, lake Huron, lake Michigan, lake Ladoga, Garabogazkol basin, Aral sea, lake Erie, Great Slave lake, lake Winnipeg, Great Bear lake, lake Ontario, lake Malawi/Nyasa/Niassa, lake Tanganyika, lake Baykal/Baikal, Ozero Khanka, Uvs lake, Issyk Kul, lago Mar Chiquita, lake Balqhash and lake Onega.

Note 3: Calibration attitude manoeuvres could be implemented to augment the on-board calibration system (e.g., Farrar et al., 2016) including views of well-characterised ocean areas with weak thermal gradients. See MRD-510

4.1.3 Coverage Requirements.

Complete mapping of the Earth surface is required with a focus on Polar Regions which implies a wide swath.

MRD-170 CIMR shall have a swath width that is >1900 km.

Note 1: A large swath width optimises coverage and revisit specified by MRD-180, MRD-190, MRD-200 and MRD-210.

MRD-180 The CIMR mission shall provide contiguous and complete (i.e. no “hole at the poles”) coverage of the Polar Regions [AD-2].

Note 1: This is a strong requirement expressed by the European Commission that acknowledges a primary focus of the CIMR mission on the Polar Regions.

Note 2: See definition of “Polar Regions”.

Note 3: Even if the focus of the CIMR mission is focused on the Arctic, measurements must be provided in the Antarctic region with the same characteristics [AD-2].

Note 4: For L-band, the impact versus benefit of "no hole at the pole" on spatial resolution must be considered against overall mission performance optimization for the application of L-band measurements during the lifetime of the CIMR Mission. The CIMR MAG (ESA-EOPSM-CIMR-MOM-4802) unanimously reaffirmed that priority must be given to the best L-band footprint resolution possible rather than preserving no hole at the pole since this would effectively degrade the entire Global L-band mission for a single pixel at the exact pole.

MRD-190

The CIMR mission shall be capable of >95% global coverage [AD-3] of all Earth surfaces every day using a single satellite and complete coverage in ≤2 days.

Note 1: This requirement excludes outages for spacecraft manoeuvres.

Note 2: Given the constraint of the OZA (MRD-270) it is anticipated that a large swath is provided by CIMR (MRD-170) resulting in ~95% global coverage per day using one satellite.

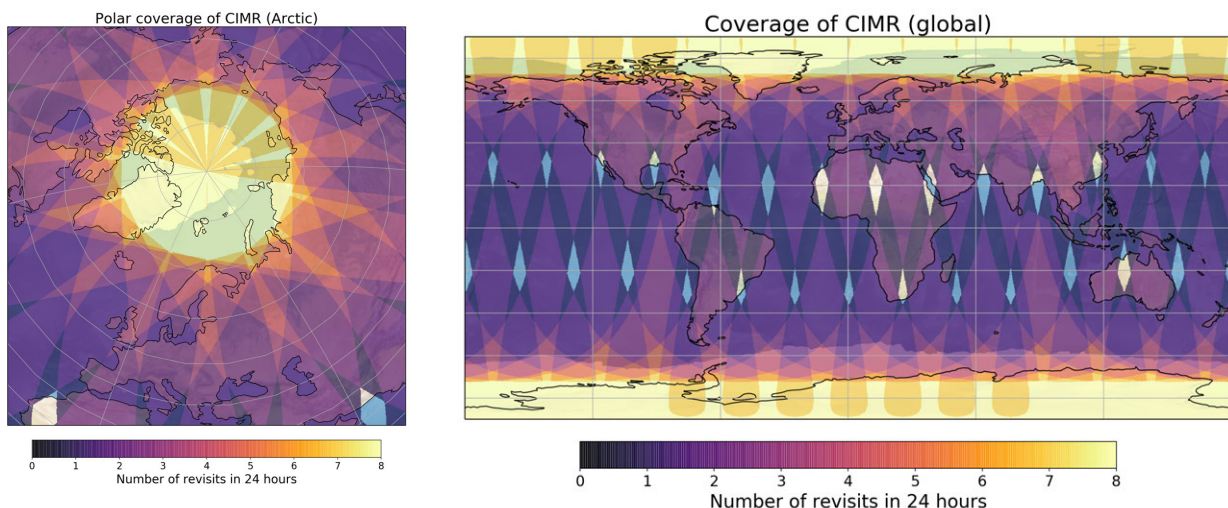


Figure MRD-4.1.2.1. Example plots showing a simulation of the expected CIMR global coverage and over the Arctic using a single satellite highlighting the number of revisits each day with no hole at the pole. Daily coverage of the Copernicus Imaging Microwave Radiometer mission in the Arctic regions. The colormap shows the number of revisit overpasses in a 24 hour period. The CIMR mission is specifically designed to ensure sub-daily coverage in all the Arctic region. Particularly, CIMR will achieve full sub-daily coverage of the Arctic region (i.e. "no hole at the pole" requirement). By symmetry, the coverage is also excellent in the Antarctic region. Over 95% of the globe will be covered on a daily basis (Lavergne, T., Pinol Sole, M. and Donlon, C.: Daily coverage of CIMR (Arctic, Antarctic, and Global views), figshare, doi:10.6084/m9.figshare.7749284.v1, 2019).

4.1.4 Temporal Resolution (Revisit) Requirements

MRD-200 The CIMR mission shall provide daily revisit of the Polar Regions and Adjacent Seas [AD-2].

Note 1: Daily revisit is a primary requirement.

Note 2: See definition of “Polar Regions” and “Adjacent Seas”.

MRD-210 The CIMR mission shall be capable of sub-daily revisit of the Polar Regions [AD-2] >55°N and >55°S latitude.

Note 1: See definition of “Polar Regions”

Note 2: Sub-daily implies at least two measurements are available in a 24-hour period.

4.2 Level-1 Observation Requirements

4.2.1 General Requirements

MRD-220 The CIMR mission shall continuously acquire measurement data in all channels over all Earth surfaces.

Note 1: This requirement implies that the instrument provides a ‘carpet mapping’ approach.

Note 2: MRD-778 requests data is acquired during manoeuvres when this is possible.

MRD-230 On-board calibration measurements shall be used to maintain the calibration of all CIMR channels within requirements at any time during measurement operations.

Note 1: This requirement is developed to always ensure full calibration of CIMR measurement data.

Note 2: It is expected that calibration of the CIMR radiometer will drift as the instrument temperature drifts around the orbit. The task is to design a radiometer that does not change temperature rapidly (e.g., with appropriate thermal design) and then to acquire sufficient calibration data from calibration reference measurements that are able to account for calibration drift.

Note 3: As calibration measurements are inherently noisy, sufficient measurements are required to obtain a smooth estimate of the calibration gain and offset (e.g., every scan).

4.2.2 Frequency Band Requirements

The choice of CIMR frequency bands is based on the following criteria:

- Frequency sensitivity to geophysical parameters of interest,
- Historical perspective (continuity of measurement for the climate record),
- Technical feasibility,
- ITU regulatory framework.

Wilheit (1978) analysed the sensitivity of microwave emissivity of open seawater to a variety of geophysical variables including sea surface temperature, atmospheric water vapour, wind speed, and salinity as a function of frequency (as shown in figure MRD-4.2.2.1).

The frequency allocations to the Earth Exploration Satellite Service (EESS) passive are defined in Article 5 of the International Telecommunications Union (ITU) Radio Regulations (RR) (ITU, 2016). For the allocation of frequencies, the world has been divided into three Regions and specific regulations and allocations apply to each: as Earth Observation is global, the regulations for all Regions (i.e. worldwide) must be considered. In bands used for satellite passive remote sensing, the required minimum availability of sensor data for each band, and the permissible interference level is defined in Recommendation ITU-R RS.2017. “Active Services” are defined in ITU Radio Regulations Article 5 (ITU, 2016) operating either in adjacent bands or in the same band as

EESS(passive) allocations must comply with the regulatory constraints of the RR. Cases of harmful interference to passive sensors must be reported for resolution by the Administration responsible for the active station causing the RFI (See Recommendation ITU-R RS.2106). ITU RR indicate that the receivers should use equipment with appropriate selectivity (RR No 3.12), and this is particularly important for passive sensors to increase robustness against active services operating in adjacent bands.

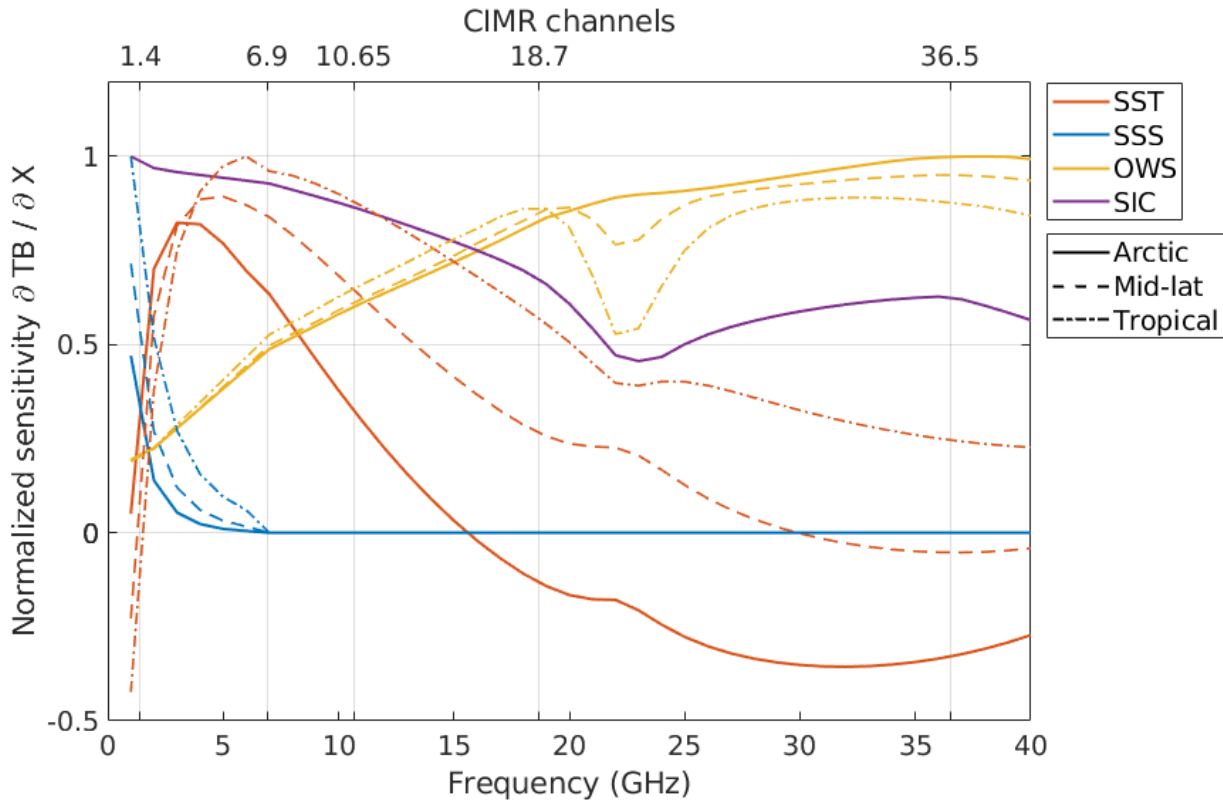


Figure MRD-4.2.2.1 Location of CIMR bands and sensitivity of brightness temperature for open seawater over a range of observing frequencies in the microwave band for a set of key geophysical parameters This figure clearly highlights why CIMR channels are chosen to maximize the information available in the 1.4–37 GHz frequency range. See Figure MRD-2.4.1.1 for CIMR frequency relationships for SIC. The figure illustrates the sensitivities of the low passive microwave brightness temperature at the top-of-the-atmosphere, in terms of Sea Surface Temperature (SST), Sea Surface Salinity (SSS), Ocean Wind Speed (OWS) and Sea Ice Concentration (SIC) as a function of frequency from 1 to 40 GHz. The Copernicus Imaging Microwave Radiometer (CIMR) channels are indicated at the top of the figure. Three different geophysical conditions are considered: arctic, mid-latitude and tropical. For each parameter the sensitivity is normalized by the maximum of sensitivity between the three considered environments, for the full frequency range from 1 to 40 GHz. The sensitivities have been computed using the ocean radiative transfer model of Remote Sensing Systems (Meissner and Wentz, 2012), the sea ice emissivity estimated from the ESA sea ice Round Robin Data Package (Pedersen et al., 2019), and the atmospheric radiative transfer model of Rosenkranz (Rosenkranz, 2017). (Credit: Kilic, et al, 2020)

CIMR must be able to detect data polluted by RFI and take steps taken to mitigate their impact. The selectivity of CIMR channels within EESS(passive) bands shall consider the RFI environment, as otherwise it may result in undesirable increased risk of Radio Frequency Interference from adjacent bands. It is important to note that when using for passive sensing frequency bands with no allocation to the EESS(passive), implies that no protection can be claimed from potential interferers. CIMR will use a dedicated on-board processor system to detect RFI and mitigate the

impact of RFI on the measurements made. Recently the Cubesat radiometer radio frequency interference technology validation mission (CubeRRT) was developed to demonstrate real-time onboard detection and filtering of radio frequency interference (RFI) for wide bandwidth microwave radiometers (e.g., *Johnson et al.* 2020, 2021; *Lahtinen et al.* 2019). CubeRRT's onboard RFI processing capability dramatically reduces the volume of data that must be downlinked to the ground and eliminates the need for ground-based RFI processing. RFI detection is performed by resolving the input bandwidth into 128 frequency subchannels, with the kurtosis of each subchannel and the variations in power across frequency used to detect nonthermal contributions. RFI filtering is performed by removing corrupted frequency subchannels prior to the computation of the total channel power. A similar on-board RFI detection and mitigation approach will be used by CIMR allowing the mission to report infringements of ITU regulations when RFI is detected within protected bands and to increase robustness against active radio services operating in adjacent bands. In addition, such an approach allows the use of a wider bandwidth facilitating compliance to NEΔT requirements.

The fundamental characteristics of CIMR bands are set out in Table MRD-2. Figure MRD-4.2.2.1 shows the EESS Passive and Active frequency allocations showing the location of proposed CIMR bands.

Label	Mission Priority	Primary	Primary	Primary	Primary	Primary
ID-080-1-1	Addressing CIMR Objectives	ALL	ALL	ALL	ALL	ALL
ID-080-1-14 (MRD-250)	ITU EESS (passive) allocated band (GHz)	1.4 – 1.427 ¹⁵	6.425–7.250 ¹⁶	10.6-10.7	18.6-18.8	36-37
ID-080-1-2 (MRD-240)	Channel centre frequency¹⁷ [GHz]	1.4135	6.925	10.65	18.7	36.5
ID-080-1-3 (MRD-380)	Maximum channel bandwidth [MHz]	50 ¹⁸	825	100	200	1000
ID-080-1-4 (MRD-300)	footprint_size [km]	<60	≤15	≤15	≤5.5	<5 (goal=4)
ID-080-1-5 (MRD-420)	L1b Radiometric resolution [K] NEΔT, 1-sigma at 150K	≤0.3	≤0.2	≤0.3	≤0.4 (goal: ≤0.3)	≤0.7
ID-080-1-6 (MRD-430)	Dynamic Range [K]	Kmin=2.7, Kmax=340				
ID-080-1-7 (MRD-440, MRD-450, MRD-460)	L1b Radiometric Total Standard Uncertainty¹⁹ [K, zero mean, 1-sigma] at 150 K	≤0.5 (goal: for an Earth scene Tb dynamic range of ≤70 to ≤300K (MRD-620) including variable NEΔT)	≤0.5 (goal: ≤0.4) (goal: for an Earth scene Tb dynamic range of ≤75 to ≤300K (MRD-580) including variable NEΔT)	≤0.5 (goal: ≤0.45) (goal: for an Earth scene Tb dynamic range of ≤80 to ≤300K (MRD-590) including variable NEΔT)	≤0.6 (goal: ≤0.5) (goal: for an Earth scene Tb dynamic range of ≤100 to ≤300K (MRD-600) including variable NEΔT)	≤0.8 (goal: for an Earth scene Tb dynamic range of ≤110 to ≤300K (MRD-610) including variable NEΔT)
ID-080-1-8 (MRD-560)	Polarisation	Full Stokes ²⁰ (see MRD-550, MRD-560, MRD-570)				
ID-080-1-9 (MRD-170)	Swath width [km]	>1900				
ID-080-1-10 (MRD-270)	Observation Zenith Angle [deg]	52.0 ²¹ ±1.0	55.0 ±2.0			
ID-080-1-11 (MRD-470)	L1b Radiometric stability over lifetime [K, zero mean, 1-sigma]	≤0.2	≤0.2	≤0.2	≤0.2	≤0.2

ID-080-1-12 (MRD-480, MRD-490)	L1b Radiometric stability over orbit [K, zero mean, 1-sigma]	≤0.2	≤0.15 (goal=0.1)	≤0.15 (goal=0.1)	≤0.2	≤0.2
ID-090-1-13 (MRD-660)	L1b geolocation uncertainty [km]	≤1/10 of ID-080-1-4 (see MRD-660)				
Example Applications		SIT, SIC, SSS, WS, SM, SD, MMVI	SIC, SST, SIT, SIST, WS, SID, SM, SD, MMVI	SST, PCP, WS, SD, SM, MMVI	TCWV, LWP, PCP, SIC, SD, SM, SID	SIC, SST, LWP, TCWV, PCP, SIC, SWE, SD

Table MRD-2. Band specifications for CIMR instrument – see specific numbered requirements for detailed specifications. (Application (SIC = Sea Ice Concentration, SST = Sea Surface Temperature, SIT = Sea Ice thickness, SIST=Sea Ice Surface Temperature, SSS= Sea Surface Salinity, WS = Wind speed, TCWV = Total Column Water Vapour, LWP = Liquid Water Path, SD = Snow Depth on sea ice, SM = Soil Moisture, SWE = Snow Water Equivalent, SID = Sea Ice Drift, PCP=precipitation), MMVI=Multi-frequency Microwave Vegetation Indicator)

¹⁵ 27 MHz bandwidth refers to the ITU(Passive) protected band for Earth Observation. Andrews *et al.* (2022) recently explored the 500-2000 MHz RFI environment using airborne techniques concluding that wideband radiometry from 500 to 2000 MHz is viable for science applications in the majority of the regions surveyed. Additional channels within this bandwidth may improve geophysical product performances e.g. centred at 1.1 GHz and 1.7GHz. A larger bandwidth could be supported by CIMR since on-board RFI detection and mitigation approach will be used allowing the mission to report infringements of ITU regulations when RFI is detected within protected bands. Such an approach could facilitate compliance to NEAT requirements.

¹⁶ ITU RR footnote No.5458 indicates that when planning future active systems, the Administrations “should bear in mind” the needs of EESS(passive) in the band 6.425 to 7.250 GHz (6.8375 GHz centre frequency, 825 MHz bandwidth). For the band 6.425-7.075 GHz (650 MHz), this footnote indicates that “passive microwave sensors measurements are carried out over the oceans” and for the band 7.075-7.250 GHz (175 MHz) the remote sensing measurements acknowledged in general. Use of this full bandwidth may bring advantages for radiometric accuracy.

¹⁷ The channel centre frequency is not necessarily the same as the ITU EESS(passive) band centre frequency since the actual CIMR bandwidth may be larger (e.g. see footnote 18). It is fundamental to show that CIMR is able to claim protection from RFI within the allocated band. Therefore it has to be possible that, using only certain sub-bands, rejection levels outside of the allocation are met.

¹⁸ The available bandwidth was increased for the L-band channel prior to PDR in an effort to allow better compliance to NEAT requirements. If this is used, the upper part of the bandwidth allocation should be used as priority since this has better RFI characteristics. However, since this is out of the ITU(Passive) protected band for Earth Observation, the use of on-board RFI detection and mitigation together with filters and limiters to protect out of band RFI is therefore essential.

¹⁹ For CIMR Absolute Radiometric Accuracy (ARA) is not used in the traditional manner but instead we calculate the Total Standard Uncertainty (which is a “zero mean, 1-sigma” total uncertainty). It is noted that this approach, while consistent with international agreements on uncertainty specification (JCGM, 2008), is different compared to other formulations (e.g. as for the MetOp-SG(B) MWI) that do not include NEAT as part of the absolute radiometric accuracy definition.

²⁰ 3rd Stokes signals are small (typically < ±3K) and the 4th Stokes parameter is <±1K implicitly suggesting very good performance in the H- and V-polarisation CIMR measurements and polarization characterisation if these parameters are to be derived from CIMR.

²¹ The OZA for L-band is lowered to attain an improved **footprint_size**. The CIMR MAG (ESA-EOPSM-CIMR-MOM-4802) unanimously reaffirmed that priority must be given to the best L-band footprint resolution possible rather than preserving no hole at the pole since this would effectively degrade the entire global L-band mission for a single pixel at the exact pole.

MRD-240

The CIMR mission shall measure top of the atmosphere brightness temperature using channels centred on frequencies specified in Table MRD-2 ID-080-1-2.

*Note 1: Thus, there are a minimum of **two** CIMR instrument measurement channels (H and V) for each CIMR instrument band e.g., 18.7V and 18.7H and **four computed outputs that are available on ground corresponding to the full Stokes Vector.***

Note 2: See MRD-550, MRD-560 and MRD-570 that request the provision of Full Stokes Vector outputs (e.g., as part of on-board radio-frequency interference processing) as these measurements can be used to support L2 retrievals (e.g., Faraday rotation correction, wind vector measurements).

Note 3: An optimal combination of channels is needed for operational and climate SIC, SIE, and SST L2 algorithms that use different combinations of channels to derive a product.

Note 4: MetOp-SG (B) MWI alone does not provide low frequency channels, nor a sufficient spatial resolution in the channels it carries to address all CIMR objectives (see Table MRD-1).

Note 5: The 7.3 GHz band of AMSR-2 was introduced for radio frequency interference (RFI) mitigation. MWI has on-board RFI mitigation technologies that could also be used by the CIMR instrument: therefore, this channel is not included.

Note 6: The 1.4135 GHz band is required to satisfy CIMR mission objectives (notably thin sea ice thickness, sea surface salinity, Ocean Vector Winds, Soil Moisture, MMVI and other products for Copernicus Services) but should not drive the instrument design. As an additional benefit, this band will allow sea surface salinity and soil moisture measurements to be retrieved. Johnson et al. (2021) and Andrews et al. (2022) recently explored the 500-2000 MHz RFI environment and potential of wideband radiometry using airborne instruments, concluding that wideband radiometry from 500 to 2000 MHz is viable for a broad range of science applications in the majority of the regions surveyed. Additional channels within this bandwidth may improve geophysical products. A larger bandwidth could be supported by CIMR since on-board RFI detection and mitigation approach will be used allowing the mission to report infringements of ITU regulations when RFI is detected within protected bands. Such an approach could facilitate compliance to NEΔT requirements.

Note 7: Recent experience with L-band measurements of extreme wind speed over the ocean has been shown to be extremely useful to operational oceanographic and hurricane forecasting systems/teams (e.g., Reul et al. 2012b; Meissner et al., 2017) providing an additional benefit.

Note 8: A recent study on Arctic sea ice signatures strongly recommends the assimilation of microwave radiometer measurements from 6 to 37 GHz simultaneously with 1.4135 GHz to constrain fractional sea ice coverage and thickness consistently at the same time (Richer et al. 2018).

Note 9: See figure MRD 4.2.2.1.

Note 10: Should extended bandwidths be implemented to facilitate compliance to NEΔT specifications, the centre frequency may deviate from the nominal values reported in Table MRD-2 ID-080-1-2. Above 10.7 GHz the RF environment becomes worse around Europe (reflected RFI over water) and if needed, the BW should be expanded towards lower frequencies. The 10.68-10.7 GHz band has the same excellent regulatory status as 1400-1427 MHz.

MRD-250

The CIMR mission shall be compliant with the ITU Radio Regulations for the EESS(passive) service as specified in Table MRD-2 ID-080-1-14.

Note 1: "Passive Services" are defined in ITU Radio Regulations Article 1 (ITU, 2016).

Note 2: CIMR must be able to detect data polluted by RFI and take steps to mitigate their impact. The selectivity of CIMR channels within EESS(passive) bands must consider the RFI environment, as otherwise it may result in undesirable increased risk of Radio Frequency Interference from adjacent bands.

Note 3: It is important to note that when using frequency bands with no allocation to the ITU EESS(passive), no protection can be claimed from potential interferers. CIMR will use a dedicated on-board RFI detection and mitigation approach which will allow to detect RFI in the data and to report RFI in EESS(passive) bands to the ITU. This approach provides an increased robustness against active radio services operating in adjacent bands.

Note 4: The rejection level requirements shall be met at the edges of the EESS(passive) band allocations. If the selected bandwidth is wider than the EESS(passive) allocation, then it shall be possible to meet the rejection level requirements by selecting only some of the sub-bands for that channel.

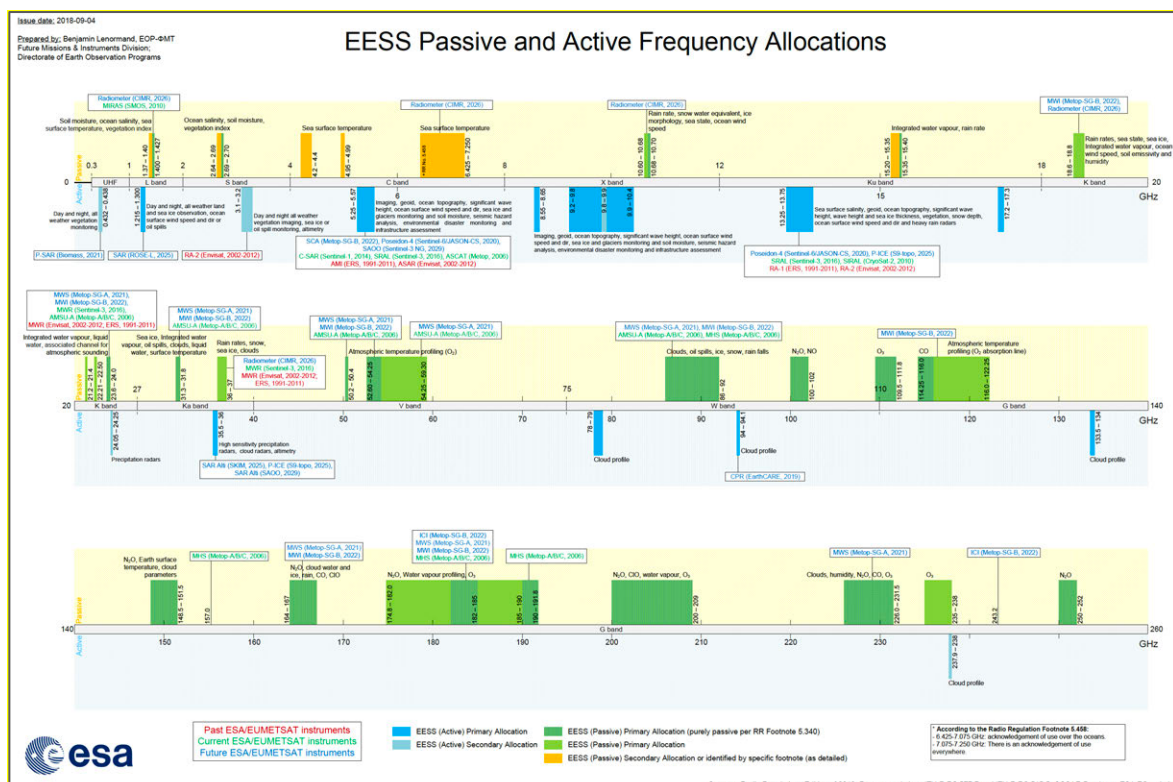


Figure MRD-4.2.2-1: ITU (2016) Earth Exploration Satellite Service (EESS) active and passive frequency allocations and the location of CIMR (and other ESA mission) instrument bands.

MRD-260 All CIMR channels shall include protective measures for unwanted RFI emissions from active services allocated in adjacent bands.

Note 1: "Active Services" are defined in ITU Radio Regulations Article 1 (ITU, 2016). Frequency allocations are defined in the ITU Radio Regulations Article 5.

Note 2: This requirement acknowledges that the use of the full bandwidth allocated to the EESS (passive) as defined by ITU Radio Regulations (ITU, 2016) for a given channel results in increased risk of Radio Frequency Interference from active services operating adjacent bands. In case of poor channel selectivity, CIMR will not be able to claim protection from the active services even in the case of having EESS(passive) a primary allocation in the band.

Note 3: The ability to claim protection from active services in adjacent bands must be achieved. In case the selected bandwidth is wider than the EESS(passive) allocation, it must be possible to select only certain sub-bands in such a way that the overall filter response with the selected sub-bands provides good rejection levels outside the EESS(passive) allocation.

4.2.3 Observation Zenith Angle Requirements

Accurate knowledge of the Observation Zenith angle (OZA) is required for accurate determination of surface emissivity and retrieval of geophysical products – see Wentz and Meissner (2000; 2007) and Meissner and Wentz (2012).

Using a high OZA also increases the swath width and therefore allows coverage and revisit requirements to be improved. However, the price to pay is that there is reduction of spatial resolution at higher OZA: resolution is decreased by $\sim 2\%/\text{OZA}_{\text{degree}}$ in the 50-55° range for an orbit similar to MetOp-SG. At C-band. The sensitivity of the surface Tb (assuming V-pol) to SST increases with OZA. At the same time, the sensitivity to wind speed of the V-pol (which acts as a noise source) decreases with increasing OZA. Ignoring secondary issues related to small increases in atmospheric path length, this favours a large OZA. This is also true for SSS. For high wind conditions (L-band, C-band), H-pol data are preferred in the retrieval and the sensitivity is also larger at high OZA. However, the OZA for L-band can be lowered to attain an improved **footprint_size**, which is a key user need. The CIMR MAG (ESA-EOPSM-CIMR-MOM-4802) unanimously reaffirmed that priority must be given to the best L-band footprint resolution possible rather than preserving no hole at the pole since this would effectively degrade the entire Global L-band mission for a single pixel at the exact pole.

For comparison, the OZA of AMSR-2 and AMSRE is 55°, for SSMI it is 53° and for WindSat at 18 GHz it is 55.6°. For CMIS (one of the proposed payloads for NPOESS although not developed) an OZA of 58.13° was proposed for one of the channels. A higher OZA is preferred from a radiative transfer modelling point of view as it increases sensitivity and thus reduces retrieval error.

MRD-270 All CIMR imaging microwave radiometer channels shall view the surface of the Earth at a boresight observation zenith angle consistent with ID-080-1-10 in Table MRD-2.

Note 1: The intention of this requirement is to maintain a constant OZA for all channels/feeds (see Note 6 and Note 7). The Actual OZA is a combination of radiometer design and in-flight pointing.

Note 2: Accurate knowledge of the Observation Zenith angle (OZA) is required for accurate determination of surface emissivity and retrieval of geophysical products – see Wentz and Meissner, 2000; 2007 and Meissner and Wentz, 2012.

*Note 3: An OZA of ~55° is required to prevent a hole at the pole (MRD-180) while minimising the size of measurement **footprint_size**.*

Note 4: Emissivity of the target source is a function of OZA, band frequency and channel polarisation. It is influenced by surface properties (e.g., wind induced isotropic roughness (waves, capillary diffraction waves, foam, ice/snow surface properties) and by subsurface properties (dielectric coefficient and scatter-size of the target material).

Note 5: For an increasingly rough sea surface, microwave emission increases and polarization differences decrease. At OZA > 55° and a rough sea surface, the vertical polarisation emission begins to decrease. See Wentz and Meissner, 2000; 2007 and Meissner and Wentz, 2012.

Note 6: The OZA may vary from band to band depending on the feed horn accommodation hence a tolerance of ±2.0° is provided.

Note 7: The allocation of the OZA to the feed horn/antenna design should consider high beam efficiency. The nominal OZA should be designed for average distance from spacecraft to ground.

Note 8: Knowledge of the OZA around the orbit is required for L1 and L2 algorithms as specified by geo-location requirements (Section 4.2.16).

Note 9: The OZA has implications for the spatial resolution by about 2.0 - 2.5% per deg. around 53° assuming a MetOp-SG orbit.

Note 10: For sea ice concentration mapping the V and H polarization difference is important for both ice and water. The H and V polarisation difference is a function of OZA

*Note 11: The OZA for L-band is lowered to attain an improved **footprint_size**. The CIMR MAG (ESA-EOPSM-CIMR-MOM-4802) unanimously reaffirmed that priority must be given to the best L-band footprint resolution possible rather than preserving no hole at the pole since this would effectively degrade the entire Global L-band mission for a single pixel at the exact pole.*

4.2.4 CIMR Scanning Requirements

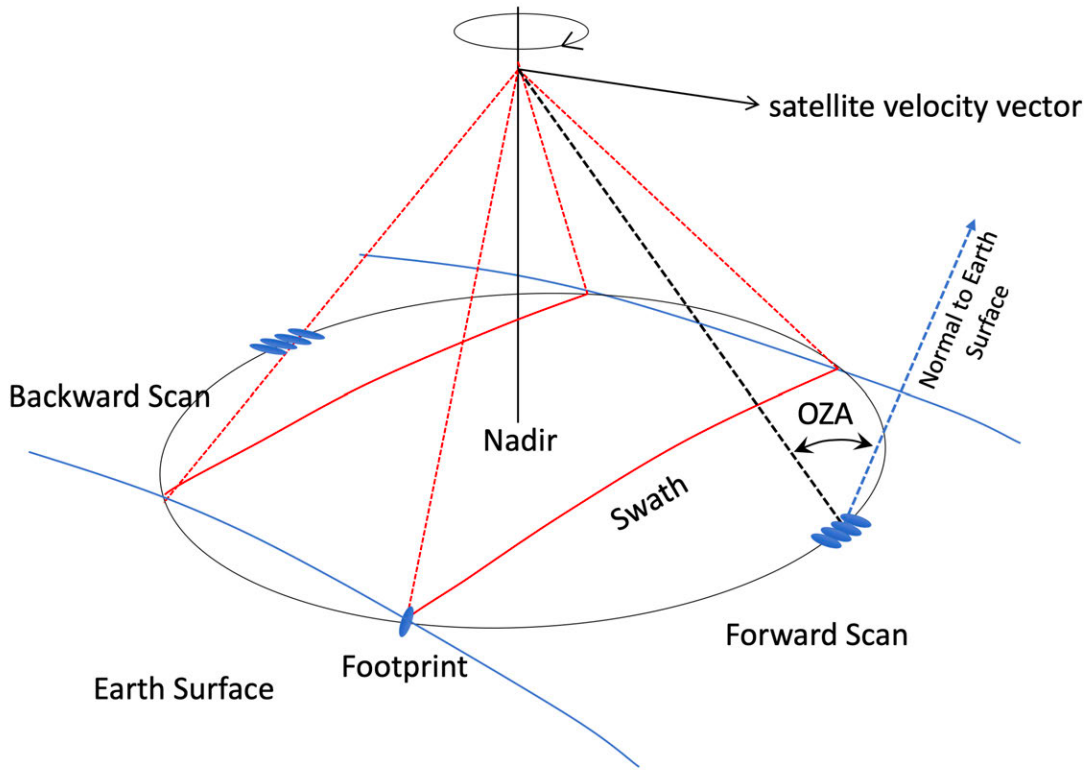


Figure MRD-4.2.4 Schematic overview of CIMR scanning approach and geometry (Donlon, C.; Vanin, F. (2019): Scanning Geometry of the CIMR instrument. Figshare <https://doi.org/10.6084/m9.figshare.7749398.v1>)

The azimuth position and rotation rate of the CIMR antenna are fundamental quantities that for re-analysis and for uncertainty modelling.

- MRD-280** CIMR shall provide continuous sample measurements along the scan arc in the flight direction ('forward scan') and along the scan arc in the opposite direction ('backward scan').

Note 1: Assuming a satellite altitude of 820 km, with OZA=55°, the forward and backward views along the satellite ground track are separated by ~1880 km. Assuming a satellite velocity of 7.2 km/s, the time separation between each view of the surface is ~260s. During this time, the surface conditions of either the SIC at 5 km resolution or SST at <15 km resolution are not expected to change significantly. However, the atmosphere may change from a non-precipitating to a precipitating state.

Note 2: It is assumed that two measurement scan arcs will be necessary to allow for accommodation of calibration data acquisition and potential blinding by the spacecraft solar array.

Note 3: Using both a forward and a backward view of the same scene separated by ~260 s it is expected that significant noise reduction of up to 29% (factor of $1/\sqrt{2}$) could be gained in L2 data processing by using two views of the same area. This applies to geophysical products where the state change in ~260s is negligible

which includes SST and sea ice concentration in non-precipitating atmospheric conditions.

Note 4: For some circumstances where surface characteristics have view angle dependence (e.g., roughness, scattering) independent information may be retrievable from each view. For example, the dual view can help to mitigate Sun glint effects.

Note 5: For some secondary variables, particularly precipitation, the state and location can change in a non-negligible manner in ~260s at CIMR channel resolutions. In such cases, having two views provides two temporal samples, improving robustness of measurements.

Note 6: See Figure MRD-4.2.4 that provides a schematic overview of the OZA.

Note 7: Forward and backward scan data over coastal and island features can be used to study geolocation performance in flight (e.g., Purdey et al 2006).

Note 8: Separate forward and backward scans can be useful in post launch adjustments to the post-launch direct and reflected galaxy corrections since the reflected galaxy typically appears only in the forward or the backward look (Meissner et al. 2022).

MRD-285 The scan azimuth position of each measurement sample shall be available in a L1b product.

Note 1: This requirement ensures that essential azimuth position data are available to the ground processors, for re-analysis and for uncertainty modelling.

MRD-290 Forward and backward scan measurements shall be maintained separately in the L1b products.

Note 1: This requirement allows data from each view to be treated independently from the other during ground processing and facilitates the use of data by standard image processing tools.

Note 2: Forward and backward scan data over coastal and island features can be used to study geolocation performance in flight (e.g., Purdey et al 2006).

Note 3: Separate forward and backward scans can be useful in post launch adjustments to the post-launch direct and reflected galaxy corrections since the reflected galaxy typically appears only in the forward or the backward look (Meissner et al. 2022).

MRD-295 It shall be possible to identify forward and backward measurements of the same scene.

Note 1: It is expected that while forward scan and backward scan measurements are separate, they will be provided in a single L1b data product.

4.2.5 Spatial Resolution Requirements

Figure MRD-4.2.5-1 describes the basic principle of measurement acquisition for a conical scanning antenna referring to the terminology used for CIMR.

The fundamental ability to resolve spatial features for any satellite-based microwave radiometer instrument is linked to the -3dB beamwidth of the instrument for a given band. The Observation Zenith Angle (MRD-270) used by CIMR to observe the Earth's surface means that the CIMR -3dB beamwidth describes an ellipse when projected onto the ground (also known as Instantaneous Field of View, IFoV, or simply footprint). The major and minor axis of the IFoV are termed **a** and **b** as shown in Figure MRD-4.2.5-1(a). For each CIMR band there is a different IFoV and a different value for **a** and **b**. The CIMR requirement MRD-300 uses a linear distance, **footprint_size** (defined as the average of the IFoV major and minor axis length) to characterize the spatial resolution of a CIMR L1b measurement as explained in the following paragraphs.

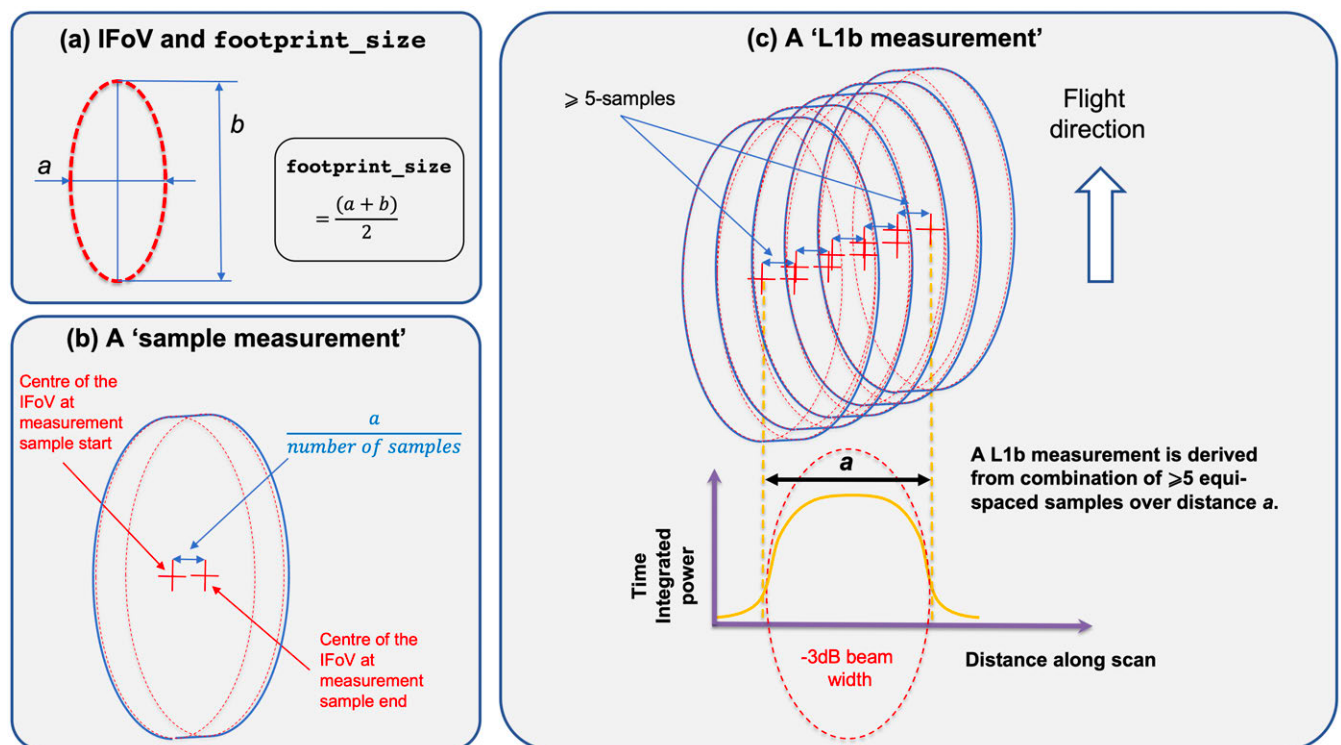


Figure MRD-4.2.5-1 Schematic representation of CIMR L1b measurements. (a) dimensions of a CIMR instantaneous Field of View, IFoV, (or footprint) and definition of **footprint_size**. (b) description of a CIMR sample measurement highlighting the centre position of the centre of the IFoV at the start and end of the sample measurement and the elongated elliptical shape formed on the ground as the antenna rotates and the satellite flies forwards. The sample measurement width is governed by the number of samples chosen for a L1b measurement and the size of the IFoV minor axis. (c) describes a CIMR L1b measurement composed of ≥ 5 sample measurements. It highlights the impact of both along-track scanning and satellite velocity leading to an elongated area covered on ground. The time integrated power obtained during the formation of a L1b measurement forms a shape that approximates the -3dB beamwidth of the antenna main beam for each CIMR band.

CIMR continuously integrates the received signal collected by the rotating antenna and forms discrete measurements across the instrument swath to meet coverage and revisit requirements (MRD-180, MRD-190, MRD-200, MRD-210). Figure MRD-4.2.5-1(b) describes a **CIMR sample measurement**. Due to the rotating beam and satellite velocity, sample measurements are ‘smeared’ in both the flight direction and the scan direction. This outcome is common to all to all conically scanning microwave radiometers.

Figure MRD-4.2.5-1(c) illustrates a **CIMR L1b measurement** and shows how the antenna -3dB footprint ellipse (IFOV) scans over a surface during a L1b measurement time (integration time). CIMR will provide an along scan L1b measurement every -3db footprint minor axis distance (distance **a**). To reach performance requirements at L1b (i.e. not at sample measurement level and not using samples from adjacent scans), there are ≥ 5 sample measurements in each **L1b measurement** (see MRD-340) that are combined (e.g., by weighted or linear averaging, a choice for implementation) in the along scan direction. Since the IFoV minor axis, **a**, is, by definition, **<footprint_size**, a sample width could depend on the size of the IFoV minor axis, **a**, and the number of samples requested for a L1b measurement e.g.:

$$\text{sample_width} = \frac{a}{\text{number of samples}}$$

Figure MRD-4.2.5-1(c) illustrates that the resulting ‘time integrated power’ of the L1b measurement approximates an ‘effective -3dB beamwidth’ of the main antenna beam, considering the antenna gain within the footprint ellipse and, the time spent of that gain shape over the scanned surface. The important thing to note is that instrument resolution, i.e. the distance between the -3dB points, is approximately maintained even though the instrument scans.

A CIMR L1b measurement must meet NE Δ T requirements (see MRD-420) and the criteria set such that the distance between the centre of the first IFoV of the first sample measurement and the centre of the last IFoV of the last sample measurement **<footprint_size** requirements (MRD-300).

Finally, considering a given location on the Earth surface, sample measurements at that location will be measured many times by the CIMR instrument – particularly in Polar Regions. Depending on the azimuth position of the sample measurement within the instrument conical scan cycle, the major and minor axis of the IFoV will have different orientation at that Earth location. For these reasons, the CIMR **footprint_size** is considered the spatial resolution of the CIMR instrument L1B measurement.

As an example, for illustration purposes only, we consider a L1b measurement spatial resolution at Ka-band of <5 km. To simulate the approach described above, we assume a perfect 1D Gaussian beam with a -3dB minor axis of 3.5 km (representing the IFOV) as shown in the orange curve in Figure MRD-4.2.5-2. If we integrate over the minor axis distance (i.e. 3.5 km), the effective -3dB width of the L1b measurement is slightly larger (4.4 km) as shown in the blue curve (which has been normalised in terms of power since there is more power in the integrated measurement). This satisfies the L1b measurement spatial resolution at Ka-band of <5 km requirement constrained by **footprint_size**.

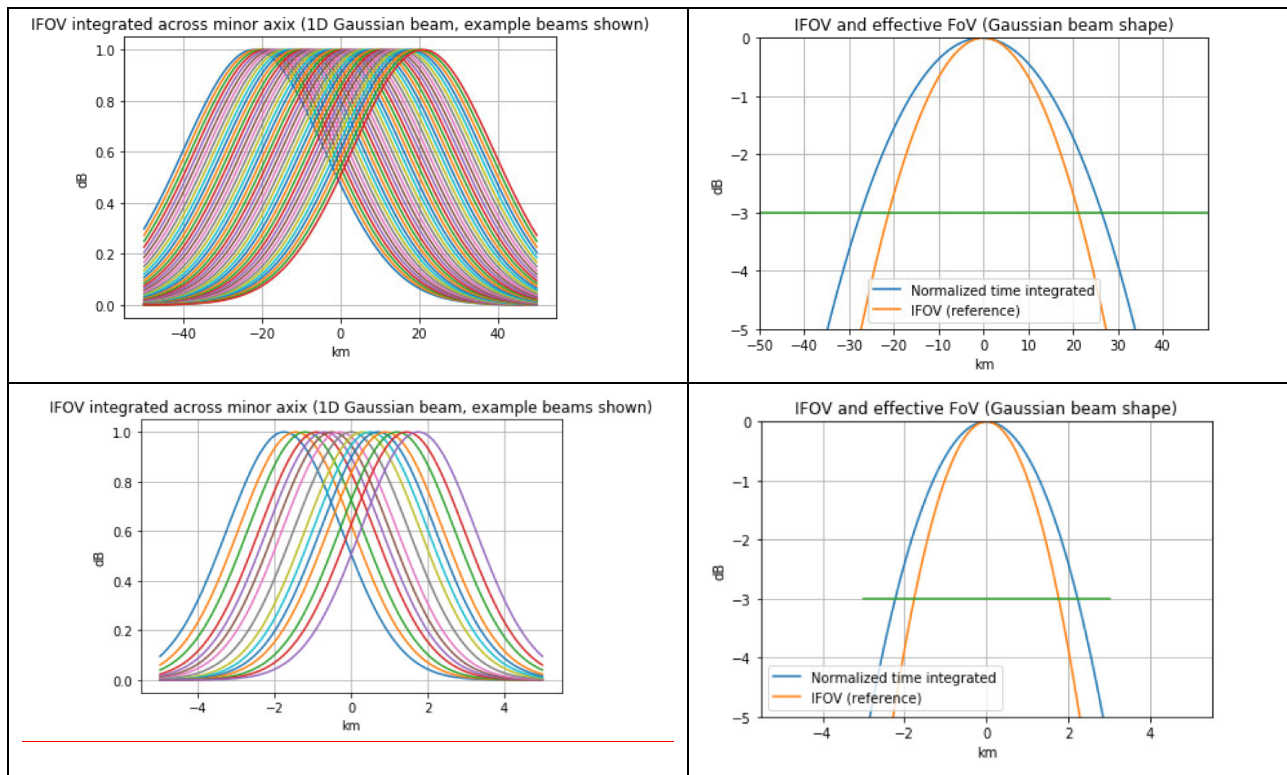


Figure MRD-4.2.5-2. Simulation results for a hypothetical L1b measurement assuming a 1D Gaussian beam. (top) for L-band with a mirror axis of 43 km and (bottom) with a minor axis, $a=3.5$ km. Left plot illustrates example measurements (in practice this is a continuous integration) taken as the beam scans across the swath. Right plot shows the reference IFOV (orange curve) and the slightly wider normalized time integrated L1b measurement (blue curve). The -3dB level is shown by the green line.

Clearly, an individual CIMR sample integrates over a smaller time compared to a L1b measurement, therefore a sample measurement has a larger NEAT compared to a L1b measurement. For some applications this is acceptable (e.g., detecting the sea ice edge or strong gradients in an SST field). Note that RFI mitigation (see MRD-630) will modify NEAT if part of the signal is removed during on-board RFI processing.

Since a L1b measurement represents a smeared area measurement at a given location in the azimuth (i.e. varies around the azimuth) geolocation must be evaluated using a precise approach. For CIMR, geolocation should be evaluated for each beam, at the antenna boresight position on ground, corresponding to mid-point along the beam scan that lies exactly between the centre of the first IFOV of the first measurement and the last IFOV of the last measurement, for a given measurement integration interval. See MRD-660.

Figure MRD-4.2.5.3 compares the CIMR L1b measurement -3dB field of view to MetOp-SG(B) MWI, GCOM-W AMSR2, ESA SMOS (L-band only) and NASA SMAP (L-band only) missions. In the case of L-band, it must be recalled that SMOS has a range of spatial resolution (35 to 60 km) depending on the position of the pixel (incidence angle) in question. SMAP (applying a similar definition of spatial resolution as CIMR) has a constant instantaneous spatial resolution of ~41 km (-3dB footprint is 36 x 47 km).

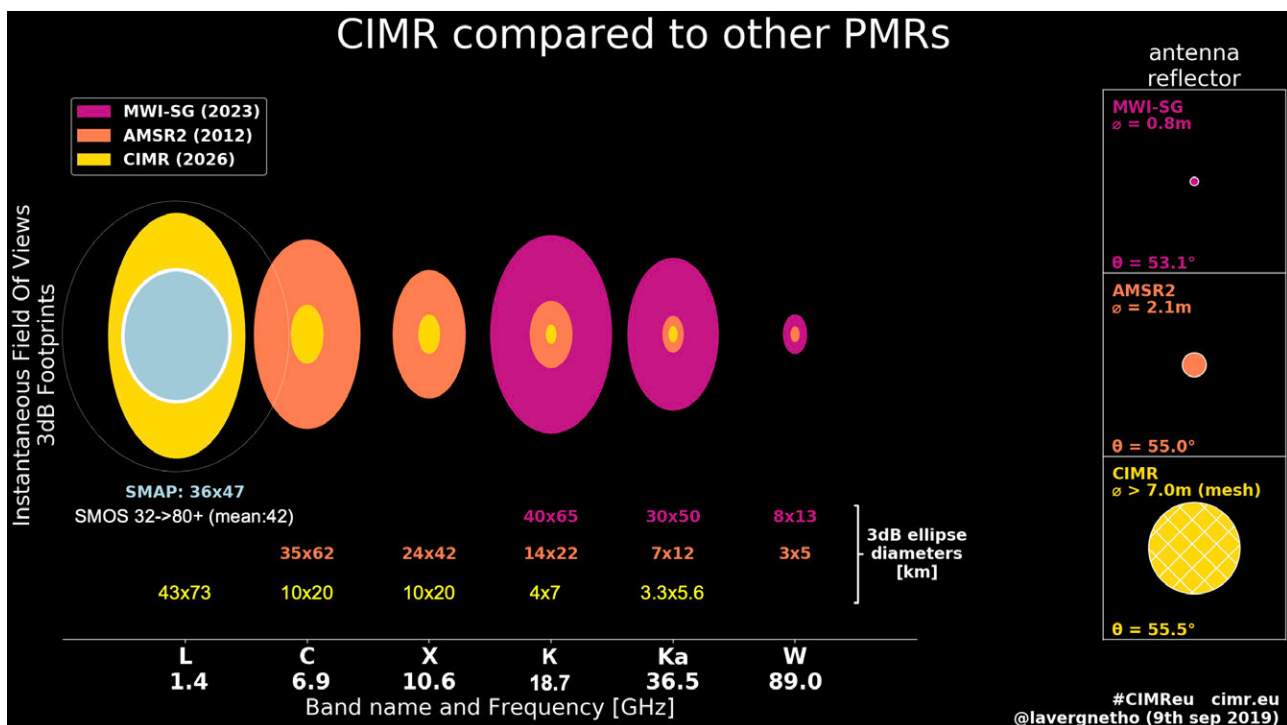


Figure MRD-4.2.5-3. Illustration of the frequency channels of the CIMR mission, and their targeted spatial resolution. CIMR is also compared to other similar Microwave Radiometers: JAXA AMSR2 in orbit since 2012, and the MWI to fly on-board the European EPS-SG satellites from ~2023 (MWI-SG).

SMAP (in orbit since 2015) and SMOS (in orbit since 2009). SMOS has a variable resolution depending on the OZA shown in white starting as close to circular and increasing as an ellipse at higher OZA (After Lavergne, Thomas (2019), Figshare <https://doi.org/10.6084/m9.figshare.7177730.v7>)

The ability of CIMR to resolve strong contrast features on the ground (such as sea ice and open water) is linked to the characteristics of both sample and L1b measurements. Therefore, to provide flexibility of processing by different applications (e.g., for SIC discrimination), a L1b product also contains all samples for each L1b measurement (MRD-640 and MRD-650). While CIMR has a constant L-band resolution of <60 km, it is anticipated that L-band products (after data processing) will be made available at ~40 km spatial resolution by exploiting the large, oversampled characteristics of this channel.

MRD-300 The spatial resolution of a CIMR measurement at L1b shall comply with ID-080-1-4 in Table MRD-2 and is computed by combining a number of measurement samples (specified in MRD-340) acquired during the measurement integration time.

Note 1: See definition of `footprint_size`.

Note 2: The spatial resolution of a CIMR measurement at L1b is translated for implementation into the `footprint_size` that considers the instantaneous field of view and the natural behaviour of the instrument (smearing) - see Figure MRD-4.2.5.1.

- Note 3: This implies a high-resolution instrument real aperture instantaneous field of view with low side-lobe characteristics (i.e., good beam formation) and measurement oversampling.*
- Note 4: In addition to the L1b measurement, L1b products will include all measurement samples made during a measurement integration time according to MRD-340.*
- Note 5: See definition of integration time.*
- Note 6: It is anticipated that resampling/gridding techniques will be employed in L2 processing to achieve an L-band gridded spatial resolution of < 50 km (goal: 40 km, commensurate with SMOS/SMAP) in all L2 and higher products.*
- Note 7: Other CIMR channels may be used in synergy with the L-band channel to sharpen geophysical products at L2.*
- Note 8: CIMR produces a continuous stream of measurement samples that are combined on-ground to derive a level-1b measurement.*
- Note 9: The 36.5 GHz channel is required for high-resolution SIC algorithms and in addition SST, TCWV, LWV, PCP, SIC, SWE, SDE. This was confirmed at the CIMR MAG #01, ESTEC, April 12-13th 2018.*
- Note 10: A goal for the 36.5GHz channel is a `footprint_size` of 4 km. This was confirmed at the CIMR MAG #01, ESTEC, April 12-13th 2018.*
- Note 11: The CIMR MAG (ESA-EOPSM-CIMR-MOM-4802) unanimously reaffirmed that priority must be given to the best L-band footprint resolution possible rather than preserving no hole at the pole since this would effectively degrade the entire Global L-band mission for a single pixel at the exact pole.*
-

MRD-310

L1b products shall include all measurement samples acquired during a measurement integration time according to MRD-340.

- Note 1: L1b measurements are foreseen to be computed on-ground from L1b measurement samples that are continuously acquired during a L1b measurement integration time according to MRD-340.*
- Note 2: In addition to the L1b measurement, all samples are included in L1b products to allow users working on applications over complex terrain (e.g., SIC determination in the marginal ice zone), to use samples in addition to L1b measurements to enhance that have a higher noise but smaller size compared to a L1b measurement.*
- Note 3: A L1b file contains only samples allowing users to translate samples directly to L2 products. It is foreseen that an appropriate Open-Source tool is available to assist users in the manipulation of L1b samples.*
-

4.2.6 Sampling Requirements

The `footprint_size` of each CIMR frequency band is different and limited to first order by the size of the antenna reflector. In addition, the Earth location of a footprint centre for each frequency corresponding to the same sample may differ depending on the final location of individual feed horns on the focal plane.

The effective spatial resolution of a measurement is determined by the antenna gain pattern and the measurement integration period.

The antenna pattern acts as spatial filter of the surface brightness distribution limiting the contribution to the observed radiance to a portion of the scene.

The antenna gain pattern is particularly important for the construction of L1b measurement data as it can be used to compensate for unwanted but significant contributions from outside the -3dB footprint measurements. L1b processing typically starts from L1a data products and can include amongst other aspects:

- Application of all calibration data.
- Removal of spill-over effects.
- Removal of antenna reflector self-emission.
- Removal of cross-polarised contamination.
- Correction for OZA variation around the orbit.
- Removal of other contributions (e.g., from the instrument structure or cold space).
- Removal of antenna shape aspects (e.g., grating lobe contributions caused by reflector faceting effects if present).
- Removal of sidelobe contributions from the antenna pattern.
- Computation of geolocation parameters for each measurement.
- Computation of fractional land area inside the main lobe for each measurement.
- Computation of standard total uncertainty for each measurement.

Accurate characterisation knowledge of the antenna gain pattern (e.g., including side-lobe and grating lobe patterns if present) for each channel is required to derive L1 and L2 products and is therefore required by the application community to develop, test, and reanalyse CIMR data.

In a conically scanning radiometer design, the antenna is scanning during the integration period, and the effective antenna gain is a smeared version of the antenna pattern. The performance of the CIMR mission TOA radiances for each channel footprint requires an excellent Antenna Pattern Correction (APC) – including all significant lobe contributions outside the main beam - to meet Mission Requirements in terms of spatial resolution and radiometry at L1b.

Following *Meissner et al.* (2011), for an antenna that is taking spatial samples at a rate that is at least twice the spatial frequency response (Nyquist rate) where the spatial frequency response is characterized by L , (the `footprint_size` in km), then samples need to be taken every $L/2$ km or more. For the GMI instrument, only channels 1-7 (10.7 – 37.0 GHz) are at least Nyquist sampled. The AMSR-E and AMSR/2 instruments record measurements at equal intervals of 10 km (5 km for the 89 GHz channels) along the scan to satisfy the Nyquist criteria along-scan. However, there remain gaps in the 89 GHz antenna patterns (*Maeda et al.*, 2016) preventing contiguous sampling between scans at the 89GHz frequency (i.e., no overlap). The SMAP radiometer makes an along-scan sample every 11 km, which is smaller than the 20-km Nyquist criterion ($L=40$ km). With the spacecraft moving at 6.8 km/s speed over ground, the across scan sampling at centre of swath is 28 km - slightly lower than the 24-km Nyquist criterion (*Piepmeier et al.*, 2016).

The antenna gain pattern is a fundamental input to the instrument measurement and may vary as a function of azimuth and elevation. To facilitate procession from L1a to L1b, uncertainty characterisation, reprocessing and calibration/ validation activities, access to 2D antenna gain patterns as sufficient resolution to resolve all side-lobes and grating lobes is required.

MRD-320

The full antenna gain pattern shall be known and made available to users for all channels and all feeds with sufficient information to resolve all side-lobes and grating lobes.

Note 1: This information is fundamental for the proper production of L1b measurement data from L1a data because the energy from side lobe and grating-lobe locations must be: (1) determined from the CIMR measurements and (2) used in L1b algorithms to adjust the calculated brightness temperature to compensate for these additional out of field radiance sources (3) the gain patterns are required for use in the L1b uncertainty modelling.

Note 2: Users may choose to apply different methods to L1b data product production depending on the specific application.

Note 3: This information is typically derived from on-ground characterisation.

Note 4: See MRD-440, MRD-450, MRD-460, MRD-470 and MRD-480 where this information is applied in L1b processing.

Note 5: The antenna gain pattern may vary as a function of azimuth and must be well known with cuts sufficient to resolve all side-lobes and grating lobes.

Note 6: The uncertainty of the antenna gain patterns will be used in the CIMR end to end uncertainty budget and performance.

MRD-330

CIMR spectral response functions for all CIMR channels shall be known and made available to users.

Note 1: This was a strong request from the MWI user community and CIMR Mission Advisory Group (MAG) as a lesson learned.

Note 2: The spectral response function is relevant for RFI characterisation and reconstruction of NEΔT calculations on ground.

Note 3: These quantities are required for radiative transfer model application in Level-2 retrievals and reprocessing activities.

When the Nyquist criterion is not met spatial aliasing occurs and signals from individual footprints become indistinguishable from each other when combined resulting in artificial artefacts and distortion. Kemppinen and Hallikainen (1992) set out an approach to determine the ideal scanning method for a scanning radiometer and suggest an overlap of ~30% was required in the MIMR case. The approach of AMSR, AMSR/2 and SSM/I was a compromise to ensure continuity of the highest frequency band(s) measurements in the flight direction.

The CIMR situation to satisfy the Nyquist sampling criteria L/2 is as follows:

Beam centre frequency (GHz)	Beam Target resolution, L (km)	Nyquist sampling criteria, L/2 (km)
1.4135	<60	30
6.9	≤15	7.5
10.65	≤15	7.5
18.7	≤5	2.5
36.5	<5	2.5

In the case of CIMR, an overlap in the along-scan direction is required for all channels. Lower frequency CIMR bands (1.4 to 10.65 GHz) must be strongly oversampled to allow interpolation schemes used in higher-level processing schemes to work most effectively. Furthermore, lower frequency bands are expected to have demanding antenna pattern corrections as beam efficiency falls due to the limited size of the CIMR reflector with respect to 1.4 and 6.9 GHz: oversampling will help reduce this aspect.

As a starting point, and to facilitate the application of L1b sample data for complex scenes (e.g., marginal ice zone, coastal transitions, strong SST frontal boundaries) CIMR will provide access to a discrete sample that are combined to generate a L1b measurement. Five samples are chosen as a starting point to allow L1b measurements to be centred on a definite sample (odd number of samples) although more could be provided depending on the implementation.

It should be noted that care must be given to the sampling characteristics of different channels relative to each other to facilitate the use of different channels together.

MRD-340 The CIMR radiometer shall provide at least five equi-spaced samples along-scan during a L1b measurement integration time.

*Note 1: Five samples is a **minimum** requirement. It is beneficial to have oversampling in the along scan direction with more than 5 samples when reconstructing gridded fields.*

Note 2: For specific applications (e.g., SIC) access to higher noise and more frequent sampling can be beneficial. To limit smearing and the size of an EFoV, the number of samples may be increased at the cost of a higher NEΔT.

Note 3: NEΔT is computed for the L1b measurement full integration time. Individual samples are likely to have a higher NEΔT and may be computed separately.

Note 4: Samples allow the intra-measurement noise characteristics to be monitored.

Note 5: For the 36.5 GHz channel this results in minimum separation of samples at ~1 km.

Note 6: Given that oversampling is highly desirable to reduce uncertainties in post processing when aligning different channels to each other. Ideally, a sampling strategy is required in which channels are sampled in a manner that allows the L1b processor to co-align samples on ground.

Note 7: A suitable arrangement of the radiometer feed horns/array will be required due to the different beam size of each channel.

MRD-350 The CIMR radiometer shall sample the target scene in the along-track direction **and** the along-scan direction by overlapping L1b measurements by ≥20% for all channels.

Note 1: The approach of AMSR, AMSR2 and SSM/I ensured at least contiguity (i.e. limited or no overlap) of the highest frequency band in the flight direction was attained.

Note 2: It is essential that a significant overlap in the across-scan direction is achieved for all channels below 18.7 GHz to allow satisfactory noise reduction when

interpolating low-spatial resolution data to high spatial resolution data. Kemppinen and Hallikainen, (1992) suggest an overlap in the across scan direction of 30% although this is particularly challenging.

Note 3: For X-band marginal compliance to oversampling may be permissible.

Note 4: A suitable arrangement of the radiometer feed horns/array will be required due to the different beam size of each channel.

Note 5: This requirement applies at the centre point of the forward and backwards swath. Due to the conical scanning principle the remainder of the swath will be automatically oversampled.

MRD-360

The CIMR radiometer shall sample the target scene with at least contiguous footprints in the along-track direction for 18.7 GHz channels.

Note 1: The approach of AMSR, AMSR/2 and SSM/I ensured at least contiguity (i.e. limited or no overlap) of the highest frequency band in the flight direction was attained.

Note 2: At Ku band the key scientific driver is high spatial resolution of 5 km. In this case, a compromise configuration could foresee a contiguous footprint arrangement in the along-track direction with no overlap of beams but with the major axis of each footprint at least tangential with the next in all parts of the forward and backward scan.

Note 3: This requirement applies at the centre point of the forward and backwards swath. Due to the conical scanning principle the remainder of the swath will be automatically oversampled.

MRD-370

The CIMR radiometer shall sample the target scene so that discontinuities between footprints shall be ≤ 1.3 km in the along-track direction for 36.5 GHz channels.

Note 1: Discontinuities may be permissible ≤ 1.3 km in the along-track direction.

Note 2: The approach of AMSR, AMSR/2 and SSM/I ensured at least contiguity (i.e. limited or no overlap) of the highest frequency band in the flight direction was attained.

Note 3: At Ka band the key scientific driver is high spatial resolution of 4 - 5 km. In this case, a compromise configuration could foresee a near-contiguous footprint arrangement in the along-track direction with no overlap of beams but with the major axis of each footprint tangential with the next for the majority of the forward and backward scan. In this arrangement, small discontinuities (e.g., ≤ 1.3 km) in an angular sector in around the along track direction in the forward and backward scan could be permissible.

Note 4: This requirement applies at the centre point of the forward and backwards swath. Due to the conical scanning principle the remainder of the swath will be automatically oversampled.

4.2.7 CIMR Spectral Performance Requirements

MRD-380 The maximum CIMR channel bandwidth shall be within the limits set by ID-080-1-3 in Table MRD-2.

Note 1: CIMR channel bandwidth shall be defined together with the frequency stability, Δf_0 , as each channel must comply with the EESS(passive) frequency allocations in the ITU radio-regulations. A larger bandwidth could be supported by CIMR since on-board RFI detection and mitigation approach will be used allowing the mission to report infringements of ITU regulations when RFI is detected within protected bands. Such an approach could facilitate compliance to NEΔT requirements.

Note 2: Channel bandwidths set within the limits of ID-080-1-3 in Table MRD-2 and will correspond to -30dB-power bandwidths, unless justified. If the full allocated band is not used then the -30dB will apply at the edge of the band as a minimum.

Note 3: CIMR channel central frequency, depends on the selected channel bandwidth and is not necessarily the same as the centre of the EESS(passive) allocated band.

Note 4: ITU note that for C-band, the passive frequency allocation is 6.425 to 7.250 GHz (6.8375 GHz centre frequency, 825 MHz bandwidth) with footnote 5.458 that states: "6.425-7.075 GHz: acknowledged for use over the oceans" and "7.075-7.250 GHz: there is an acknowledgement of use everywhere". Use of this full bandwidth may bring advantages for radiometric accuracy.

Note 5: The overall RFI contamination in the passive band 1400-1427 MHz is a significant challenge. Different types of RFI sources have been identified by SMOS and SMAP radiometers and typically these are detected as individual RFI sources. Three main categories: (1) excessive unwanted emissions from radars in adjacent band, (2) unauthorised equipment (e.g., radio links, surveillance cameras, etc.) operating in-band and (3) malfunctioning equipment in adjacent bands (e.g., IM or harmonics, frequency shifts, etc). In addition, since Oct 2011 it is observed over Japan and extended RFI over urban areas (aggregated impact of hundreds of individual RFI sources). The cause found is due to poor shielding in IF circuits (L-Band) of 12 GHz Home-TV Satellite Receivers. ESA has been able to report and claim protection for SMOS thanks to the excellent selectivity of the SMOS radiometer ($F_0 = 1413.5$ MHz, BW_{3dB} limited to 20 MHz, and more than 30 dB rejection at the edges of the allocated band: 1400 MHz and 1427 MHz).

Note 6: For salinity, soil moisture and thin sea ice thickness measurements a channel at 1.4GHz within the narrow ITU protected band will have least amount of RFI and maintains continuity with past missions. However, other channels in the 1.0-2.0 GHz band are of interest since the sensitivity to salinity peaks at ~600 MHz. Andrews et al. (2022) recently explored the 500-2000 MHz RFI environment using airborne techniques concluding that wideband radiometry from 500 to 2000 MHz is viable for science applications in the majority of the regions surveyed. Additional channels within this bandwidth may improve geophysical product performances e.g., centred at 1.1 GHz and 1.7GHz. A larger bandwidth could be supported by CIMR since on-board RFI detection and mitigation approach will be used allowing the mission to report infringements of ITU regulations when RFI is detected within protected bands. Such an approach could facilitate compliance to NEΔT requirements.

Note 7: There is a trade-off between the bandwidth of the 36.5 GHz channel and the end-to-end performance of the channel especially in terms of the reflectivity of the antenna mesh. The current specification uses that of AMSR-2.

Note 8: This requirement acknowledges that the use of the full bandwidth allocated to the EESS (passive) as defined by ITU Radio Regulations (ITU, 2016) for a given channel results in increased risk of Radio Frequency Interference from active services operating adjacent bands. In case of poor channel selectivity, CIMR will not be able to claim protection from the active services even in the case of having EESS (passive) a primary allocation in the band.

Note 9: The ability to claim protection from active services in adjacent bands shall be achieved. In case the selected bandwidth is wider than the EESS (passive) allocation, it shall be possible to select only certain sub-bands in such a way that the overall filter response with the selected sub-bands provides good rejection levels outside the EESS(passive) allocation.

MRD-390 CIMR shall provide frequency selectivity to guarantee that received RFI can be uniquely identified to originate from within the ITU allocated bands.

Note 1 Typically, CIMR channel out-of-band (OOB) rejection shall be >30 dB at the edges of the allocated bandwidth per channel.

Note 2 The OOB rejection refers to the complete chain from the antenna aperture to the instrument output. This is to protect from adjacent band activities (e.g., active radars etc)

MRD-400 CIMR channel out-of-band rejection, specified at the receiver input shall ensure protection and non-destructive impact from high power transmitters (mainly radars) in adjacent or near-by bands.

Note 1: The purpose of this requirement is to make sure that the receiver is able to withstand very high-power radars in adjacent bands that could cause damage or stress.

MRD-410 CIMR shall be able to withstand potentially damaging RFI sources.

Note 1: This requires evaluation of signal levels as in the case of SMOS withstanding high-power radars in band that blinded the instrument for a few seconds.

4.2.8 Radiometric resolution ($\text{NE}\Delta T$) Requirements

In cold polar regions $\text{NE}\Delta T$ is a limiting factor for L-band measurements of SSS and is a fundamental requirement. For SST, C-band and X-band $\text{NE}\Delta T$ is a fundamental requirement in order to satisfy Copernicus SST performance requirements. For sea ice concentration at Ka/Ku band, $\text{NE}\Delta T$ is more relaxed since the operational algorithms employed employ difference ratios.

-
- | | |
|---------|--|
| MRD-420 | The $\text{NE}\Delta T$ of each CIMR channel at L1b shall comply with ID-080-1-5 in Table MRD-2. |
|---------|--|
-

Note 1: CIMR is focussed on Polar Regions where sea ice has a typical (frequency dependent) dynamic range of e.g., <100 to ~260 K @18.7 GHz. Therefore, radiometric resolution ($\text{NE}\Delta T$) is specified as 1σ at a reference temperature (T_{ref}) of 150 K as for AMSR-2.

Note 2: See definition of $\text{NE}\Delta T$.

Note 3: $\text{NE}\Delta T$ is a significant performance specification.

Note 4: $\text{NE}\Delta T$ is computed using a combination of all samples acquired for a L1b measurement MRD-340.

Note 5: An uncertainty of 0.1 K in T_b leads to an uncertainty of ~0.3 psu in SSS in cold Arctic waters. Thus L-band $\text{NE}\Delta T$ is stringent.

Note 6: C-band is a primary channel for SST and has a very stringent $\text{NE}\Delta T$ of 0.2K if the required uncertainty in cold Arctic waters is to be met.

4.2.9 Dynamic Range Requirements

-
- | | |
|---------|---|
| MRD-430 | The dynamic range of each CIMR channel shall comply with ID-080-1-6 in Table MRD-2. |
|---------|---|
-

Note 1: K_{\min} allows a view of deep space (cold sky) for absolute calibration purposes.

Note 2: K_{\max} allows a view of the largest Sea Surface Temperature values plus a margin of ~10 K headroom for RFI processing.

Note 3: The large dynamic range has implications for the calibration approach. Ideally the reference calibration sources should span the expected range of Earth scene brightness temperatures to constrain the calibration appropriately and minimise uncertainties introduced due to non-linearity of derived calibration parameters.

4.2.10 Radiometric Uncertainty and Stability Requirements.

From Bell (1999) accuracy (or rather inaccuracy) is not the same as uncertainty. Unfortunately, usage of these words is often confused. Correctly speaking, ‘accuracy’ is a qualitative term (e.g., one could say that a measurement was ‘accurate’ or ‘not accurate’). Uncertainty is quantitative. When a ‘plus or minus’ figure is quoted, it may be called an uncertainty, but not an accuracy.

For CIMR Absolute Radiometric Accuracy (ARA) is not used in the traditional manner but instead we calculate the Total Standard Uncertainty (which is a “zero mean, 1-sigma” total uncertainty). The strength of this approach is that each component of the total standard uncertainty can be validated (which is not the case for ARA which implies a reference of “truth”). It is noted that this approach, while consistent with international agreements on uncertainty specification (JCGM, 2008), is different compared to other formulations (e.g., as for the MetOp-SG(B) MWI) that do not include NEΔT as part of the absolute radiometric accuracy definition.

The Total Standard Uncertainty is comprised of components having individual requirements: NEΔT (MRD-420), end-to-end lifetime radiometric stability (MRD-470) and orbital stability (MRD-480 and MRD-490) and a bias (e.g., associated with pre-launch characterisation uncertainty).

The total standard uncertainty for a single measurement (in one channel) is the combination of uncertainty from random and systematic effects. These correctly combine in quadrature:

$$u_{total} = \sqrt{u_{random}^2 + u_{systematic}^2} + 0 \quad (\text{Eqn. 4.2.10.1})$$

Channel NEΔT addresses the uncertainty from random effects in the instrument that could be derived in-flight from repeat measurements of the calibration reference sources over several scans. The ‘+ 0’ is a formalism included to represent the unknown unknowns’ in the uncertainty equation.

The stability requirements limit the excursions of the calibration from “truth” on slower timescales: the orbit stability requirement constrains the drift of the calibration on orbital timescales; the lifetime stability constrains the degree of drift of calibration over the mission lifetime; and one further component is required to obtain the total standard uncertainty, namely the beginning of life uncertainty of pre-launch calibration knowledge (u_{pl-cal}) e.g., derived from ground characterisation). In particular, the uncertainties associated with pre-flight calibration (from unit to instrument level), u_{pl-cal} , imply a rigorous pre-launch characterisation of the CIMR instrument (and thus links to the CIMR calibration and validation plans). This is consistent with the definition of all quantities as zero-mean, 1-sigma standard deviations in the MRD requirements. Therefore, the requirements adhere to the formulation of Total Standard Uncertainty:

$$u_{total}^2 \cong u_{NE\Delta T}^2 + u_{orbit-stability}^2 + u_{lifetime-stability}^2 + u_{pl-cal}^2 + 0 \quad (\text{Eqn. 4.2.10.2})$$

For CIMR (using the data in Table MRD-2) these evaluate as (at zero mean, 1-sigma) for the goal values in Table MRD-2 as follows:

GHz	U_{total}	U_{NEΔT}	U_{orbit-stability}	U_{lifetime-stability}	U_{pl-cal*}
1.4135	0.5	0.3	0.2	0.2	0.2
6.9	0.4	0.2	0.1	0.2	0.2
10.65	0.45	0.3	0.1	0.2	0.2
18.7	0.6	0.4	0.2	0.2	0.2
36.5	0.8	0.7	0.2	0.2	0.2

*pl_cal=payload characterisation on ground

MRD-440 CIMR 1.4135, 6.9, and 10.65 brightness temperature measurements at L1b shall ensure a total standard uncertainty of ≤ 0.5 K, 6.9 GHz goal ≤ 0.4 K and 10.65 GHz goal ≤ 0.45 K (zero mean, 1-sigma) consistent with Table MRD-2 ID-080-1-7.

Note 1: This implies an accurate representation of the antenna gain patterns for all feeds is convolved with the measurement data set to correct for side-lobe and other aspects (e.g., grating lobes) contributions to the measurement of interest.

Note 2: This requirement applies to scientific measurements at top of atmosphere.

Note 3: This implies that the calibration subsystem is performing to specification. e.g., all components within the calibration chain (e.g., temperature of the reflector, losses, receiver noise etc).

Note 4: L1b product corrections should be pursued to maintain the performance of CIMR as close to radiometric discontinuities (e.g., land sea transitions etc).

Note 5: See definition of total standard uncertainty.

Note 6: Vicarious calibration targets (e.g., the sea surface, deserts, salt-flats, Dome-C in Antarctica etc) are not traceable to SI and are not suitable as reference measurements.

Note 7: This requirement implies that calibration reference target(s) used to validate this requirement are part of the CIMR on-board calibration system and have been thoroughly characterised and are traceable to SI before flight.

MRD-450 CIMR 18.7 GHz brightness temperature measurements at L1b shall ensure a total standard uncertainty of ≤ 0.6 K, goal ≤ 0.5 (zero mean, 1-sigma) consistent with Table MRD-2 ID-080-1-7.

Note 1: This implies an accurate representation of the antenna gain patterns for all feeds is convolved with the measurement data set to correct for side-lobe and other aspects (e.g., grating lobes) contributions to the measurement of interest.

Note 2: This requirement applies to scientific measurements over at top of atmosphere.

Note 3: This implies that the calibration subsystem is performing to specification.

Note 4: L1b product corrections should be pursued to maintain the performance of CIMR as close to radiometric discontinuities (e.g., land sea transitions etc).

Note 5: See definition of total standard uncertainty.

Note 6: Vicarious calibration targets (e.g., the sea surface, deserts, salt-flats, Dome-C in Antarctica etc) are not traceable to SI and are not suitable as reference measurements.

Note 7: This requirement implies that calibration reference target(s) used to validate this requirement are part of the CIMR on-board calibration system and have been thoroughly characterised and are traceable to SI before flight.

MRD-460	CIMR 36.5 GHz brightness temperature measurements at L1b shall ensure a total standard uncertainty of ≤ 0.8 K (zero mean, 1-sigma) consistent with Table MRD-2 ID-080-1-7.
	<p><i>Note 1: This implies an accurate representation of the antenna gain patterns for all feeds is convolved with the measurement data set to correct for side-lobe and other aspects (e.g., grating lobes) contributions to the measurement of interest.</i></p> <p><i>Note 2: This requirement applies to scientific measurements at top of atmosphere.</i></p> <p><i>Note 3: This implies that the calibration subsystem is performing to specification.</i></p> <p><i>Note 4: L1b product corrections should be pursued to maintain the performance of CIMR as close to radiometric discontinuities (e.g., land sea transitions etc).</i></p> <p><i>Note 5: See definition of total standard uncertainty.</i></p> <p><i>Note 6: Vicarious calibration targets (e.g., the sea surface, deserts, salt-flats, Dome-C in Antarctica etc) are not traceable to SI and are not suitable as reference measurements.</i></p> <p><i>Note 7: This requirement implies that calibration reference target(s) used to validate this requirement are part of the CIMR on-board calibration system and have been thoroughly characterised and are traceable to SI before flight.</i></p>
MRD-470	The CIMR radiometer shall demonstrate instrument end-to-end (i.e. following full-calibration) radiometric stability to ≤ 0.2 K (zero mean, 1-sigma) for all channels over the lifetime of the mission.
	<p><i>Note 1: This requirement is fundamental to the utility of the data in the context of any long-term multi-satellite record.</i></p> <p><i>Note 2: The overall radiometric stability of the instrument is also dependent on the stability of the end-to-end calibrated system (i.e. reflector, calibration reference sources, detector, A/D etc.).</i></p> <p><i>Note 3: The minimum lifetime of the mission is 7 years after a commissioning period of 6 months.</i></p>
MRD-480	The CIMR radiometer shall demonstrate instrument end-to-end (i.e. following full-calibration) radiometric stability to ≤ 0.2 K (zero mean, 1-sigma) for 1.4315, 18.7 and 36.5 GHz channels for each orbit.
	<p><i>Note 1: To deal with any bias adequately in flight when retrieving geophysical parameters, adequate radiometric stability around an orbit, driven by the geophysical parameter is, required. In order not to compromise the geophysical uncertainty, this stability needs to be, order-of-magnitude, half of the geophysical uncertainty value in the channels used. This is not averaged down by using both forward and backward scans. In order not to compromise the SST uncertainty, this stability needs to be, order-of-magnitude, half of the SST uncertainty value in the SST channels. This is not averaged down by using both fore and aft, so the factor is \sim emissivity.</i></p>

Note 2: The overall radiometric stability of the instrument is also dependent on the stability of the end-to-end calibrated system (i.e. reflector, calibration reference sources, detector, A/D etc.).

MRD-490

The CIMR radiometer shall demonstrate instrument end-to-end (i.e. following full-calibration) radiometric stability to ≤ 0.15 K (zero mean, 1-sigma) with a goal of ≤ 0.1 K for 6.9 and 10.65 GHz channels for each orbit.

Note 1: To deal with any bias adequately in flight in retrieving geophysical parameters adequate radiometric stability around an orbit, driven by the geophysical parameter is required. In order not to compromise the geophysical uncertainty, this stability needs to be, order-of-magnitude, half of the geophysical uncertainty value in the channels used. This is not averaged down by using both forward and backward scans. In order not to compromise the SST uncertainty, this stability needs to be, order-of-magnitude, half of the SST uncertainty value in the SST channels. This is not averaged down by using both fore and aft, so the factor is ~ emissivity.

Note 2: The radiometric stability of the instrument is also dependent on the stability of the end-to-end calibrated system (i.e. reflector, calibration reference sources, detector, A/D etc.).

Note 3: This requirement applies at any point during the CIMR mission lifetime and implies that knowledge of calibration parameters are included in Level-1b products.

4.2.11 Calibration System Requirements

MRD-500

The calibration of L1b brightness temperature in all channels shall be maintained during science measurement acquisition using an on-board calibration system with at least two reference values that are traceable to SI.

Note 1: Options to provide reference values include hot and cold load sources (including active cold loads and noise diodes).

Note 2: The means that for all CIMR on-board calibration reference value temperatures should be reference to the International Temperature scale 1990 (ITS 1990) – see Preston-Thomas (1990)

Note 3: More than two calibration points could be used to account for non-linearity if needed to constrain the CIMR calibration in flight.

Note 4: The reflector characteristics must be known, and the reflector temperature monitored in flight (either by measurement or using a high-performance modelling approach correlated to in-flight measurements i.e. temperature sensors located at strategic positions along the support boom and antenna frame).

Note 5: Vicarious calibration targets are not traceable to SI. Therefore, the CIMR on-board calibration system must be thoroughly characterised before flight and a strategy developed to periodically check calibration.

MRD-510 The CIMR radiometer shall be capable of viewing deep space as a cold calibration reference target.

Note 1: This implies that specific spacecraft manoeuvres are required.

Note 2: The number of deep space views is a function of the calibration system implementation and must be derived based on the implementation of CIMR.

Note 3: Other calibration attitude manoeuvres could be implemented to augment the on-board calibration system (e.g., Farrar et al., 2016) or views of well-characterised ocean areas with weak thermal gradients.

Note 4: The invariability of the Moon emissivity makes it well suited as a reference target to assess the long-term stability of sensor calibration (e.g., Burgdorf et al., 2016). A constant phase angle eliminates the need for a model of the Moon's brightness when checking the stability of an instrument.

MRD-520 All on-board calibration data and supporting engineering data required to recalibrate CIMR science measurements shall be available to users.

Note 1: Access to engineering data such as thermistor values, instrument state, scan position etc is essential to monitor the performance of the CIMR calibration systems and to re-calibrate the instrument on-ground if required as part of reanalysis.

Note 2: Supporting engineering data includes any on-board information considered necessary to reconstruct the calibration of CIMR and is specific to the implementation of the on-board calibration system e.g., thermistor values, scan position, feed temperature etc.

Note 3: It is anticipated that this information will be available to users via L1a data products.

4.2.12 Inter-channel calibration.

The consistency of brightness temperature retrievals from CIMR bands and CIMR channels is important as L2 algorithms will use a combination of channels to derive measurements contained in geophysical products. In addition, depending on the implementation, CIMR may use multiple feeds each with their own characteristics in terms of calibration. The following requirements are designed to ensure that there is consistency both within a channel (regardless of the implementation used e.g., multiple feed chains) and between different bands in requirements addressing inter-channel and inter-band differences.

MRD-530 Brightness temperature differences for the same target area measured at different frequencies (bands) and polarisations (channels) by any combination of two footprints shall be ≤ 0.2 K when compared to the theoretical brightness temperature derived using the Raleigh-Jeans approximation of for an infinite uniform target scene represented as a perfect blackbody at a temperature of 290 K.

Note 1: This requirement addresses the fact that L2 geophysical retrievals will use a combination of different channel data from potentially multiple feeds and consistency of performance between channel data must be guaranteed.

Note 2: 290 K is used as a blackbody physical temperature to facilitate on ground testing.

Note 3: It is assumed that this requirement is to be verified prior to launch by analysis and testing.

MRD-540 Brightness temperature differences for the same target area measured at the same frequency (band) and polarisation (channel) by any combination of two footprints shall be ≤ 0.1 K when compared to the theoretical brightness temperature derived using the Raleigh-Jeans approximation of for an infinite uniform target scene represented as a perfect blackbody at a temperature of 290 K.

Note 1: The requirement addresses the fact that multiple feeds are required to meet sampling requirements and each feed chain (reflector, feed-horn, back end electronics, calibration etc.) may be slightly different. However, from a user perspective, these differences should be minimised so that data within a given channel, regardless of the feed chain used, are essentially uniform.

Note 2: 290 K is used as a blackbody physical temperature to facilitate on ground testing.

Note 3: It is assumed that this requirement is to be verified prior to launch by analysis and testing.

4.2.13 Polarisation Requirements.

Polarisation is an important quantity for CIMR since channel polarisation differences and ratios are used in retrieval algorithms.

MRD-550 All CIMR bands shall acquire data in two channels: one with a vertical linear polarisation (V) and a second with a horizontal linear polarisation (H).

Note 1: The wind roughened surface mixes the vertical and horizontal polarizations of the specular surface, and the mixing increases with increasing emissivity of the specular surface e.g., Meissner and Wentz, (2012).

*Note 2: There are a minimum of **two** CIMR instrument measurement channels (H and V) for each CIMR instrument band e.g., 18.7V and 18.7H and **four computed outputs in a L1b product that are available on ground corresponding to the full Stokes Vector.***

Note 3: Vertical Polarisation (V) is defined as the electric field being parallel to the plane of incidence.

Note 3: Full Stokes Vector is requested in MRD-560. 3rd Stokes signals are small (typically < $\pm 3K$) and the 4th Stokes parameter is < $\pm 1K$ implicitly suggesting very good performance in the H- and V-polarisation CIMR measurements and polarization characterisation if these parameters are to be derived from CIMR.

The degree of polarisation is extremely useful in CIMR L1 (e.g., correction for Faraday Rotation) and L2 (e.g., potential retrieval of wind vector over the ocean) processing and is conveniently expressed in the full Stokes Vector. In principle, with appropriate hardware, this can be derived as an output from the radiometer feeds or as part of the RFI processing system.

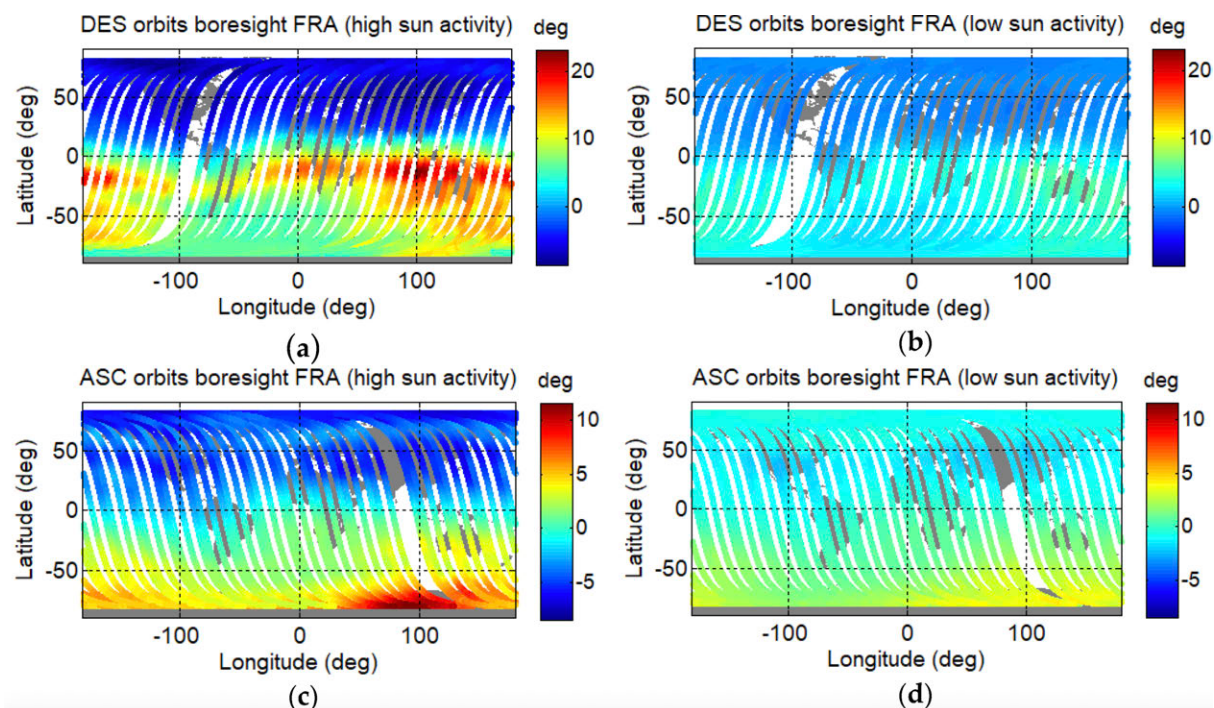


Figure 4.2.13-1. Faraday rotation in the Soil Moisture and Ocean Salinity (SMOS) boresight coordinates for 3 days in different periods: (a) descending orbits in March 2014 (high sun activity), (b) descending orbits in January 2011 (low sun activity), (c) ascending orbits in March 2014 (high sun activity), (d) ascending orbits in January 2011 (low sun activity). From Rubino et al (2020).

The CORIOLIS WindSat (Gaiser et al., 2004) mission was developed to evaluate the potential of polarimetric microwave radiometry to retrieve ocean surface wind vectors. The polarization properties of an electromagnetic wave can be fully characterized by measuring the modified Stokes vector. The modified Stokes vector includes the vertical and horizontal polarizations and the third and fourth Stokes parameters. Because the wind direction dependence differs for the 4 Stokes parameters it is possible to retrieve an estimate of the ocean surface wind vector free of ambiguities without the use of an ancillary numerical weather prediction field.

Narvekar et al (2011) note that during most of the year, the absolute value of the 10.7- and 37-GHz 3rd and 4th Stokes signals over sea ice is below 1 K (Narvekar et al, 2020), which is small compared to those observed over the sea surface (~ 2 K) (Yueh et al, 2006) the land surface (~ 2 K) (Narvekar et al, 2007) the Antarctic (~ 7 K) (Narvekar et al, 2010) and Greenland (~ 15 K) (Li et

al., 2008) ice sheets. During the summer months, parts of the Arctic sea ice show larger 3rd and 4th Stokes signals. The 37-GHz 3rd Stokes component shows a large signal over the large area extending from the Beaufort Sea to the New Siberian Islands. These occurred mainly during the period of June 22–27. From the analysis of the year 2003, it was found that, for most of the year, the absolute value of 3rd and 4th Stokes remains close to 0.25 K, which is the standard measurement noise of WindSat (Gaiser *et al* 2004). A larger signal in the 37-GHz 3rd Stokes channel was observed during early summer (June 24, 2003). Before this period, the signal was below 1 K. Yueh *et al* (2006) develop a model function for the WindSat polarimetric radiometer and note that the third and fourth Stokes parameters are less sensitive to cloud and water vapor as demonstrated in aircraft measurements (e.g., Yueh, 1997) and are more suitable for the ocean wind direction measurements over a broader range of weather conditions. Thus, 3rd Stokes signals are small (typically $< \pm 3\text{K}$) and the 4th Stokes parameter is $< \pm 1\text{K}$ (e.g., Quilfen *et al*, 2007) implicitly suggesting very good performance in the H- and V-polarisation CIMR measurements and polarization characterisation if these parameters are to be derived from CIMR.

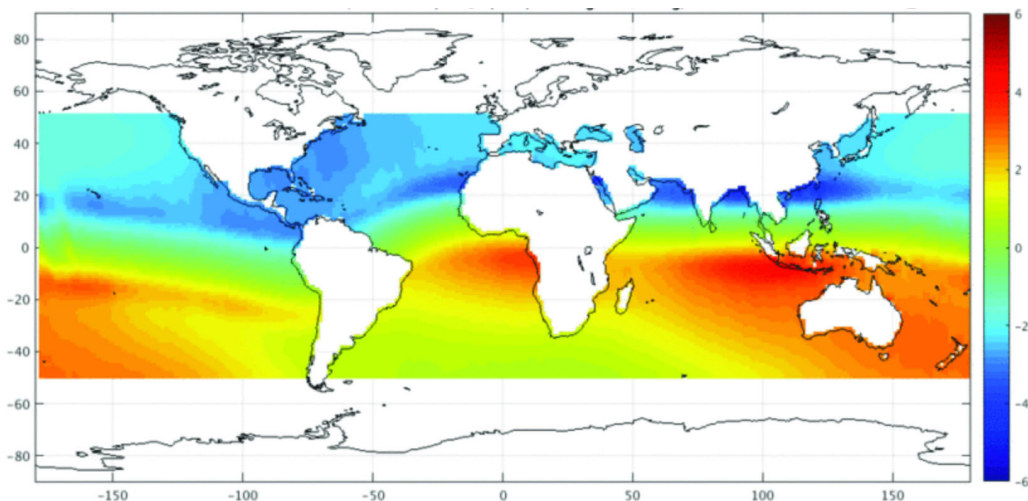


Figure 4.2.13-2. The mean annual distribution of the 3rd Stokes signal (an indication of Faraday rotation) derived from SMAP for 2016 (From Soldo *et al*, 2019).

Faraday rotation is a change in the polarization vector that occurs as electromagnetic waves propagate through the ionosphere and is important for measurements made at the low microwave frequencies. For example, at L-band the rotation of the polarization vector can range from a few degrees to more than 15 degrees depending on viewing angle and the solar cycle (Le Vine and Abraham, 2002). The corresponding change in apparent brightness temperature can be several Kelvin (e.g., Yueh, 2000). Seung-Bum *et al.* (2011) highlight the effect of antenna cross-polarization coupling on the brightness temperature retrieval at L-Band for the Aquarius L-band satellite radiometer. Peng and Ruf (2008) note that, for vertical and horizontal polarization channels of a fully polarimetric radiometer, the quadrature components of correlation between them will represent the third and fourth Stokes parameters. Very low and known cross-polarisation between H- and V-polarised channels is important.

Measurement of the third and fourth Stokes parameters of microwave thermal emission can be degraded by non-ideal radiometer characteristics. Meissner and Wentz (2006) discuss the effects of spacecraft attitude and Faraday rotation polarization rotation and the third Stokes parameter. Of particular importance in the case of incoherent radiometry where 3rd and 4th Stokes parameters are computed from H- and V-polarised Tb (e.g., Peng and Ruf (2008)). Thus, the level of polarization

purity and the knowledge of polarization impurity (e.g., Ruf, 1998) must be well characterized to minimize uncertainties on L1b brightness temperature.

Of particular note is that for SMAP, strong 4th Stokes parameter signals are observed in the presence of RFI and at land/water boundaries (e.g., coast lines) that can be exploited for RFI detection (e.g., Soldo *et al*, 2019).

MRD-560 CIMR shall estimate the Full Stokes Vector for each frequency band with polarisation purity cross coupling of <2%.

Note 1: 2% is approximately -33dB.

Note 2: Phase stability of the H&V channels must be known and stable because variations in H&V channel phase will directly impact the determination of the 3rd and 4th modified Stokes parameters required for on-board RFI detection and required on ground for L2 products.

Note 3: The provision of full Stokes Vector outputs is foreseen as part of on-board radio-frequency interference processing that are downlinked to ground. However, further processing may be necessary on ground to meet performance requirements. 3rd Stokes signals are small (typically < ±3K) and the 4th Stokes parameter is < ±1K implicitly suggesting very good performance in the H- and V-polarisation CIMR measurements and polarization characterisation if these parameters are to be derived from CIMR and remain useful.

Note 4: Stokes vector measurements are used to support L2 retrievals (e.g., Faraday rotation correction, salinity, wind vector measurements).

MRD-570 The polarization rotation angle (PRA) shall be maintained within an alignment within ±1° and maintained with a knowledge ≤ 0.05° for both the bias and random components.

*Note 1: Coupling occurs when the spacecraft polarization basis is rotated with respect to the earth surface polarization basis. This form of coupling can be corrected by a matrix multiplication that can be used to correct the alignment. See Gaiser *et al* (2004).*

*Note 2: If the cross-polarisation coupling level is low on-orbit vicarious calibration techniques may be used to estimate the cross-coupling level to within 0.05% using global ocean, land, and ice measurement data (e.g., Farrar *et al* 2016).*

Note 3: Phase stability of the H&V channels must be known and stable because variations in H&V channel phase will directly impact the determination of the 3rd and 4th modified Stokes parameters required for on-board RFI detection and required on ground for L2 products.

*Note 4: This is the heritage WindSat specification (see Gaiser *et al*, 2004) that limits polarisation purity cross coupling to -30dB with a polarisation rotation angle <0.05° (random and bias components) and an alignment of ±1°.*

Note 5: Stokes vector measurements are used to support L2 retrievals (e.g., Faraday rotation correction, wind vector measurements).

Note 6: Over the ocean we may expect typical TbV - TbH differences of ~50K. To limit uncertainties to 0.1K or better we require cross polarization knowledge of 0.2% or better.

4.2.14 Antenna main beam requirements.

Following Kaefer and Harrington (1983), the *main-beam* efficiency of a microwave radiometer specifies the integral of power over the main beam divided by the integral over the complete antenna pattern. For reference, the beam width used by the AMSR-2 sensor are shown in Table 4.2.14.1. In the case of CIMR, the main beam is defined as 2.5 x -3dB footprint contour. It represents the fraction of the power received through the main beam if the antenna was in an isothermal enclosure.

Table 4.2.14.1. AMSR-2 beam characteristics and sampling specification (from Imaoka et al., 2010).

Frequency (GHz)	Beam width (3dB, deg.)	Spatial resolution (km)	Sampling interval (km)
6.9	1.8	35 x 62	10
10.65	1.2	24 x 42	10
18.7	0.65	14 x 22	10
36.5	0.35	7 x 12	10

In the case of CIMR we consider sources within the *wide beam* defined as 3 x -3dB footprint contour. The fraction of power received from all angles other than the wide beam, $1 - \varepsilon$, originates from sources other than the scene being observed and, in general, is not accurately known. The effective antenna temperature, T_a , then consists of two parts:

$$T_a \approx \varepsilon T_{\text{scene}} + (1 - \varepsilon) T_{\text{other}}$$

The second term must be removed by assuming a temperature distribution for T_{other} and integrating over all the side lobes, back lobes and e.g., grating lobes. This process is simple if most of the power is in the first side lobe and the scene is homogeneous, such as an ocean scene. But, for example, if the wide beam is viewing the ocean and the side lobes and e.g., grating lobes, back lobes, spillover etc, are partially viewing land or sea ice, it may be impossible to make the correction to the required accuracy if knowledge of the antenna characteristics is poor and/or the target scene is extremely heterogeneous Kaefer and Harrington (1983). The use of properly computed uncertainty estimates including these effects at L1b will be necessary to capture the quality of an individual measurement in challenging conditions. Nevertheless, the larger the beam efficiency, the easier it is to correct for the unwanted received radiation.

The required beam efficiency is highly dependent on the required measurement accuracy, side-lobe structure, and scene heterogeneity. It is possible to obtain wide beam efficiencies $\varepsilon \sim 98\%$ with certain types of horn antennas for a uniformly illuminated reflector antenna (e.g., Gaiser et al., 2004). Since the required wide-beam efficiency is dependent on the particular observation, it is

difficult to specify a general requirement on ϵ for a broad range of measurements other than to say that ϵ should be as high as possible.

One approach is to investigate the impact of main beam contamination using radiative transfer modelling. Simulated SST Level-2 retrievals (using only channels at 6.925, 10.65 and 18.7 GHz) using a radiative transfer model following the approach of *Pearson et al.* (2018) have been performed to quantify the impact of an additional bias induced by side-lobe contamination in steps of 0.1K for a 50 x 50 km area and a straight boundary. In this simulation, the same bias is applied to all the retrievals and all channels. To limit the impact on SST bias to 0.2 K the Tb contributions from side-lobes and grating-lobes must be ~0.1 K. The estimated impact of a 0.5 K side-lobe and grating lobe contribution on SST bias is ~0.8 K.

Practically, the impact of side-lobe and e.g., grating lobe contamination at L1b can be estimated and mitigated by analysing the contribution of power from the full beam (including side and other lobes) compared to the -3dB footprint ellipse using accurate antenna gain patterns and knowledge of the brightness temperature characteristics of surrounding CIMR measurements. This requires that accurate antenna gain, and grating-lobe pattern knowledge is available for each channel and feed (if multiple feeds are employed) and a L1a to L1b data processing approach is used to adjust the -3dB measurement and compensate for side-lobe contamination.

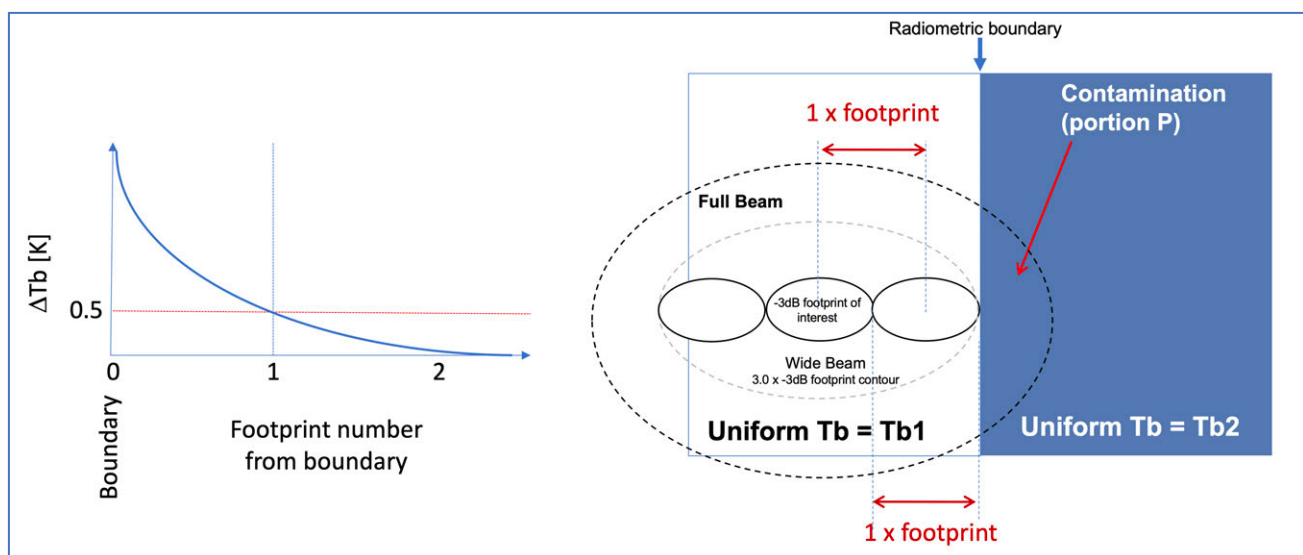
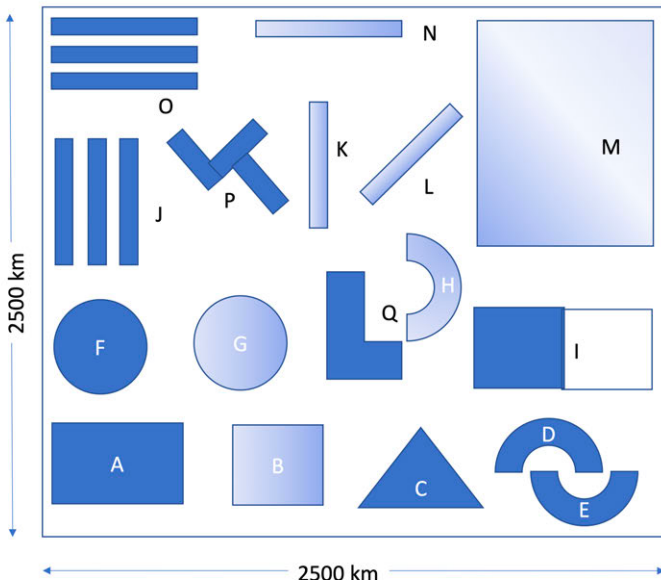


Figure MRD-4.2.14.1. Schematic example of how Tb changes as it approaches a boundary to illustrate the meaning of MRD-580, MRD-590, MRD-600, MRD-610 and MRD-620.

As CIMR is focussed on the Polar Regions, the following requirements are specified for transitions between open water to first year ice in horizontal polarisation although each requirement provides an additional specification for Land and Ocean surfaces. The approach to be used to address each requirement is summarised in Figure MRD-4.2.14.1.

CIMR-Test Card—'Picaso v3.0' (2500 x 2500 km)



Test Scene to test side lobe AND grating lobe corrections at L1B.

Objective: select the most appropriate facet size on the reflector. 2500 km x 2500 km Scene includes limits commensurate with MRD distance to coast requirements.

Principle shall be to develop geometric shapes that challenge lobe corrections.

1. Gradients
2. Spatial features of variable complexity
3. Uncertainty

One Test Card for each Channel with following specification

Background temperature=uniform 250K
Uncertainty :+/-2K
Lband: gradient [70->230 K], shape=70K
Cband: gradient [75 -> 250 K], shape=75K
Cband: gradient [80 -> 250 K], shape=80K
KuBand: gradient [100 -> 250 K], shape=100K
Kaband: gradient [135 -> 250 K], shape=135K

Figure MRD-4.2.14.2. Example synthetic test scene that can be used to assess CIMR “Distance to Coast” and Total Standard Uncertainty.

As a guide to assessing the performance of MRD-580 to MRD-620, and as part of the CIMR total standard uncertainty assessment (Eqn. 4.2.10.2) MRD-440 to MRD-490, a synthetic scene provides a powerful means to control the assumptions used (both geometrically and radiometrically) when performing an assessment. An example scene is provided in Figure 4.2.14.2 as a starting point from which a viable test scene can be appropriately tailored.

MRD-580

The impact of radiometric discontinuities (e.g., thermal ocean fronts, at a coastal boundary, sea ice edge [AD-2] or ice shelf edge etc) on 6.9 GHz L1b horizontally polarised brightness temperature measurements shall not be ≥ 0.5 K at 1 footprint from a hypothetical and infinite high contrast target scene, with top of the atmosphere brightness temperatures of 75 K and 250 K at each side of a straight boundary.

Note 1: As CIMR is focused on the Polar Regions, the following requirements are specified for transitions between open water to first year ice (the marginal ice zone), to address the need for measurements close to coastal boundaries and at strong SST frontal gradients in the ocean. But it should be recalled that because CIMR has a high spatial resolution it may “see” lakes close to hot land surfaces.

Note 2: Over land surfaces at C-band $T_{min}= 200$ K, $T_{max}= 300$ K.

Note 3: Over ocean surfaces at C-band $T_{min}= 75$ K, $T_{max}= 150$ K).

Note 3: In terms of open-water (OW) to first-year ice (FYI) sea-ice transition cases that are the most common cases (OW to Multi-Year Ice (MYI) transitions are less common) the TB contrasts in H-polarization (that are always larger than the contrast in V-pol) $T_{min}(Hpol)= 75$ K and $T_{max}(Hpol)= 250$ K. These are average “realistic” transitions that also consider the variability of conditions around the mean SIC algorithm tie-points.

Note 4: This requirement is designed to ensure that side-lobe and e.g., grating lobe corrections, when applied, result in useful measurements allowing accurate computation of geophysical parameters.

Note 5: This requirement implies a well-formed antenna beam and well characterised antenna side lobes and grating lobe patterns to be used in L1b processing.

Note 6: This requirement implies that a suitable algorithm is used to compensate for side-lobe and e.g., grating lobe contamination at L1b.

Note 7: This requirement will be assessed theoretically by analysis.

Note 8: It is expected that the “worst case” will be in the coastal region (see definition) where there are large radiometric discontinuities (temperature, emissivity, varied terrain and elevation etc).

Note 9: See Figure MRD-4.2.14.1

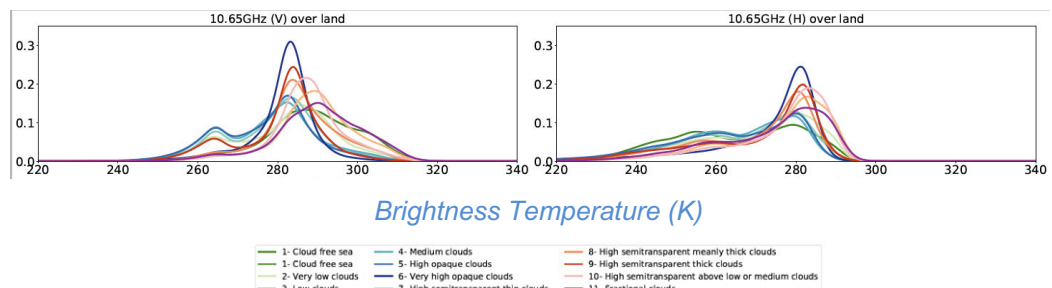
Note 10: See specification of Coastal Boundary defined in MRD-852.

MRD-590

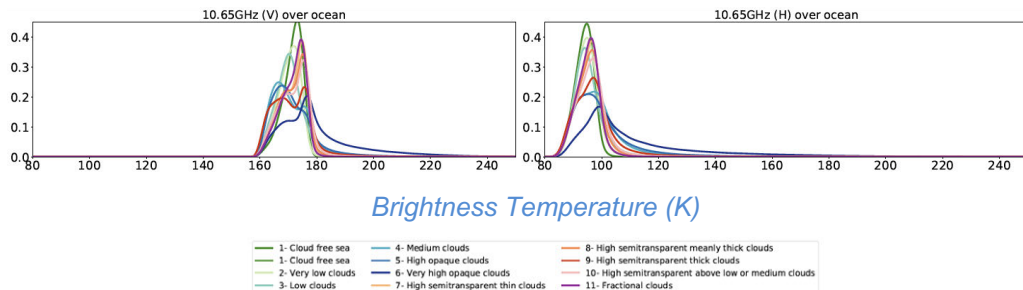
The impact of radiometric discontinuities (e.g., thermal ocean fronts, at a coastal boundary, sea ice edge [AD-2] or ice shelf edge etc) on 10.65 GHz L1b horizontally polarised brightness temperature measurements shall not be ≥ 0.5 K at 1 footprint from a hypothetical and infinite high contrast target scene, with top of the atmosphere brightness temperatures of 80 K and 250 K at each side of a straight boundary.

Note 1: As CIMR is focused on the Polar Regions, the following requirements are specified for transitions between open water to first year ice (the marginal ice zone), to address the need for measurements close to coastal boundaries and at strong SST frontal gradients in the ocean. But it should be recalled that because CIMR has a high spatial resolution it may “see” lakes close to hot land surfaces.

Note 2: The distribution of GPM-GMI (having an incidence angle of 53.5° similar to CIMR at 55°) data over land surface within the METEOSAT disk (i.e. no polar regions) for both H an V polarization averaged over 6 days per month for a year (2015) is provided as a guide to more realistic scenarios below. $T_{min}(Vpol) = 240$ K, $T_{max}(Vpol) = 320$ K, $T_{min}(Hpol) = 220$ K, $T_{max}(Hpol) = 300$ K,



Note 3: The distribution of GPM-GMI (having an incidence angle of 53.5° similar to CIMR at 55°) data over ocean surface within the METEOSAT disk (i.e. no polar regions) for both H an V polarization averaged over 6 days per month for a year (2015) is provided as a guide to more realistic scenarios below. $T_{min}(Vpol) = 150$ K, $T_{max}(Vpol) = 240$ K, $T_{min}(Hpol) = 80$ K, $T_{max}(Hpol) = 140$ K.



Note 4: In terms of open-water (OW) to first-year ice (FYI) sea-ice transition cases that are the most common cases (OW to Multi-Year Ice (MYI) transitions are less common) the TB contrasts in H-polarisation (that are always larger than the contrast in V-pol) $T_{min}(Hpol) = 80\text{K}$ and $T_{max}(Hpol) = 250\text{K}$. These are average "realistic" transitions that also consider the variability of conditions around the mean SIC algorithm tie-points.

Note 5: This requirement is designed to ensure that side-lobe and e.g., grating lobe corrections, when applied, result in useful measurements allowing accurate computation of geophysical parameters.

Note 6: This requirement implies a well-formed antenna beam and well characterised antenna side lobes and grating lobe patterns to be used in L1b processing.

Note 7: This requirement implies that a suitable algorithm is used to compensate for side-lobe and e.g., grating lobe contamination at L1b.

Note 8: This requirement will be assessed theoretically by analysis.

Note 9: It is expected that the "worst case" will be in the coastal region (see definition) where there are large radiometric discontinuities (temperature, emissivity, varied terrain and elevation etc).

Note 10: See Figure MRD-4.2.14.1

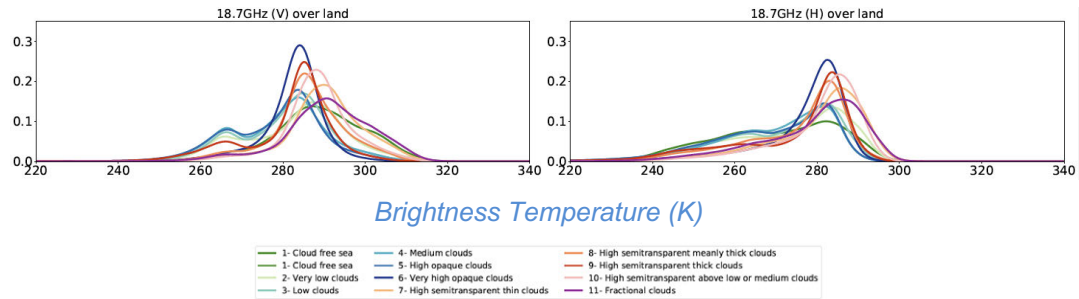
Note 11: See specification of Coastal Boundary defined in MRD-852.

MRD-600

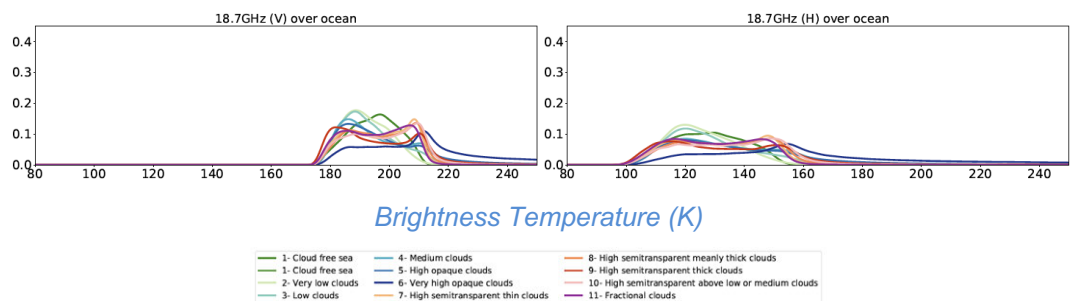
The impact of radiometric discontinuities (e.g., thermal ocean fronts, at a coastal boundary, sea ice edge [AD-2] or ice shelf edge etc) on 18.7 GHz L1b horizontally polarised brightness temperature measurements shall not be $\geq 0.5\text{ K}$ at 1 footprint from a hypothetical and infinite high contrast target scene, with top of the atmosphere brightness temperatures of 100 K and 250 K at each side of a straight boundary.

Note 1: As CIMR is focused on the Polar Regions, the following requirements are specified for transitions between open water to first year ice (the marginal ice zone), to address the need for measurements close to coastal boundaries and at strong SST frontal gradients in the ocean. But it should be recalled that because CIMR has a high spatial resolution it may "see" lakes close to hot land surfaces.

Note 2: The distribution of GPM-GMI (having an incidence angle of 53.5° similar to CIMR at 55°) data over land surface within the METEOSAT disk (i.e. no polar regions) for both H and V polarization averaged over 6 days per month for a year (2015) is provided as a guide to more realistic scenarios below. $T_{min}(Vpol) = 240\text{ K}$, $T_{max}(Vpol) = 320\text{ K}$, $T_{min}(Hpol) = 220\text{ K}$, $T_{max}(Hpol) = 310\text{ K}$.



Note 3: The distribution of GPM-GMI (having an incidence angle of 53.5° similar to CIMR at 55°) data over ocean surface within the METEOSAT disk (i.e. no polar regions) for both H and V polarization averaged over 6 days per month for a year (2015) is provided as a guide to more realistic scenarios below. $T_{min}(Vpol) = 170\text{ K}$, $T_{max}(Vpol) = 250\text{ K}$, $T_{min}(Hpol) = 100\text{ K}$, $T_{max}(Hpol) = 250\text{ K}$.



Note 4: In terms of open-water (OW) to first-year ice (FYI) sea-ice transition cases that are the most common cases (OW to Multi-Year Ice (MYI) transitions are less common) the TB contrasts in H-polarization (that are always larger than the contrast in V-pol) $T_{min}(Hpol) = 100\text{K}$ and $T_{max}(Hpol) = 250\text{K}$. These are average "realistic" transitions that also consider the variability of conditions around the mean SIC algorithm tie-points.

Note 5: This requirement is designed to ensure that side-lobe and e.g., grating lobe corrections, when applied, result in useful measurements allowing accurate computation of geophysical parameters.

Note 6: This requirement implies a well-formed antenna beam and well characterised antenna side lobes and grating lobe patterns to be used in L1b processing.

Note 7: This requirement implies that a suitable algorithm is used to compensate for side-lobe and e.g., grating lobe contamination at L1b.

Note 8: This requirement will be assessed theoretically by analysis.

Note 9: It is expected that the "worst case" will be in the coastal region (see definition) where there are large radiometric discontinuities (temperature, emissivity, varied terrain and elevation etc).

Note 10: See Figure MRD-4.2.14.1

Note 11: See specification of Coastal Boundary defined in MRD-852.

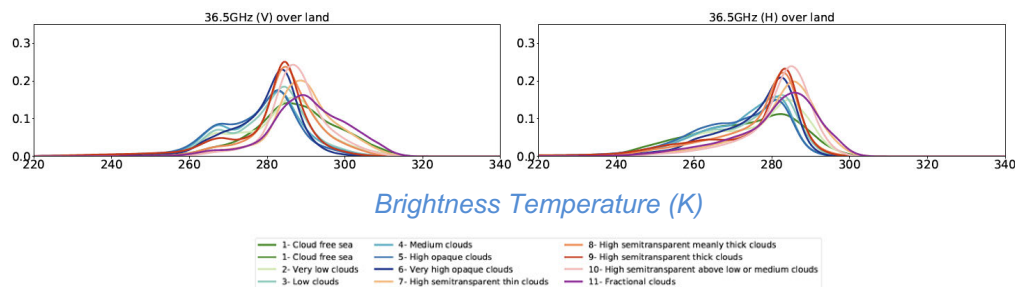
MRD-610

The impact of radiometric discontinuities (e.g., thermal ocean fronts, at a coastal boundary, sea ice edge [AD-2] or ice shelf edge etc) on 36.5 GHz L1b horizontally polarised brightness temperature measurements shall not be $\geq 0.5\text{ K}$ at 1 footprint from a hypothetical and infinite high contrast target scene, with top of the

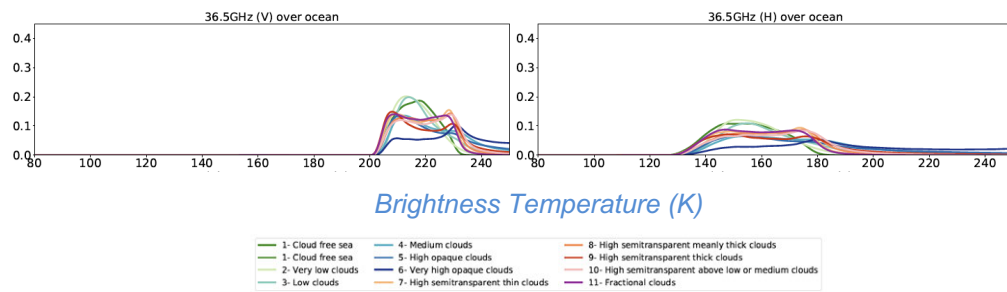
atmosphere brightness temperatures of 135 K and 250 K at each side of a straight boundary.

Note 1: As CIMR is focused on the Polar Regions, the following requirements are specified for transitions between open water to first year ice (the marginal ice zone), to address the need for measurements close to coastal boundaries and at strong SST frontal gradients in the ocean. But it should be recalled that because CIMR has a high spatial resolution it may “see” lakes close to hot land surfaces.

Note 2: The distribution of GPM-GMI (having an incidence angle of 53.5° similar to CIMR at 55°) data over land surface within the METEOSAT disk (i.e. no polar regions) for both H an V polarization for averaged over 6 days per month for a year (2015) is provided as a guide to more realistic scenarios below. $T_{min}(Vpol) = 240$ K, $T_{max}(Vpol) = 320$ K, $T_{min}(Hpol) = 220$ K, $T_{max}(Hpol) = 310$ K



Note 3: The distribution of GPM-GMI (having an incidence angle of 53.5° similar to CIMR at 55°) data over ocean surface within the METEOSAT disk (i.e. no polar regions) for both H an V polarization for averaged over 6 days per month for a year (2015) is provided as a guide to more realistic scenarios below. $T_{min}(Vpol) = 200$ K, $T_{max}(Vpol) = 260$ K, $T_{min}(Hpol) = 130$ K, $T_{max}(Hpol) = 250$ K.



Note 4: In terms of open-water (OW) to first-year ice (FYI) sea-ice transition cases that are the most common cases (OW to Multi-Year Ice (MYI) transitions are less common) the T_B contrasts in H-polarization (that are always larger than the contrast in V-pol) $T_{min}(Hpol) = 135$ K and $T_{max}(Hpol) = 250$ K. These are average "realistic" transitions that also consider the variability of conditions around the mean SIC algorithm tie-points.

Note 5: This requirement is designed to ensure that side-lobe and e.g., grating lobe corrections, when applied, result in useful measurements allowing accurate computation of geophysical parameters.

Note 6: This requirement implies a well-formed antenna beam and well characterised antenna side lobes and grating lobe patterns to be used in L1b processing.

Note 7: This requirement implies that a suitable algorithm is used to compensate for side-lobe and e.g., grating lobe contamination at L1b.

Note 8: This requirement will be assessed theoretically by analysis.

Note 9: It is expected that the “worst case” will be in the coastal regions (see definition) where there are large radiometric discontinuities (temperature, emissivity, varied terrain and elevation etc).

Note 10: See Figure MRD-4.2.14.1. Note 11: See specification of Coastal Boundary defined in MRD-852.

MRD-620 The impact of radiometric discontinuities (e.g., thermal ocean fronts, at a coastal boundary, sea ice edge [AD-2] or ice shelf edge etc) on 1.4315 GHz L1b horizontally polarised brightness temperature measurements shall not be ≥ 0.5 K at 1 footprint from a hypothetical and infinite high contrast target scene, with top of the atmosphere brightness temperatures of 70 K and 230 K at each side of a straight boundary.

Note 1: As CIMR is focused on the Polar Regions, the following requirements are specified for transitions between open water to first year ice (the marginal ice zone), to address the need for measurements close to coastal boundaries and at strong SST frontal gradients in the ocean. But it should be recalled that because CIMR has a high spatial resolution it may “see” lakes close to hot land surfaces.

Note 2: Over land surfaces at L-band $T_{min} = 250$ K (Amazon Rainforest), $T_{max} = 300$ K (Sahara Desert).

Note 3: Over ocean surfaces at L-band $T_{min} = 70$ K, $T_{max} = 130$ K).

Note 4: In terms of open-water (OW) to first-year ice (FYI) sea-ice transition cases that are the most common cases (OW to Multi-Year Ice (MYI) transitions are less common) the TB contrasts in H-polarization (that are always larger than the contrast in V-pol) $T_{min}(Hpol) = 70$ K and $T_{max}(Hpol) = 230$ K. These are average “realistic” transitions that also consider the variability of conditions around the mean SIC algorithm tie-points.

Note 5: This requirement is designed to ensure that side-lobe and e.g., grating lobe corrections, when applied, result in useful measurements allowing accurate computation of geophysical parameters.

Note 6: This requirement implies a well-formed antenna beam and well characterised antenna side lobes and grating lobe patterns to be used in L1b processing.

Note 7: This requirement implies that a suitable algorithm is used to compensate for side-lobe and e.g., grating lobe contamination at L1b.

Note 8: This requirement will be assessed theoretically by analysis.

Note 9: It is expected that the “worst case” will be in the coastal regions (see definition) where there are large radiometric discontinuities (temperature, emissivity, varied terrain, and elevation etc).

Note 10: See Figure MRD-4.2.14.1

Note 10: See specification of Coastal Boundary defined in MRD-852.

4.2.15 Radio Frequency Interference (RFI) Mitigation Requirements.

Radio Frequency Interference (RFI) is an increasing problem in most of the frequency bands used for Earth observation. Historical data from SMOS, SMAP, AMSR-E/AMSR2 reveal RFI contamination at L-band, C-band and X-band from a variety of sources on ground and via reflection of satellite television broadcast channels at the sea surface from space. RFI must be detected and mitigated when using low frequency (i.e. L-, C- and X-band) channels in geophysical retrieval algorithms (e.g., Maeda *et al.*, 2011; Soldo *et al.*, 2017). Nielsen *et al.* (2018) show that an Optimal Estimation retrieval is very efficient to filter out RFI effects in C- and X-band channels. The JAXA AMSR2 adopted a different strategy and included separate bands at 6.9 GHz and 7.3 GHz to mitigate RFI (the assumption is that RFI will not, in general, pollute both channels). However, the AMSR2 “brute force” approach must handle more data in the ground segment operations and provides limited knowledge of the RFI characteristics and their evolution. Other implications include discarding excessively polluted data or incorrectly flagged data with a direct impact on Copernicus Users.

Spectral RFI filtering detects and mitigates RFI pollution by removing polluted parts of the measurement bandwidth. In addition, such an approach allows the use of a wider bandwidth facilitating compliance to NEΔT requirements. The NASA SMAP mission piloted a strategy based on on-board and on-ground RFI mitigation using approaches initially developed in Europe (e.g., Balling *et al.* 2011). Recently, the CubeSat radiometer radio frequency interference technology validation mission (CubeRRT) was developed to demonstrate real-time onboard detection and filtering of RFI for wide bandwidth microwave radiometers (e.g., Johnson *et al.*, 2020, 2021; Lahtinen *et al.* 2019). RFI detection is performed by resolving the input bandwidth into 128 frequency subchannels, with the kurtosis of each subchannel and the variations in power across frequency used to detect non-thermal contributions. RFI filtering is performed by removing corrupted frequency subchannels prior to the computation of the total channel power. CubeRRT's onboard RFI processing capability dramatically reduces the volume of data that must be downlinked to the ground and eliminates the need for ground-based RFI processing.

It is recognised that this type of approach on-board the satellite has the potential to offer enhanced performance, particularly if configurable time-domain and frequency-domain sub-channelling for all measurements is used to optimise the detection and mitigation of RFI while preserving the radiometric fidelity of the measurements.

MRD-630 The CIMR mission shall detect and mitigate Radio Frequency Interference (RFI) on board the spacecraft and on-ground for all channels.

Note 1: RFI is a source of significant uncertainty in L1 products and must be clearly identified and mitigated from the measurement data if they are to be scientifically useful by the operational user community.

Note 2: See MRD-640 describing data to be sent to ground for analysis if RFI is detected and mitigated on-board.

Note 3: To support the correct verification and evolution of on-board processor RFI detection and mitigation algorithms in a changing RFI environment (e.g., 5G networks) on-ground RFI management activities and re-processing is required.

MRD-640 When Radio Frequency Interference (RFI) of a measurement is detected and mitigated by on-board processing, both the original measurement data (i.e. that unprocessed by the RFI system) **and** the RFI mitigated measurement shall be available to users.

Note 1: This requirement allows the performance of RFI filtering on-board to be assessed by the scientific and operational user community.

Note 2: In case of on-board RFI processor failure, access to original data for further on-ground processing will be required to continue the mission.

Note 3: It is expected that RFI mitigated and unmitigated data are available in L1a and L1b products.

MRD-650 When Radio Frequency Interference (RFI) of a measurement is detected and mitigated by on-board processing, relevant data generated by the RFI processor for the affected measurement shall be available to users.

Note 1: This requirement allows the performance of RFI filtering on-board to be assessed by the scientific and operational user community. This is important since the NEΔT for a measurement that has been ‘cleaned’ for RFI will be modified.

Note 2: “relevant data” in this requirement would include all data samples computed and used in a time-frequency assessment matrix, and statistical indicators such as thresholds and kurtosis, etc.

Note 3: Data compression approaches may be used to minimise the volume of data (e.g., selecting specific data of use for re-computation of NEΔT, re-filtering or identifying RFI sources).

Note 4: RFI sources may be used as a validation source for geolocation – see note in MRD-680.

Note 5: It is expected that RFI mitigated and unmitigated data are available in L1a and L1b products.

Historically, space systems have neglected their entitlement to radio protection and have not reported RFI (radio frequency interference) to the ITU-R. This situation has led to external erroneous assertions that the space services, including the Earth Exploration Satellite Service (EESS) and the Space Research Service (SRS), do not experience any significant RFI.

Important work has been performed for the past years to increase awareness of the RFI affecting space services and to improve the means to report it in different fora, such as the Space Frequency Coordination Group, and the ITU have developed the Satellite Interference Reporting and Resolution System (SIRRS), an online tool for reporting RFI to satellite system. SIRRS allows satellite operators to report RFI affecting radiometers. In short, when radiometers experience RFI, they can document these instances and report them to SIRRS. That information is then shared with the ITU and the National administration where the RFI source is located.

Efforts must be continued and intensified by raising concern among the different countries and relevant organisations about the detrimental impact of RFI in the operation and in the scientific return of scientific space missions. ESA has extensive experience with RFI monitoring and reporting with the national regulatory authorities thanks to the SMOS mission (e.g., Uranga *et al.*

2018). Claiming protection from interference is a right and it ensures that the number of interference cases decrease or do not grow despite the number of wireless equipment that can be a potential source of interference that has been growing exponentially over the last 10 years. There are other satellite missions and terrestrial radio astronomy organizations also claiming protection and reporting. It is important to try to coordinate all these efforts, as ESA SMOS is currently doing with the NASA SMAP mission. To be even more effective, ESA has set up a procedure to coordinate RFI reports with NASA, who operates a single channel L-band microwave radiometer mission (SMAP) in the same band as SMOS. As a result, the two agencies are now submitting RFI reports to the same administrations at the same times, which is beneficial to both agencies.

Building on this established foundation, CIMR RFI cases should be reported via SIRRS in the same way as done today for SMOS. In addition, as done by SMOS today, CIMR should maintain monthly global statistics (e.g., spatial distribution, intensity, persistence in time, statistical moments, amongst others as necessary) for all CIMR channels throughout the CIMR mission lifetime.

MRD-655	Radio Frequency Interference (RFI) cases and monthly global statistics (e.g., spatial distribution, intensity, persistence in time, statistical moments and others as necessary) shall be maintained for all CIMR channels throughout the CIMR mission lifetime.
---------	--

Note 1: These activities use data from the CIMR on-board RFI processors via the ground segment. RFI statistics with global scope in space and in time are necessary to commission the RFI processing system.

Note 2: As the RFI environment changes, it may be necessary to reconfigure on-board RFI processor coefficients on a periodic basis. By actively monitoring the characteristics and evolution of RFI sources (in space and in time), the performance of the CIMR on-board RFI processor can be continuously assessed (i.e. minimal false positives and false negatives etc). To accommodate a shift in the global RFI environment (which is a regular occurrence), the ground-based RFI monitoring function provides the evidence necessary to reach a decision as it if/when an update of the CIMR onboard RFI processor algorithm configuration is required.

Note 3: A database of RFI must be maintained that is updated every orbit by the CIMR ground segment RFI management service.

MRD-657	CIMR RFI cases shall be reported via the International Telecommunications Union (ITU) Satellite Interference Reporting and Resolution System (SIRRS) platform.
---------	--

Note 1: Formal RFI reports have to follow the ITU template for reporting (i.e. Recommendation ITU-R RS.2106) and they have to include images or other information as requested by the National Authorities. The exact content of the reporting will be developed in collaboration with the ESA Frequency Management team at ESTEC.

Note 2. Strategies are in place at ESA to mitigate the impact of RFIs in particular the collaboration established with National Frequency Regulatory Authorities for the investigation of interference cases and for the enforcement of the in-force

regulatory framework, which may include switching-off the unauthorised RFI sources.

4.2.16 Geo-location Requirements.

One of the most important downstream applications of CIMR SIC is the merging with high-resolution data from other sources and (mainly Sentinel-1 SAR, L-band SAR or altimeter data) information to allow automatic ice charting. The focus will be on locating the sharp gradient regions (MIZ). This places strong constraints on an accurate geolocation for all channels. Furthermore, a km-scale geolocation error is likely too poor for Sea Ice Drift retrievals. The impact of geolocation error on Sea Ice Drift retrievals strongly depends on if it is a “noise” (random) or a systematic error (e.g., along-track). Geo-location is also important to ensure that the location of CIMR measurements is correct with reference to the WGS-84 ellipsoid and for co-registration with MetOp-SG(B1) MWI and SCA data. The spatial resolution of MetOp-SG(B1) MWI measurements at the highest resolution are 10 km. The geolocation accuracy is set at < 2.5 km (1σ , zero-mean). The nominal spatial resolution of MetOp-SG(B1) SCA is 25 km gridded cells although 12.5 km gridded products will be available. The geolocation accuracy is set at < 1 km (1σ , zero-mean see *Rostan et al. 2016*).

Retrieval of geophysical products from CIMR requires simultaneous use of data taken at different frequencies, and that all involved channels represent the same regions of the Earth’s surface or atmosphere. As the data are typically taken by different feedhorns and the same antenna reflector, they may point to different regions on the Earth, in addition they have different spatial resolutions.

Due to the impact of conically scanning and satellite velocity (discussed in Sec. 4.2.4 and Sec. 4.2.5), CIMR sample measurements are ‘smeared’ in both the flight direction and the scan direction. This outcome is common to all to all conically scanning microwave radiometers. *Wiebe et al. (2007)* present an approach for AMSR-E that retrieves parameters for the viewing angles of the satellite instrument with which a more accurate projection of measured brightness temperatures to latitude and longitude coordinates can be achieved. The method to improve the geolocation of AMSR-E data is to determine optimal constant offsets for all off-nadir and initial scan angles of the measurements given in the AMSR-E Level 1 data. Based on these values, the latitude and longitude boresight coordinates for each footprint are recalculated.

Purdy et al. (2006) discuss Geolocation and pointing uncertainty analyses of WindSat flight data. Beam pointing knowledge uncertainty is critical to support accurate polarimetric radiometry. Pointing uncertainty was improved and verified using geolocation analysis using matchups comparing coastlines indicated in imagery data with their known geographic locations to identify geolocation discrepancies.

However, coastlines appear as dramatic temperature changes at land water boundaries caused by the significant differences in brightness temperatures for land and water although the transition from water to land typically occurs over a blended region due to side-lobe contamination. Alternatively, the local maximum temperature gradient along scan and cross scan can be computed and the partial derivative of the sampled radiometer data with respect to the scan contains information about the antenna gain function in the along-scan direction. In particular, an estimate may be made of the position of the “mean” shoreline in terms of the location associated with the maximum of the partial derivative of the sampled data. A smoothed first derivative of the radiometer samples with respect to the sample number can be used to solve for the fractional sample number associated with the peak of the derivatives. Using the latitude and longitude coordinates for the sampled data the fractional sample number to latitude and longitude coordinates (associated with the peak of the gain function) can then be computed and used to

estimate geolocation uncertainty. In the case of WindSat, this method represents the coastline to an uncertainty of less than 2 km (*Purdy et al.*, 2006).

Over the open ocean where no reference ground targets are available, geo-location relies on knowledge gained from instrument and platform pointing. Pointing errors may be systematic affecting all beams or may be attributable to individual beams (*Purdy et al.*, 2006). The CIMR 36.5 GHz channel has the smallest 3-dB footprint of ~3 x 5 km. Thus, achieving good geolocation accuracy depends on excellent knowledge of several in-flight parameters including OZA (beam elevation), beam azimuth position, feed boresight position, roll, pitch, yaw uncertainty and pre-launch characterisation knowledge – all depending on the implementation of CIMR. This information must also be supplemented using a variety of statistical analyses used to validate geolocation uncertainty based on the use of in-flight data, ground control points and coastline/coastline gradient analyses (e.g., *Purdy et al.* 2006) and/or other methods.

It is important to select a reference location for a L1B measurement for geolocation uncertainty validation which in the case of CIMR will be beam dependent. The antenna boresight provides the position of the peak of the -3dB antenna gain and is thus the location on the Earth surface that is most representative of the signal received.

MRD-660	The geo-location uncertainty of CIMR L1b measurement shall be $\leq 1/10$ of the footprint_size (1σ , zero mean) as specified in Table MRD-2 ID-090-1-13 evaluated for each beam, at the antenna boresight position on ground, corresponding to mid-point along the beam scan that lies exactly between the centre of the first IFOV of the first measurement and the last IFOV of the last measurement, for a given measurement integration interval.
---------	---

Note 1: AMSR-E geolocation studied by Wiebe et al. (2008) demonstrates that accuracy varies with frequency (6 to 89 GHz) from 1500 to 250 m. WindSat geolocation accuracy is studied by Purdy et al (2006) which proposes several techniques based on the analysis of coastal features and gradients. These could be used by CIMR.

Note 2: Geolocation is computed from L0 to L1a and is included in L1b. When CIMR launches, "pre-launch" values for all parameters needed to compute geolocation (theoretical orbit, attitude, OZAs for all feeds, etc...) will be available to compute "pre-launch" geolocation. During commissioning, it is expected that coastlines, islands, and other points of interest will be used to assess the geolocation performance of CIMR. Any systematic deviation observed during commissioning will be analysed and adjustments for all relevant parameters.

Note 3: CIMR geolocation assessment is a continuous monitoring challenge throughout the mission.

Note 4: Geolocation applies to all frequencies and all polarisations and all samples. The smallest granule of information available from CIMR will be a sample that should also include geolocation information.

Note 5: For performance assessment, this requirement is to be met at L1b. Since a L1b is composed of samples, each sample must be geolocated. The geolocation performance is to be met at L1b measurement which is the average of ≥ 5 samples and represents a smeared area measurement. Since geolocation is specified for a given location in the azimuth (i.e. varies around the azimuth) geolocation must be evaluated using a precise approach.

Note 6: For CIMR, geolocation should be evaluated for each beam, at the antenna boresight position on ground, corresponding to mid-point along the beam scan that lies exactly between the centre of the first IFOV of the first measurement and the last IFOV of the last measurement, for a given measurement integration interval. For example, should 5 samples be used, the antenna boresight position on ground (i.e. the peak of the -3dB antenna gain on Earth), then the Barrycentre of the L1b measurement would be used to asses performance. Clearly, L1b samples must also be assessed to evaluate their geolocation consistency and stability within the context of a L1b measurement.

Note 7: Accurate positioning of RFI sources (especially via potential processing of grating lobe signals) could be extremely useful to report RFI at the international level (SMOS is better than 5 km after post processing). It is expected that CIMR should be able to locate RFI sources to within +/- 5 km.

MRD-665 On-board Attitude Orbit Control System data shall be made available at the same time as CIMR instrument data to achieve L1b geolocation requirements specified in Table MRD-2 ID-090-1-13.

Note 1: Geolocation accuracy at L1b is an important aspect of the CIMR Mission. Timeliness to NRT1H is also important for several L2 products. To facilitate data processing on ground the necessary platform position/pointing information should be available in a timely manner. Ideally this information should be available such that processing does not need to wait for AOCS data downlinked separately to proceed with the processing.

Note 2: In order to compute the OZA for L1b processing and geolocation, pointing information is required from the AOCS.

Note 3: CIMR NRT1H requirements imply that AOCS must be available at the same time as CIMR instrument data.

Geolocation is inextricably linked to Absolute Performance Error (APE) of the instrument pointing accuracy (attitude) and the uncertainty of this parameter expressed as an Absolute Knowledge Error (AKE, see ESSB-HB-E-003, 2011). These parameters are important inputs to the L1 and L2 scientific processing systems. In addition, application of polarized data (e.g., for L2 wind vector measurements, use for surface roughness calculations etc.) are typically derived from very small differences in polarization pairs (e.g., Gaiser et al, 2004). Therefore, pointing errors have a large impact on the validity of the derived geophysical parameters, primarily because of the impact of OZA variations on the brightness temperature and polarization rotation angle variations on the cross-polarization coupling.

MRD-670 The CIMR Observation Zenith Angle shall be known with an Absolute Knowledge Error (AKE) of <0.05° per axis.

Note 1: Accurate knowledge of the OZA is required for accurate determination of surface emissivity and retrieval of geophysical products – see Wentz and Meissner, 2000; 2007 and Meissner and Wentz, 2012.

Note 2: Emissivity of the target source is a function of OZA, frequency and polarisation. It is influenced by surface properties (e.g., Wind induced isotropic roughness

(waves, capillary diffraction waves, foam, ice/snow surface roughness and scattering properties) and by subsurface properties (dielectric coefficient of the target material). For an increasingly rough sea surface, microwave emission increases and polarization differences decrease. At OZA > 55° and a rough sea surface, the vertical polarisation emission begins to decrease. See Wentz and Meissner, 2000; 2007 and Meissner and Wentz, 2012.

MRD-680 The combined CIMR platform pointing shall be known with an Absolute Knowledge Error (AKE) of <0.01°.

Note 1: The 18.7 GHz channel is considered as the pointing reference channel.

Note 2: AKE on relative pointing for AMSR-E was < 0.07 (Wiebe et al. 2008). For WindSat this was split into Coriolis/WindSat was designed to provide knowledge errors of ±0.05° bias and ±0.05° random components in each OZA and Polarisation Rotation Angle (Gaiser et al 2006).

Note 3: The combined pointing AKE is composed of a fixed bias component that could be verified at land/ocean crossing points and a variable component that must be estimated.

Note 4: A key aspect is to ensure stability of pointing during extended periods where no ground verification is possible.

MRD-690 In addition to any on-board AOCS solution, individual unprocessed attitude sensor data (e.g., from each star-tracker) shall be available to users.

Note 1: Due to the stringent pointing requirements for the CIMR mission and large rotating reflector, individual star tracker, angular position of the antenna and other relevant data will be required on ground to precisely reconstitute CIMR pointing and as input to L2 retrieval algorithms applied by the user community.

4.3 Product Requirements.

The CIMR mission product suite is focussed on providing the maximum flexibility and utility for operational users while preserving the radiometric integrity of measurement data.

4.3.1 CIMR Product types

Figure 4.3.1-1 provides a simplified flow chart highlighting the relationship between Level-1a, Level-1b, Level-1c and Level-2 products.

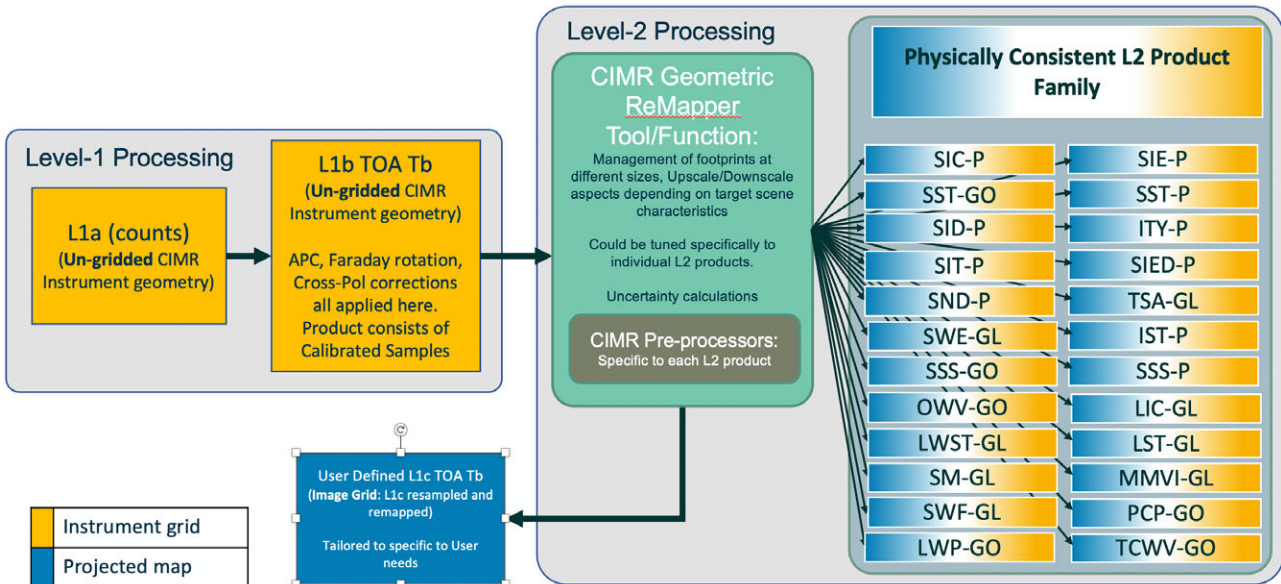


Figure MRD-4.3.1-1. Schematic overview of the main data products for the CIMR mission. TOA=Top of Atmosphere, Tb=Brightness Temperature, SIC=Sea Ice Concentration, SIE=Sea Ice Extent, SST=Sea Surface Temperature, SID=Sea Ice Drift, ITY=Ice Type/stage of Development, SIT=Sea Ice thickness, SIED=Sea Ice Edge, TSA=Terrestrial Snow Area (extent), SND=Snow Depth on Sea Ice, SWE=Snow Water Equivalent, SSS=Sea Surface Salinity, LIC=Lake Ice Concentration, OVW=Ocean Vector Wind, LWST=Lake Water Surface Temperature, MMVI=Microwave Multichannel Vegetation Indicators, SM=Soil Moisture, PCP=Precipitation, SWF=Surface Water Fraction, TCWV=Total Column Water Vapour (atmosphere), LWP Liquid Water Path, G=Global, P=Polar, O=Ocean, T=terrestrial.

For a conically scanning radiometer such as CIMR, the most efficient way to manage CIMR products is to store and manipulate measurement data in the native instrument scan geometry. Figure 4.3.1-2 shows a schematic representation of the CIMR samples on ground for a hypothetical and idealised implementation in which samples are returned at the integration time of Ka/Ku band. The actual implementation of CIMR may differ.

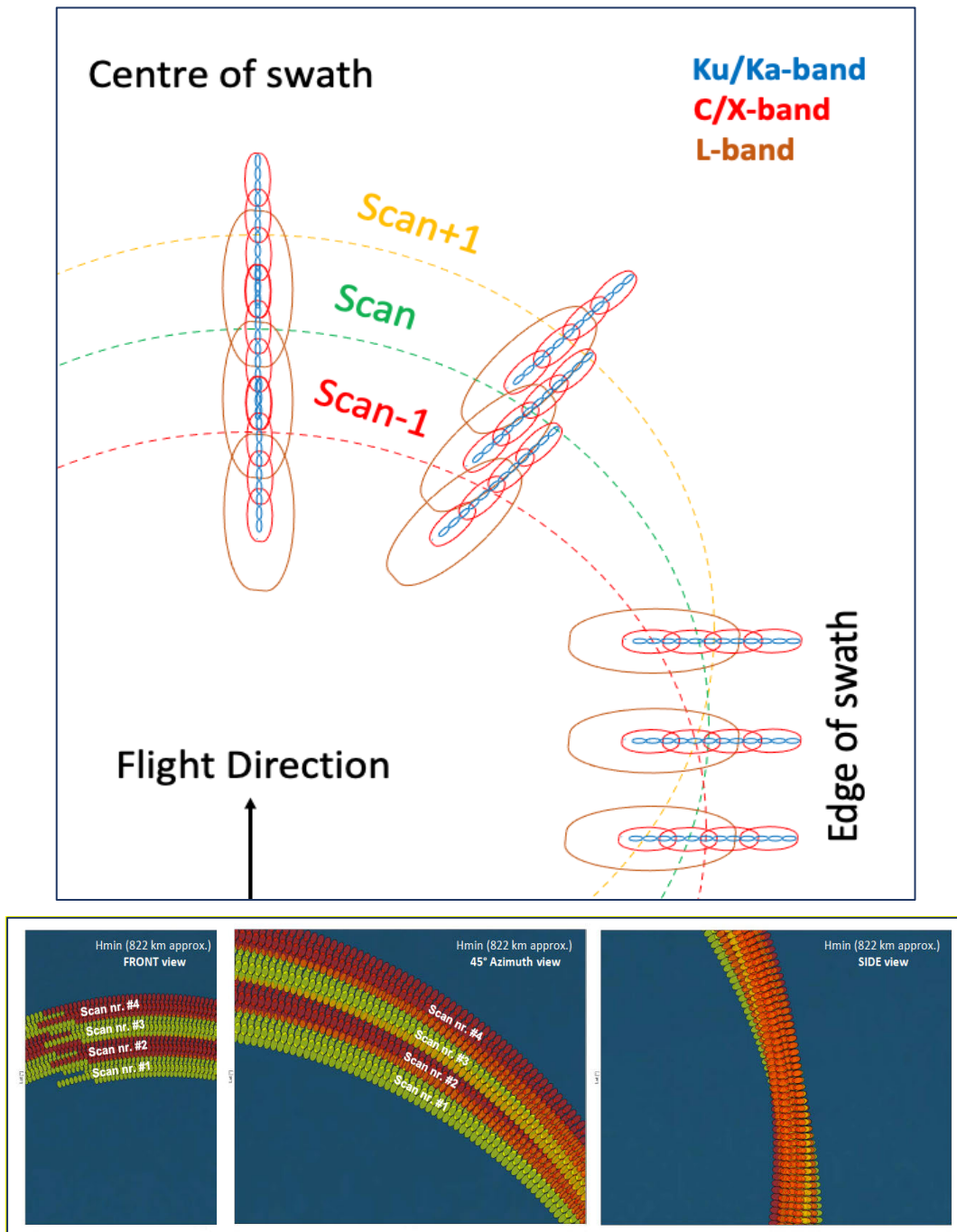


Figure 4.3.1-2. Schematic representation of idealised CIMR footprints for a hypothetical system with the footprint characteristics set out in this MRD. A small number of example measurement footprints are shown at 90°, 45° and 0° azimuth for a single quadrant of the CIMR scan for three consecutive scans as the satellite flies forwards. The L-band feed has an OZA $\sim 52^\circ$ whereas all other footprints have an OZA of $\sim 55^\circ$. Thus, the L-band feed is offset from the other feeds having a narrower swath. In reality, the full swath will be populated with many more sample measurements. It highlights how the relative location of each set of scan-line footprints changes around the azimuth. The lower plot shows many more example footprints at C-band and the large oversampling capability anticipated from CIMR toward the edge of the swath (figure courtesy of TAS-I). The actual implementation of CIMR may be different from this hypothetical example.

It is important to recognise that toward the edge of the swath oversampling increases. In Figure 4.3.1-2, not all samples are shown for clarity.

The CIMR instrument sampling approach provides:

- Measurement **samples** (≥ 5 for each L1b measurement) are the primary measurement likely to be sent to ground for further processing necessary to meet L1b requirements per feed, per frequency band,
- Measurement samples have a quasi-elliptical footprint over the ground from each feed and the orientation of the sample with reference to the Earth surface changes around the scan azimuth,
- Each measurement sample has a different size footprint depending on the band frequency (L-band < 60 km, C/X-band ≤ 15 km, Ka/Ku-band < 5 km),
- Because the instrument must use different feed horns for each band (and potentially multiple feedhorns for that band), measurements for each CIMR band within L1a and L1b data products will view different Earth locations with different size footprints at a given time. The mismatch in spatial resolution becomes a critical consideration when observations at different frequencies must be combined to retrieve geophysical parameters that are not generally homogeneous over such large dimensions (*Robinson et al., 1992*).
- Samples are acquired along a scan arc in a forward view and separately in a scan arc of a backward view. Temporal differences are expected to be very small for a given set of measurements and scan arc. However, the temporal difference and view direction (impacting Bio-directional Reflectivity Distribution Function (BRDF) assumptions) between the forward and backward scan data are significant. Forward and backward scan data are therefore requested as separate data streams in L1 products for users to manipulate according to the application requirements.
- Samples are overlapped by at least 20% in both the scan and flight direction (with exceptions for X-, Ku- and Ka-band),
- Each sample sent to ground includes four measurements (full Stokes Vector) if RFI is not detected. If RFI is detected, each sample includes four measurements without RFI processing applied, and four measurements with RFI processing applied. In addition, the RFI mitigation matrix used to mitigate RFI and quality indicators are also included. It is anticipated that 20% of Earth coverage may be RFI contaminated based on L-band SMAP mission statistics.
- L-band measurements use smaller OZA thus the coverage of L-band data is less (smaller swath width) than for other channels: the L-band swath is ~ 170 km smaller.

Since the orientation of a sample relative to the flight direction varies around the azimuth relative to the Earth surface, L1a, L1b and L2 products are specified in native instrument scan geometry, while L1c products are processed to deliver resampled and gridded products (images). This allows users to apply their own re-gridding algorithms starting from the L1b products (the purest radiometric information) should that be required. Furthermore, users can re-grid and project Level-2 products as required by their specific application. Re-gridding introduces additional uncertainties due to re-sampling; choices will need to be made regarding which samples to use in the grid – especially toward the scan edges where orphan measurements may emerge and/or data may be interpolated to “cosmetically fill” a grid cell as in the case of other conically scanning radiometers such as the Sentinel-3 SLSTR. This is discussed in the following sections.

4.3.1.1 Un-gridded products

CIMR L1a, L1b and Level-2 products are un-gridded products.

Un-gridded products contain measurement samples in the native CIMR scan geometry.

Un-gridded products preserve the radiometric properties of each sample measurement in the native conical scan geometry of the CIMR design. All data are retained on the original instrument frame of reference, arranged by scan and sample indices. Thus, there is a direct correspondence between the contents of a product record and the contents of a CIMR instrument scan.

L1a data contain counts and are designed to be as close to a Level-0 product as possible (i.e. calibration information is included but not applied to the data). L1b products have all calibration information applied with geolocation computed and associated with each sample. When displaying a native un-gridded data, any geophysical features will appear distorted due to the conical scanning geometry of the instrument. However, the advantages of this approach are:

- Radiometric data are retained in their original, time ordered coordinate frame.
- It is a simple process to re-grid to form an image using scan, sample, and channel information.
- Product size is reduced since there are no additional cosmetic pixels or orphan pixel data to store (which is the case for image grid products).
- No unfilled pixels at the edges of the image swath will be generated.
- L1 processing can easily be split into time-sliced segments.
- The transformation from un-gridded to gridded products is a relatively simple operation.

4.3.1.2 Gridded products

CIMR L1c products are nominally gridded products (some users may prefer products as un-gridded swath products similar to L1 products).

Gridded products contain geolocated projected images. Geolocation derives the Earth-locations of the acquired footprints and maps these onto an appropriate image grid using a particular projection.

The Equal-Area Scalable Earth (EASE2, https://nsidc.org/data/ease/ease_grid2.html) grid is one approach designed for Polar Regions. These grids were originally conceived at the US NSIDC and have been used to archive several satellite instrument data sets including SMMR, SSM/I, SSMIS and AMSR-E. It is also the scheme adopted by the SMAP mission, and several ESA CCI data records. For CIMR, adopting EASE2 in the Polar Regions provides user convenience, facilitates continuity of historical data grid formats, and enables re-use of heritage gridding and extraction software tools already developed. Because they are equal area grids, visualization and inter-comparison operations are greatly simplified and data analysis is more convenient.

However, the EASE2 format may not be convenient for other products and alternative choices could be made such as Equal Area Cylindrical projection for land and global products.

4.3.2 L0 Products

L0 data products contain native instrument source packets data downlinked from the spacecraft.

4.3.3 L1a Un-gridded Products

CIMR products at L1 will be provided in native instrument geometry (sometimes called “swath” products) with no convolution applied (i.e. preserving the “pure” radiometric content of the measurements) so that every sample measurement acquired is available to users.

L1a is the foundation CIMR product that carries all information from CIMR with all calibration and geolocation data available but not applied (i.e. the data remain in counts and instrument scan geometry and very close to a L0 product). The intention is to provide a L1a data product that could be used as the starting point for re-processing activities.

Table 4.3.3-1. Overview of CIMR L1a products

Product	Description
CIMR L1a	<p>Observed sensor engineering data for each channel in instrument geometry at native channel resolution. L1a data are derived from L0 data that have been reconstructed and ordered into orbit files.</p> <p>Data are unprocessed instrument data (counts) at full resolution (i.e., all samples, from all feeds, in all polarisations), time-referenced, and annotated with ancillary information, including radiometric and geometric calibration coefficients (e.g., thermistor counts etc.) and geo-referencing parameters (e.g., platform ephemeris) and auxiliary information (e.g., relevant solar angles etc) computed and appended.</p> <p>No calibration or instrument corrections are applied to L1a data: it is designed as the starting point for all higher-level ground processing and, in particular, reanalysis.</p> <p>See JAXA (2005), Aqua AMSR-E Level 1 Product Format Description Document, MAS-100045A as an example.</p>

MRD-700 L1a data products shall be produced and made available to users.

Note 1: This essential requirement provides flexibility for the ground processors and end user community because L1a products maintain data in native scan geometry with pure radiometry.

Note 2: See definition of product levels.

Note 3: MRD-1100 for availability and timeliness requirement.

A NetCDF like format has been chosen for CIMR L1a data products (<https://www.unidata.ucar.edu/software/netcdf/>). However, as cloud processing and new IT technologies are emerging at a rapid rate, alternative file formats may be more widely used at the time of CIMR that may provide a more useful format that cannot be dismissed.

MRD-710 L1a products shall be formatted in a NetCDF like format.

*Note 1: Network common Data format (NetCDF) see
<https://www.unidata.ucar.edu/software/netcdf>*

*Note 2: It is recommended that L1a products follow accepted conventions such as the Climate and Forecast (CF) Convention and latest Attribute Convention for Data Discovery (ACDD) discovery metadata convention see
<http://cfconventions.org/> and
http://wiki.esipfed.org/index.php/Category:Attribute_Conventions_Dataset_Discovery*

Note 3: The L1a product format may evolve to align to state-of-the-art solutions.

MRD-720	CIMR L1a products shall remain in instrument swath geometry with calibration and geolocation available as part of the product but not applied to the data.
MRD-730	<p>A CIMR L1a product shall contain sufficient information for CIMR re-processing activities.</p> <p><i>Note 1: This is a foundation product that is as close to a Level-0 product as possible implying that a significant amount of engineering/calibration data is also part of the product.</i></p> <p><i>Note 2: L1a is the foundation CIMR product that carries all information from CIMR with all calibration and geolocation data available but not applied (i.e. the data remain in counts and instrument scan geometry and very close to a L0 product). The intention is to provide a L1a data product that could be used as the starting point for re-processing activities while deep archiving L0 data.</i></p> <p><i>Note 3: See Table 4.3.3-1 for an overview of CIMR L1a products</i></p>

4.3.4 L1b Un-gridded Products

L1b data are derived from L1a data to form L1b measurements that are calibrated and geolocated. All engineering corrections and calibration parameters (e.g., side-lobe and grating lobe contributions, Faraday and geometric rotation corrections, calibration measurement targets, geolocation adjustment if required) are applied. L1b products remain in native instrument geometry and L1b measurement resolution (i.e., no gridding or mapping projections are implemented). Except for the construction of a L1b-measurement from samples, no further resampling or interpolation of data will be performed to reach this product level. The intention is to provide measurement data with minimum data processing so that the L1b represents the purest calibrated top-of-atmosphere radiometry in instrument geometry.

Table 4.3.4-1. Overview of CIMR L1b products

Product	Description
L1b	<p>Top of the atmosphere calibrated brightness temperature (full modified Stokes parameters) for each channel in instrument geometry.</p> <p>L1b products include all measurement samples (MRD-340) used to derive the L1b measurements. L1b data also include all RFI data – but only when RFI is detected and mitigated (MRD-640 and MRD-650).</p> <p>All engineering corrections (e.g., side-lobe and grating lobe contributions, Faraday and geometric rotation corrections, calibration measurement targets quantities and other relevant calibration information per scan, geolocation adjustment linked to geolocation tie-points (TBC) etc) have been computed and (as appropriate) applied to each sample, radiometric calibration parameters have been applied to each sample to output top-of-atmosphere spectral brightness temperatures (Tb) in units of Kelvin, modified Stokes parameters are included, all RFI</p>

	<p>information and supporting data when RFI is detected are included.</p> <p>Uncertainties per-pixel are computed and included. Quality flags, per pixel, are computed and included. Geometric information is computed using a tie-point approach (TBC) and linked to each sample (i.e. there is no reprojection or resampling to a gridded product). Preliminary pixel classification (e.g., land/ocean/ice etc) is included in the product, as well as uncertainty information, and sub-footprint land area fraction. The coefficients converting brightness temperatures to radiance allowing conversion between the two quantities.</p> <p>For illustrative purposes only, a simplified description of L1b data consists of:</p> <pre> foreach(scan) { • scan_calibration_data[feed[], quality_flag[], calibration_total_standard_uncertainty[]], • geolocation_tie_points, foreach(L1b-measurement) { • L1b_H_polarisation_samples[TOA_Tb[], quality_flags[bitfield e.g standard flags, NEΔT etc], total_standard_uncertainty[],pixel_classification[bitfield e.g., land/ocean/ice etc], (TBC) sub_footprint_water_fraction_area[intent is to exclude land, ice sheets, ice shelves based on pixel_classification], /* needs to be handled in the L1b processor */, (TBC) sub_footprint_land_fraction_area[intent is to exclude land, ice sheets, ice shelves based on fixed masks], /* needs to be handled in the L1b processor , useful for geolocation*/; o if (RFI_detected) {same as above but with RFI_mitigated_Tb[]; RFI_time_frequency_matrixp[];} • L1b_V_polarisation...[as for L1b_V_polarisation above] • L1b_Stokes3.....[as for L1b_V_polarisation above] • L1b_Stokes4.....[as for L1b_V_polarisation above] } } </pre>
--	--

As noted by Jimenez *et al.* (2021), for L-band, additional processing is required, including the calculation of the Faraday rotation angle, estimation of the Sun and Galactic glint contributions for the given viewing geometry, and calculation of main beam TBs below the ionosphere. The Sun and Galactic glint components can be calculated using different methodologies developed (e.g., Reul *et al.*, 2007, 2008; Tenerelli *et al.*, 2008; Meissner *et al.* 2017; 2022). For that purpose, an L-band sky map is generated, including the hydrogen HI line, the L-band continuum, and the cosmic background.

4.3.4.1 Mitigating the impact of galactic radiation on CIMR L-band Tb

Radiation from the galaxy (in addition to the constant Cosmic Microwave Background, CMB, radiation) constitutes a significant contamination of L1b Tb and is the potential source of systematic errors at L-band (e.g., Le Vine and Abraham 2004; Reul *et al.* 2008; Meissner *et al.* 2017, 2018; Dinnat *et al.* 2018; Meissner *et al.* 2022). This poses a challenge for applying L-band

measurements for geophysical retrievals – particularly retrieving ocean surface salinity with CIMR, considering the very stringent accuracy requirement of 0.3 pss. (SEC-OBJ-09).

The galactic radiation can enter the CIMR measurement system in the following ways:

1. Directly through the antenna back-lobes.
2. Through reflection from the wind roughened ocean surface.

The magnitude of either direct or reflected galaxy brightness temperature is in the order of 0.2 K – 5 K. Following the experience from SMOS (*Reul et al.* 2008), Aquarius (*Meissner et al.* 2017, 2018) and SMAP (*Meissner et al.* 2022), the correction is applied when going from Level 1 to Level 2. If the performance of CIMR SSS L2 products (MRD-980 and MRD-985) are to be met, a correction to be applied at L1b must be derived and applied.

The basis of an accurate pre-launch derivation of the direct and reflected galactic radiation is based on L-band galactic Tb maps (*Le Vine and Abraham* 2004; *Reul et al.* 2008; *Dinnat et al.* 2018). The latest version of the galactic TB map was provided by *Dinnat et al.* (2018) for the centre frequency (1.41 GHz) and bandwidth (about 25 MHz) of Aquarius and SMAP.

If the CIMR L-band centre frequency and band width differs significantly from Aquarius and SMAP, the galactic TB map might need to be recomputed. Extending the galactic TB map to a very wide L-band (1.1 – 1.7 GHz) is not straightforward and may result in additional uncertainties. The L-band galactic radiation consists of a narrow line absorption at 1420 MHz and a continuum absorption, which has very different spectral characteristics. The continuum absorption has been surveyed close to the line, which is very close to the Aquarius and SMAP centre frequency (*Dinnat et al.* 2018). For a very wide L-band, uncertainties due to the galactic continuum and their impact on the accuracy of the sea surface salinity must be quantitatively assessed.

The pre-launch computation of the direct galaxy is based on folding the galactic TB map with the back-lobe gain of the antenna pattern (*Meissner et al.*, 2017). It can be cast as a table that depends on time of the year and position within orbit.

The pre-launch computation of the reflected galaxy is based on folding the galactic TB map after reflection from the Earth surface with the gain of the antenna pattern. Over the ocean, wind roughening of the surface must be taken into account. Following Aquarius and SMAP (*Meissner et al.* 2017, 2018), one can model the rough ocean surface as an ensemble of tilted facets, whose slopes are randomly distributed according to Gaussian probability distribution whose variance is determined by the surface wind speed (geometric optics model). It can be cast as a table that depends on:

- Time of the year.
- Orbit position.
- Scan position.
- Surface wind speed.

During post-launch processing, the computation of the reflected galaxy requires ocean surface wind speed as ancillary input. This requires a wind speed value from either:

- An external numerical weather prediction model being available during L1 to L2 processing.
- The L1 to L2 processing for the L-band TB uses the retrieval output ocean wind speed from the L2 processing based on the higher frequency channels (C, X, Ku, Ka-bands). That means the ocean wind vector retrieval would need to be completed before the L-band L1 to L2 processing.

The pre-launch computation of the direct and reflected galaxy require a precise knowledge of the following CIMR parameters:

- Orbit,

- Scan system geometry,
- Antenna pattern,
- L-band spectral response function.

Analysis of the Aquarius and SMAP salinity retrievals (*Meissner et al. 2017, 2018, 2022*) have shown that the pre-launch computation of the direct and reflected galaxy for these sensors has an accuracy of about 90 – 95%. One should expect and be prepared for post-launch adjustment to some of the components, for example to the variance of the tilted facet slope distribution of the geometric optics model. The CIMR forward and backward scan capability can strongly aid in achieving this, since the reflected galaxy typically appears only in the foreword or the backward look (*Meissner et al. 2022*).

MRD-732 The impact of cosmic background and galactic radiation on CIMR Brightness Temperature shall be compensated at Level-1b.

Note 1: Radiation from the galaxy (in addition to the constant Cosmic Microwave Background, CMB, radiation) constitutes a significant contamination of L1b Tb and is the potential source of systematic errors at L-band (e.g., Le Vine and Abraham 2004; Reul et al. 2008; Meissner et al. 2017, 2018; Dinnat et al. 2018; Meissner et al. 2022).

Note 2: The pre-launch computation of the direct galaxy is based on folding the galactic TB map with the back-lobe gain of the antenna pattern (Meissner et al, 2017).

Note 3: Over the ocean, wind roughening of the surface must be taken into account. Following Aquarius and SMAP (Meissner et al. 2017, 2018), one can model the rough ocean surface as an ensemble of tilted facets, whose slopes are randomly distributed according to Gaussian probability distribution whose variance is determined by the surface wind speed (geometric optics model).

Note 4: During post-launch processing, the computation of the reflected galaxy requires ocean surface wind speed as ancillary input. This requires a wind speed value from either: (1) An external numerical weather prediction model being available during L1 to L2 processing. (2) The L1 to L2 processing for the L-band TB uses the retrieval output ocean wind speed from the L2 processing based on the higher frequency channels (C, X, Ku, Ka-bands). That means the ocean wind vector retrieval would need to be completed before the L-band L1 to L2 processing.

4.3.4.2 Mitigating the impact of Faraday rotation on CIMR L-band Tb

Faraday rotation is a significant error source at L-, C- and X- band. Faraday rotation is the change in polarization that occurs when an electromagnetic signal propagates through the ionosphere. At L-band this change can be significant, and it can be an important consideration for remote sensing of soil moisture and ocean salinity retrievals. All L-band radiometers launched in space (SMOS, Aquarius and SMAP) include polarimetric channels to estimate the Faraday rotation angle using the ratio of the third Stokes parameter, T3, and second Stokes parameter Q = Tv – Th, as proposed by Yueh (2000).

CIMR determines the 3rd Stokes parameter which allows the size of Faraday rotation to be determined. Since the spectral response of Faraday rotation is clear and well behaved as 1/frequency², if it is determined at 1 frequency (e.g., L-band) it can be known at the other

frequencies. Faraday rotation must be compensated in the L1b Tb for all relevant channels (i.e. L-, C- and X-band).

MRD-734 The impact of Faraday rotation on CIMR Brightness Temperature shall be compensated at Level-1b.

Note 1: CIMR determines the 3rd Stokes parameter which allows the size of Faraday rotation to be determined. Since the spectral response of Faraday rotation is clear and well behaved as 1/frequency², if it is determined at 1 frequency (e.g., L-band) it can be known at the other frequencies.

4.3.4.3 General requirements for Level-1b products

MRD-740 L1b products shall be produced in instrument swath geometry from corresponding L1a data.

Note 1: L1b products are the starting point for further L1c and L2 processors.

Note 2: There must be a direct mapping from L1a products to corresponding L1b products to facilitate reanalysis activities.

Note 3: L1b products require that a suitable algorithm is used to calibrate data, correct for antenna spill over, antenna gain patterns, other contributions in wide beam (e.g., grating lobes), attitude and pointing errors, to compute and provide geolocation information etc. Ancillary and auxiliary data sets will be required as input to the L1b algorithm

Note 4: L1b data products remain in the native instrument conical scan geometry.

Note 5: L1b products include all samples used to construct a L1b measurement within the product.

Note 6: L1b data also include all RFI data – but only when RFI is detected and mitigated (MRD-640 and MRD-650).

MRD-750 Each measurement sample from each feed horn in all polarisations (full modified Stokes) shall be provided in L1b products.

Note 1: L1b data may include low-level data processing choices that may result in a change of the pure radiometric signals (e.g., averaging of samples over footprint_size to reduce noise, resampling etc.) that may not easily be reversible. Access to sample data is therefore required.

Note 2: Different users may wish to combine data using different approaches and resolutions depending on the application. This is particularly relevant in the Marginal Ice Zone, at the coastal zones and in areas of strong SST gradients.

Note3: This requirement ensures that the purest radiometric measurement data at L1b from the CIMR instrument are available to users

A NetCDF like format has been chosen for CIMR L1b data products (<https://www.unidata.ucar.edu/software/netcdf/>). However, as cloud processing and new IT technologies are emerging at a rapid rate, alternative file formats may be more widely used at the time of CIMR that may provide a more useful format and cannot be dismissed.

MRD-760 L1b products shall be formatted in a NetCDF like format.

*Note 1: Network common Data format (NetCDF) see
<https://www.unidata.ucar.edu/software/netcdf>*

Note 2: It is recommended that L1 products follow accepted conventions such as the Climate and Forecast (CF) Convention and latest Attribute Convention for Data Discovery (ACDD) discovery metadata convention see <http://cfconventions.org/> and http://wiki.esipfed.org/index.php/Category:Attribute_Conventions_Dataset_Discovery (Note CF- convention now includes elements related to tie-point geolocation standardisation)

Note 3: The L1b product format may evolve to align to state-of-the-art solutions depending on the resources available within the CIMR system.

Note 4: Selected operational users include Numerical Weather Prediction Centres request BUFR format product. In future, as radiance-based data stimulation scenes become more prolific at operational centres, larger uptake of BUFR format products may emerge. It may be sufficient to provide a capability to convert the L1b products into Binary Universal Form for the Representation of meteorological data (BUFR) is requested to facilitate operational data assimilation systems (e.g., ECMWF). Challenges are evident since BUFR transmission via the WMO Global Telecommunications System (GTS) is limited to ~50 Mb per orbit placing significant restrictions on the product content. The WMO BUFR user guide is available at <https://www.ecmwf.int/sites/default/files/elibrary/2008/18140-bufr-users-guide.pdf>.

MRD-765 L1b data products shall be produced and made available to users.

Note 1: This essential requirement provides flexibility for the ground processors and end user community because L1b products maintain data in native scan geometry with pure radiometry.

Note 2: See definition of product levels.

Note 3: MRD-1100 for availability and timeliness requirement.

MRD-770

A CIMR L1b data product shall contain the L1b information necessary to generate all L2 products and populate the CIMR L1b uncertainty model.

Note 1: The exact content of L1b data products depends on the final implementation of CIMR. See Table 4.3.4-1 overview of CIMR L1b products.

Note 2: The following parameters are expected: the time of measurement; calibrated brightness temperatures for each channel in native instrument geometry at a resolution of 0.01K; the Earth-fixed location of each measurement at the centre of each footprint; earth incidence angle, earth azimuth angle, solar zenith angle, solar azimuth angle, land/ocean fraction for effective(integrated) footprint, ionosphere, Moon and Galaxy relevant parameters; uncertainty estimates for each measurement; calibration parameters applied to the data.

Note 3: L1b files use NetCDF4 Groups to structure the information.

Note 4: Tie points could be used to provide the Earth-fixed location of each measurement and/or extended to other angular quantities that have a smooth variation over the scan to reduce product size if required. This is the approach adopted for MetOp-SG(1B) MWI and ICI due to the large number of samples, in order to reduce product size.

*Note 5: **As an example**, the following NetCDF global Attributes are provided:*

Title	“CIMR L1b product”
disposition_mode	(“Test” “Commissioning” “Operational” “Validation”)
product_ID	Unique identification of the product
processing_level	L1b (note for convenience we also define “L1a” “L1b” “L1c” “L2”)
production_date	Product creation date (UTC) e.g., 2025-07-29T07:14:29.000Z
sensing_start_time_utc	UTC time of start of sensing data formatted in CF date and time format with millisecond precision
sensing_end_time_utc	UTC time of end of sensing data formatted in CF date and time format with millisecond precision
orbit_start	Absolute orbit number at sensing_start_time_utc
orbit_end	Absolute orbit number at sensing_end_time_utc
processing_centre	Data processing centre
contact_id	Name (e.g., European Space Agency)
processor_flag_description	Explanation of processor data flags
quality_flag_description	Explanation of quality data flags
science_flag_description	Explanation of science data flags
netcdf_version	Version of NEtCDF used
CF_version	Version of CF convention used
ACDD_version	Version of ACDD used
TBD	TBD

*Note 5: **As an example**, the following NetCDF Group: Satellite (all orbital values) fields are provided:*

orbit parameters:	<ul style="list-style-type: none"> • Epoch time in UTC of the orbital elements, • Semi major axis of the orbit at epoch time, • Eccentricity of the orbit • Inclination of the orbit • Argument of perigee of the orbit
-------------------	--

	<ul style="list-style-type: none"> Right ascension of the orbit
Location Summary	<ul style="list-style-type: none"> Latitude and longitude of subsatellite point at start of the product referenced to Earth Ellipsoid. Latitude and longitude of subsatellite point at end of the product referenced to Earth Ellipsoid.
State Vector and Attitude (all in Earth Fixed Reference Frame)	<ul style="list-style-type: none"> Time of the state vector and attitude items X,Y,Z position of the state vector X,Y,Z velocity of the state vector Yaw, Roll, Pitch attitude error
Leap Second Information	<ul style="list-style-type: none"> Time and “direction” of leap second event if one occurs during the product.
Manoeuvre Information (See MRD-775)	<ul style="list-style-type: none"> Number of manoeuvres during the product Time of start and end of each Manoeuvre
TBD	TBD

Note 6: As an example, the following NetCDF Group: Processing fields are provided

processor_name	“CIMR_L1b”
reprocessing_ID	Unique identification of the reprocessing run
Versions	Versions of the processor software, of the file format, of the input parameters (if any), of the ATBD describing the processor, etc...
processing_mode	NRT1H NRT3H, NTC, reprocessing.
upstream_source	name of the upstream file (typically L1a file)
creation time	time when the processor is run to generate this product
TBC	TBC

Note 7: As an example, the following NetCDF Group: Calibration Data (to be adapted to CIMR calibration strategy) fields are provided:

NEΔT	NEΔT at calibration loads
parameters	offset, gain, non-linear parameters
counts	“counts” at the calibration loads
temperatures	temperature readings relevant for calibration
TBD	TBD

Note 8: As an example, the following NetCDF Group: Navigation Data (one for each forward and backward scan) fields are provided:

time	time for each observation
observation position and geometry	The Earth-fixed location of each measurement;(at the centre of integrated footprint); - earth incidence angle, earth azimuth angle, solar zenith angle, solar azimuth angle, land/ocean fraction for effective(integrated) footprint, terrain elevation, sun glint angle, parallax latitude and longitude shift,
Other parameters	Ionosphere, Moon and Galaxy relevant parameters.
Platform information at the time of each observation	Orbit angle, spacecraft altitude, sub-satellite lat/lon,
Brightness temperature to radiance conversion coefficients	Coefficients for each channel and conversion equations in L1b product document allowing user to transform Brightness Temperature (K) to radiance (W/m ² -sr) quantities.
TBD	TBD

Note 9: *As an example, the following NetCDF Group: Measurement Data (one for each forward and backward scan) fields are provided:
See Table 4.3.4-1 for more information on this group*

Scan calibration	Calibration information from calibration subsystem for each scan <code>scan_calibration_data[feed[], quality_flag[], calibration_total_standard_uncertainty[], other_calibration_information (TBD)</code>
Geolocation	<code>geolocation_tie_points /* for this scan line of data */</code>
L1b sample brightness temperatures for each feed	L1b samples used to compute L1b measurement Tb for each feed (with at least 1/100K precision): For each Feed 1 x L-band feed 4 x C-band 4 x X-band 8 x K-band 8 x Ka-band and each polarisation [H, V, 3 rd Stokes, 4 th Stokes] we have: <code>L1b_samples[TOA_Tb[], quality_flags[bitfield e.g. standard flags, NEΔT etc], total_standard_uncertainty[], pixel_classification[bitfield e.g., land/ocean/ice etc], (TBC)</code> <code>sub_footprint_water_fraction_area[intent is to exclude land, ice sheets, ice shelves based on pixel_classification], /* needs to be handled in</code>

	<pre>the L1b processor /*, (TBC) sub_footprint_land_fraction_area[intent is to exclude land, ice sheets, ice shelves based on fixed masks], /* needs to be handled in the L1b processor , useful for geolocation*/; if (RFI_detected) {same as above but with RFI_mitigated_Tb; RFI_matrix}</pre>
lobe corrections	side and other lobes (e.g., grating lobes) corrections
Faraday rotation	Estimated Faraday rotation (needs also to be specified how this is derived in the L1 ATBD). The User may need to reverse this part of the processing (e.g., GIM model used, TEC etc)
TBD	TBD

Note 10: As an example, the following NetCDF Group: Flags (one for each forward and backward scan) fields are provided:

Quality flags	Per channel, per scan. Concerning Tbs, geolocation, calibration, navigation etc.
Surface Type	A first-guess of surface type (open ocean, sea-ice, land, lake...) based on a combination of masks (for static) and/or dynamic (sea ice) variables could also be monthly climatology for sea ice products (e.g., OSI-SAF with inputs from ESA CCI).
Processing flags	Issues/warning raised during processing
General quality	Summarized of the quality of the product (missing chunks, etc...)
TBD	TBD

MRD-775 The type of CIMR manoeuvres including the time of start and end of each manoeuvre performed within a CIMR product shall be available to users.

Note 1: This information assists users when applying the data in particular the type and number of manoeuvres during the product and the time of start and end of each manoeuvre is requested.

MRD-778 Data acquired during CIMR manoeuvres shall be available to users.

Note 1: This information assists users when applying the data and for reanalysis

Note 2: During manoeuvres, performance requirements may not be attained.

Note 3: It may be necessary to provide separate data products for data acquired during manoeuvres.

Note 4: MRD-220 requests data is acquired continuously.

MRD-780	<p>Standard total uncertainties and quality indicators shall be delivered for all CIMR measurements in a L1b data product.</p> <hr/> <p><i>Note 1: This is critical for the L1c and L2 processor design, propagation of uncertainties in the processors, and for application of higher L2 products that are used by data assimilation systems [AD-2].</i></p> <p><i>Note 2: Quality indicators are typically implemented as flags and/or numerical data attached to each measurement to provide information to users on aspects related to the measurement or processing that may impact the quality of data.</i></p> <hr/>
MRD-790	<p>The methods used to generate and propagate uncertainties and quality indicators shall be coherent across product levels and documented for users L1b data products.</p> <hr/> <p><i>Note 1: This is critical for the L1c and L2 processor design, propagation of uncertainties in the processors, and for application of higher L2 products that are used by data assimilation systems [AD-2].</i></p> <p><i>Note 2: Uncertainty estimates in higher-level products need to reflect uncertainty propagated from lower levels, if significant.</i></p> <p><i>Note 3: Quality indicators are typically implemented as flags and/or numerical data attached to each measurement to provide information to users on aspects related to the measurement or processing that may impact the quality of data.</i></p> <hr/>

4.3.5 L1c Gridded Products

L1b products are further processed to generate more user-friendly remapped products called CIMR L1c products. This demands knowledge of the measurement context in order to provide an appropriately gridded product (e.g., samples containing sea ice should be separated from those containing land or ocean). Appropriate gridding strategies and uncertainty propagation is a fundamental challenge for L1c products.

L1c products contain geolocated gridded images. Geolocation derives the Earth-locations of the acquired footprints and maps these onto an appropriate grid. The Equal-Area Scalable Earth (EASE2, https://nsidc.org/data/ease/ease_grid2.html) grid provides one approach. These grids were originally conceived at the US NSIDC and have been used to archive several satellite instrument data sets including SMMR, SSM/I, SSMIS and AMSR-E. It is also the scheme adopted by the SMAP mission, and several ESA CCI data records. Because they are equal area grids, visualization and inter-comparison operations are greatly simplified and data analysis is more convenient.

However, the EASE2 format may not be convenient for other products and alternative choices could be made such as Equal Area Cylindrical projection.

L1c products have the same content as L1b (brightness temperatures and associated quantities), but the centre points of all channels are matched to location (and resolution) of a target-frequency

channel. All other L1b data are synthesized by interpolation to the footprint of the target-frequency channels. This means that choices on how to select/compute a specific Brightness Temperature for a given grid point will need to be made since toward the edge of the swath the a given location on earth will be very oversampled. At the Centre of the swath in K- and Ka-band, small gaps between measurement scans may exist.

The L1c product will be helpful for retrievals using geophysical products combining observations at different frequencies. In the L1c product, different footprints observe different regions on the surface, and when combined to derive a value for a grid point, introduce noise that must be included in the L1c uncertainty value (i.e., L1c uncertainty values for a given grid point are different to the input L1b products since the additional uncertainty associated with re-gridding must be included).

As these products are gridded and mapped products, the standard total uncertainties that accompany each L1c grid cell must include the additional uncertainty associated with re-mapping. Furthermore, NE Δ T values may be better represented for a given grid cell rather than per L1b measurement in L1b products to account for under-sampling of high-frequency channels compared to the low frequency channels.

Table 4.3.5-1. Overview of CIMR L1c products

Product	Description
CIMR L1c	<p>Gridded Top of the atmosphere calibrated brightness temperature for each channel derived from CIMR L1b data files.</p> <p>All parameters of a L1b file are included in the corresponding L1c file.</p> <p>Additional parameters relating to the gridding process and the implications of the gridding process (e.g., uncertainty, NEΔT are likely to be different compared to native L1b etc.) will be included in a L1c file.</p> <p>L1c are geolocated images. Geolocation derives the Earth-locations of the acquired footprints and maps these onto an appropriate grid defined using an appropriate grid format e.g., for the Polar Regions the EASE2 format (<i>Brodzik et al.</i>, 2012; 2014) is well-suited to Polar Regions and utilize an equal-area projection to minimizes the amount of distortion over the poles.</p> <p>However, the EASE2 format may not be convenient for other products and alternative choices could be made such as Equal Area Cylindrical projection.</p> <p>Binary Universal Form for the Representation of meteorological data (BUFR) is important for meteorological services.</p>

It should also be noted that, for a conically scanning radiometer, the spacing between each scan will vary around the orbit due to (*Ashcroft and Wentz*, 2000):

- The elliptical satellite orbit will cause variations in the inter-scan distance.
- The oblateness of the Earth superimposes further variations with a relative phase determined by the orientation of the major axis of the satellite orbit relative to the Earth axis.
- The inter-scan distance is generally greater when measured at the centre of the swath in the flight direction compared to at the edges where multiple scans overlap.
- Earth rotation causes an asymmetry between the inter-scan distance measured at the first observation of each scan, and that measured at the last observation of each scan.

Antenna pattern matching algorithms are used to transform native L1b swath to L1c re-gridded products that demand a trade-off between noise, spatial and temporal resolution (e.g., *Long*, 2016). Conventional “drop-in-the-bucket” (DIB) approaches result in low-noise low-resolution products (*Long*, 2016). For higher resolution products (with potentially higher noise) image reconstruction techniques such as Backus–Gilbert (*Backus and Gilbert*, 1967; 1968) or the less computationally intensive radiometer form of the Scatterometer Image Reconstruction (SIR) algorithm (e.g., *Drinkwater et al* 1994; *Long and Daum*, 1998) are useful. However, *Ashcroft and Wentz* (2000) note that although the Backus–Gilbert method could in principle be used to construct effective observations corresponding to gain patterns either larger or smaller than those of the actual observations, the noise amplification for construction of smaller gain patterns (deconvolution) was deemed unacceptable. The OI method (e.g., *Stogryn*, 1978; *Poe*, 1990; *Meissner et al.* 2012) can be used to resample individual radiometer observations onto Composite Field Of View (CFOV) cells. The CFOV of all channels are shifted to a common location. In this approach, measurements are resampled around the main beam of interest defined by the -3dB footprint area of channels with lower frequencies (see definition of L1bR product (section 4.3.5)). Adjusted radiance can then be derived for each L1 product for every channel. This approach averages multiple finely sampled high-resolution measurements to lower resolution CFOV footprints with less noise. As a general rule, the finer the sampling of the measurement data, the more effective the OI method can be in finding a solution with lower noise. All of these techniques require sufficient overlap of adjacent measurements so that neighbouring pixels can contribute to the increase of the spatial resolution of the centre pixel of interest for the algorithm being applied.

All methods rely on very good instrument radiometric performance because deconvolution techniques imply an amplification of the associated radiometric noise (e.g., *Poe*, 1990; *Stogryn*, 1978; *Bauer and Bennartz*, 1998). The balance between resolution enhancement and increased noise must be evaluated by simulation and in-flight performance to obtain a satisfactory balance.

MRD-800 L1c data products shall be defined from a corresponding L1b data and contain all L1b parameters that have been geolocated and gridded to form an image grid for each channel.

Note 1: See Table 4.3.5-1 for an overview of CIMR L1c products.

Note 2: Different approaches exist on how to select/compute a specific Brightness Temperature for a given grid point. Toward the edge of the swath, a given location on earth will be very oversampled. At the Centre of the swath in K- and Ka-band, small gaps between measurement scans may exist.

Note 3: Nearest neighbour interpolation may be used to cosmetically fill gaps. These grid cells must be identified as “cosmetically filled” using an appropriate flag.

Note 4: If a grid point is oversampled redundant samples must be stored in a separate data record called orphaned pixels: These are pixels acquired by the instrument but not retained in the Level-1c gridded image, due to the Level-1c projection and nearest neighbour choice on the product grid.

MRD-810 L1c products shall be formatted in a NetCDF like format and use a projection tailored to specific coverage/geographical area (e.g., Equal Area Cylindrical projection for global products, or EASE2-like for Polar Regions).

*Note 1: Network common Data format (NetCDF) see
<https://www.unidata.ucar.edu/software/netcdf>*

*Note 2: It is recommended that L1 products follow accepted conventions such as the Climate and Forecast (CF) Convention and latest Attribute Convention for Data Discovery (ACDD) discovery metadata convention see
<http://cfconventions.org/> and
http://wiki.esipfed.org/index.php/Category:Attribute_Conventions_Dataset_Discovery*

Note 3: The L1a product format may evolve to align to state-of-the-art solutions.

Note 4: A capability to convert the L1c products into Binary Universal Form for the Representation of meteorological data (BUFR) should be considered. L1c may be well suited to address known limitations of the WMO Global Telecommunication System (GTS) that limit BUFR products to ~50 Mb per orbit.

Note 5: The final choice of grid kernel should be based on an appropriate trade-off analysis that preserves as much as possible the native structure of CIMR footprint sizes for all channels. Given the characteristics of the CIMR instrument, a grid kernel of 3 km would scale up allowing 9 km, 15 km 36 km, etc. Depending on the approach used, for example Optimal Estimation techniques, alternative solutions could be used.

MRD-815 Deleted (merged with MRD-810)

MRD-820 CIMR L1c data products shall be produced and made available to users.

Note 1: The exact content of L1c data products depends on the final implementation of CIMR.

MRD-830 Standard total uncertainties and quality indicators shall be delivered for all CIMR measurements in a L1c data product.

Note 1: This is critical for the L2 processor design and for application of higher L2 products that are used by data assimilation systems [AD-2].

Note 2: Quality indicators are typically implemented as flags and/or numerical data attached to each measurement to provide information to users on aspects related to the measurement or processing that may impact the quality of data.

MRD-840

The methods used to generate and propagate uncertainties and quality indicators shall be coherent across product levels and documented for users for all L1c data products.

Note 1: This is critical for the L2 processor design and for application of higher L2 products that are used by data assimilation systems [AD-2].

Note 2: Uncertainty estimates in higher-level products need to reflect uncertainty propagated from lower levels, if significant.

Note 3: Quality indicators are typically implemented as flags and/or numerical data attached to each measurement to provide information to users on aspects related to the measurement or processing that may impact the quality of data.

4.3.6 European ice services for SIC and SIE productsL2 Products

L2 products are generated from L1b data products using appropriate retrieval algorithms. The output data set is a field of geophysical parameter, with associated uncertainties and processing flags. Table 4.3.6-1 describes L2 products produced by the CIMR mission.

Table 4.3.6-1 General overview of CIMR L2 products.

Level	Description
CIMR L2	<p>L2 products are generated from L1b data products using appropriate retrieval algorithms. The output data set is a field of geophysical parameter(s), with associated uncertainties and processing flags. The output product products may be provided in the native instrument geometry (allowing users to regird products for their application) or, if required for a specific product or application, as gridded fields based on equal area polar and/or global projections.</p> <p>L2 are geolocated data with a latitude and longitude attached to each measurement (either directly or by using tie-point arrays).</p>

MRD-845

L2 surface geophysical data product performance requirements shall be validated using established Fiducial Reference Measurement (FRM) procedures.

Note 1: Many processes and environmental conditions can degrade the performance of surface geophysical data products e.g., precipitating conditions, RFI, sun glint coastal/sea ice boundaries etc) known to degrade performances. FRM processes strive to avoid such situations to establish a fair validation in nominal conditions for a given parameter (ie. away from costal boundaries, no precipitation etc). Further analysis is then used to study degradation in more challenging environmental conditions.

Note 2: FRM procedures for a given parameter document how to perform a fair validation measurement based on established processes and best practices including statistical averaging in space and time.

MRD-850 L2 geophysical data products shall be produced and made available to users.

Note 1: See definition of product levels.

Since different Level-2 data processing techniques and algorithms will be used in different regions (e.g., the open ocean, more complex coastal regions, within estuaries etc) and data are across a transition region that includes both land and water. A clear definition of the actual coastline and the transition zone is required. This is the purpose of the Land and Marine Mask. Level-1 products are anticipated as continuous half-orbit or full orbit products regardless of the surface type.

Global Self-consistent, Hierarchical, High-resolution Geography Database (GSHHG, Wessel and Smith (1996) is a high-resolution geography data set, amalgamated from two databases: World Vector Shorelines (WVS) and CIA World Data Bank II (WDBII). The former is the basis for shorelines while the latter is the basis for lakes, although there are instances where differences in coastline representations necessitated adding WDBII islands to GSHHG. The WDBII source also provides political borders and rivers. GSHHG data have undergone extensive processing and should be free of internal inconsistencies such as erratic points and crossing segments. The shorelines are constructed entirely from hierarchically arranged closed polygons. GSHHG combines the older GSHHS shoreline database with WDBII rivers and borders, available in either ESRI shapefile format or in a native binary format. Geography data are provided in five resolutions: crude(c), low(l), intermediate(i), high(h), and full(f). Shorelines are organized into four levels: boundary between land and ocean (L1), boundary between lake and land (L2), boundary between island-in-lake and lake (L3), and boundary between pond-in-island and island (L4). Datasets are in WGS84 geographic (simple latitudes and longitudes; decimal degrees). The full Resolution data set is provided at a resolution of 0.04 km.

MRD-852 A CIMR Geographical Mask shall be used for Level-2 data processing activities according to the following specification:

The Coastline Boundary separating land form ocean is defined by the Hierarchical, full-resolution (0.04 km) Shoreline (GSHHS) high-resolution dataset (Wessel and Smith (1996) available from <https://www.ngdc.noaa.gov/mgg/shorelines/gshhs.html>). This includes shoreline boundary of all inland seas.

Other aspects (TBD).

Note 1: See definitions of Global Ocean, Polar Regions and Adjacent Seas, Coastal Zone, Coastal Regions, and Coastal Boundary (in MRD-852).

Note 2: Global Self-consistent, Hierarchical, High-resolution Geography Database (GSHHG) is a high-resolution geography data set, amalgamated from two databases: World Vector Shorelines (WVS) and CIA World Data Bank II (WDBII). The former is the basis for shorelines while the latter is the basis for lakes, although there are instances where differences in coastline representations necessitated adding WDBII islands to GSHHG. The WDBII source also provides political borders and rivers. GSHHG data have undergone extensive processing and should be free of internal inconsistencies such as erratic points and crossing segments. The shorelines are constructed entirely from hierarchically arranged closed polygons.

Note 3: There are issues with NE Greenland in this Database that need to be corrected before use. Open Street Map (<https://www.openstreetmap.org/>) has a correct data set in this region.

Note 4: GSHHG combines the older GSHHS shoreline database with WDBII rivers and borders, available in either ESRI shapefile format or in a native binary format. Geography data are in five resolutions: crude(c), low(l), intermediate(i), high(h), and full(f). Shorelines are organized into four levels: boundary between land and ocean (L1), boundary between lake and land (L2), boundary between island-in-lake and lake (L3), and boundary between pond-in-island and island (L4). Datasets are in WGS84 geographic (simple latitudes and longitudes; decimal degrees).

Note 5: The definition does not preclude CIMR retrievals up to the Costal Boundary.

MRD-854 A CIMR Hydrology Target mask shall be used for Level-2 data processing activities according to the following specification:

The Hydrology Target Mask shall have a spatial resolution of ≤ 1 km.

It shall include fractional water surfaces with a spatial resolution $\leq 1 \times 1$ km

Inland water surfaces (lakes reservoirs, rivers, as well as wetlands) shall be identified in the database.

Both permanent and transitory water surfaces shall be identified with seasonality information.

The baseline data set shall include the Yamazaki et al. (2019) MERIT Hydro at ~90m: Global Hydrography Database available at http://hydro.iis.u-tokyo.ac.jp/~yamadai/MERIT_Hydro

The baseline data set shall include The Global Lakes and Wetlands Database (*Lernher and Doll, 2004*) at 1 km data set that can provide complementary information on the water surfaces. A GLWD2 version should soon available at 500m spatial resolution, with improved information. Auxiliary data (e.g., Digital elevation models) as required depending on the implementation of CIMR.

Other aspects as required depending on the implementation of CIMR.

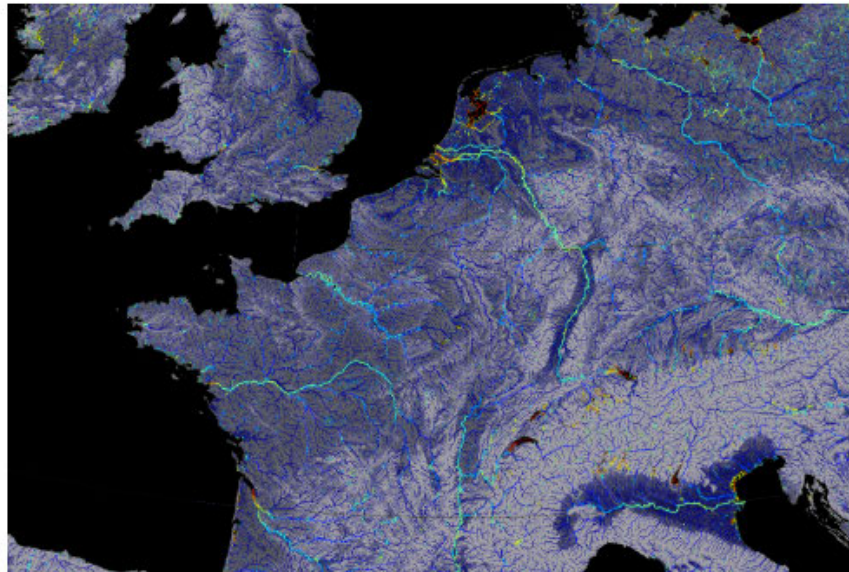
Note 1: The CIMR Hydrology Target Mask specifies lake, reservoir, and wetland targets for the CIMR mission.

Note 2: The mask considers large lakes that are greater than 5 km since Ka-band CIMR measurement footprint are <5 km.

Note 3: The Hydrology Target Mask shall be re-evaluated and uploaded to the satellite up to 4 (TBC) times per year. This is necessary since river spatial extent and position may change seasonally.

Note 4: Example maps form Yamazaki et al (2019), “MERIT Hydro river width (right) are shown below.

Note 5: Monthly masks could be considered, with possible updates during the mission.



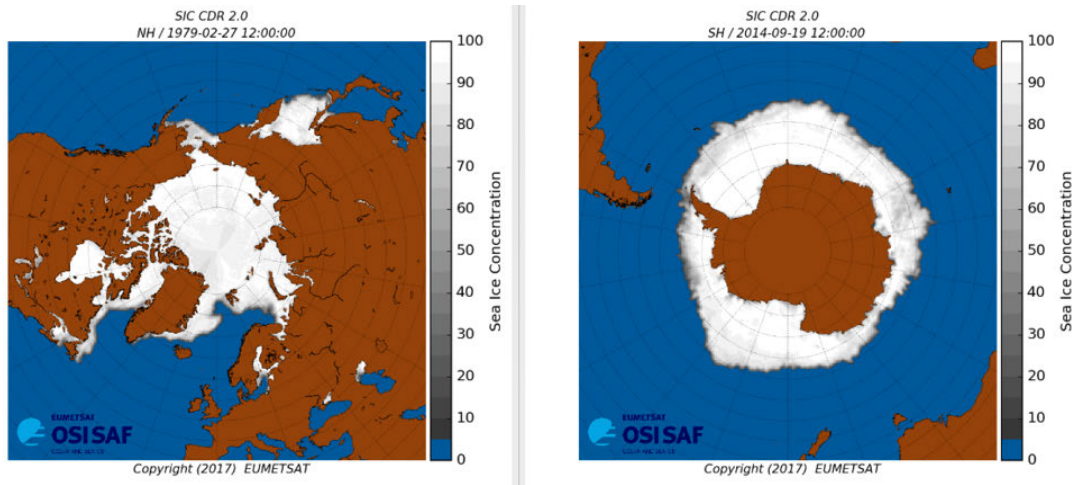
The limit of sea ice is defined in a Sea Ice Edge Mask. It is defined by largest sea ice extent in the EUMETSAT OSI-SAF record (Jan 1979-today)1979-02-27 (NH) and 2014-09-19 (SH) (OSI SAF, 2017). The maximum extents are Northern Hemisphere: 16,661,875 km² and for the Southern Hemisphere: 20,727,500 km² (Lavergne et al, 2019). The S3NG-T Sea Ice Mask is shown in Figure 5.1.3.1.

- MRD-856 For Sizing purposes, the CIMR Sea Ice Edge Mask (SIM) shall be defined as the limit of the largest sea ice extent in the EUMETSAT OSI-SAF sea ice record (OSI SAF, 2017).

Note 1: The following files serve as a starting point for system sizing purposes:

Northern Hemisphere: ftp://osisaf.met.no/reprocessed/ice/conc/osi-450/1979/02/ice_conc_nh_ease2-250_cdr-v2p0_197902271200.nc

Southern Hemisphere: ftp://osisaf.met.no/reprocessed/ice/conc/osi-450/2014/09/ice_conc_sh_ease2-250_cdr-v2p0_201409191200.nc



Example Sea Ice edge mask defined by the largest sea ice extent recorded during the period January 1979 to August 2020 (EUMETSAT OSI-SAF)

MRD-860

L2 products shall be formatted in a NetCDF like format.

*Note 1: Network common Data format (NetCDF) see
<https://www.unidata.ucar.edu/software/netcdf>*

*Note 2: It is recommended that L2 products follow accepted conventions such as the Climate and Forecast (CF) Convention and latest Attribute Convention for Data Discovery (ACDD) discovery metadata convention see
<http://cfconventions.org/> and
http://wiki.esipfed.org/index.php/Category:Attribute_Conventions_Dataset_Discovery*

Note 3: The L2 product format may evolve to align to state-of-the-art solutions.

Note 4: Level-2 products may use a projection tailored to specific coverage/geographical area (e.g., EASE2-like for Polar Regions, Equal Area Cylindrical projection) if appropriate. The preference (as in the case of MetOp MWI and ICI) is to provide Level-2 measurements in instrument swath geometry allowing users to choose the most appropriate gridding approach for a given application.

Many users work in thematic domains that make use of several geophysical measurements at the same time in their applications. In addition, products must be consistent with each other for example, ocean products must use the sea ice concentration/edge derived from CIMR as a mask and vice versa. Furthermore, Product Families reduce the overhead for the ground segment activities. For these reasons, product families have been established for the CIMR mission.

MRD-865	L2 geophysical data products shall be grouped as Product Families including a Polar Ocean Product Family (P), a Land Surface Product Family (L), a Global Ocean Product Family (O), and an Atmospheric Product Family (A) as defined in Table 6.3-1.
	<i>Note 1: See definition of product levels.</i>
	<i>Note 2: Many users work in thematic domains that make use of several geophysical measurements at the same time in their applications. Product families allow variables in thematic domains to be provided in the same container minimising overheads such as geolocation information.</i>
	<i>Note 3: As products must be consistent with each other for example, ocean products must use the sea ice concentration/edge derived from CIMR as a mask and vice versa, product Families provide a convenient way to ensure consistency of products.</i>
	<i>Note 4: Product Families reduce the overhead for the ground segment activities.</i>
MRD-870	Standard total uncertainties and quality indicators shall be delivered for all CIMR measurements in a L2 data product.
	<i>Note 1: This is critical for the L2 processor design and for uptake of L2 products by data assimilation systems [AD-2].</i>
	<i>Note 2: Standard Total Uncertainties are expected to be propagated from L1 to L2A.</i>
	<i>Note 3: Quality indicators are typically implemented as flags and/or numerical data attached to each measurement to provide information to users on aspects related to the measurement or processing that may impact the quality of data.</i>
MRD-880	The methods used to generate and propagate uncertainties shall be coherent across product levels and documented for users for all L2 data products.
	<i>Note 1: This is critical for the L2 processor design and for uptake of L2 products by data assimilation systems [AD-2].</i>
	<i>Note 2: Uncertainty estimates in higher-level products need to reflect uncertainty propagated from lower levels, if significant.</i>
	<i>Note 3: Quality indicators are typically implemented as flags and/or numerical data attached to each measurement to provide information to users on aspects related to the measurement or processing that may impact the quality of data.</i>

MRD-885 To address Copernicus User needs, CIMR Level-2 products shall be geophysically consistent with each other across all CIMR product families.

Note 1: The starting point for all CIMR Level-2 products is a common set of Level-1 inputs provided by the ESA CIMR Ground Segment starting from a same instrument acquisition.

Note 2: This implies consistency and integration of the Level-2 algorithms

Note 3: For example, sea ice should be in the similar location for all SST and SSS products depending on the temporal and spatial resolution (and therefore fidelity) of different products.

Note 4: This implies that auxiliary data sets are common to products ATBD (e.g., climatology).

Note 5: This implies the use of a common Radiative Transfer model is used by algorithm development teams (e.g RTTOV (Saunders et al., 2018) <https://nwp-saf.eumetsat.int/site/software/rttov/>)

Note 6: This implies that ATBD fully exploit the new capability of CIMR (e.g., CIMR can provide wind speed estimates that may be used in SST and SSS retrievals).

Note 7: It may not be possible to reconcile all inconsistencies due to the complexity of geophysical processes defining the signals measured by CIMR at the time and spatial resolution of the CIMR mission.

MRD-890 CIMR shall generate L2 sea ice concentration (SIC) [AD-1], [AD-2] products at a spatial resolution of ≤ 5 km and a standard total uncertainty of $\leq 5\%$ with sub-daily coverage of the Polar Regions and daily coverage of Adjacent Seas.

Note 1: This requirement addresses PRI-OBJ-1 as requested by [AD-1], [AD-2] and [AD-3].

Note 2: See also MRD-1110 that requests SIC in NRT1H.

Note 3: The target standard total uncertainty of $\leq 5\%$ is realistic for homogeneous scenes, and non-melting surface conditions. In regions of high gradient (e.g., the marginal ice zone) and under surface melt conditions, the standard total uncertainty will be larger.

Note 4: With a significant enhancement of spatial resolution compared to current and planned missions, a 6.925/10.56 GHz channels in combination with a high resolution 5 km channel at 18.7 and 36.5 GHz is an optimal channel for sea ice concentration measurements (e.g., Ivanova et al., 2015). See also Zabolotskikh, (2019).

Note 5: The best performance SIC products will be obtained when CIMR data are used together with other satellite measurements including scatterometer, SAR and optical data to help e.g., resolve melt water ponds during summer amongst other issues.

MRD-895

CIMR shall generate Sea Ice Extent (SIE) [AD-1], [AD-2] products calculated from Level-2 SIC at a spatial resolution of ≤ 5 km and a standard total uncertainty of $\leq 5\%$ with daily coverage of the Polar Regions and Adjacent Seas.

Note 1: This requirement addresses PRI-OBJ-1 as requested by [AD-1], [AD-2] and [AD-3]. SIE is a single number describing the area of sea-ice covered ocean. It has unit km^2 (typically millions km^2 for the whole Arctic). SIE is computed from a time-composite (typically a daily aggregate) of CIMR L2 SICs.

Note 2: The target standard total uncertainty of $\leq 5\%$ is realistic for homogeneous scenes, and non-melting surface conditions. In regions of high gradient (e.g., the marginal ice zone) and under surface melt conditions, the standard total uncertainty will be larger.

Note 3: With a significant enhancement of spatial resolution compared to current and planned missions, a 6.925 GHz channel in combination with a high resolution 5 km channel at 18.7 and 36.5 GHz is an optimal channel for sea ice concentration measurements (e.g., Ivanova et al., 2015).

Note 4: The best performance SIC products will be obtained when CIMR data are used together with other satellite measurements including scatterometer, SAR and optical data to help e.g., resolve melt water ponds during summer amongst other issues.

Note 5: See definition of Sea Ice Edge.

Note 6: SIE is computed from CIMR Sea Ice Concentration products. Addition processing may be required beyond Level-2 to compute SIE

MRD-900

CIMR shall generate L2 Sea Surface Temperature (SST) [AD-1], [AD-2] products at a resolution of ≤ 15 km, with a standard total uncertainty of ≤ 0.2 K for $\geq 95\%$ over the global ocean.

Note 1: See definition of Global Ocean. This requirement addresses SEC-OBJ-1 as requested by [AD-1], [AD-2] and [AD-3].

Note 2: The native footprint for 6.9 GHz channels is < 15 km. This requirement implies image-processing and analysis techniques are used to achieve a gridded resolution of 5 km.

Note 3: The achievable geophysical accuracy of SST products is linked to the uncertainties in sea surface emissivity, the ocean and atmospheric state, surface temperature dependencies amongst other physical constraints in addition to the specific retrieval algorithm used and the final CIMR instrument specification (e.g., $\text{NE}\Delta T$ and channel selection).

Note 4: Calculated for a theoretical retrieval as the mode value of daily ocean average discrepancies assuming no uncertainty in the validation data set and varying between 0.15 K to 0.45 K for cold waters (Kilic et al, 2018).

Note 5: 0.2 K SST target needs to be appraised for high latitudes in particular as it is unlikely to be met in a single retrieval sense. The SST retrieval must be considered in a 2-d sense including forward and backward views, including implications of over-sampling on noise reduction and including potential noise reduction from separation of scales, where applicable.

Note 6: The PEG accuracy is stated as 0.1 K (and is not uncertainty, but “accuracy”) and is given in context of climate – without an indication of frequency, whereas the

oceanography requirement in PEG is for 6 hourly and without an uncertainty number. Both permit a degree of temporal (multi-orbit) averaging in the specification of the SST uncertainty – i.e., the 0.2 K need not necessarily be a single-pass uncertainty to be within spirit of PEG. Whether multi-pass methods significantly reduce the uncertainty crucially depends on the instrumental sources of error and their correlation properties Practically speaking, an uncertainty of 0.2 K in a daily average SST (to be met where SST is not changing significantly within the day) would be a significant advance relative to present state of the art (particularly in the high latitudes).

Note 7: The Group for High Resolution Sea Surface Temperature (GHRSST) maintains internationally agreed product specifications for SST products. Specific SST products are required following the GHRSST approach as described in GHRSST (2012).

MRD-905

CIMR shall generate L2 Sea Surface Temperature (SST) [AD-1], [AD-2] products at a resolution of ≤ 15 km with a standard total uncertainty of ≤ 0.3 K with sub-daily coverage in the open water Polar Regions and Adjacent Seas.

Note 1: See Definition of Polar Regions and Adjacent Seas. This requirement addresses PRI-OBJ-2 as requested by [AD-1], [AD-2] and [AD-3].

Note 2: The native footprint for 6.9 GHz channels is < 15 km. This requirement implies image-processing and analysis techniques are used to achieve a gridded resolution of 5 km.

Note 3: SEC-OBJ-1 requests SST with daily coverage of the global ocean (MRD-900).

Note 4: The achievable geophysical accuracy of SST products is linked to the uncertainties in sea surface emissivity, the ocean and atmospheric state, surface temperature dependencies amongst other physical constraints in addition to the specific retrieval algorithm used and the final CIMR instrument specification (e.g., $NE\Delta T$ and channel selection).

Note 5: Calculated for a theoretical retrieval as the mode value of daily ocean average discrepancies assuming no uncertainty in the validation data set and varying between 0.15 K to 0.45 K for cold waters (Kilic et al, 2018). Thus, the uncertainty specification is relaxed to ≤ 0.3 K to accommodate the physical limitation of the cold-water regime (see Figure MRD-2.4.2.1).

Note 6: The SST uncertainty target needs to be appraised for high latitudes in particular as it is unlikely to be met in a single retrieval sense. The SST retrieval must be considered in a 2-d sense including forward and backward views, including implications of over-sampling on noise reduction and including potential noise reduction from separation of scales, where applicable.

Note 7: The PEG accuracy is stated as 0.1 K (and is not uncertainty, but “accuracy”) and is given in context of climate – without an indication of frequency, whereas the oceanography requirement in PEG is for 6 hourly and without an uncertainty number. Both permit a degree of temporal (multi-orbit) averaging in the specification of the SST uncertainty – i.e., the 0.2 K need not necessarily be a single-pass uncertainty to be within spirit of PEG. Whether multi-pass methods significantly reduce the uncertainty crucially depends on the instrumental sources of error and their correlation properties Practically speaking, an uncertainty of 0.2 K in a daily average SST (to be met where SST is not changing significantly within the day) would be a significant advance relative to present state of the art (particularly in the high latitudes).

Note 8: The Group for High Resolution Sea Surface Temperature (GHRSST) maintains internationally agreed product specifications for SST products. Specific SST products are required following the GHRSST approach as described in GHRSST (2012).

MRD-910	<p>CIMR shall generate thin (≤ 0.5 m) sea ice thickness [AD-1], [AD-2] L2 data products in freezing conditions at a spatial resolution of ≤ 60 km, with a thickness standard total uncertainty goal of $\leq 10\%$ and daily coverage of the Marginal Ice Zone in the Polar Regions and Adjacent Seas.</p> <hr/> <p><i>Note 1: This requirement addresses SEC-OBJ-2 as requested by [AD-1], [AD-2] and [AD-3]. The requirement is relevant to freezing conditions.</i></p> <p><i>Note 2: There is a need to significantly oversample L-band measurements in the across-scan and flight direction and make use of additional channels to sharpen L-band products</i></p> <p><i>Note 3: Channels that can measure thin sea ice thickness up to a depth of ~ 0.5 m includes 1.4315 GHz.</i></p> <p><i>Note 4: Channels that can measure thin sea ice thickness up to a depth of ~ 0.2 m includes 6.9 GHz.</i></p> <p><i>Note 5: Standard uncertainty assumes uniform, level ice within the L1b measurement. If a mixture of ice types and open water prevail in the L1b measurement the uncertainty is expected to be higher.</i></p> <p><i>Note 6: Assuming uniform, level ice within the L1b measurement. If a mixture of ice types and open water prevail in the L1b measurement the uncertainty is expected to be higher. Kaleschke et al (2016) note that an uncertainty of $<30\%$ is possible based on SMOS tSIT measurements although validation remains a challenge using aircraft and in situ data sets.</i></p> <p><i>Note 7: As a Secondary Objective, this requirement does not drive the instrument design.</i></p> <hr/>
---------	---

MRD-915	<p>CIMR shall generate L2 Sea Ice Edge (SIED) [AD-1], [AD-2] products at a spatial resolution of ≤ 5 km with a confidence of $>85\%$ or <10 km (whichever is smaller) with sub-daily coverage of the Polar Regions and daily coverage of Adjacent Seas.</p> <hr/> <p><i>Note 1: Sea Ice Edge is a surface classification product that assigns ocean grid cells to sea-ice classes (e.g., Open Water, Very Open Drift Ice, Open Drift Ice, Closed Ice, etc.). For the CIMR product, classes are TBD depending on the implementation of CIMR. The EUMETSAT OSI SAF and C3S both provide sea-ice edge products with the following classes: Open Water ($\sim <30\%$ SIC), Open Ice ($\sim 30\text{--}70\%$ SIC) and Closed Ice ($\sim \geq 70\%$ SIC). See Aaboe et al. (2018).</i></p> <p><i>Note 2: The SIED product is a refined ICE/NO_ICE mask, that can be used for navigation and used masking sea-ice signal in other CIMR products and/or satellite missions (e.g., altimeter-based SSH, IR-radiometer-based SSTs, OC products, etc.).</i></p>
---------	--

Note 3: The uncertainty specification assumes a confidence matrix is used to discriminate the sea-ice classes when compared to SAR and Scatterometer data (e.g., Aaboe et al, 2016).

Note 4: An alternative uncertainty characterization of the SIED product is the mean distance to SAR/ice-chart sea-ice edge, expressed in km (Aaboe et al, 2016). In this case, the requirement would be < 10 km.

Note 5: See definition of Sea Ice Edge.

MRD-920 CIMR shall generate daily sea ice drift (SID) vector [AD-1], [AD-2] L2 products with a standard total uncertainty of $\leq 3 \text{ cm s}^{-1}$ at a spatial resolution of $\leq 25 \text{ km}$ with daily coverage of the Polar Regions and Adjacent Seas.

Note 1: This requirement addresses SEC-OBJ-3 as requested by [AD-1], [AD-2] and [AD-3].

Note 2: As a secondary objective, this requirement does not drive the instrument design.

Note 3: 3 cm/s is the required uncertainty for each gridded components (dx and dy) of the drift vector, separately. This is furthermore the uncertainty for a reference 24 hours drift duration, equivalent to 2.6 km for a 24h drift vector. Drift vectors for shorter drift duration might perform better, drift vectors for longer drift duration might perform worse, see Fig. 5 in Lavergne et al. (2021). OSI-SAF product <http://osisaf.met.no/p/ice/index.html#lrdrift>. CMEMS also has an all-year Sentinel-1 SAR based sea ice drift product at 10 km resolution, produced by DTU (<http://www.seaice.dk>). This product has gaps in daily polar coverage due to limited Sentinel-1 duty-cycle and swath acquisitions in some parts of the polar regions. The microwave radiometer product has a 62.5 km resolution but complete coverage of 2-day sea-ice drift. The 62.5 km could potentially be improved to 25 km with CIMR.

Note 4: The CIMR L2 SID product is a swath-to-swath product (Lavergne et al., 2021).

Note 5: 3- cm/s is the required uncertainty for each gridded components (dx and dy) of the drift vector, separately. This is furthermore the uncertainty for a reference 24-hour drift duration, equivalent to 2.6 km for a 24h drift vector. Drift vectors for shorter drift duration might perform better, drift vectors for longer drift duration might perform worse, see Fig. 5 in Lavergne et al. (2021).

MRD-930 CIMR shall generate L2 sea ice stage of development/Ice type [AD-1], [AD-2] and [AD-3] products discriminating FYI from MYI with a confidence of $\geq 85\%$ at a spatial resolution of $\leq 15 \text{ km}$ with sub-daily coverage [AD-1] of the Polar Regions and Adjacent Seas.

Note 1: This requirement addresses SEC-OBJ-5 as requested by [AD-1] and [AD-2].

Note 2: As a secondary objective, this requirement does not drive the instrument design.

Note 3: Ice type is provided as a number of defined categories (typically new ice, first year ice, second year ice, multi-year ice, fast ice) according to specific spectral signatures.

Note 4: This requirement will benefit from a combination of microwave radiometer data with scatterometer and SAR data from other satellite missions.

Note 5: Uncertainty assumes a confidence matrix is used to discriminate FYI from MYI when compared to SAR and Scatterometer data (e.g., Zhang et al, 2019).

MRD-940 CIMR shall generate snow depth on sea ice [AD-1], [AD-2] L2 products in freezing conditions with a standard total uncertainty of ≤ 10 cm at a spatial resolution of ≤ 15 km with daily coverage of the Polar Regions and Adjacent Seas.

Note 1: This requirement addresses SEC-OBJ-6 as requested by [AD-1], [AD-2] and [AD-3]. The requirement is relevant to freezing conditions.

Note 2: As a secondary objective, this requirement does not drive the instrument design.

MRD-950 CIMR shall generate L2 products of terrestrial snow cover extent (SCE) [AD-1], [AD-2] with a standard total uncertainty of $\leq 10\%$ and a spatial resolution of ≤ 15 km with daily coverage of the Polar Regions.

Note 1: This requirement addresses SEC-OBJ-6 as requested by [AD-1], [AD-2] and [AD-3].

Note 2: Channels that can measure terrestrial snow cover include 18.7 and 36.5 GHz, both polarizations.

Note 3: As a Secondary Objective, this requirement does not drive the instrument design.

MRD-960 CIMR shall generate L2 products of terrestrial snow water equivalent (SWE) [AD-1], [AD-2] with an uncertainty ≤ 40 mm at a spatial resolution of ≤ 15 km with daily coverage of the Polar Regions.

Note 1: This requirement addresses SEC-OBJ-7 as requested by [AD-1], [AD-2] and [AD-3].

Note 2: Channels that can measure terrestrial snow water equivalent include 18.7 and 36.5 GHz, both polarizations.

Note 3: As a Secondary Objective, this requirement does not drive the instrument design.

MRD-970 CIMR shall generate L2 products of Sea Ice Surface Temperature (SIST) [AD-1], [AD-2] and [AD-3] in freezing conditions with a standard total uncertainty of ≤ 1.0 K at an effective spatial resolution of ≤ 15 km with daily coverage of the Polar Regions and Adjacent Seas.

Note 1: This requirement addresses SEC-OBJ-9 as requested by [AD-1], [AD-2] and [AD-3]. The requirement is relevant to freezing conditions.

Note 2: As a secondary objective, this requirement does not drive the instrument design.

Note 3: For SIST measurements, 6.925 GHz channels with significant enhancement of spatial resolution compared to current and planned missions, in combination with thermal infrared imagery, is required.

Note 4: SIST is typically retrieved using thermal infrared (TIR) measurements that are confounded by the presence of clouds. At microwave frequencies, an effective temperature (Teff) of the emitting layer due to the finite emission depth at a given frequency is retrieved. At 6.925 GHz (for example) this is more representative of the snow-ice interface temperature than the snow surface temperature in contact with the atmosphere.

Note 5: Additional thermal infrared satellite imagery will be required to achieve a true SIST.

MRD-980	CIMR shall generate daily L2 products of sea surface salinity (SSS) [AD-3] over $\geq 95\%$ global ocean at a resolution of <60 km (goal:40 km) and a standard total uncertainty of $\leq 0.3 \pm 0.2$ pss over monthly timescales.
<i>Note 1: Salinity is a ratio and has no units - see definition of sea surface salinity</i>	
<i>Note 2: This requirement addresses SEC-OBJ-9.</i>	
<i>Note 3: As a secondary objective, this requirement does not drive the instrument design.</i>	
<i>Note 4: A primary band for sea surface salinity measurement is 1.4315 GHz. However other CIMR bands should be used to sharpen the native L-band spatial resolution of SSS products.</i>	
<i>Note 5: There is a co-dependency of SSS with SST measurements. SSS has a strong dependency on SST at L-band.</i>	
<i>Note 6: Successful SSS retrievals require a measurement of ocean surface roughness ideally from CIMR itself and from co-located and contemporaneous measurements from, for example, scatterometer data such as MetOp-SG (B) SCA.</i>	
<i>Note 7: Full Stokes parameters will be extremely useful to account for Faraday Rotation.</i>	

MRD-985	CIMR shall generate daily L2 products of sea surface salinity (SSS) [AD-3] in the Polar Regions and Adjacent seas at a resolution of <60 km (goal:40 km) and a standard total uncertainty of $\leq 0.3 \pm 0.2$ pss over monthly timescales.
<i>Note 1: Salinity is a ratio and has no units - see definition of sea surface salinity. However, the use of PSS to indicate that the PSS scale has been used is appropriate.</i>	
<i>Note 2: This requirement addresses SEC-OBJ-9. In the Polar Regions a cold-water dependency on the measurement introduces and additional uncertainty hence the inclusion of a ± 0.2 pss specification.</i>	

- Note 3: As a secondary objective, this requirement does not drive the instrument design.*
- Note 4: A primary band for sea surface salinity measurement is 1.4315 GHz. However other CIMR bands should be used to sharpen the native L-band spatial resolution of SSS products.*
- Note 5: There is a co-dependency of SSS with SST measurements. SSS has a strong dependency on SST at L-band.*
- Note 6: Successful SSS retrievals require a measurement of ocean surface roughness ideally from CIMR itself and from co-located and contemporaneous measurements from, for example, scatterometer data such as MetOp-SG (B) SCA.*
- Note 7: Full Stokes parameters will be extremely useful to account for Faraday Rotation.*
- Note 8: ~1% undetected or mis-detected sea-ice concentration results in an SSS error of 5 pss (on monthly time scales and 60-km spatial scales).*
- Note 9: For the purpose of validating this requirement and to avoid the expected degradation in proximity to coastal boundaries and sea ice, performance metrics must be calculated at least 3 L-band **footprint_size** from these boundaries.*
-

MRD-990

CIMR shall generate daily L2 products of wind speed and direction over $\geq 95\%$ global ocean at a resolution of ≤ 40 km and a standard total uncertainty of $\leq 2 \text{ ms}^{-1}$ and $\leq 20^\circ$ in direction at wind speeds $\geq 6 \text{ ms}^{-1}$.

Note 1: The modified Stokes vector includes the vertical and horizontal polarizations and the third and fourth Stokes parameters that provides sufficient information to retrieve an estimate of the ocean surface wind vector. Because the wind direction dependence differs for the 4 Stokes parameters it is possible to resolve the vector wind ambiguities without the use of an ancillary numerical weather prediction field.

Note 2: At wind speeds below 6 m s^{-1} , the wind direction signal from microwave radiometry is small in all polarizations leading to noisy wind direction estimates. At 6 m s^{-1} , the uncertainty of WindSat wind direction is 20° (Hilburn et al., 2016). Above 8 m s^{-1} , the uncertainty is $10\text{--}15^\circ$ and is similar to that derived from scatterometers (Ricciardulli et al., 2012; Hilburn et al., 2016). At high winds (above 10 m s^{-1}) the wind direction signal derived from microwave radiometry is strong in all 4 Stokes parameters.

Note 3: It should be feasible to generate wind speed at a spatial resolution of $\leq 15 \text{ vkm}$ at least for winds between $6\text{--}18 \text{ m s}^{-1}$.

Note 4: Retrieval of wind speed is valid in non-precipitating conditions.

MRD-995

CIMR shall generate daily L2 products of wind speed and direction over the Polar Regions and Adjacent Seas at a resolution of ≤ 40 km and a standard total uncertainty of $\leq 2 \text{ ms}^{-1}$ and $\leq 20^\circ$ in direction at wind speeds $\geq 6 \text{ ms}^{-1}$.

Note 1: The modified Stokes vector includes the vertical and horizontal polarizations and the third and fourth Stokes parameters that provides sufficient information to

retrieve an estimate of the ocean surface wind vector. Because the wind direction dependence differs for the 4 Stokes parameters it is possible to resolve the vector wind ambiguities without the use of an ancillary numerical weather prediction field.

Note 2: At wind speeds below 6 m s^{-1} , the wind direction signal from microwave radiometry is small in all polarizations leading to noisy wind direction estimates. At 6 m s^{-1} , the uncertainty of WindSat wind direction is 20° (Hilburn et al., 2016). Above 8 m s^{-1} , the uncertainty is $10\text{--}15^\circ$ and is similar to that derived from scatterometers (Ricciardulli et al., 2012; Hilburn et al., 2016). At high winds (above 10 m s^{-1}) the wind direction signal derived from microwave radiometry is strong in all 4 Stokes parameters.

Note 3: It should be feasible to generate wind speed at a spatial resolution of $\leq 15\text{ km}$ at least for winds between $6\text{--}18\text{ m s}^{-1}$.

Note 4: Retrieval of wind speed is valid in non-precipitating conditions.

Note 5: Wind direction retrievals typically result in ambiguities, which need to be resolved using an ambiguity removal algorithm (e.g., median filter). For WindSat, CMIS, WSF the wind direction accuracy requirement referred to the CLOSEST ambiguity (closest to true).

MRD-1000 CIMR shall generate terrestrial lake surface water temperature (LSWT) L2 data products in non-freezing conditions at a spatial resolution of $\leq 15\text{ km}$, with a standard total uncertainty of $\leq 0.75\text{ K}$ and daily coverage for inland water areas that have no land within 20 km of a target defined by a Hydrology Target mask.

Note 1: Channels that can measure lake surface water temperature include 6.9 and 10.6 GHz (both polarizations).

Note 2: As a Secondary Objective, this requirement does not drive the instrument design.

Note 3: The requirement requests validation is performed for targets that "...have no land within 20 km of a target defined by a Hydrology Target mask" since smaller targets are numerous and are often not equipped with in situ instrumentation.

Note 4: In terms of implementation, it is anticipated that the land surface temperature products would include many more lake targets that are smaller than the definition given here. The difference is that validation of LSWT would be confined to the large lakes.

MRD-1010 CIMR shall generate terrestrial lake ice cover (LIC) L2 data products in freezing conditions at a spatial resolution of $\leq 5\text{ km}$, with a standard total uncertainty of $\leq 10\%$ and daily coverage for inland water areas that have no land within 20 km of a target defined by a Hydrology Target mask.

Note 1: Channels that can measure lake ice cover include 18.7 and 36.5 GHz.

Note 2: As a Secondary Objective, this requirement does not drive the instrument design.

- MRD-1020 CIMR shall generate a surface binary freeze/thaw state (FT) L2 product with <60 km spatial resolution and a mean spatial classification accuracy of $\leq 10\%$ with daily temporal coverage of the Polar Regions.
-
- Note 1: The primary band for freeze/thaw state measurement is 1.4315 GHz.*
- Note 2: There is a need to significantly oversample L-band measurements in the across-scan and flight direction and make use of additional channels to sharpen L-band products.*
- Note 3: As a Secondary Objective, this requirement does not drive the instrument design.*
-
- MRD-1030 CIMR shall generate land surface temperature (LST) L2 data products at a spatial resolution of ≤ 15 km, with a standard total uncertainty of ≤ 3 K and daily global land coverage.
-
- Note 1: This requirement addresses SEC-OBJ-10*
- Note 2: Channels that can measure land surface temperature include 6.9, 10.65, 18.7 and 36.5 GHz, both polarizations.*
- Note 3: As a Secondary Objective, this requirement does not drive the instrument design.*
-
- MRD-1040 CIMR shall generate L2 products of soil moisture (SM) at a spatial resolution of <60 km, with standard total uncertainty of $\leq 0.04 \text{ m}^3 \text{m}^{-3}$ and daily global land coverage.
-
- Note 1: This requirement addresses SEC-OBJ-10*
- Note 2: A primary band for soil moisture measurement is 1.4315 GHz. The significant oversample of L-band measurements in the across-scan and flight directions as well as CIMR bands at 6.9 GHz and 10.6 GHz should be used to sharpen the spatial resolution of SM products.*
- Note 3: There is a co-dependency of SM with LST. Information on surface water extent is required for SM retrieval. Vegetation absorption and scattering properties (e.g., VOD, MMVI) are retrieved together with soil moisture.*
- Note 4: As a Secondary Objective, this requirement does not drive the instrument design.*
-
- MRD-1050 CIMR shall generate L2 products of Multi-frequency Microwave Vegetation Indicators (MMVI) at a spatial resolution of ≤ 60 km with standard total uncertainty of $\leq 30\%$ band daily global land coverage.
-
- Note 1: Channels that can be used to estimate MMVI are 1.4315, 6.9, and 10.6 GHz. At least two indicators to account for absorption and scattering of vegetation.*

Note 2: MMVI is obtained simultaneously with the soil moisture retrieval.

Note 3: MMVI measures the degree of absorption and scattering of microwave through vegetation canopy constituents -branches, stems, leaves, depending on the frequency- and can be related to other important vegetation characteristics such as vegetation water content (VWC) and above-ground biomass.

Note 4: As a Secondary Objective, this requirement does not drive the instrument design.

Note 5: An appropriate algorithm must be developed and tested building on the existing radiative transfer inversion approaches (i.e., those estimating canopy parameters such as VOD) to implement this requirement.

MRD-1060 CIMR shall generate L2 products of surface water fraction over land (SWF) at a spatial resolution of ≤ 15 km with a standard total uncertainty of $\leq 10\%$ and daily coverage.

Note 1: This requirement addresses SEC-OBJ-10

Note 2: Channels that can measure surface water extent include 18.7 and 36.5 GHz, both polarizations.

Note 3: As a Secondary Objective, this requirement does not drive the instrument design.

MRD-1070 CIMR shall generate precipitation rate over ocean (liquid phase only, $[\text{mm h}^{-1}]$) L2 data products between 0.1 and 100.0 mm h^{-1} at a spatial resolution of ≤ 10 km (goal 5 km), with a standard total uncertainty $\leq 80\%$ at 1 mm h^{-1} or $\leq 50\%$ above 10 mm h^{-1} .

Note 1: Validation of this product is usually performed by inter-comparison with other products over ocean, due to the paucity of in-situ measurements. Usually, biases are observed among various products. For the CIMR-derived product, the bias in instantaneous rain rates should not exceed 80% at 1 mm h^{-1} or 50% at 10 mm h^{-1} .

Note 2: For consistency, Water vapor, cloud liquid water, and precipitation estimates should be retrieved simultaneously. Their retrievals are highly interdependent and should not be tempted separately.

MRD-1080 CIMR shall generate cloud liquid water over ocean $[\text{kg m}^{-2}]$ L2 data products at a spatial resolution ≤ 15 km (goal=5 km), with a standard total uncertainty $\leq 50\%$.

Note 1: See Jacob et al (2019).

Note 2: Water vapor, cloud liquid water, and precipitation estimates should be retrieved simultaneously, for consistent products. Their retrievals are highly interdependent and should not be tempted separately.

MRD-1090 CIMR shall generate the total water vapor column over ocean (kg m^{-2}) L2 product at a spatial resolution $\leq 15 \text{ km}$ (goal=5 km), with a standard total uncertainty of $\leq 10\%$ (with a minimum uncertainty of $\leq 2 \text{ kg m}^{-2}$)

Note 1: Water vapor, cloud liquid water, and precipitation estimates should be retrieved simultaneously, for consistency. Their retrievals are highly interdependent and should not be tempted separately.

4.3.7 Product Delivery Latency

In keeping with the existing Copernicus ground segment for the first-generation Sentinel series, a near real time timeliness of ≤ 3 hours at the point of data pickup (NRT3H) and non-time critical (NTC) products available ≤ 30 days at the point of pickup are specified for the CIMR mission. Specific products are requested with an additional timeliness of NRT1H in support of Arctic navigation and safety systems.

- MRD-1100 The CIMR mission shall deliver to users L1a, L1b, L1c and L2 products in Near Real Time 3-hour (NRT3H) with $\geq 97\%$ availability.

Note 1: For navigational needs in the Polar Regions, a more stringent NRT1H timeliness is required which is covered by MRD-1110.

Note 2 See definition of Near Real Time 3-hour.

Note 3: This requirement implies that L1 products are available not later than 2 hours after satellite measurement acquisition.

- MRD-1105 The CIMR mission shall deliver to users L1a, L1b, L1c and L2 products in Non Time Critical (NTC) with $\geq 97\%$ availability.

Note 1: See definition of Non Time Critical.

Note 3: This requirement implies that L1 products are updated compared to NRT3H data based on improved orbit, quality control, uncertainty estimates and calibration data.

Given that CIMR is focused on the timely delivery of data to support activities in the Arctic Ocean, including operational aspects associated with shipping, exploration, general operations, and other applications requiring real-time access to information, a more stringent timeliness requirement of < 1 hour is anticipated by European ice services for SIC and SIED products. At short (hourly) temporal scales, changes in the sea-ice cover are mainly driven by dynamics, and a short latency of sea-ice drift information strengthens situation awareness and leads to better short-range forecasting. In addition, timely information about high wind speed over the ocean is critical for safe navigation in the Arctic waters where local and intense Polar Lows events are hard to forecast. NRT1H timeliness will enable the services to combine CIMR data with Sentinel-1 (and other) SAR imagery in support of nowcasting for tactical navigation needs. Automated ice charting systems are also in active development with participation of the Finnish, Danish/Greenlandic and Norwegian Ice Services as well as their research departments (e.g., *Carrières et al.*, 2017). The current generation of automatic processing systems use a combination of Sentinel-1 SAR and AMSR2 data and minimize the latency from acquisition of data to delivery to end users. In the future CIMR would replace AMSR2.

The EC Polar Expert Group timeliness requirements call for timeliness of 1 hour for SIC and Thickness of thin-ice, and 6 hours for SST as well as Sea Ice type/stage (ITY), and Ice Surface Temperature (IST). The ice service requirement for Sentinel-1 is delivery of L1 SAR data < 1 hour after acquisition (for their main areas of interest, which is the Baltic and the European/Atlantic sector of the Arctic and subarctic). Other Ice Services such as the Canadian, Russian and the USA

would certainly appreciate a similar low latency. It is important to realize that the value of ice observations in the dynamic regions of the North Atlantic/Arctic for tactical navigation decreases exponentially with time. Considering a target 5 km resolution, it is worth noting that in dynamic cases, sea ice may move 1-2 km each hour. From reception of satellite data at the ice services to delivery of the automatic products to the end user, the ice service timeliness is <15 minutes. Finally, it should be noted that communication in the Polar Regions remains a challenge with limited coverage for data delivery using conventional approaches.

A direct broadcast capability for data from the CIMR mission in the Polar Regions has been considered but due to the expected challenges in data processing (e.g., compensation for grating lobes and side-lobes if a mesh antenna is implemented) this would require an extensive on-board processing capability. A better solution is to focus on the improvement of on-ground data processing and employ a system that can downlink and process polar region data in the most efficient manner.

A NRT1H capability of CIMR should focus on exploiting the high-resolution imagery (Ku and Ka-band) for rapidly evolving phenomena (e.g., SIC, SID, OWS). For support to safe navigation in the Arctic, NRT1H lower resolution imagery (L, C, X-band) and their derived products would not bring much added-value (wrt waiting for NRT3H). An NRT1H capability should also distribute brightness temperatures (Ku and Ka-band, 2 polarizations) so that time-critical downstream services can use them in visual interpretation (including sea-ice charting), and their own automated products (e.g., ITY). Well established and fast algorithms exist for SIC, SIED, SID, and OWS from Ku- and Ka-band only (e.g., for SIC and SIE: *Lavergne et al. (2019)*, for SID: *Lavergne et al. (2021)*, and for OWS *Meissner and Wentz (2012)*).

MRD-1110 In support of Arctic polar navigational applications, CIMR Sea Ice Concentration (SIC), Sea Ice Edge (SIED), Sea Ice Drift (SID), and as a goal: Ocean Wind Speed (OWS), shall be available over specific regions of the Polar Arctic in Near Real Time 1-hour (NRT1H).

Note 1: Communication in the Polar Regions remains a challenge with limited coverage for data delivery using conventional approaches. Given that CIMR is focussed on the timely delivery of data to support activities in the Arctic Ocean, including operational aspects associated with shipping, exploration, general operations, and other applications requiring real-time access to information enhanced timeliness in the polar regions is highly desirable.

Note 2: Several ice service providers (also providing ice charts to CMEMS) state that a major advantage of an operational high-resolution microwave radiometer is in the synergy with Sentinel-1 for which the requirement is <60 minutes from data downlink over specific regions. This synergy can involve artificial intelligence (AI) techniques, for combining the active and passive data.

Note 3: In ice charting the validity and utility of data decrease exponentially with the delay from sensing since ice is dynamic.

Note 4: An option to address this requirement could include the use of a pass-through downlink transmitting acquired data to a core ground station while the data is being acquired by the instrument (as used by Sentinel-1 over specific areas).

Note 5: Users in other Polar regions and adjacent Seas may have similar requirements that are to be confirmed.

Note 6: The coverage of the station(s) used for data downlink shall be compatible with the polar areas where NRT1H data access is required.

Note 7: NRT1H Tbs and L2 products may have a higher uncertainty.

Note 8: Other products of relevance indicated in [AD-1] could include Sea Ice Thickness (SIT) and Ice Type/Stage of development (ITY).

Note 9: The ice service requirement for Sentinel-1 is delivery of L1 SAR data <1 hour after downlink. CIMR will be used in Synergy with these Sentinel-1 data.

Note 10: This requirement may have implications for the selection and number of ground stations required.

Note 11: The order of importance for NRT1H products is 1) Tbs (Ku- and Ka-band, H and V pol), 2) SIC, 3) OWS, 4) SID, 5) SIED. Strategies should be investigated to speed-up processing, and to make available data products as fast as they are processed (i.e., do not wait for all products to be produced before issuing) and within 1H of sensing.

Note 12: This requirement implies that navigation information is available (e.g., interleaved) with science data during the downlink to ensure processing can start as soon as possible.

4.4 User Service Requirements

4.4.1 Routine Processing Requirements

MRD-1120 The users shall have access to the generated mission data products and all relevant information to allow the mission data products exploitation, including auxiliary data.

Note 1: This includes e.g., data quality information, system anomalies, planning for upcoming operations, production performance, product descriptions, changes in production baseline (processor update/reprocessing campaign) etc.

Note 2: This includes offering a catalogue of the mission data products.

Note 3: Any significant change in the data generation or processing should be communicated to all data users in a timely manner. A timely manner means when a chance is known it is communicated well in advance of that change.

Note 4: A catalogue of all CIMR mission data product files should be maintained, storing all relevant identification information and be available to the users. This is essential to services and users in the operational domain that wish to perform reanalyses.

Note 5: It should be possible for users to access CIMR mission data products stored in the historical archive.

MRD-1130 The user shall be able to search for mission data products using various search criteria and be able visualize their contents with a response time sufficiently rapid to enable interactive usage.

Note 1: This could be a web-based service.

Note 2: The criteria, such as e.g., time window, area of interest are specified by the Ground Segment.

MRD-1140 The User Service shall inform Users of all significant activities or events planned with a lead time of at least 4 weeks.

Note 1: This is essential to services and users in the operational domain.

Note 2: For more immediate changes (e.g., Reactive decisions were required) communication should be immediate (e.g., via email list)

MRD-1150 deleted

MRD-1160 User Guides providing information about the mission and guidance for exploitation of the data products shall be available to users and maintained up to date.

Note 1: This could be a web-based service.

MRD-1170 deleted

MRD-1180 deleted

MRD-1190 It shall be possible for users to access any CIMR data product.

Note 1: This could be a web-based service.

Note 2: This service should allow temporal, geographical, and product-type sub-setting.

4.4.2 Reprocessing Requirements

MRD-1200 It shall be possible to reprocess data products at Levels L0, L1a, L1b, L1c and L2.

Note 1: Reprocessing is a fundamental part of the CIMR mission.

Note 2: While L1a products are considered the nominal starting point for re-processing as specified in MRD-730, a capability to reprocess data from L0 may be required in

the future as part of dedicated climate reprocessing activities (which has been historically found to be the case for many missions).

Note 3: It is expected that L0 data will be retained in the archive for climate data stewardship and future reprocessing if required by the Copernicus Climate Change Service.

MRD-1210 The Reprocessing Service shall be sized such that it can reprocess all data from Level 1a to Level 2 including intermediate L1b and L1c products at least every two years as a goal.

Note 1: This is essential if meaningful reprocessing is to be achievable.

MRD-1220 All data acquired during Phase-E1 of the mission shall be reprocessed into Level 2 products after completion of Phase E1.

Note 1: This is essential for external and internal calibration and validation teams to provide meaningful results for the mission.

Note 2: Adequate resources and planning is required to achieve this requirement.

MRD-1230 Users shall be able to retrieve L1 data products for a L2 data file.

Note 1: This requirement means that users can easily retrieve L1 data products for a L2 data file and implies that all L2 products are generated from corresponding L1a, L1b, and L1c data files.

Note 2: Ideally, there should be an obvious and easy to use mapping of L1a to L1b, L1c and L2 data for all CIMR data products within the CIMR data archive.

MRD-1232 Reprocessing of any archived product to derive and archive new products or new versions of any product shall have no impact on the nominal operations.

Note 1: Reprocessing is a fundamental part of a satellite mission required to maintain consistent high quality data sets as the mission progresses and more validation data are used to assess in-flight performance. This requirement allows the ground segment to be sized appropriately for operations including reprocessing which will be essential for CIMR given the challenges of RFI.

Note 2: Reprocessing should be foreseen at least once per year as part of normal operations to ensure a fully consistent data set form the CIMR system.

Note 3: Depending on the stability of the CIMR instrument longer intervals between reprocessing may be appropriate.

4.5 Calibration and Validation Requirements

Calibration and validation will, principally, be carried out during the commissioning and verification phases. *Calibration* addresses aspects of the measurement system, which need to be addressed in the generation of the level 1b data products. Since they are concerned with the conversion from the instruments' measurement quantities into standard physical units, they may be addressed by many techniques. The geolocation accuracy is to be quantified and -if possible- improved as part of the Calibration step. *Validation*, is a term used in the context of the conversion of these instrument measurements into the geophysical quantities. Validation is concerned with the characterisation of uncertainty in the L1b, L1c and L2 parameters. Commonly, this is achieved by suitable analysis of the level 2 data themselves, often in combination with *Fiducial Reference Measurements*.

- MRD-1240 All the contributing sources of uncertainty in L1b, L1c and L2 data products shall be identified in a CIMR uncertainty model documented as part of a Scientific Calibration and Validation Concept Document.

Note 1: The Calibration and Validation Concept document provides the framework upon which the activities defined in a Calibration and Validation Plan are based.

Note 2: The Calibration and Validation Concept document includes the sources of uncertainty in the geo-location of level 1b data products.

Note 3: It is anticipated that the CIMR uncertainty model will be established using the principles set out by the European Commission FIDUCIO project (<http://www.fiduceo.eu/>).

Note 4: the CIMR uncertainty model will require access to instrument pre-launch calibration and characterisation data.

- MRD-1250 A technique for the quantification and propagation of each of the contributing sources of uncertainty in the L1b, L1c and L2 data products shall be identified in the Scientific Calibration and Validation Concept Document.

Note 1: For example, techniques may include validation campaigns using dedicated ships/aircraft, use of existing fiducial Reference Measurements, or comparison with other satellite data.

Note 2: In designing such techniques and associated methods, care needs to be taken with the spatial and temporal scales and correlation of the uncertainties.

Note 3: Techniques to quantify and -if possible - improve the geo-location accuracy should be identified as well (e.g., against land contours, Wiebe et al. 2008).

MRD-1260 A Scientific Calibration and Validation Implementation Plan shall be established that describes how all measurements and techniques identified as necessary in the Scientific Calibration and Validation Concept will be implemented.

Note 1: The Scientific Calibration and Validation Implementation Plan should identify responsible entities for all calibration and validation measurements and techniques.

Note 2: The Calibration and Validation Implementation Plan should identify the schedule for all activities planned.

MRD-1270 A Scientific Calibration and Validation Team (CIMR-VT) shall be established to assist in the implementation of the Scientific Calibration and Validation Plan.

Note 1: The Scientific Calibration and Validation team should be linked to existing infrastructure and that can perform long-term (i.e., beyond Phase E1) calibration and validation activities according to the Scientific Calibration and Validation Plan.

4.6 Software Requirements

MRD-1280 A community, open source, modular library (CIMRL1BDEV), including a Radiative Transfer Model (RTM) shall be made available and maintained through the lifetime of the mission to simulate CIMR L1b test data sets from gridded geophysical quantities at Earth's surface.

Note 1: The satellite simulator is to support Copernicus Services and Weather Prediction Centres, in the task of directly assimilating CIMR TB observations into geophysical models. It should thus be designed so that it allows comparison of simulated vs measured CIMR data in swath projection.

Note 2: As a limit case (by bypassing the RTM), the satellite simulator is limited to a geometric operator that aggregates geo-reference surface gridded fields (e.g., TB, T2m from a NWP model, ...) to any L1a, L1b sample and field-of-view.

Note 3: The most common geographic projections must be supported as input (including but not limited to: EASE2, polar stereographic, rotated lat/lon,...).

Note 4: The satellite simulator should, as much as possible, re-use existing open-source libraries.

Note 5: "modular" means the interfaces of the software implementing the various stages of the simulator are well defined and documented, so that a user can change parts of the simulator (e.g., the RTM) or access intermediate data.

Note 6: The accurate simulation of the L1B observations may require that L1A footprints are simulated (including contribution by side- and grating-lobes) and the L1A->L1B side-grating-lobe correction algorithm (as used in the operational processing chain) be applied. The need for this should be assessed with reference to the case of simulating sea-land boundaries.

Note 7: The same software module (or part of) can be used to support the development of CIMR L2 algorithms, by easing the task of collocating auxiliary fields (e.g., NWP and Ocean re-analysis and forecasts fields) with the L1b observations.

Note 8: By using an open source approach this tool will facilitate the development of the maximum potential of CIME early on in the mission lifetime through collaborative development.

Note 9: Open source implies distribution under a version of the Free/Open-Source Software License.

MRD-1290 A community, open source, modular library software to generate L1b, L1c and L2 products (CIMRL2DEV) shall be made available and maintained through the lifetime of the mission to facilitate algorithm development and evolution.

Note 1: The principle of CIMRL2DEV is to ensure there is continuous improvement in the CIMR products in an open and transparent manner throughout the mission lifetime.

Note 2: CIMRL2DEV will facilitate the exploitation and evolution of CIMR data to the full capability offered by the mission.

Note 3: It is anticipated that CIMRL2DEV will be a shared responsibility between ESA and EUMETSAT.

Note 4: By using an open source approach this tool will facilitate the development of the maximum potential of CIME early on in the mission lifetime through collaborative development.

Note 5: Open source implies distribution under a version of the Free/Open Source Software License.

MRD-1300 Open access to L1a, L1b, L1c and L2 ATBD documents shall be possible.

Note 1: This is required to implement CIMRL2DEV.

Note 2: This is required to implement and manage the CIMR uncertainty budget throughout the mission.

Note 3: Open access implies distribution under a version of the Free/Open-Source Software License.

Building on the heritage of Copernicus Sentinel-5P and EE7 Biomass activities, a Copernicus Expansion Missions Product Algorithm Laboratory (CEM-PAL) will be implemented to allow Copernicus scientists monitoring mission performance and tasked with evolving algorithms to work to jointly, and transparently, develop version-controlled code for CIMR L1 and L2 algorithms. CEM-PAL may integrate the CIMR ATBD, CIMRL1BDEV and CIMRL2DEV open-source libraries and host all test data sets. In this way, CEM-PAL provides an on-line platform-based resource that lies at the core of L1/L2 algorithm evolution and refinement throughout the CIMR mission development and operations. In addition, CEM-PAL may be used during Phase E1 during scientific cal/val activities. Elements of CEM-PAL could provide: a standardised validation and verification

approach; access to end-to-end performance simulator forward and retrieval models allowing optimisation of the E2E performance (e.g., compensation for side-lobes and grating lobes on-board calibration filtering etc); include the detection, mitigation, characterisation and monitoring of RFI in-flight and on-ground; host the development of alternative approaches that are not formally part of the CIMR system (but could be brought into the system); foster the inclusion of end-user communities. The CEM-PAL approach can reduce considerably the risk of failures in the Level-1 and Level-2 performance through independent critical review of the developments. Sentinel-5P has implemented this approach and an on-line version of this approach is provided by the Biomass mission at: <https://portal.val.esa-maap.org/portal-val/ESA/home>.

- MRD-1310 A Copernicus Expansion Missions Product Algorithm Laboratory (CEM-PAL) shall be established as an on-line platform-based resource for Copernicus L1/L2 algorithm evolution and refinement throughout the CIMR mission development.

Note 1: CEM-PAL may integrate the CIMR ATBD, CIMRL1BDEV and CIMRL2DEV open-source libraries and host all test data sets in support of development reviews.

Note 2: The CEM-PAL could provide resources to support an efficient operations environment for the CIMR L1/L2 algorithm evolution and refinement.

5 PRELIMINARY SYSTEM CONCEPT(S) AND CHARACTERISTICS

5.1 CIMR mission preliminary system characteristics

Working exclusively from the User requirements set out in [AD-1], [AD-2] and [AD-3] the following CIMR mission characteristics are established:

- The mission will take advantage of the long-standing experience of Microwave Radiometer development and data utilisation in Europe (starting with science team contributions to the Scanning Multi-frequency Microwave Radiometer (SMMR) on Nimbus-7 in 1978) [AD-2], the ESA Multichannel Imaging Microwave Radiometer (MIMR, e.g., *Pullainen et al.* 1993) studied for the USA EOS-PM Polar Platform³¹ and MetOp preparatory programme, the EPS-SG system, the Sentinel-3 Microwave Radiometer (MWR), the ESA Microwat (*Donlon*, 2009, *Prigent et al.* 2013) activity (2010-2015) and related ESA activities on large antenna technologies.
- A multi-frequency microwave instrument with a wide swath is considered the only possibility to address sub-daily revisit requirements in the Polar Regions [AD-2] with a spatial resolution and dedicated spectral channels for SIC (~5 km) and SST retrievals (~15 km) [AD-2].
- A swath width that offers at least daily revisits in the Polar Regions and Adjacent Seas to observe the associated geophysical parameters with the required spatial and temporal resolutions and coverage requirements is needed [AD-2].
- The mission must offer the best solution from technical, scientific, and operational viewpoints (operational daily observations of polar regions and Adjacent Seas in non-precipitating atmospheric conditions, day, and night) [AD-2].
- The mission must include protection from Radio Frequency Interference. The mission must also include advanced detection and mitigation of Radio Frequency Interference.
- A high degree of synergy with measurements provided by sensors flying on other satellites may be highly advantageous. More generally, the use of a microwave radiometry mission in synergy with active microwave sensors (e.g., wind scatterometer, radar altimeter, SAR imagers) and with optical VIS/IR sensors (e.g., MetOp-SG(A) MetImage) is expected to provide powerful tools/techniques/synergy improve geophysical products and their accuracy for the cryosphere, ocean, land, and atmosphere domains. Ice services already make use of AMSR-2 data as a prerequisite for automation of Sentinel-1 SAR SIC retrievals.
- The MetOp-SG (1B) Microwave Imager (MWI) and SCA Scatterometer [AD-2] could be used in synergy with CIMR with the additional benefit of enhanced multi-satellite products (note that AMSR-E and AMSR-2 fly in the NASA A-train (<https://atrain.nasa.gov/>) to derive similar synergy benefit).
- The MetOp-SG (1A) MetImage sensor could be used in synergy with CIMR with the additional benefit of enhanced multi-satellite thermal infrared and microwave radiometer products.

³¹ Post-EPS Mission Requirements Document, EUM/PEPS/REQ/06/0043, v2D Draft, 2009 included requirements for a Microwave Radiometer with channels centred at 6.9 and 10.65 GHz.

- The end-to-end mission concept must ensure enhanced continuity of an AMSR-type instrument (specifically of AMSR-2 data on GCOM-W1 that is now close to end of life) [AD-2].
- An L-Band channel is required to address mission objectives - specifically to retrieve thin (< 0.5m) SIT and SSS and provide continuity to SMOS and SMAP type L-band capability.
- The mission must include a C-band channel (6.9 GHz) with significantly improved spatial resolution to ensure enhanced continuity of AMSR-2 measurements. This frequency, if a resolution of ~15 km can be achieved, offers accurate measurement of SIC and SST in combination with other high spatial-resolution channel data (e.g., a 5 km channel at 18.7 GHz). Furthermore, with the addition of a C-band channel, SST can be measured in the Polar Regions and Adjacent Seas (note that at higher X-band frequencies, the brightness temperature is insufficiently sensitive to changes in SST below ~290 K (*Gentemann et al., 2010*) [AD-2]).
- The Arctic policy document is a baseline driver for a Polar Ice and Snow mission with the Antarctic being more related to Climate Change when considered together with Arctic. However, a focus is given to the Arctic, related areas and adjacent seas with observations over the Antarctic considered as much as possible [AD-2].
- The mission will be operated in parallel with the Sentinel constellation currently under deployment and/or in operations. In this context, it is assumed that for new missions the same operating paradigm as to the current Sentinel constellation will be applied. The global architecture (Copernicus Ground Segment and its operations) should follow the same standards as the current Sentinel constellation [AD-2].
- This Copernicus mission will not include on-demand rapid tasking of the satellite.

The final form of the CIMR mission depends on implementation choices.

5.2 CIMR mission preliminary system concept

A preliminary mission concept is focused on the provision of one or more multi-frequency conical scanning microwave radiometers using a large antenna flying in synergy with the MetOp-SG(B) and MetOp-SG(A) satellites in the polar regions. The MetOp-SG(B) MicroWave Imager (MWI) offers frequency bands and channels that are similar to AMSR-2 (in particular the high-frequency channels). In addition, co-located and near-contemporaneous measurements from the MetOp-SG(B) SCA scatterometer will be possible. Scatterometer data are ideal to estimate the surface roughness of the ocean and are used in conventional retrievals of SIC, SST, SSS, sea ice type classification, amongst others. MetOp-SG(A) Spatial resolution, radiometric performance and revisit have significantly limited previous and currently planned missions for the primary applications of CIMR. To address this concern, the mission will provide enhanced continuity of AMSR-2-type capability including mandatory band frequencies and spatial resolution of 6.925 (~10-15 km), 10.65 (~10-15 km), 18.7 (~5 km) and 36.5 GHz (<5km). By taking advantage of MWI, the CIMR instrument can focus on improving the spatial resolution and radiometric fidelity of low frequency (\leq 18.7 GHz) channels that are best suited to the primary objectives for the mission (SIC and SST).

Compliance to the requirement for SST is based primarily on the performance of vertically and horizontally polarised channels at 6.925 and 10.65 GHz but with a much higher (~10-15 km) spatial resolution than other missions. Furthermore, polarised channels located at 6.925 GHz, provide the best spectral separation between open water and sea ice in SIC retrieval algorithms - but only if a higher spatial resolution can be attained. Using these channels together with polarized channels at 18.7 GHz having a spatial resolution of \leq 5 km, Europe will be able to provide a superior solution

to heritage measurements of SIC and SST without the need for an 89 GHz channel as flown by AMSR-2. The 89 GHz channel, in any case, is compromised by atmospheric attenuation and scattering requiring additional manipulation.

Based on an analysis of Copernicus observational needs, high-level Mission Requirements are derived and articulated for the CIMR mission. Secondary parameters requested by PEG-II and CMEMS, will also make full use of the low frequency channels at high resolution with optimal performance and enlarge the range of ice parameters in non-precipitating atmospheric conditions of interest to Copernicus. The implementation of an additional channel at 1.4315 GHz (L-band) to address requirements for thin sea ice thickness and sea surface salinity products, expressed by PEG and CMEMS, is proposed.

6 DATA PRODUCTS AND USAGE

6.1 Level-0 data products

Level-0 (L0) products complex products that are used by the ground segment.

Table 6.1-1 Overview of CIMR L0 products.

Level	Description
CIMR L0	<p>Reconstructed, unprocessed instrument and payload data at full resolution, with any and all communications artefacts (e.g., synchronization frames, communications headers, duplicate data) removed.</p> <p>Level-0 (L0) products are used by the ground segment.</p>

6.2 Level-1 data products

Level-1 (L1) products are foreseen to be available to the End User community.

L1a products are designed to be as close to L0 products as practically possible (i.e. all calibration data available in a product but not applied to the measurement data set). L1a products are particularly important for a conically scanning radiometer since different choices can be made when combining samples and deriving/applying calibration information to form L1b products.

L1b products have all calibration data applied to provide top of atmosphere brightness temperatures in native instrument geometry. These products are designed to provide feed-specific, L1b samples and L1b measurements with the purest radiometric qualities (i.e. no interpolation or merging of data from scan-to-scan) for users wishing to implement their own L2 algorithms.

L1c products provide a gridded product that contains L1b data in a more convenient gridded image format but with additional uncertainty associated with the gridding process. While the gridding operation is common to most applications of CIMR data and the L1c data relieve users of this task, there are different approaches to gridding L1b data, both the L1b and L1c products are required.

Table 6.2-1 Overview of CIMR L1 products.

Product ID P=Polar Regions and Adjacent Seas, G=Global, L=land,	Description	Coverage Domain	Spatial Resolution (km)	Total Standard Uncertainty	Delivery Timeliness (NRT1H, NRT3H)	Revisit	MRD REQ
L1A-G	Observed sensor engineering data for each channel in instrument geometry at native channel resolution. L1a data are derived from L0 data that have been reconstructed and ordered into orbit files (instrument geometry, swath based).	Global coverage.	Defined by feedhorn	N/A	NRT1H in limited areas of the Arctic Polar Region. NRT3H global	Swath based	MRD-520, MRD-640, MRD-650, MRD-660, MRD-690, MRD-700, MRD-710, MRD-720, MRD-730

	Data are unprocessed instrument data (counts) at full resolution (i.e., all samples, from all feeds, in all polarisations), time-referenced, and annotated with ancillary information, including radiometric and geometric calibration coefficients (e.g., thermistor counts etc.) and geo-referencing parameters (e.g., platform ephemeris) and auxiliary information (e.g., relevant solar angles etc) computed and appended. No calibration or instrument corrections are applied to L1a data: it is designed as the starting point for all ground processing and reanalysis.						
L1B-G	<p>Top of the atmosphere calibrated brightness temperature sample and L1b measurement data for each channel in instrument geometry at native channel resolution, derived from a corresponding L1a file (instrument geometry, swath based).</p> <p>Forward scan and backward scan data are provided separately in the same data product.</p> <p>All engineering (e.g., corrections for side-lobes and e.g., grating lobes) corrections have been applied to each L1b sample, radiometric calibration parameters have been applied to each sample to output top-of-atmosphere spectral brightness temperatures (Tb) in units of Kelvin. Geometric information is computed and appended to each L1b sample (i.e. there is no reprojection or resampling to a gridded product). Preliminary pixel classification is included in the product.</p> <p>Data provided is individual orbit files linked to corresponding L1A data allowing users to easily move between L1a and L1b data.</p>	Global coverage.	Variable, defined by channel	Variable, defined by channel	NRT1H in limited areas of the Arctic Polar Region. NRT3H global	Daily	MRD-290, MRD-300, MRD-310, MRD-340, MRD-420, MRD-440, MRD-450, MRD-460, MRD-500, MRD-550, MRD-560, MRD-640, MRD-650, MRD-660, MRD-690, MRD-740, MRD-750, MRD-760 , MRD-770, MRD-780, MRD-790
L1C-G	Gridded top of the atmosphere calibrated brightness temperature for each channel	Global coverage.	Variable, defined	Variable, defined	NRT3H	Daily	MRD-800, MRD-810, MRD-815,

	<p>derived from a corresponding L1B data in a swath based gridded image product.</p> <p>Forward scan and backward scan data are provided separately in the same data product.</p> <p>Data provided is individual orbit files linked to corresponding L1b data.</p>		by channel	by channel			MRD-820, MRD-830, MRD-840
--	--	--	------------	------------	--	--	---------------------------------

6.3 Level-2 data products

Level-2 (L2) products provide geophysical products and can be derived from L1b or L1c depending on the user and are foreseen to be available to the End User community. Table 6.3.1 describes L2 products that are foreseen from the CIMR mission.

Table 6.3-1 Detailed overview of CIMR Level 2 products. Product Families include Polar Ocean (P), Global Land (L), Global Ocean (O), Global Atmosphere (A).

Product ID	Product family	Description	Coverage Domain	Spatial Resolution (km)	Total standard Uncertainty	Delivery Timeliness (NRT1H, NRT3H, NTC)	Revisit	MRD REQ
SIC-P	P	Sea Ice Concentration	Polar Regions and Adjacent Seas	≤5 km	≤5%	NRT3H NTC	Sub-daily in Polar Regions, Daily in Adjacent Seas	MRD-890, MRD-1100, MRD-1105
SIC-P1H	P	Sea Ice Concentration	For limited areas of the Arctic Polar Region.	≤5 km	≤15%	NRT1H	Sub-daily in Polar Regions, Daily in Adjacent Seas	MRD-1110
SIE-P	P	Sea Ice Extent	Polar Regions and Adjacent Seas	≤5 km	≤5%	NTC	Daily in Polar Regions, and Adjacent Seas	MRD-895, MRD-1100, MRD-1105, MRD-1110

SST-P	P	Sea Surface Temperature	Polar Regions and Adjacent Seas	≤ 15 km	≤ 0.3 K ³²	NRT3H NTC	Sub-daily in Polar Regions, Daily in Adjacent Seas	MRD-905, MRD-1100, MRD-1105
SST-O	O	Sea Surface Temperature	Global ocean	≤ 15 km	≤ 0.2 K ¹⁹	NRT3H NTC	Daily	MRD-900, MRD-1100, MRD-1105
SIT-P	P	Thin Sea Ice Thickness	Polar Regions and Adjacent Seas	< 60 km	$\leq 10\%$	NRT3H NTC	Daily	MRD-910, MRD-1100, MRD-1105, MRD-1110
SIED-P	P	Sea Ice EDge	Polar Regions and Adjacent Seas	≤ 5 km	Confidence of >85% or < 10 km (whichever is smaller)	NRT3H NTC	Daily	MRD-915, MRD-1100, MRD-1105, MRD-1110
SIED-P1H	P	Sea Ice EDge	For limited areas of the Arctic Polar Region.	≤ 5 km	Confidence of >85% or < 10 km (whichever is smaller)	NRT1H	Daily	MRD-915, MRD-1100, MRD-1110
SID-P	P	Sea Ice Drift	Polar Regions and Adjacent Seas	≤ 25 km	$\leq 3 \text{ cm s}^{-1}$	NRT3H NTC	Sub-daily in Polar Regions, Daily in Adjacent Seas	MRD-920, MRD-1100, MRD-1105
SID-P1H	P	Sea Ice Drift	For limited areas of the Arctic Polar Region.	≤ 25 km	$\leq 3 \text{ cm s}^{-1}$	NRT1H	Sub-daily in Polar Regions, Daily in Adjacent Seas	MRD-920, MRD-1100
ITY-P	P	Ice stage of development / type	Polar Regions and Adjacent Seas	≤ 15 km	$\geq 85\%$ confidence to discriminat	NRT3H NTC	Sub-daily in Polar Regions, Daily in	MRD-930, MRD-1100, MRD-1105,

³² Calculated for a theoretical retrieval as the mode value of daily ocean average discrepancies noting anticipated theoretical discrepancies varying between 0.15 K (warm waters) to 0.45 K for (cold <280K waters). A standard total uncertainty of ≤ 0.2 K for $\geq 95\%$ global coverage and standard total uncertainty of ≤ 0.3 K in the Polar Regions and Adjacent Seas is requested for L2 products.

					e FYI from MYI		Adjacent Seas	MRD- 1110
SND-P	P	Snow Depth on Sea Ice	Polar Regions and Adjacent Seas	≤15 km	≤10 cm	NRT3H NTC	Daily	MRD-940, MRD-1100, MRD-1105, MRD-1110
TSA-L	L	Terrestrial Snow Area	Global – Focus on Polar Regions and Adjacent Seas	≤15 km	≤10%	NRT3H NTC	Daily	MRD-950, MRD-1100, MRD-1105
SWE-L	L	Terrestrial Snow Water Equivalent	Global land ³³	≤15km	≤40mm	NRT3H NTC	Daily	MRD-960, MRD-1100, MRD-1105
SIST-P	P	Sea Ice Surface Temperature	Polar Regions and Adjacent Seas	≤ 15 km	≤1.0 K	NRT3H NTC	Daily	MRD-970, MRD-1100, MRD-1105, MRD-1110
SSS-O	O	Sea Surface Salinity	Global ocean	< 60 km	≤0.3 pss	NRT3H NTC	Daily	MRD-980, MRD-1100, MRD-1105
SSS-P	P	Sea Surface Salinity	Polar Regions and Adjacent Seas	< 60 km	≤0.3 pss	NRT3H NTC	Daily	MRD-985, MRD-1100, MRD-1105
OWV-P	P	Ocean Surface Wind Vector	Polar Regions and Adjacent Seas	≤ 40 km	2 ms-1 and ≤20° in direction at wind speeds ≥6 ms-1	NRT3H NTC	Daily	MRD-995, MRD-1100, MRD-1105, MRD-1110
OWS-P1H	P	Ocean Surface Wind Speed	For limited areas of the Arctic Polar Region.	≤ 40 km	2 ms-1 at wind speeds ≥6 ms-1	NRT1H	Daily	MRD-995, MRD-1100,

³³ Land Products include the Coastal Zone (see definition of Coastal Zone)

								MRD-1110
OWV-O	O	Ocean Surface Wind Vector	Global ocean	≤ 40 km	2 ms $^{-1}$ and $\leq 20^\circ$ in direction at wind speeds ≥ 6 ms $^{-1}$	NRT3H NTC	Daily	MRD-990, MRD-1100, MRD-1105
L SWT-L	L	Lake Surface Water Temperature	Global land according to specified L SWT mask	≤ 15 km	≤ 0.75 K	NRT3H NTC	Daily	MRD-1000, MRD-1100, MRD-1105
LIC-L	L	Lake Ice Cover	Global land according to specified L SWT mask	≤ 15 km	$\leq 10\%$	NRT3H NTC	Daily	MRD-1010, MRD-1100, MRD-1105
FT-L	L	Freeze/thaw state	Global land	< 60 km	$\leq 10\%$	NRT3H NTC	Daily	MRD-1020, MRD-1100, MRD-1105
LST-L	L	Land Surface Temperature	Global land	≤ 15 km	$\leq 3K$	NRT3H NTC	Daily	MRD-1030, MRD-1100, MRD-1105
SM-L	L	Soil Moisture	Global land	< 60 km	≤ 0.04 m 3 m $^{-3}$	NRT3H NTC	Daily	MRD-1040, MRD-1100, MRD-1105
MMVI-L	L	Multi-frequency Microwave Vegetation Indicators (MMVI)	Global land	< 60 km	$\leq 30\%$	NRT3H NTC	Daily	MRD-1050, MRD-1100, MRD-1105
SWF-L	L	Surface Water Fraction	Global land	≤ 15 km	$\leq 10\%$	NRT3H NTC	Daily	MRD-1060, MRD-1100, MRD-1105
PCP-A	A	Precipitation rate	Global Atmosphere	≤ 15 km (g=5 km)	$\leq 80\%$ at 1 mm h $^{-1}$ or $\leq 50\%$ above 10 mmh $^{-1}$.	NRT3H NTC	Daily	MRD-1070, MRD-1100, MRD-1105

LWP-A	A	Liquid Water Path	Global Atmosphere	$\leq 15 \text{ km}$ (g=5 km)	$\leq 50\%$	NRT3H NTC	Daily	MRD-1080, MRD-1100, MRD-1105
TCWV-A	A	Total Column Water Vapour	Global Atmosphere	$\leq 15 \text{ km}$ (g=5 km)	$\leq 10\%$	NRT3H NTC	Daily	MRD-1090, MRD-1100, MRD-1105

From an end user perspective, separate multi-parameter products would be extremely useful. For example, a product that include all ocean parameters, one including all Polar Regions parameters, one for land products and one for atmospheric products. This should be considered.

6.3.1 Polar Sea Ice Concentration algorithm

Many SIC retrieval algorithms from microwave radiometer observations exist, using most of the available frequency channels. The development of SIC algorithms from microwave radiometer data is an active field of research, and by the time CIMR flies other approaches might have matured further. One of these is multi-variate optimal estimation (OE) that combines more frequency channels and relies less on ancillary input.

Algorithms combining K-band (~19 GHz) and Ka-band (~37 GHz) frequency channels are by far the most common because of long time availability (SMMR, SSM/I, SSMIS, AMSR-E/2), relative moderate noise levels compared to near 90 GHz algorithms, and spatial resolution. Examples are the *Comiso*, (1995) Bootstrap algorithm, the NASA Team algorithm (*Cavalieri*, 1991), the Bristol algorithm (*Smith*, 1996), the OSISAF algorithm (*Andersen et al.*, 2006), the SICCI2 algorithms (*Lavergne et al.*, 2018), mostly developed for SSM/I and being applied to SMMR, SSM/I, SSMIS, and AMSR-E and AMSR2 data. These algorithms are used operationally at many processing centres, such as EUMETSAT OSISAF (feeding into CMEMS), U.S. NSIDC, JAXA, CMA, etc. These SIC products are used to initialize operational global and regional model forecasts, e.g., at ECMWF, at CMEMS and at national meteorological and marine forecasting centre.

Having K-band (18.7GHz) and Ka-band (36.5GHz) on board CIMR ensures that this type of algorithms can be used to derive SIC at a high accuracy (<5%) and higher resolution (<5 km) than before. A generic form for a SIC algorithm is expressed by:

$$C(\vec{T}) = \frac{\hat{v} \cdot (\vec{T} - \langle \vec{T}^W \rangle)}{\hat{v} \cdot (\langle \vec{T}^I \rangle - \langle \vec{T}^W \rangle)} \quad (\text{Eqn. 6.3.1.1})$$

where $C(T)$ is the sea-ice concentration computed from T (an n-dim vector of L1b Tb, for example $T=[T_{18.7V}, T_{36.5V}, T_{36.5H}]$ triplet for a 3D algorithm like Bristol or SICCI2). $\langle T^W \rangle$ and $\langle T^I \rangle$ are respectively the open water and consolidated sea-ice mean signature, i.e. the water and ice tie-points. v is a unit vector holding the coefficients of the algorithms.

Today's state-of-the-art SIC algorithms include dynamic tuning of the algorithm coefficients (dynamic tie-points, and dynamic weather filters). This is a key feature to implement as it provides algorithms that are more robust to 1) inter-seasonal and inter-annual changes of open water and sea-ice emissivity, 2) update of channel calibration, 3) changes in auxiliary data. Because tie-points and weather filter thresholds are derived dynamically, the coefficient values entering the algorithms (including the $\langle T^W \rangle$, $\langle T^I \rangle$, and v above) cannot be pre-computed (although good pre-launch first-guess and fail-over values can be made).

Today's state-of-the-art SIC algorithms include RTM-based correction for atmospheric and surface noise contributions. This requires additional auxiliary information from NWP analysis and forecast such as those from ECMWF. At present, air temperature at 2m height (T2m), wind-speed, and Water Vapour fields are routinely used in operational processing chains (e.g., at EUMETSAT OSI SAF).

L2 uncertainties have (at least) two components: the algorithm uncertainty and the smearing uncertainty, that are combined (in terms of variance) into a total uncertainty by:

$$\sigma_{total}^2 = \sigma_{algorithm}^2 + \sigma_{smear}^2 \quad (\text{Eqn. 6.3.1.2})$$

Algorithm uncertainty $\sigma_{algorithm}$ are propagated from those at Level-1B (the NEΔTs) but are dominated by the variability of the Water and Sea Ice tie-points:

$$\Sigma_C = \frac{1}{(\hat{\nu} \cdot (\langle \vec{T}^I \rangle - \langle \vec{T}^W \rangle))^2} [\hat{\nu} \Sigma_T \hat{\nu}^T + (1 - C)^2 \times \hat{\nu} \Sigma_W \hat{\nu}^T + C^2 \times \hat{\nu} \Sigma_I \hat{\nu}^T] \quad (\text{Eqn. 6.3.1.3})$$

where Σ_C is σ_{algo}^2 and Σ_T , Σ_W and Σ_I are covariance matrices for the L1b uncertainty, the Water signature variability, and the Ice signature variability.

The smearing uncertainty σ_{smear} expresses the additional uncertainty arising from combining frequency channels with different locations and/or resolution. It is difficult to express analytically and is typically computed via proxies.

Lavergne et al. (2020) describes the prototype CIMR SIC algorithm in an Algorithm Theoretical Basis Document (ATBD). It builds upon the experience from EUMETSAT Ocean and Sea Ice Satellite Application Facility (OSI SAF) and ESA Climate Change Initiative (ESA CCI) R&D efforts and includes 1) explicit atmospheric correction of the Tbs, 2) Open Water Filters, 3) dynamic tuning of the tie-points and algorithms, and 4) per-pixel uncertainties.

Explicit atmospheric correction. Many geophysical variables contribute to the Top-Of-Atmosphere (TOA) sensed Tb in addition to SIC, e.g., ocean surface parameters (wind speed, skin temperature, etc.), sea-ice and snow characteristics (sea-ice type, salinity, snow depth, layering, grain size, etc.), and atmosphere parameters (water vapour, cloud liquid and ice water content, etc.). Some of these effects can be partially corrected for on-the-fly (e.g., using auxiliary information from NWP forecasts and Radiative Transfer Models, RTM) while others cannot. The reduced accuracy due to these imperfect corrections are quantified and delivered as uncertainties together with the SIC retrieval.

Open Water Filters. Over the free ocean, even limited SIC noise of few percent (1 standard deviation) can prove an issue for downstream applications like data assimilation, forcing, or retrieval of other parameters like Sea Surface Temperature (SST). It is thus customary to add an Open Water Filter (OWF, aka Weather Filter, *Cavalieri et al., 1996*) to the SIC algorithm. The role of the OWF is to flag (True/False) measurements that are ice-free with high (but not absolute) confidence. The OWF combine frequency channels, typically at Ku- and Ka-bands, and apply a threshold-based classification between two classes (sea-ice and ice-free). The classification is however ambiguous in cases with low SIC and applying OWF necessarily results in removing (flagging as ice-free) conditions that have some amount of true sea-ice, especially along the Marginal Ice Zone (MIZ). Because removal of true low-concentration sea-ice can be an acute issue for some applications, the CIMR L2 product will hold both a “filtered” and an “unfiltered” SIC field. The OWF can be tuned via the choice of channel combination and the value of the thresholds.

Dynamic tuning. Experience -among others- from the EUMETSAT Ocean and Sea Ice Satellite Application Facility (OSI SAF) and ESA Climate Change Initiative (ESA CCI) R&D efforts advocate for implementing dynamical tuning of the SIC algorithm coefficients, and of the OWF threshold (*Tonboe et al. 2016, Lavergne et al. 2019*). This ensures low bias at 0% and 100% SIC despite the regional, inter-seasonal, and inter-annual changes in emissivity as well as inter-sensor calibration

differences or ageing. This also ensures that the OWF behave consistently through time when it discards true, low concentration (typically SIC < 10% or 15%) sea-ice conditions, as ice-free. The CIMR SIC algorithm should perform well over the whole range of SIC values, thus achieve optimal accuracy both at OW and Closed Ice (CI) conditions. This is best achieved by “hybrid” algorithms, that compute SIC as the combination of two SIC algorithms, one optimized for 0% and the low concentration range, and the other optimized for 100% and the high concentration range.

Per-pixel uncertainties. At Level-2, the total uncertainty is a combination of three independent contributions. The algorithm uncertainty quantifies the impact of the geophysical noise of the OW and CI signature (tie-points), the radiometric uncertainty measures the impact of the Tb, ΔT , and the footprint mismatch uncertainty quantifies the noise due to the CIMR FoVs not imaging exactly the same area at the surface.

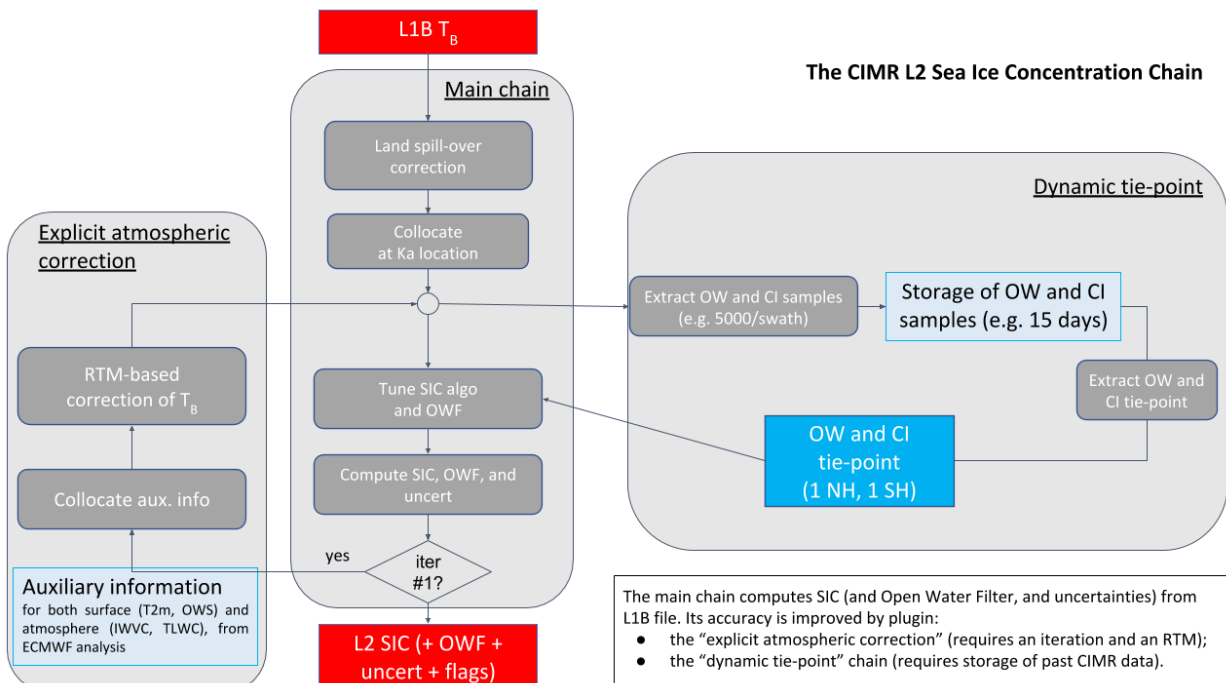


Figure MRD-6.3.1.1 Prototype CIMR NRT3H L2 Sea Ice Concentration product processing chain.

Processing algorithms for NRT1H L2 SIC products (MRD-1110) can be made simpler by e.g., not running the explicit atmospheric correction step, limiting the number of channels entering the SIC formula Eqn. 6.3.1.1, and limiting the time spent in estimating uncertainties. A prototype CIMR QRT L2 SIC processing chain is shown in Figure MRD-6.3.1.2.

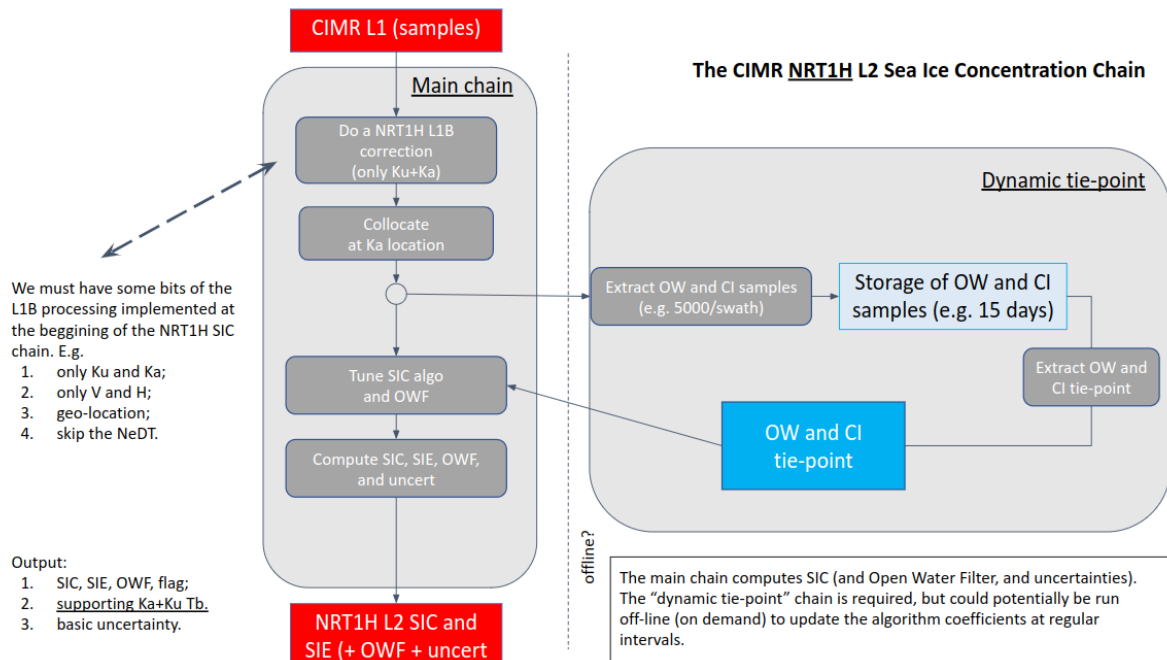


Figure MRD-6.3.1.2 Prototype CIMR NRT1H L2 Sea Ice Concentration product processing chain.

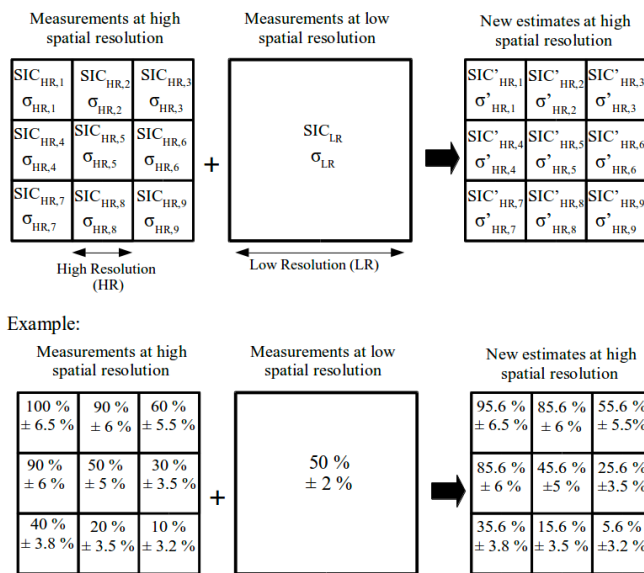


Figure MRD-6.3.1.3 : Illustration of the data fusion method: combination of the SIC retrievals at high resolution with the SIC retrieval at low resolution in the case of the CIMR instrument configuration (top).

Another retrieval framework has been specifically developed to estimate the SIC from CIMR observations between 6 and 36 GHz (Kilic et al., 2020). Different frequency combinations can be used, to minimize the uncertainty or to maximize the spatial resolution of the products. A solution is proposed to optimize both, using all the frequency range from 6 to 36 GHz. It is a two-step

algorithm. First, the SIC is estimated at the low spatial resolution of the 6 GHz, using 6 and 10 GHz observations (both polarizations), and at the high spatial resolution of the 18 GHz, using the 18 and the 36 GHz (both polarizations). Second, the high spatial resolution 18+36GHz results within a low-resolution 6+10GHz pixel are bias-corrected to match the 6+10GHz result, taking into account the respective errors of the products (see Figure MRD-6.3.1.3). This is the IceCREAM algorithm. The algorithm has been tested with AMSR2 observations, with collocated MODIS estimates. It is also tested for the full polar regions, winter and summer, under clear and cloudy conditions. The IceCREAM results provides both low errors related to the low frequency observations and high spatial resolution obtained from the high frequencies for both North and South Poles (*Prigent et al., 2020*).

6.3.2 Global and Polar Sea Surface Temperature algorithm

SST retrievals from microwave radiometer measurements have been tested early, as soon as 1978, with dual polarization channels at 6.6, 10.7, 18, 21, 37 GHz from SMMR. It was followed by TMI on board TRMM with better calibrated instruments and spatial resolution (~50 km spatial resolution for the SST estimate) although limited to latitudes of ~40° N/S. Since 2002, AMSR-E and now AMSR-2 also measure using 6.9 GHz.

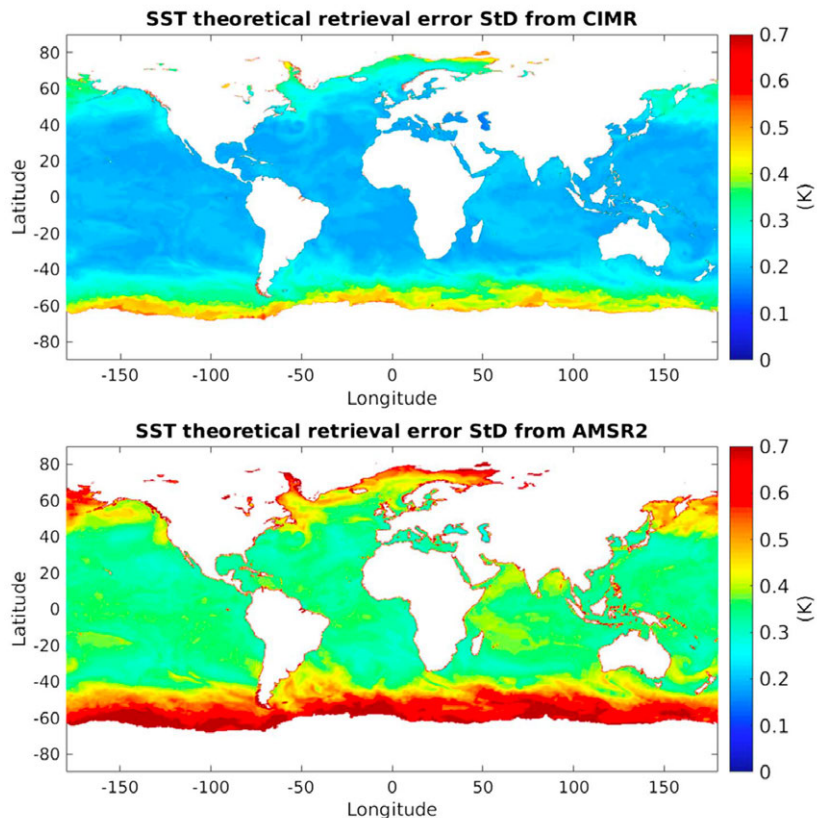


Figure MRD-6.3.2.1. The theoretical retrieval error SD on SST for 1 day (15 June 2008) at global scale, estimated from radiative transfer simulations and realistic ocean and atmospheric fields, with the instrument specifications of CIMR (top) and of AMSR2 (bottom). SST = sea surface temperature; CIMR = Copernicus Imaging Microwave Radiometer; AMSR2 = Advanced Microwave Scanning Radiometer 2; SD = standard deviation (from *Kilic et al., 2018*).

Many SST studies, from TMI or from AMSR, are derived from retrievals from Wentz and colleagues (e.g., *Wentz et al., 2000*). The algorithms are based on radiative transfer simulations on

a large data set of atmospheric/ocean conditions. The resulting simulated brightness temperatures are typically used to train multi-regression algorithms. Operational AMSR2-based SSTs are provided by Remote Sensing Systems (RSS). Prigent *et al.* (2013) tested a Neural Network inversion on different subsets of frequencies from AMSR-E, at global scale, with results comparable to the previous algorithm for the full set of AMSR-E channels. An optimal estimation technique has been developed within the European Space Agency Climate Change Initiative (ESA-CCI) at DMI to retrieve SST from AMSR-E. A comprehensive matchup database with drifting buoy observations is used to develop and test the algorithm setup (Nielsen-Englyst *et al.*, 2018). Pearson *et al.* (2018) also tested an optimal estimation method to prioritize the different window channels from 6 to 36 GHz for SST retrievals. The colder the water, the more important the role of the 6.9 GHz frequency. Outside polar and high-latitude regions, the sensitivity to SST becomes strong enough at 10.7 GHz so that this higher frequency can be given a more prominent role. This can be used to provide higher resolution SSTs outside the high-latitude regions and justify a separate global SST product.

A detailed analysis of CIMR capability to derive SST, OWS and SSS is provided in Kilic *et al.* (2018) who analyse the performances of the CIMR mission in terms of theoretical retrieval precision and spatial resolution on the SST, SSS, OWS and, SIC products based on the CIMR instrument specification set out in this MRD. A careful information content analysis (see Prigent *et al.*, 2013) is conducted and the derived CIMR performances are compared with the AMSR2 and SMAP missions. Maps of the retrieval precision based on realistic conditions are computed. CIMR will provide SST, SSS, and SIC with a spatial resolution of 15, 55, and 5 km and a precision of 0.2 K, 0.3 pss, and 5%, respectively (see Figure MRD-6.3.2.1). The SST and SIC will be retrieved at better than 30 km from the coast. The figure above provides an estimate of theoretical retrieval errors for CIMR SST compared to AMSR2 SST. Jimenez *et al.* (2021) implemented a two step consistent estimation retrieval of all the ocean variables (see Figure MRD-6.3.2.2). They also conducted a thorough evaluation of the SST retrieval performances (along with SSS, OWS, and SIC) with CIMR, using the End-to-End CIMR simulator developed during the ESA Algorithm Development and Performance Evaluation project (CIMR-APE). It showed that the SST retrieval (as well as the retrieval of the other ocean variables) was conforming with the mission requirements.

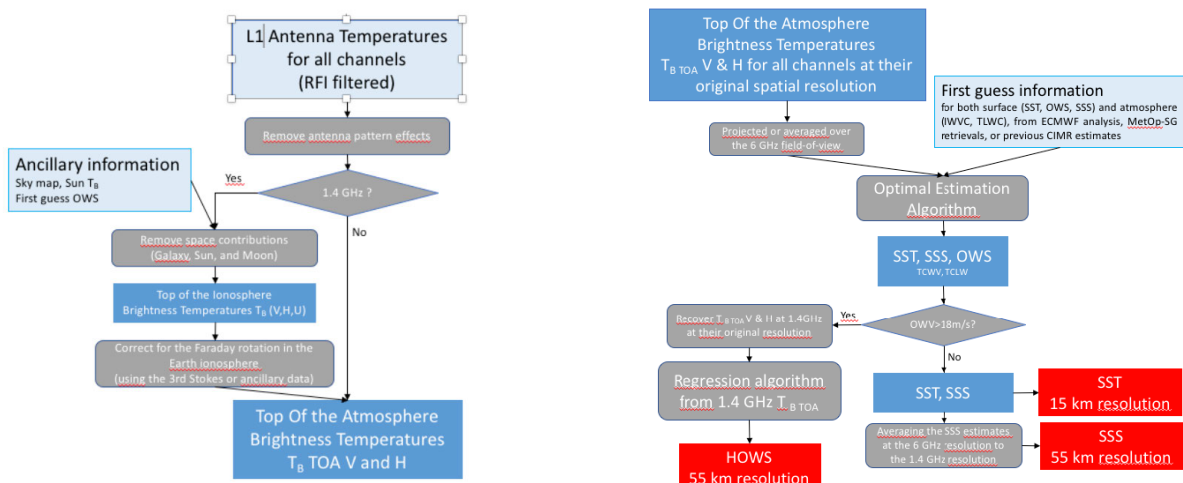


Figure MRD-6.3.2.2 Prototype CIMR L2 Optimal Estimation retrieval overview (includes SST, ocean surface winds and SSS). See CIMR-APE reports and Jimenez *et al.* (2021).

For the ice-free ocean, consistent retrievals of SST, OWS, SSS, High Ocean wind Speed (HOWS), and OWV, along with the cloud and precipitation retrieval are highly desirable.

6.3.3 Polar Thin Sea Ice Thickness algorithm

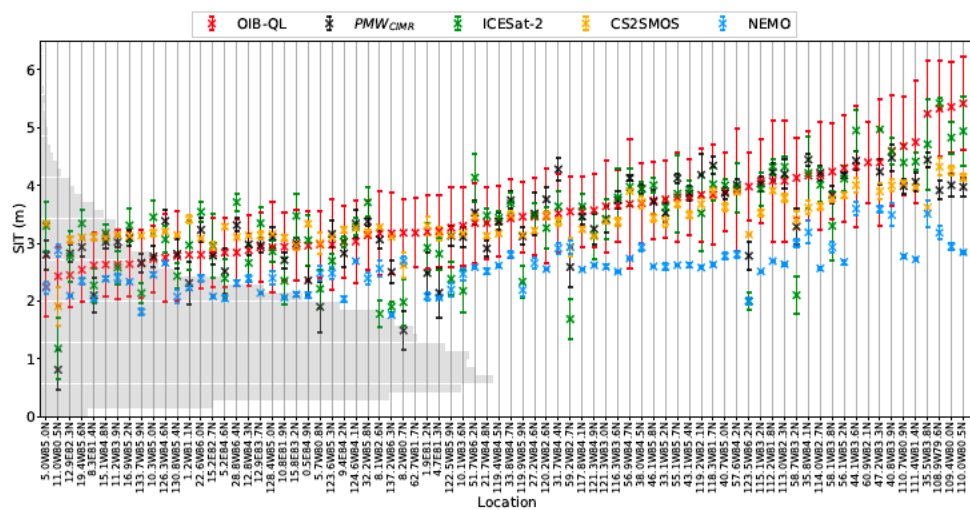
Kaleschke et al (2010; 2016) describe a method to exploit brightness temperatures at 1.4 GHz (L-band) measured by the Soil Moisture and Ocean Salinity (SMOS) Mission to derive the thickness of sea ice. The retrieval method is applicable only for relatively thin ice and not during the melting period. Ice thicknesses derived from the surface elevation measured by an airborne laser scanner and from simultaneous EMIRAD-2 brightness temperatures correlate well up to 1.5m which is more than the previously anticipated maximal SMOS retrieval thickness.

Operational products of thin sea ice thickness (up to 0.5–1.0 m maximum thickness) retrieved from SMOS observations (since 2010) are today available from two independent retrieval procedures based on observations at different incidence angle ranges. While the procedure by *Kaleschke et al.* (2010) (algorithm baseline in *Tian-Kunze et al.*, 2014) uses intensity at incidence angle below 40°, the procedure by *Huntemann et al.* (2014) relies on intensity and polarization difference between 40° to 50° (<https://seacie.uni-bremen.de/thin-ice-thickness>). Currently, the SMOS SIT retrieval is being transferred to the L band sensor SMAP launched in 2015 (*Patilea et al.*, 2018; *Schmitt and Kaleschke*, 2018).

The retrieval of thickness of thin sea-ice works only during the cold season (~October to ~April in the Arctic), and have been routinely demonstrated only in the Arctic.

CIMR will be able to exploit both L-, C- and X-band channels to improve the determination of thin Sea Ice Thickness.

Recent developments showed the potential of AMSR-like frequencies to estimate the SIT over the full SIT range (Lee et al., 2021; Chi and Kim 2021). Soriot et al. (under review) specifically developed a retrieval methodology to provide SIT from the full range of CIMR frequencies, using a NN methodology trained on IceSat SIT estimation. The method shows performances that are similar to IceSat and CS2SMOS SIT estimates, as compared to campaign measurements (Figure MRD-6.3.3-1).



6.3.4 Polar Sea Ice Type / Stage of Development algorithm

Temporal and spatial variation of sea ice type in the Polar Regions is an indicator of regional and global change. Sea ice can be classified into two major categories: multiyear ice (MYI) and first-year ice (FYI). Since the start of satellite records, Arctic sea ice extent has declined by about 4% per decade with MYI has declined at a higher rate during the same period and FYI dominates the Arctic ocean. This change of proportion leads to changes in weather and climate through different radiation and dynamic properties (*Zhang et al. 2019*). Recently, MYI area has decreased by 42%, (*Kwok et al. 2009*): the replenishment of MYI with thinner, easily deformed FYI increases the heat exchange between the atmosphere and the ocean (*Stroeve et al., 2012*). Such a reduction of MYI cover benefits Arctic shipping with less risks and more convenience (*Zhang et al. 2019*).

A variety of ice-type classification methods exist (e.g., *Zhang et al. 2019*, *Cavalieri and Parkinson, 2012*, *Comiso and Kwok, 1996*) that rely on microwave radiometer brightness temperature, or combinations of brightness temperature with scatterometer and Synthetic Aperture Radar (SAR) measurements. The state of snow (wetness) increases Tb and therefore complicates the signature separation of MYI and FYI used by classification algorithms complicating sea ice-type discrimination particularly in the summer melt season or during warm air outbreaks. This sea ice type products remain challenging during summer seasons. Nevertheless, microwave radiometer Tb constitute the long-term record for sea ice classification. CIMR will bring a unique capability focused on low-frequency, high-resolution Tb to discriminate sea ice type and stage of development.

Ice-type is typically derived from scatterometers (e.g., MetOp ASCAT) in combination with microwave radiometry measurements (e.g., AMSR-2 or SSMI), e.g., as in the current operational OSI-SAF and CMEMS catalogue. Historically, the 19 and 37 GHz gradient has been used for ice type classification into first- and multiyear ice types (*Swift and Cavalieri, 1985*).

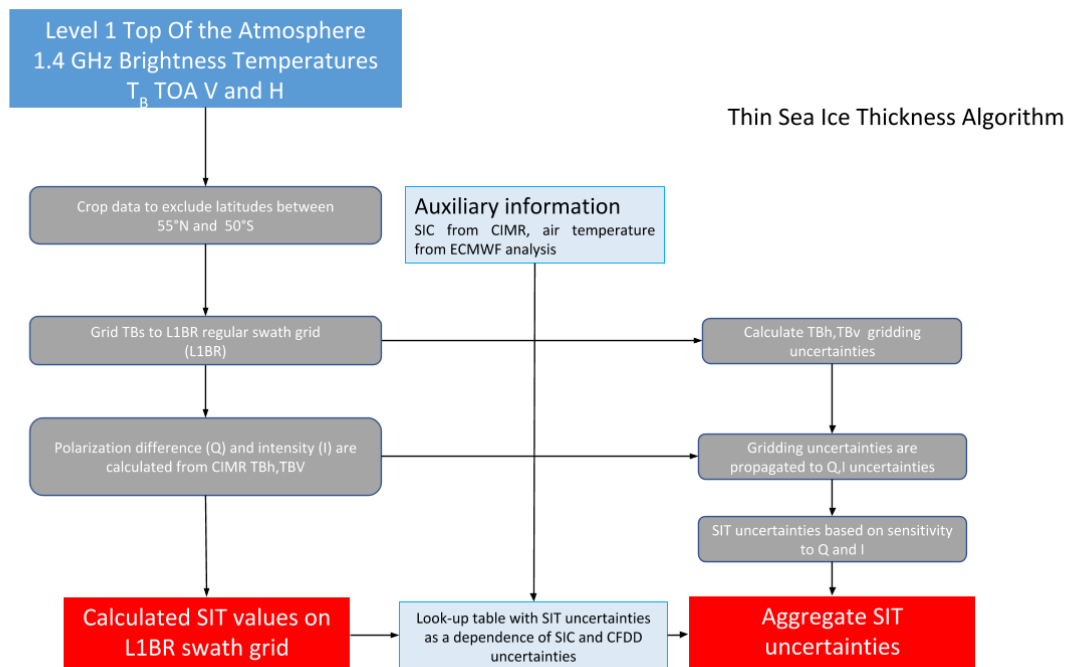


Figure MRD-6.3.3.1 Prototype CIMR L2 Thin Sea Ice thickness algorithm overview.

A retrieval method specifically for the multiyear ice (MYI) concentration first uses input data from active and passive microwave instruments (radar scatterometer and radiometer, respectively) as

well as distributions of typical brightness temperatures and radar backscatter coefficients for the ice types and open water and then retrieves the concentration of each ice type by a constrained optimisation method. The frequencies used are Ku band or C band for the scatterometer, and 18 and 37 GHz, H and V polarisation for the radiometer. Next, it applies several correction schemes on the MYI concentration to account for the effect of melt-refreeze processes, snow metamorphosis and sea ice drift on the sea ice type retrieval, which has proven to eliminate unphysical behaviour of MYI as retrieved from active and/or passive microwave instrument data (Ye *et al.*, 2016a, b).

Using radiometry and scatterometry limit the retrieval period to the cold season (~October to ~April in the Arctic) although post-processing and filtering tests such as those of Ye *et al.* (2016 a, b) can extend the period to mid-September (onset of freezing) to mid-May (onset of surface melt-ponding).

Because of the many types of sea ice and the dynamic nature of their radiometric signature, state-of-the-art algorithms dynamically adapt their coefficients to cope with inter-seasonal and interannual variability.

6.3.5 Polar Sea Ice Edge algorithm

Aaboe *et al.* (2016;2018) describe Sea Ice Edge detection algorithms. Sea Ice Edge is a surface classification product that assigns ocean grid cells to sea-ice classes (e.g., Open Water, Very Open Drift Ice, Open Drift Ice, Closed Ice, etc.). For the CIMR product, classes are TBD depending on the implementation of CIMR. The EUMETSAT OSI SAF and C3S both provide sea-ice edge products with the following classes: Open Water (~<30% SIC), Open Ice (~ 30-70% SIC) and Closed Ice (~>=70% SIC). The SIED product is a refined ice/no-ice mask, that can be used for navigation and used masking sea-ice signal in other CIMR products and/or satellite missions (e.g., altimeter-based SSH, IR-radiometer-based SSTs, OC products, etc.).

The uncertainty specification assumes a confidence matrix is used to discriminate the sea-ice classes when compared to SAR and Scatterometer data (e.g., Aaboe *et al.*, 2016). An alternative uncertainty characterization of the SIED product is the mean distance to SAR/ice-chart sea-ice edge, expressed in km (Aaboe *et al.*, 2016). In this case, the requirement would be < 10 km.

6.3.6 Polar Sea Ice Drift algorithm

The vast majority of satellite-based sea-ice drift algorithms work by analysing a pair of satellite images and attempting to explain the change in intensity patterns between the images by two-dimensional shifts of small blocks of pixels. There is no limitation as to what the type of imager is used (active/passive), the type of wavelength (visible, microwave, etc...) nor the actual property that is imaged (snow, ice type, ocean in leads, melt pond patterns, ...). This leads to the same algorithms being easily applied to several types of sea ice images, with adaptations that are often driven by the need for better processing speed when using finer resolution images (typically SAR).

A variety of ice drift products, which are obtained from different satellite-borne sensors, different time intervals for detecting ice motion, and/or different algorithms for deriving drift vectors, are available (e.g., Kwok *et al.*, 1998; Fowler, 2013; Lavergne *et al.*, 2010; Girard-Ardhuin and Ezraty, 2012). As noted by Sumata *et al.* (2014), the advantages of such products in comparison to *in situ* data are an Arctic-wide spatial coverage with a constant time interval and gridded data format, which makes the products easily suitable for evaluating the model-observation misfit of basin-scale sea-ice simulations. Sumata *et al.* (2014) perform an inter-comparison of four different Arctic Ocean low-resolution ice-drift products derived from satellite observations at monthly timescales, and examined their differences to buoy drift data. In high ice concentration areas (99–100%), the

mean differences of drift vectors are small ($0.6\text{--}0.8 \text{ cm s}^{-1}$) and they gradually increase to $0.9\text{--}4.4 \text{ cm s}^{-1}$ in 89–90% ice concentration areas. In thicker ice areas ($4.5\text{--}5.0 \text{ m}$), mean differences of the drift range from 0.5 to 0.8 cm s^{-1} depending on a combination of the products, whereas those in thinner ice areas ($0.5\text{--}1 \text{ m}$) range from 0.7 to 1.9 cm s^{-1} . Direct comparisons with the buoy-based drift speeds indicate that the error also depends on the drift speed. In all products, faster ice drift speed generally gives larger errors; the error is roughly less than 1 cm s^{-1} for ice drift speeds slower than 3 cm s^{-1} while the error exceeds 1.6 cm s^{-1} for ice drifts larger than 5 cm s^{-1} . However, many of the characteristics described pertain to monthly fields, not necessarily the sustaining daily fields.

Algorithms for sea-ice drift are mature (e.g., *Lavergne et al.*, 2010), and used operationally on a wide variety of instruments and channels. The most basic algorithms are even integrated in popular off-the-shelf software packages (motion detection is a field of computer vision).

One of the limitations of the sea-ice drift products available from AMSR-2 and SSMIS from OSISAF is that they are L3c-type products, generated only once a day, from daily averaged maps of brightness temperature. This reduces the accuracy of the drift vectors, wastes geographical coverage (several vectors a day could be retrieved at many locations, instead of just one), and greatly reduces timeliness (daily averaged maps must be built before a product is generated). CIMR, with its increased spatial resolution and repeat cycle, will provide the possibility to produce so-called swath-to-swath drift products (*Lavergne et al.*, 2021), that is computing vectors from pairs of swaths, instead of pairs of daily-averaged maps.

In addition to the swath-to-swath processing approach, the increased resolution of CIMR grants higher resolution ($\sim 25 \times 25 \text{ km}$) and better accuracy. Note that high-resolution 18.7 GHz channels have the potential to provide year-round sea-ice drift vectors (Ka-band and above are challenged by surface melt and atmospheric noise during the melt season).

6.3.7 Polar Snow Depth on Sea Ice algorithm

Snow lying on top of sea ice plays an important role in the radiation budget because of its high albedo, the Arctic freshwater budget, and influences the Arctic climate: it is fundamental climate variable. Importantly, accurate snow depth products are required to convert satellite altimeter measurements of ice freeboard to sea ice thickness (SIT). Due to the harsh environment and challenging accessibility, in situ measurements of snow depth are sparse. The quasi-synoptic frequent repeat coverage provided by satellite measurements offers the best approach to regularly monitor snow depth on sea ice. A number of algorithms are based on satellite microwave radiometry measurements and simple empirical relationships (for a review see *Braakmann-Folgmann and Donlon*, 2019). Reducing their uncertainty remains a major challenge.

Snow Depth on sea ice has been estimated using a combination of AMSR-E or AMSR-2 brightness temperatures (e.g., using 18.7 and 36.5, GHz) using a spectral gradient approach (e.g., *Markus et al.*, 2006; *Comiso et al.*, 2003). Although the method is confounded in the presence of snow melt water and sensitive to the ice roughness below, potentially this can allow direct snow measurements to replace the Warren snow climatology (*Warren et al.*, 1999). Several studies investigated the uncertainty bounds of the microwave SD retrieval in the Arctic and Antarctic (e.g., *Markus et al.*, 2006; *Stroeve et al.*, 2006) and the current retrieval methods have a Scientific Readiness Level (SRL) of 4 or higher. In the Arctic, the traditional 19/37 GHz gradient ratio retrieval, however, is limited to first-year ice. Recently, the method was extended to work over multiyear ice in spring and more reliable over first-year ice by inclusion of the 6.9 GHz channels (*Rostosky et al.*, 2018).

Maass et al. (2013, 2015) and *Zhou et al.* (2018) proposed the use of L-band radiometer data for snow depth retrieval over thicker Arctic sea ice, where the sensitivity of L-band measurements

towards ice thickness shift to snow depth. Similarly, it was demonstrated by *Rostosky et al.* (2018) that the use of C-band in combination with Ku-band has retrieval skills over thicker old ice.

The performance and uncertainty of the Snow Depth retrieval is well quantified by several studies (e.g., *Markus et al.*, 2006; *Stroeve et al.*, 2006; *Rostosky et al.*, 2018). This the method can be considered mature. However, due to the high variability of snow properties (e.g., layering, ice lenses, liquid water content, salinity) and the underlying sea ice (e.g., roughness, salinity) conceptually there are significant uncertainties (RMSD approx. 10 cm) for the retrieved SD.

Kilic et al. (2018b) describe an approach to estimate the snow depth, the snow-ice interface temperature, and the effective temperature of Arctic sea ice using AMSR2 and Ice Mass Balance buoys data. At low microwave frequencies, the sensitivity to the atmosphere is low, and it is possible to derive sea ice parameters due to the penetration of microwaves in the snow and ice layers. The snow depth over sea ice is estimated with an error of 5.1 cm, using a multilinear regression of 6, 18, and 36 GHz vertical polarisation data.

Braakmann-Folgmann and Donlon (2019) explore a new approach to retrieve snow depth on sea ice from multi-frequency satellite microwave radiometer measurements using a neural network approach. Neural networks have proven to reach high accuracies in other domains and excel in handling complex, non-linear relationships. using airborne snow depth measurements from Operation Ice Bridge (OIB) campaigns and compare them to products from three other established snow depth algorithms. Neural networks outperform other algorithms in terms of accuracy when compared to the OIB data. The estimated snow depth covers the full range of measured OIB snow depths and our approach works over both FYI and MYI without requiring a map of ice types to distinguish between both.

6.3.8 Polar Sea Ice Surface Temperature algorithm

The Snow/Ice Interface Temperature (or Ice Surface Temperature (IST)) can be estimated using the 6 GHz radiometer measurements. Snow is mostly transparent at 6 GHz and the sea ice have a very stable emissivity. The vertical snow and sea ice description in models is now advancing and requires information on the vertical temperature profile (*Tonboe et al.* 2011).

Recent developments using satellite microwave radiometer data at 6.9, 18.6 and 36.5 GHz with empirical algorithms suggest that the snow-ice interface temperature, the effective temperature, and the snow depth in terms of brightness temperature can be retrieved (*Kilic et al.*, 2018b).

Another field of progress which is currently limited by the low resolution of existing 6 GHz sensors will be the simultaneous retrieval of atmospheric and surface parameters from microwave radiometer observations at higher frequencies using an optimal estimation method. This has been a standard for open ocean for many years and is subject to ongoing research over sea ice (*Melsheimer et al.* 2008, *Scarlat et al.* 2017).

6.3.9 Global Terrestrial Snow Area algorithm

The CIMR channels are very good fit for remote sensing of terrestrial snow. The Ka-/Ku-band information from earlier microwave radiometers have been applied quite successfully for estimation of snow water equivalent (SWE) over the terrestrial domain on hemispheric scale. The information from X to Ka-band has been applied for snow detection, and there have been preliminary studies to complement these retrieval approaches using L-/C-band data. However, there has not been an opportunity to study the whole suite of L- to Ka-band data for snow monitoring up to date, and the unprecedented high spatial resolution of CIMR will likely benefit snow remote sensing as snow cover is often very heterogeneous and dynamic in nature. The analysis of terrestrial snow with

microwave radiometers has typically been limited to observations at one or two frequencies at a time.

Terrestrial snow cover can be detected using a combination of 19 and 36.5 GHz. There are a number of well-established snow cover and snow-melt estimation algorithms that work on hemispherical and Global scales (e.g., *Hall et al.* 2002, *Kelly et al.* 2003, *Takala et al.* 2009, *Li and Kelly*, 2017). In addition to detecting the extent of snow cover, detection of wet snow and snowmelt is straightforward and reliable. There are several operational services providing daily snow extent and wet snow information on regional and hemispherical scales (e.g., EUMETSAT H SAF, ESA GlobSnow). The methodologies for Snow area estimation can be considered mature but must be extended to consider to new opportunities presented by CIMR multifrequency approaches.

6.3.10 Global Terrestrial Snow Water Equivalent algorithm

From the available set of observed frequencies, the algorithms for retrieval of SWE employ a 36-37 GHz (or 31.4 GHz) and a 18-19 GHz channel in combination. These being the key required frequencies, allowing for SWE retrieval, without the 37GHz (or 31.4GHz) channel the retrieval is in practice not feasible. The scattering of a 19 GHz signal in snow is notably smaller when compared to 37 GHz, while the emissivity of frozen soil and snow is estimated to be largely similar at both frequencies. Observing the brightness temperature difference of the two channels allows to establish a relation with the detected signal and snow depth, with the additional benefit that the effect of variations in physical temperature on the measured brightness temperature is reduced. Similarly, observing a channel difference reduces or even cancels out systematic errors of the observation, provided that the errors in the two observations are similar (e.g., due to using common calibration targets on a space-borne sensor). Typically, the vertically polarized channel is preferred due to the inherent decreased sensitivity to snow layering (e.g., *Rees et al.*, 2010).

The existing globally operational snow mass retrieval algorithms are currently based on microwave radiometer sensors (e.g., *Kelly*, 2009; *Takala et al.*, 2011). Applying microwave radiometers for snow cover detection is appealing due to the availability of a daily time series with global coverage, extending back almost 40 years to 1979. While the detection of certain snow cover characteristics, such as snow extent and snow melt-off (*Takala et al.*, 2009), is relatively straightforward, estimation of SWE is more challenging. The main challenges hampering retrieval skill are related to the separation of the effect of increasing snow mass from other varying structural properties of the snowpack, and on the other hand, mitigating for mixed pixel effects in the coarse scale microwave radiometer observations over heterogeneous landscapes.

The underlying principle in all microwave radiometer algorithms for retrieval of SWE is based on observing the effect of snow cover on the naturally emitted brightness temperature from the ground surface. Ground brightness temperature is scattered and absorbed by the overlying snow medium, resulting in decreasing brightness temperature with increasing snow mass, up to a frequency-dependent point of saturation when self-emission from the snow itself matches the rate of extinction of the ground radiation (e.g., *Mätzler et al.*, 1982). The rate of extinction can be approximated by dividing extinction into absorption and scattering mechanisms following the radiative transfer theory. The rates of absorption and scattering depend on the wavelength, the amount of snow in the signal path, and the dielectric and structural properties of the snow cover. Scattering intensity increases as the wavelength approaches the size of the scattering particles. Considering that individual snow particles are measured in millimetres, high microwave frequencies (short wavelengths) will be scattered more than low frequencies (long wavelengths). The intensity of absorption can be related to the dielectric properties of snow, with snow density largely defining the permittivity for dry snow.

Several retrieval algorithms have been proposed in the literature and implemented in an operational context. Studies by *Kelly et al.* (2003) and *Kelly* (2009) form the basis of the current

NASA AMSR-E SWE product ('NASA SWE Standard' algorithm), as well as the JAXA AMSR2 SWE product. A recent adjustment to the algorithm ('NASA SWE Prototype' algorithm) has been presented by Tedesco and Jeyaratnam (2016). An approach introduced by Pulliajainen (2006) and Takala *et al.* (2011), based on numerical inversion of a snow emission model and assimilation of in situ data, is applied in the Copernicus Global Land Monitoring Service (<https://land.copernicus.eu/>) and ESA GlobSnow (www.globsnow.info). The in-situ data regulates the retrieval by both calibrating the forward model at sites where in situ data on snow depth are available, and finally through providing a first guess value for SWE through Kriging interpolated background fields of snow depth.

Applying physical models in SWE retrieval requires a robust forward modelling scheme capable of reproducing the emission signatures from snow-covered landscapes. Available snow emission models are mostly based on radiative transfer analysis, treating the snowpack as a scattering medium with varying degrees of complexity (e.g., Tsang *et al.*, 1985; Tsang *et al.*, 2000; Wiesmann *et al.*, 1999; Pulliajainen *et al.*, 1999; Picard *et al.*, 2013). Forward models for vegetation and other features can also be applied to mitigate the effects of heterogeneous land cover (Kruopis *et al.*, 1999; 2011; Lemmetyinen *et al.*, 2011; Roy *et al.*, 2012; Kontu *et al.*, 2014; Cohen *et al.*, 2015). However, actual retrieval schemes are forcibly limited to relatively simple emission models, in particular due to the lack of detailed ancillary input parameters (e.g., snow stratification; detailed vegetation information; lake ice properties) on a global scale.

Microwave radiometer retrievals of SWE have a long history, but regardless of efforts retrieval skill remains a limitation in the current products (e.g., Larue *et al.*, 2016 and Hajnsek *et al.*, 2017). While fairly good results have been achieved using the GlobSnow approach (Takala *et al.*, 2011), the overall accuracy of satellite radiometer-based SWE estimates are slightly better or on par with current land surface model capabilities (e.g., Brun *et al.*, 2013). A known challenge with the usability of the GlobSnow approach is the fact that the final SWE product is reliant on surface observations and cannot thus be considered as an independent observation for merging with e.g., meteorological reanalysis data. As was found in the ESA SnowPex study, standalone SWE retrievals from microwave radiometer sensors exhibit even larger errors, limiting their usability for most applications.

In general, microwave radiometer retrievals at current frequencies are limited to snow depth between approximately 0.05 m – 1.00 m in thickness, and only under dry snow conditions. Depths of less than 0.05 m cannot be detected as detected brightness temperature difference between the 19 and 37 GHz frequencies used falls below the 1-2 K radiometric resolution of space borne instruments. With snow depths greater than about 1 m, the brightness temperature signal at 37 GHz saturates. Moreover, even a relatively small amount of liquid water will contaminate the detected signal making detection of SWE impossible. Separating the effects of extinction efficiency and of the total amount of snow also remains an issue in the interpretation of microwave radiometer observations of snow cover for stand-alone approaches.

The coarse spatial resolution of microwave radiometer sensors in space remains a serious handicap for observations over heterogeneous land surfaces and mountain regions, as spatial resolutions at frequencies relevant for snow parameter retrieval are on the order of tens of kilometres, an improved resolution of about 5km would improve the situation notably. Currently, mixed pixel effects from vegetation, topography and subnivean conditions complicate the microwave signal. The natural variability of snow cover itself is also notable, as the distribution of snow is strongly affected by meteorological conditions, interaction with vegetation, and changes in surface topography and land cover. As a result, in addition to snow height and SWE, properties such as stratigraphy and snow microstructure change both spatially and over time, affecting the microwave signature and adding an additional challenge for SWE retrieval.

The methodologies for SWE retrieval from 19GHz and 37GHz are mature and being conducted in operational fashion within (e.g., Copernicus Global Land Service and EUMETSAT H SAF services), the improved resolution of the proposed mission would be a game changer for operational SWE monitoring and would benefit a large array of downstream services.

6.3.11 Global Sea Surface Salinity algorithm

The brightness temperature measurement at L-band 1.4 GHz is proportional to the surface skin temperature (SST) and to the sea emissivity, which depends strongly on the salinity (SSS) at this frequency and to a lesser extent to the OWS. In practice, however, numerous additional external factors (galactic noise contamination, ionosphere) also contribute to the signal and must be accounted for. The 1.4 GHz brightness temperature sensitivity in SSS is ~ 0.5 K/pss, which is rather weak given that spatial and temporal variability of SSS does not exceed several pss. The algorithms are based on the reasonable knowledge of the emissivity radiative transfer at this frequency. *Reul et al.* (2012) describe the initial SMOS algorithm and evaluate the products, and *Brucker et al.* (2014) present the developments for the Aquarius mission.

While a challenging measurement to make from space (e.g., *Yueh et al.*, 2001), for warmer waters great progress has been made using 1.4315 GHz measurements from the ESA SMOS (e.g., *Reul et al.*, 2012a) and NASA Aquarius (e.g., *Yueh et al.*, 2014) and SMAP missions (e.g., *Meissner and Wentz*, 2016). Radio Frequency Interference (RFI) must be mitigated when using low-frequency L-X band channels, in geophysical retrieval algorithms (e.g., *Soldo et al.*, 2017; *Mohammed et al.*, 2016). New algorithms, recently developed at the Barcelona Expert Centre (BEC) to improve the quality of L-band measurements show that for the first time cold-water SSS maps from SMOS data can be derived (*Olmedo et al.*, 2017; *Garcia-Eidell et al.*, 2017) to observe the variability of the SSS in the higher north Atlantic and the Arctic Ocean. Also, BEC has proposed a methodology to mitigate systematic errors produced by the contamination of the land over the sea that allows obtaining SMOS SSS fields over enclosed seas such as the Mediterranean (*Olmedo et al.*, 2018). *Buongiorno Nardelli et al.*, 2012 and 2016 demonstrated that SST can be used together with SSS data to produce L4 SSS products with higher resolution and improved accuracy and to directly estimate the sea surface density (SSD) fields. This method is now adopted by CMEMS to produce global reanalysis of SSS and SSD (1993-2016) at $1/4^\circ$ spatial resolution available from the CMEMS catalogue since April 2018 (*Droghei et al.* 2016, *Droghei et al.* 2018). The NRT3H SSS and SSD production is planned for end of 2018.

The L-band measurements are also sensitive to the SST and the OWS (and to a much lesser extent to atmospheric parameters). CIMR having both L-band and C, X, Ku, and Ka bands, a joint analysis of the bands can provide simultaneously consistent SSS, SST, and OWS information. A detailed analysis of CIMR capability to derive SST, OWS, and SSS is provided in *Kilic et al.* (2018) who analyse the performances of the CIMR mission in terms of theoretical retrieval precision and spatial resolution. An optimal estimation method has been tested to provide simultaneously these parameters with the current CIMR instrument characteristics (the ESA CIMR-APE project). NN inversion algorithms could also be developed, with similar retrieval performances, but faster processing (*Prigent et al.*, 2013). *Jimenez et al.* (2021) tested the combined SST, OWS, and SSS optimal estimation retrieval within the End-to-End CIMR simulator (CIMR-APE ESA study) and showed that the SSS retrieval performances agreed with the requirements.

6.3.12 Global Soil Moisture algorithm

Microwave observations are sensitive to soil moisture because moisture affects the dielectric constant of the surface and thus the land surface emissivity. Vegetation and surface roughness reduce the microwave sensitivity to soil moisture and are more pronounced as microwave frequency increases. At L-band frequencies the soil moisture emission originates from deeper in

the soil (a few centimetres), giving a more representative measurement of conditions below the surface or skin layer. Measurements at C-band range are sensitive to soil moisture, but primarily in regions of low vegetation. The attenuation by vegetation and the shallow sensing depth of ~1 cm for bare soil impose limitations on the retrieval of soil moisture. See *Njoku et al.* (2003) for information on the application of AMRE for Soil Moisture retrieval. The CIMR channel at 1.4315 GHz is ideally suited to soil moisture measurements complemented by the other channels at higher frequencies. Recent research has shown that retrieval algorithms that estimate both soil moisture and the degree of attenuation through vegetation can improve the soil moisture retrieval at C- and X- bands (see *Owe et al.*, 2001, 2008, *de Jeu et al.*, 2003, *Karthik et al.*, 2019) and L-band (*Konings et al.*, 2016; *Fernández-Moran et al.*, 2017; *Konings et al.*, 2017). Also, techniques have been developed to simultaneously exploit observations at diverse frequencies using AI algorithms based on Neural Network trained on land surface models (*Aires et al.*, 2005, *Kolassa et al.*, 2016, 2017). At ECMWF, the current operational algorithm for SMOS soil moisture is based on NN, trained on the land surface model (*Rodriguez-Fernandez et al.*, 2015-2019).

6.3.13 Global Precipitation (rain rate) algorithm

Precipitation is a key hydrological and climate variable and includes both the liquid (rain) and solid (snow and ice) forms. Precipitation occurs when a particle formed by the condensation of water vapour becomes heavy enough to fall under the force of gravity. Precipitation rate estimates are a fundamental component of the water cycle characterization. The physical basis for retrieving precipitation from microwave radiometer measurements depends on distinguishing the radiation from Earth's surface from the radiation emitted from precipitation (e.g., *Hilburton and Wentz*, 2008). Microwave emission from the ocean surface is strongly polarized, while the emission from rain drops is un-polarized. Thus, precipitation can be accurately distinguished from the underlying ocean surface using measurements of the vertically and horizontally polarized radiation (see examples at <http://www.remss.com/measurements/rain-rate/>). CIMR will be able to provide estimates of precipitation rate, although further algorithm development is required, in particular to exploit forward and backwards views together.

Precipitation rate retrieval algorithms have been developed in Europe (e.g., *Casella et al.* 2017, *Sanò et al.* 2018) to work with data from the conically scanning Global Precipitation Measurement (GPM) Microwave Imager (GMI) and AMSR-2. CIMR will be able to provide estimates of precipitation rate, although further algorithm development is required, in particular to exploit forward and backwards views together.

6.3.14 Global Ocean Surface Wind Vector/Speed algorithm

Multi-channel microwave radiometers have been used to measure ocean surface winds for several decades (at NWP centres, or at Remote Sensing System for instance). With CIMR, it has been already shown that the available frequency combination can provide consistent OWS, SST, and SSS, within an optimal estimation framework (*Kilic et al.*, 2018), at least for wind speed below 18m/s. See the section on SST, and SSS retrievals above. For wind speed above 18m/s, the current sea surface emissivity models encounter difficulties, and empirical parameterization have been developed, to estimate the wind speed, using essentially the L-band observations (e.g., *Reul et al.*, 2017).

The first space-based fully polarimetric microwave radiometer, WindSat, (*Gaiser et al.* 2004) was launched in January 2003 with a primary mission is to provide measurements to evaluate the potential of polarimetric microwave radiometry to retrieve the ocean surface wind vector. The polarization properties of an electromagnetic wave can be fully characterized by the modified Stokes that includes the vertical and horizontal polarizations and the third and fourth Stokes parameters. As discussed by *Bettenhausen et al.* (2006), modelling and aircraft measurements

have shown that the vertical and horizontal Stokes components are even periodic functions of the relative wind direction whereas the 3rd and 4th Stokes parameters are odd periodic functions. Thus, a fully polarimetric radiometer such as CIMR, provides sufficient information to, at least in principle, retrieve the ocean surface wind vector.

Bettenhausen et al. (2006) develop a nonlinear iterative retrieval algorithm for wind vector retrievals from WindSat data. The algorithm can easily be adapted to use different subsets of measured s , and therefore, it can easily be adapted for use with future polarimetric microwave radiometers. The accuracy of the retrievals is limited by measurement noise and the accuracy of the forward model. It is important to note that minimizing measurement noise in the 3rd and 4th Stokes measurements is important for measuring wind direction with a polarimetric microwave radiometer. The RMS difference between WindSat and QuikSCAT wind speed retrievals is less than 1.0 ms^{-1} for wind speeds below 10 ms^{-1} . The wind direction performance results are primarily wind speed dependent.

Bourassa et al (2019) review the current capability of ocean wind measurements from space. If the estimation of the OWS is reliably estimated from passive microwave observation, at wind speeds below 6 m s^{-1} , the wind direction signal from microwave radiometry is small in all polarizations leading to noisy wind direction estimates. The magnitude of the wind direction signal becomes greater than the noise in the measurements around 4 ms^{-1} . Above 6 ms^{-1} RMS wind speed differences are $\leq 15^\circ$ ($\leq 9^\circ$ above wind speeds $> 10 \text{ ms}^{-1}$) between co-located WindSat and QuickScat measurements and is similar to that derived from scatterometers (*Ricciardulli et al.*, 2012; *Hilburn et al.*, 2016). At high winds (above 10 m s^{-1}) the wind direction signal derived from microwave radiometry is strong in all 4 Stokes parameters.

The application of L-band measurements to measure extreme wind speed over the ocean has been pioneered by *Reul et al.* (2017). Efficient masking of the areas over the oceans, where geophysical parameter retrievals are objectively impossible due to non-transparent atmosphere, is still an important issue for satellite radiometer measurements working at frequency higher or equal than C-band. As demonstrated for Tropical cyclones (*Reul et al.*, 2012b, 2016, 2017, *Meissner et al.*, 2017) L-band radiometer data can provide a direct way to probe surface wind speed in extreme weather events, being almost transparent to the atmosphere. Estimation of the total atmospheric absorption can be also done from the $\sim 10 \text{ GHz}$ channel with high accuracy due to the weak influence of liquid water and especially water vapour (*Zabolotskikh et al.*, 2013). This helps to refine a new filter to considerably reduce masking ocean areas in e.g., AMSR2 radiometer data for severe weather systems such as PL, characterized by high wind speeds and moderate atmospheric absorption. Combining, X- with C- and L-band channels, a methodology can be proposed to jointly retrieve sea surface wind speed and sea surface temperature in PL.

The combined use of both CIMR multi-channel, full Stokes measurements and MetOp-SG(B) active microwave sea surface wind estimates will provide an unprecedented wind speed/vector data set at high spatial and temporal resolution for application in Copernicus.

The combined usage of both CIMR passive and MetOp-SG(B) active microwave sea surface wind estimates will demonstrate the potential of the highest spatial and temporal resolution in the investigation of PL intensity. The ability to better measure warm SST PLs wakes thanks to X/C band combination for SST and L-band wind retrievals will also help in better characterizing feedbacks of PLs to impact sea-ice formation.

6.3.15 Global Water Vapor, Cloud Liquid Water, and Precipitation algorithms

Microwave multichannel radiometers have historically produced measurements of liquid water path and total water vapor column for many years and CIMR will be able to continue records of these parameters (e.g., *Jacob et al.* (2019)).

Water vapor, cloud liquid water, and rain rate are key parameters in the global hydrological cycle, a component of climate change and ocean–atmosphere energy exchange studies. The physical basis for retrieving water vapor and liquid water from microwave radiometer measurements depends on the ability of distinguishing the radiation from Earth’s surface from the radiation emitted from the atmosphere (e.g., *Hilburton and Wentz*, 2008). Regular long-term observations of water vapour, cloud liquid water and precipitation over the open seawater are provided by satellite microwave radiometer instruments (see examples at <http://www.remss.com/measurements/> and related papers from that group). See also *Kazumori* (2012) or *Zabolotskikh and Chapron* (2017), for application with AMSRE and AMSR2. Water vapour changes in the Arctic are poorly described because of a lack of direct observations and large sea ice cover over which atmospheric water retrievals are either complicated or impossible (e.g., *Vihma*, 2014).

The water-vapour and liquid water sensitive channels (mainly 18.7 and 36.5 GHz) of the CIMR mission can provide consistent estimates of the integrated water vapor and liquid water contents of the atmosphere, over ocean, along with the ocean surface parameters, to insure the consistency of all the ocean and atmospheric parameters. The CIMR capability to estimate these atmospheric parameters, along with the surface parameters has been shown, within the optimal estimation framework developed for the retrieval of the SST, OWS, and SSS (*Kilic et al.*, 2018), and tested in the CIMR-APE report. Once the total liquid water content is estimated, it is possible to partition it into cloud and precipitation. This is what is being done operationally in the Remote Sensing System algorithms. See also *Greenwald et al.* (2018) for a recent study about the partitioning of the cloud and rain in passive microwave algorithms.

The physical basis for retrieving precipitation from microwave radiometer measurements depends on distinguishing the radiation from Earth’s surface from the radiation emitted from cloud and precipitation (e.g., *Hilburton and Wentz*, 2008). The total atmospheric liquid water content can be estimated, and the rain rate can be deduced by partitioning the cloud and rain contributions (*Greenwald et al.* 2018).

Precipitation rate retrieval algorithms have been developed in Europe (e.g., *Casella et al.* 2017, *Sanò et al.* 2018) to work with data from the conically scanning Global Precipitation Measurement (GPM) Microwave Imager (GMI) and AMSR-2. CIMR will be able to provide estimates of precipitation rate, although further algorithm development is required, in particular to exploit forward and backwards views together.

6.3.16 Global Land Surface Temperature algorithm

A significant challenge for Land Surface Temperature (LST) when retrieved from Thermal Infrared Radiometer (TIR) measurements is the presence of clouds that preclude the retrieval. With ~60% cloud cover in average over the globe, there is a need for “all weather,” long record, and real-time estimates of land surface temperature (LST) from microwave satellite radiometers. Microwave radiometer data operating in the 6-37 GHz frequency range can overcome this primary difficulty and have been successfully used to retrieve LST. An efficient methodology has been developed to estimate LST at the global scale using microwave radiometer observations between 18 and 37 GHz from SSM/I, SSMIS, AMSR-E or AMSR-2 (*Prigent et al.*, 2016, *Jimenez et al.*, 2017, *Ermida et al.*, 2017). It is based on a neural network scheme, using pre-calculated land surface emissivity atlases at the same frequencies. The method is currently applied for the ESA LST CCI project. The

errors on these LSTs are slightly larger than for their infrared counter parts, but the estimates are available ~90% of the time (compared to less than ~40% of the time with the infrared estimates). Another example of LST retrieval is based on AMSR-E data together with estimates of vegetation in an optimal estimation framework (Zhao *et al.*, 2017). The CIMR mission will be able to estimate LST using a priori estimates of vegetation coverage.

Prigent et al. (2016) describe a simple yet accurate methodology to derive the land surface temperature from microwave conical scanner observations, with the help of pre-calculated land surface microwave emissivity estimates. Very good agreement is obtained for well-controlled stations in vegetated environments (RMSE of ~2.5 K for several stations). The methodology can encounter difficulties under cold conditions due to the large variability of snow and ice surface emissivity that must be addressed for CIMR in the Polar Regions. This algorithm is applied to produce the all weather LST for the ESA LST CCI, to complement the IR LST under cloudy conditions (<https://climate.esa.int/en/odp/#/project/land-surface-temperature>, Jimenez *et al.*)

6.3.17 Landscape freeze/thaw state (FT) algorithm

Seasonal freezing occurs on approximately 51% of the land surface in the Northern Hemisphere, while permafrost areas cover 24% (*Smith and Brown*, 2009). Seasonal Soil freezing affects surface radiation balance and exchange rates of latent heat and carbon with the atmospheric boundary layer (*Skoglund et al.*, 1988, *Zhang*, 2003), and partially control water uptake and thus photosynthesis of vegetation in the spring (*Hollinger et al.* 1999).

Using suitable frequencies, the freeze/thaw (F/T) state of the soil surface layers can be observed directly by means of passive microwave remote sensing. In particular, the low L-band frequency has a theoretical penetration depth in soils beyond 10 cm in certain conditions, yielding an advantage over higher frequencies. Consequently, geophysical products on soil F/T have been developed for the currently operational L-band missions, i.e., the Soil Moisture Active Passive (SMAP) and SMOS missions (*Derksen et al.*, 2017; *Rautiainen et al.*, 2016). However, frequencies up to Ka band have been used to derive products on total landscape F/T (*Kim et al.*, 2011), applying in situ measured air temperatures for tuning of the retrieval algorithm.

CIMR promises to provide a unique opportunity for land surface F/T observations, considering the range of relevant frequencies on the same platform. This will enable a multispectral approach to F/T detection, also considering the presence and state (dry or wet) of seasonal snow cover. The CIMR lower frequencies (1.41, 6.925 and 10.65 GHz) provide increasing penetration into both standing vegetation and the soil surface, providing information on surface vegetation and soil F/T at different depths, while higher frequencies (18.7 and 36.5 GHz) are sensitive to freezing processes in the immediate ground surface and standing vegetation (forest canopy). The higher frequencies are also suitable for detection of seasonal snow cover.

Together, information on both snow cover and soil F/T state are highly relevant for simulating processes of the soil active layer in permafrost regions. While information on the soil F/T state can potentially be assimilated in land surface models (e.g., *Gao et al.*, 2020), snow cover has a large influence on permafrost active layer evolution due to its insulating properties (e.g., *Hrbáček et al.*, 2021). CIMR has the potential to provide information on both by means of a combining CIMR snow and soil FT product over permafrost regions.

Considering retrievals over heterogeneous landscapes such as the boreal forest region, it will be necessary to further improve existing forward modelling tools of microwave signatures of soil, snow, vegetation, wetlands, and freshwater bodies (lakes and rivers). In particular, recent research points to previously disregarded dynamics of forest canopy transmissivity in winter (*Li et al.*, 2019; *Schwank et al.*, 2020), affecting all surface parameter retrievals from passive microwave (e.g., *Li et al.*, 2020). Recent advances in simulation of microwave propagation in snow (*Picard et al.*, 2018)

should be fully exploited in the forward model environment. Advanced forward modelling of CIMR observations also facilitates the development and implementation of techniques to assimilate CIMR data to permafrost models.

6.3.18 Multi-frequency Microwave Vegetation Indicators (MMVI) algorithm

For CIMR terrestrial variables algorithms could be directly inherited from previous sensors operating either at L-band, or at C and X-bands. There are soil Moisture (SM) and Vegetation Optical Depth (VOD) products available from these three bands (e.g., *Baur et al.*, 2019; *De Jeu and Owe*, 2003; *Fernandez-Moran et al.*, 2017). CIMR will leverage an approach capitalizing on the inherent multi-channel and multi-resolution instrument characteristics to go beyond single-channel products. SM differences in sensing depth across frequencies is minimal (1 to 5 cm, with higher frequencies being insensitive under presence of low vegetation).

CIMR measurement characteristics in terms of simultaneous multi-channel microwave measurements enables a unique set of land surface products and applications over land. These characteristics go beyond what previous microwave radiometers (e.g., AMSR series, SMAP and SMOS) provide, and therefore allow unique approaches to inversion of brightness temperatures. Across CIMR channels, the L-band frequencies have the highest sensitivity to soil moisture. Measurements at C and X-bands are also sensitive to soil moisture, yet their attenuation by vegetation is higher and they have a shallower sensing depth (of ~1 cm vs. ~5 cm). To meet requirements for global soil moisture estimation, it is essential to develop advanced algorithms exploiting the CIMR L-, C-, and X-band multi-frequency ensemble for a better characterization of vegetation properties, electromagnetic soil surface roughness and soil-plant interactions in the soil moisture inversion process. Information on effective temperature and terrestrial surface water extent is required in the soil moisture retrieval and can be obtained from CIMR higher frequencies (Ku and Ka bands).

Canopy microwave parameters such as the Vegetation Optical Depth (VOD) parameter is very different when estimated at L-band (sensitive to trunks and branches) or at C and X-band (sensitive to upper canopy and mostly leaves). CIMR Multi-frequency Microwave Vegetation Indicators (MMVI) is a more appropriate approach. There are very few studies directly exploring retrievals using the three frequencies, and further work is required to define the vegetation absorption and scattering properties that can be derived from CIMR. In addition, spatial resolution differences are particularly important for land and CLMS (e.g., some users may prefer C-band retrievals at 15-km compared to L-band retrievals at 60 km). The detailed application of multi-frequency multi-resolution retrievals for measuring moisture status in soil and plant components must be further developed for CIMR.

CIMR will generate Multi-frequency Microwave Vegetation Indices (MMVI) that relate mechanisms of energy loss (scattering and absorption) to vegetation properties such as biomass (dry) and water content (e.g., *Baur et al.* 2019, *Konings et al.* 2016 and *Momen et al.* 2017).

The potential of the CIMR frequencies for vegetation parameter estimation has been estimated, and the synergies between the CIMR frequencies has been quantified (*Prigent and Jimenez*, 2021). The study shows that the CIMR frequency combination can provide improved Above Ground Biomass (AGB) estimate, as compared to L-band alone, while also providing additional vegetation related to the foliage photosynthesis activity (with NDVI as a proxy).

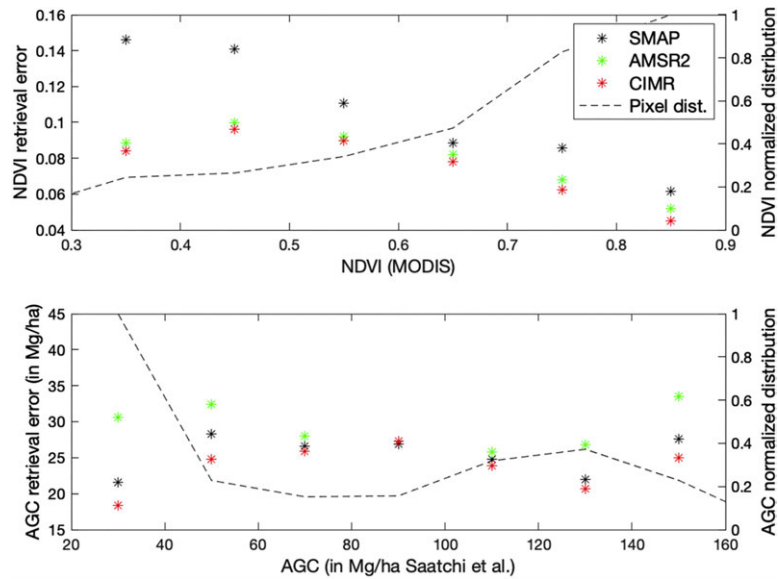
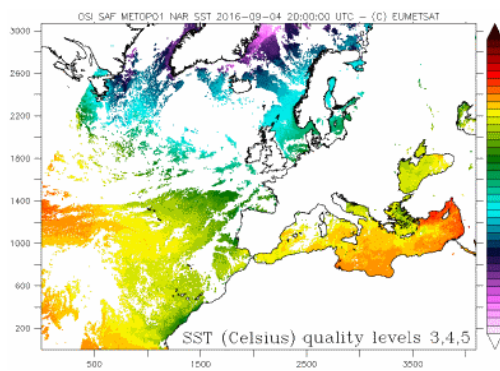


Figure MRD-6.3.18-1. Bottom: Above Ground Carbon (AGC), as a function of AGC, for SMAP, AMSR2, and CIMR frequency combinations. The normalized AGC distribution is also indicated in dashed line (see left axis). Top: Same for the NDVI. From Prigent and Jimenez (2021).

6.4 Example European Operational Users

6.4.1 EUMETSAT OSI-SAF:

Utilising specialist expertise from the EUMETSAT Member States, Satellite Application Facilities (SAFs) are dedicated centres of excellence for processing satellite data. They form an integral part of the distributed EUMETSAT Application Ground Segment. SAFs develop, generate, and distribute operational satellite products including long-term data records.



SAF products are designed to serve operational users: primarily Meteorological Services and other operational services in the member states and international organisations (Copernicus, ECMWF). The OSI SAF develops, processes, and distributes, in near real-time, products related to key parameters of the ocean-atmosphere interface. The OSI SAF team focuses on Sea Surface Temperature (SST) and Sea Ice Surface Temperature (IST), scatterometer winds (and soon microwave winds from MetOp-SG(B) MWI), radiative fluxes: Solar Surface Irradiance (SSI) and Downward

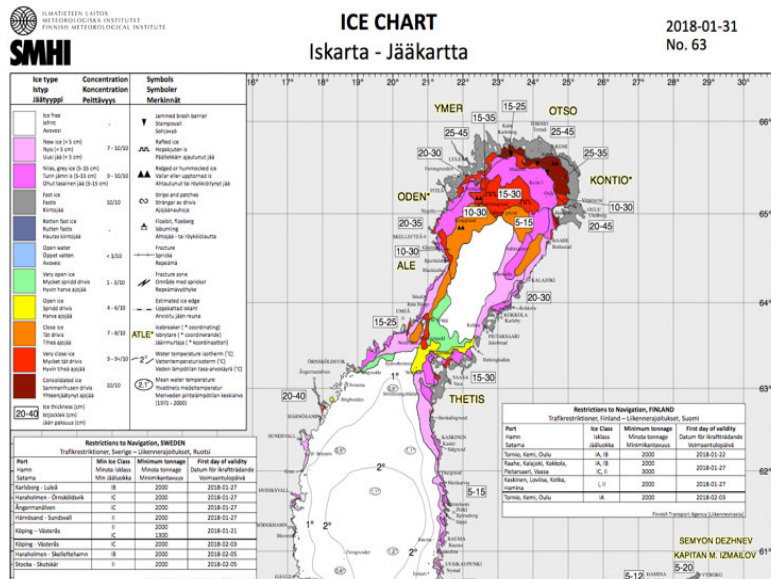
Longwave Irradiance (DLI), sea ice concentration, edge, type, emissivity, drift. See also <http://www.osi-saf.org>.

6.4.2 FMI – Finnish Meteorological Institute

The Finnish Meteorological Institute (FMI) is a research and service agency under the Ministry of Transport and Communications.

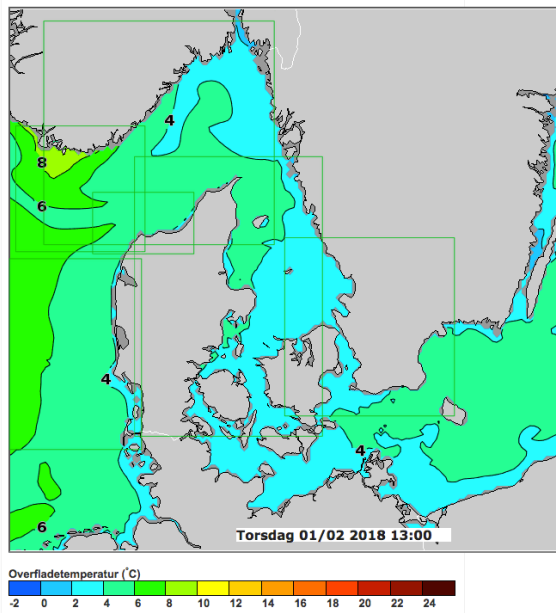
The main objective of the Finnish Meteorological Institute is to provide the Finnish nation with the best possible information about the atmosphere above and around Finland, for ensuring public safety relating to atmospheric and airborne hazards and for satisfying requirements for specialized meteorological products. The Finnish Meteorological Institute offers various services on the Baltic Sea and other seas and oceans also.

The services include real time observations, forecasts, and expert analyses. The most common services are the ice service, wave, and sea level services. The detailed Finish Ice Report including ice charts for the whole Baltic Sea is published in the autumn twice a week and daily when the amount of ice increases until ice break-up in spring. It represents the current ice situation and traffic restrictions in the Baltic Sea. More info at <http://en.ilmatieteenlaitos.fi/ice-conditions>.



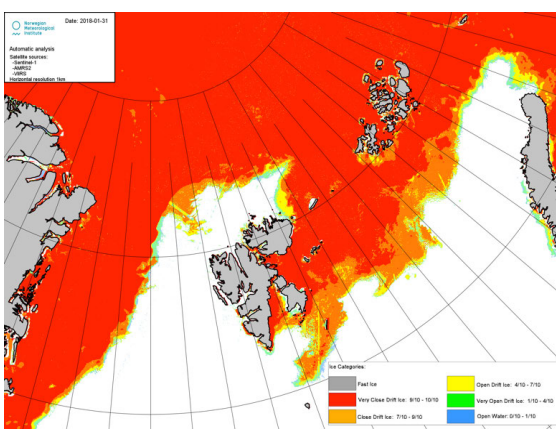
6.4.3 DMI- Denmark Meteorological Institute

DMI provides meteorological services in the Commonwealth of the Realm of Denmark, the Faroe Islands, Greenland, and surrounding waters and airspace. Meteorological services include forecasting and warnings and monitoring of weather, climate, and related environmental conditions in the atmosphere, on land and at sea. Purpose of all activities is to safeguard human life and property. DMI's many activities also act as background knowledge in terms of planning and decision-making in economic and environment sectors - especially within transport and industry businesses. DMI collects and processes meteorological, climatological, and oceanographic measurements/observations, and measures, collects and compiles related geophysical parameters throughout the Realm. Conducting research and development within its area of expertise, DMI ensures efficient operations and state-of-the-art quality in all productions while monitoring and conducting research on global warming and the stratospheric ozone balance.



The DMI's ocean forecast products for Danish waters include several parameters visualised as strength fields and direction fields. Ice maps are produced at DMI/Lyngbyvej in Denmark in cooperation with the ice monitoring station in Greenland based on satellite information and observations collected locally.

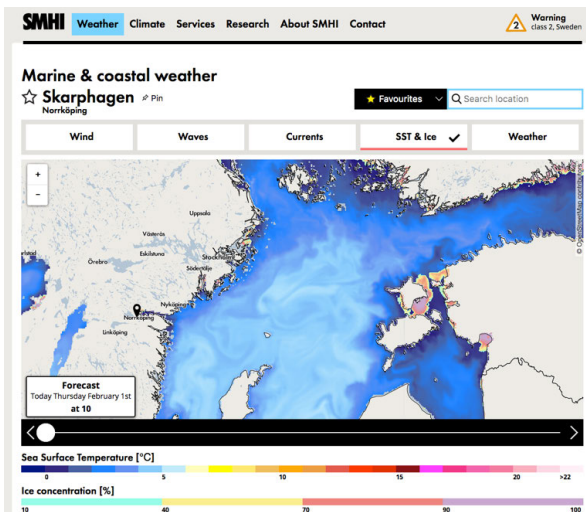
6.4.4 MET Norway – Norwegian Meteorological Institute



The Norwegian Meteorological Institute forecasts weather monitors the climate and conducts research. Since the institute was established, Norwegian meteorologists have figured prominently in the development of the discipline. The Norwegian Meteorological Institute is today a leading international centre of expertise. The forecasting service in the High North is extensive and ranges from forecasting the extent and thickness of the ice, to warning of icing on vessels. Since 2015 the Norwegian Meteorological Institute together with the Nansen Environmental and Remote Sensing Centre and the Institute of Marine Research, have had the responsibility of monitoring and measuring the ocean and sea ice conditions in the High North and the Arctic, including in the CMEMS Arctic MFC. See also <http://cryo.met.no>

MET Norway leads the high-latitude node of the EUMETSAT OSI SAF (see Sec. 6.4.2) and the Sea Ice Thematic Assembly Centre (SI TAC) of the CMEMS (see Sec. 6.4.1). MET Norway is also involved in the Copernicus Climate Change project (C3S) and the Copernicus Atmosphere Monitoring Service (CAMS).

6.4.5 SMHI – Swedish Meteorological and Hydrological Institute



SMHI, the Swedish Meteorological and Hydrological Institute, is an expert agency under the Ministry of the Environment and Energy. Through unique expertise in meteorology, hydrology, oceanography, and climatology, SMHI contributes towards greater public welfare, increased safety and a sustainable society. More info at <https://www.smhi.se/en/about-smhi>

MHI provides daily forecasts to the public and societal functions and issues warnings when faced with severe weather and water events. SMHI also offers products and services that function as vital support in the decision-making of, for example, Swedish authorities, organisations, and municipalities. SMHI produce operational sea

surface temperature and sea ice concentration services at <https://www.smhi.se/en/weather/sweden-weather/marine-coastal-weather/q/Skarphagen/Norrk%C3%B6ping/2678060#ws=wpt-a,proxy=wpt-a,parameter=ice>

6.4.6 MetOffice – United Kingdom Meteorological Office

The MetOffice provides global services for weather, operational oceanography, and climate. It provides weather and climate-related services to the Armed Forces, government departments, the public, civil aviation, shipping, industry, agriculture, and commerce. The MetOffice runs an operational oceanography system and develops operational short-range forecast configurations of community models driven by atmospheric forcing from the Unified Model, and where appropriate using marine data assimilation (<https://www.metoffice.gov.uk/weather/specialist-forecasts/coast-and-sea>). Applied research supports users of the models and develops decision tools for marine operations based on model outputs. The MetOffice is a core contributor to the CMES system maintaining and operating a global CMEMS ocean forecasting system model and a number of regional models for CMEMS. Both SST and SIC are fundamental variables used in all aspects of its operations. See <https://www.metoffice.gov.uk/>.

6.4.7 ECMWF – European Centre for Medium Range Weather Forecasting

ECMWF is an independent intergovernmental organisation founded in 1975 and supported by 34 states. It produces global numerical weather forecasts for users worldwide. ECMWF produces operational ensemble-based analyses and predictions that describe the range of possible scenarios and their likelihood of occurrence. ECMWF's forecasts cover time frames ranging from medium-range, to monthly and seasonal, and up to a year ahead. ECMWF provides current forecasts, climate reanalyses, and specific datasets. These are available to the Member and Co-operating States, as well as through licensing to the World Meteorological Organization (WMO) and the academic and commercial sectors. All forecast systems at ECMWF are coupled to an ocean model. The ensemble and seasonal forecast systems use a coupled atmosphere-ocean model, which includes a simulation of the general circulation of the ocean and the associated coupled feedback processes that exist.

The current operational ensemble forecast systems model sea ice dynamically using the LIM2 model within NEMO ocean model to represent the dynamic and thermodynamic evolution of sea ice within the coupled forecast system.

ECMWF uses the community ocean model NEMO (Nucleus for European Modelling of the Ocean) as part of the IFS. The NEMO model provides the dynamic ocean model used in the ensemble prediction system and the seasonal forecast system (S4). The ensemble prediction system of the medium and monthly range forecasts runs the ocean model at 0.25-degree horizontal resolution with 75 levels in the vertical and is initialised with the NEMOVAR (3D variational assimilation system) OCEAN5. The seasonal forecast system (S4) uses a 1-degree horizontal resolution with 42 levels in the vertical and is initialised with NEMOVAR OCEAN4. Since 2013 the ensemble forecasts have coupled the atmosphere-wave-ocean model from the start of the forecast. This is important to allow capturing the two-way feedback between the atmosphere and the sea surface temperatures, for example when a tropical cyclone is slow moving it can cool the sea surface. Since November 2014 the ensemble forecasts have been run with 0.25-degree horizontal resolution with the sea ice model active. Both sea ice and SST data sets are required for use in ECMWF operations.

ECMWF uses the Tiled ECMWF Scheme for Surface Exchanges over Land incorporating land surface hydrology (HTESSEL) as part of the IFS. HTESSEL accounts for snow, with snow water equivalent, snow density and snow albedo being the model prognostic variables. It represents soil water and heat transfer based on using four-layer model (0-7cm, 7-28cm, 28-100cm, 100-289cm) and solving the Richards equation. Sub grid scale land cover and snow conditions allows to represent up to 8 tiles per model grid-box. ECMWF currently analyses in operations soil moisture and temperature, and snow water equivalent, density, and temperature. SWE is of great interest for ECMWF coupled land-atmosphere data assimilation. See <https://www.ecmwf.int/>.

6.4.8 Vandersat (NL)

Vandersat (<https://vandersat.com/>) is an example Copernicus downstream user of microwave satellite products with a mission to build the best satellite products to solve the global water and food crisis. It specializes in soil moisture that influences hydrological and agricultural processes, runoff generation, drought development and many other processes. It also impacts on the climate system through atmospheric feedbacks. Soil moisture is a source of water for evapotranspiration over the continents and is involved in both the water and the energy cycle and is a recognised Essential Climate Variable (ECV). Vandersat has over 900 users distributed across the world serving operational solutions to the insurance industry based on turnkey indices tuned to specific regions and applications, agriculture (crop monitoring, soil moisture, land surface temperature), water resources (drought monitoring, hydropower) and science.

CIMR will provide a unique data set of low-frequency high spatial resolution microwave radiometer measurements in support of downstream users such as Vandersat. Importantly, continuity of L-band measurements together with full Stokes information at L1b are a fundamental input to the work of Vandersat and other downstream users.

7 SYNERGIES AND INTERNATIONAL CONTEXT

A summary of historical and contemporary microwave imaging radiometers is provided in Table 7-2, which is derived from the extensive information provided within the World Meteorological Organisation (WMO Observing Systems Capability analysis and Review Tool (OSCAR, <https://www.wmo-sat.info/oscar/>). It is clear from this Table that there is a long heritage of missions carrying a variety of microwave radiometer channels that are suitable for Polar sea ice and ocean monitoring applications.

Table 7-2. Summary of Microwave imaging radiometer missions (from the World Meteorological Organisation Observing systems Capability analysis and Review Tool (OSCAR, <https://www.wmo-sat.info/oscar/>).

Acronym	Full name	Channels GHz (Polarisations: H = horizontal, V = vertical, P = + 45°, M = - 45°, L = left-hand circular, R = right- hand circular)	Space Agency	Satellites	Usage from	Usage to
SHF	MW Radiometer	7.5 (V&H), 19.4 (V&H), 22.22 (V&H) and 37.5 (V&H)	Roscosmos	Meteor-P1 Meteor-P2 Meteor-P3 Meteor-P6	1974	1983
ESMR	Electrically Scanning Microwave Radiometer	19.0 (H) 37.0 (V&H)	NASA	NIMBUS 5 ESMR 19H planar antenna NIMBUS 6 ESMR 37 H&V conical scan	1972/ 1975	1977/ 1983
SMMR	Scanning Multichannel Microwave Radiometer)	6.6 (V&H), 10.7 (V&H) 18 (V&H) 21 (V&H) 37.0 (V&H)	NASA	Nimbus-7 SeaSat	1978	1987
SSM/I	Special Sensor Microwave - Imager	19.35 (V&H), 22.235 (V), 37.0 (V&H), 85.5 (V&H)	DoD	DMSP-F08 DMSP-F10 DMSP-F11 DMSP-F12 DMSP-F13 DMSP-F14 DMSP-F15	1987	2017
TMI	TRMM Microwave Imager	10.65 (V&H), 19.35 (V&H), 21.3 (V), 37.0 (V&H), 85.5 (V&H)	NASA	TRMM	1997	2015
Delta-2D	Scanning Microwave Radiometer	6.9 (V&H), 13.0 (V&H),	Roscosmos	Okean-O-1	1999	2000

		22.3 (V&H), 37.5 (V&H).				
MSMR	Multi-frequency Scanning Microwave Radiometer	6.6 (V&H), 10.65 (V&H), 18.0 (V&H), 21.0 (V&H).	ISRO	OceanSat-1 (IRS-P4)	1999	2010
MTVZA	Imaging/Sounding Microwave Radiometer	20-frequency, band 18.7 - 183	Roscosmos	Meteor-3M	2001	2006
AMSR	Advanced Microwave Scanning Radiometer	6.925 (V&H), 10.65 (V&H), 23.8 (V&H), 36.5 V&H, 50.2 (V&H), 53.8 (V&H), 89 (V&H)	JAXA	ADEOS-2	2002	2003
AMSR-E	Advanced Microwave Scanning Radiometer for EOS	6.925 (V&H), 10.65 (V&H), 18.7 (V&H), 23.8 (V&H), 36.5 (V&H), 89.0 (V&H).	JAXA	Aqua	2002	2011
SSMIS	Special Sensor Microwave - Imager/Sounder	21 frequencies, 19.35 – 183.	DoD	DMSP-F16 DMSP-F17 DMSP-F18 DMSP-F19 DMSP-S20	2003	2025
WindSat	WindSat	6.8 (V&H), 10.7 (V, H, P, M, L, R), 18.7 V, H, P, M, L, R, 23.8 (V&H), 37.0 V, H, P, M, L, R)	DoD	Coriolis	2003	2020
MTVZA-OK (MW)	Combined Microwave-Optical Imaging/Sounding Radiometer (MW component)	22-frequency 6.9 to 183 GHz various polarisation	NSAU/ Roscosmos / Ros-HydroMet	SICH-1M	2004	2006
MWRI	Micro-Wave Radiation Imager	10.65 (V&H), 18.7 V&H), 23.8 (V&H), 36.5 (V&H), 89.0 (V&H).	CMA	FY-3A FY-3B FY-3C FY-3D FY-3F FY-3G	2008	2026

MTVZA-GY	Imaging/Sounding Microwave Radiometer - improved	21-frequency 10.6 - 183 GHz V&H polarisations	Roscosmos	Meteor-M N1 Meteor-M N2 Meteor-M N2-1 Meteor-M N2-2 Meteor-M N2-3 Meteor-M N2-4 Meteor-M N2-5 Meteor-M N2-6	2009	2028
MIRAS	Microwave Imaging Radiometer using Aperture Synthesis	1.4315 (V&H)	ESA	SMOS	2009	TBD On-orbit at present
MADRAS	Microwave Analysis & Detection of Rain & Atmospheric Structures	18.7 (V&H), 23.8 (V), 36.5 (V&H), 89.0 (V&H), 157.0 (V&H)	ISRO	Megha-Tropiques	2011	2017
MWI	Microwave Radiometer	6.6 (V&H), 10.7 (V&H), 18.7 (V&H), 23.8 (V), 37.0 (V&H).	NSOAS	HY-2A	2011	2016
Aquarius	Pushbroom L-band sensor	1.4 full polarisation	CONAE, INPE, BASA	Aquarius	2011	2015
AMSR-2	Advanced Microwave Scanning Radiometer-2	6.925 (V&H), 7.3 (V&H), 10.65 (V&H), 18.7 (V&H), 23.8 (V&H), 36.5 (V&H), 89.0 (V&H).	JAXA	GCOM-W1	2012	2025
GMI	GPM Microwave Imager	10.65 (V&H), 18.7 (V&H), 23.8 (V), 36.5 (V&H), 89.0 (V&H), 166.0 (V&H), 183.3 (V)	NASA	GPM Core Observatory	2014	2022+
SMAP	Soil Moisture Active-Passive radiometer	1.4 full polarisation	NASA	SMAP	2015	2022+

SMOS	Soil Moisture and Ocean Salinity	1.4 H and V	ESA	SMOS	2009	2022+
MWI	Microwave Radiometer	6.6 (V&H), 10.7 (V&H), 18.7 (V&H), 23.8 (V), 37.0 (V&H).	NSOAS	HY-2B	2018	2023
COWVR	Compact Ocean Wind Vector Radiometer	18.7 (Full), 23.8 (Full), 33.9 (Full).	NASA, US DoD	ORS-6	2021	2024+
AMSR-3	Conical scanning microwave radiometer	6.925 (V&H), 7.3 (V&H), 10.65 (V&H), 18.7 (V&H), 23.8 (V&H), 36.5 (V&H), 89.0 (V&H), 165.5 (V), 183±3 (V), 183±7 (V).	JAXA	GOSAT-3	2023	2030
MWRI	Conical scanning microwave radiometer	10.65 (V&H), 18.7 (V&H), 23.8 (V&H), 36.5 (V&H), 89.0 (V&H).	CMA, NRSCC	FY-3F FY-3G	2023+ >2024	2029 >2030
WSF-MWI	Weather Satellite Follow-On Microwave Imager	10.85 (Full), 18.85 (Full), 36.5 (Full), 23.8 (V), 89.0 (V&H)	US DoD	WSF-M1 WSF-M2	2024	2035
MWI	Conical scanning microwave radiometer	18.7 (V&H), 23.8 (V&H), 31.4 (V&H), 50.3 (V&H), 52.61 (V&H), 53.24 (V&H), 53.75 (V&H), 89.0 (V&H), 118.75 (V), 166.9 (V), 183.31 (V).	ESA/ EUMETSAT	MetOp-SG (B1, B2 and B3)	2025	2046
FPIR	Full-polarized Interferometric synthetic aperture microwave radiometer	1.4135, 2.695, 6.9 GHz all full polarisation	CAS	WCOM	?	?

PMI	Passive Microwave Imager	6.8 (V&H), 10.7 (Full), 18.7 (Full), 23.8 (V&H), 37.0 (Full), 89.0 (V&H)	CAS	WCOM	?	?
-----	--------------------------	---	-----	------	---	---

Table 7.2 reveals that more channels, with multiple polarisations, are provided toward the contemporary era of satellite imaging microwave radiometers. However, the provision of lower frequency channels (<18.7 GHz) is sporadic and variable likely due to the challenges of finding a single antenna technology that can accommodate the wide range of frequencies at an affordable mass with an appropriate instantaneous field of view (IFOV). In terms of application in the Polar-regions and global oceans, the limited use of low frequency channels is largely due to the poor spatial resolution of these channels rather than the information content (see the SIC and SST discussions in sections above).

In terms of continuity, bands above 10.65 GHz are well provisioned by the international constellation (missions from Russia, China USA, and Europe). The Chinese National Ocean Satellite Application Centre (NSOAS) HY2 series of satellites carry a Microwave Imager (MWI) with 6.6 (V&H), 10.7 (V&H), 18.7 (V&H), 23.8 (V&H) and 37.0 V&H) channels but with a very large instantaneous field of view (6.6 GHz is 80 x 120 km). The WMO OSCAR database suggests that there are no plans to continue the HY- series MWI instrument beyond HY-2B (i.e. loss of capability in ~2023).

The future European Microwave Imager (MWI) on the MetOp-SG satellites developed for the EPS-SG EUMETSAT programme will eventually secure continuation of the United States Special Sensor Microwave Imager (SSM/I) series of coarse resolution radiometry for climate monitoring but will not fulfil the requirements for medium resolution (~10 km) sea ice concentration which is needed in the near future by operational ice/ocean models [AD-2]. The MWI instrument on MetOp-SG does not provide access to frequencies below 18.7 GHz and therefore cannot provide continuity of AMSR-2 measurements of SST alone [AD-2], nor can it provide an equivalent spatial resolution in other channels.

The CMA/NRSCC MWRI instrument does carry a 10.65 GHz channel to~2026 (FY-3F and FY-3G) but this is insufficient for SST and SIC monitoring in the Polar regions and Adjacent Seas as the spatial resolution is too large (the antenna is ~1.8m in diameter) and the fact that a poor sensitivity to SST at water temperatures less than ~290 K (e.g., Gentemann *et al.*, 2010) means that a useful SST cannot be retrieved.

Extensive capability is offered by the WindSat, SMOS and SMAP missions. WindSat allows a retrieval of ocean vector winds over the ocean using a fully polarimetric capability (but there is no follow-on mission) and the L-band missions retrieve sea surface salinity, sea ice thickness and high wind speeds over the ocean. But beyond SMOS and SMAP there are no microwave radiometry imaging missions planned that will provide access to the 1.4 GHz frequency delivering thin sea ice thickness and sea surface salinity (e.g., Olmedo *et al.*, 2017) in the Polar Regions. Copernicus services (i.e., CMEMS in the polar ocean case) cannot solely rely on non-European contributing missions to maintain the current quality of its service [AD-3].

The JAXA AMSR-2 instrument is currently active although it is not clear how long the instrument will maintain its current performance. The rotating joint for the antenna scan mechanism of the predecessor instrument (AMSR-E) degraded within ~9.5 years of launch. The design lifetime of AMSR2 was 5 years and clearly a replacement is urgently needed.

To continue and improve current capability of water cycle/climate monitoring, JAXA is now developing the Global Observing SATellite for Greenhouse gases and Water cycle (GOSAT-GW)

including an Advanced Microwave Scanning Radiometer 3 (AMSR3). It is the successor of AMSR2 and is scheduled to be launched in 2023. Orbit specification of the GOSAT-GW satellite was decided to satisfy requirements from both AMSR3 and TANSO-3 missions. Ascending orbit will be during daytime (same as GCOM-W), orbit altitude is same as GOSAT, and local sun time is same as GCOM-W. Orbiting number of one recurrent day is 44 and smaller compared to that of GCOM-W (233), so there are some differences in observation frequency. Unlike AMSR2, AMSR3 cannot cover global area within 2-day and small missing areas are remained in tropics. Observation frequency of AMSR3 is not homogeneous for every longitude due to fewer orbiting number compared to AMSR2, and there are fixed areas less than 1 observation/day.

AMSR3 has 8-frequency with 21-channel. Sensor characteristics and channel sets, including centre frequency, bandwidth, polarization, instantaneous field of view (FOV) of AMSR3 are indicated in Table 7-3. The basic concept is almost equivalent to that of AMSR2; a conical scanning system with 2-m diameter offset parabolic antenna; feed horn cluster to realize multi-frequency observation; external calibration with two temperature standards; and total-power radiometer systems. Due to lower orbit altitude compared to the GCOM-W satellite, FOV of each channel is slightly smaller and swath width of the sensor is slightly narrower.

Table 7-3. JAXA AMSR-3 channel characteristics.

Center frequency [GHz]	Polarization	Band width [MHz]	NEDT (1σ)	Beam width (field of view)
6.925 / 7.3	H/V	350	< 0.34 K	1.8° (34 km x 58 km)
10.25	H/V	500	< 0.34 K	1.2° (22 km x 39 km)
10.65	H/V	100	< 0.70 K	1.2° (22 km x 39 km)
18.7	H/V	200	< 0.70 K	0.65° (12 km x 21 km)
23.8	H/V	400	< 0.60 K	0.75° (14 km x 24 km)
36.42	H/V	840	< 0.70 K (TBD)	0.35° (7 km x 11 km)
89.0 A/B	H/V	3000	< 1.20 K	0.15° (3 km x 5 km)
165.5	V	4000	< 1.50 K	0.30° (4 km×9 km)
183.31±7	V	2000×2	< 1.50 K	0.27° (4 km×8 km)
183.31±3	V	2000×2	< 1.50 K	0.27° (4 km×8 km)

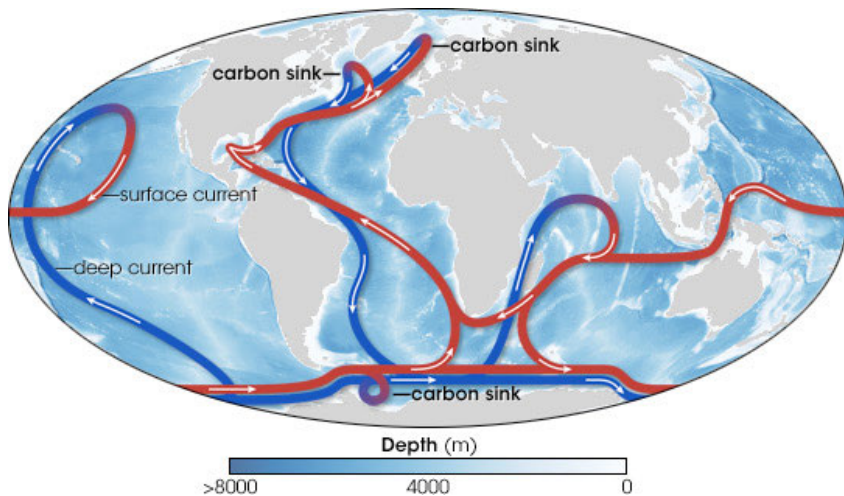
* Bold indicates changes from AMSR2.

Table 7-3 shows that AMSR3 will not fulfil the joint requirements of resolution and accuracy for polar SIC and SST ([AD-1]).

There is a potential loss of capability of 1.4 GHz bands in the mid 2020's and no sensors are capable of meeting the requirements set out in [AD-1 to AD-5]. Without acting, the long-term continuity of microwave space observations at these frequencies will be broken by a data gap in European and non-European satellite missions that provide a unique capability for SIC, SST, thin-SIT and other sea ice parameters in non-precipitating atmospheric conditions is required by Copernicus Services [AD-1 to AD-5].

Complementarity of the CIMR mission in the Arctic under the Carbon and hydrologic cycles is very strong. The CIMR mission is relevant considering the complex interplay between the hydrological cycle and the carbon cycle in the atmosphere and in the ocean. The presence of sea-ice can prevent CO₂-rich water from releasing its CO₂ to the atmosphere (Roberts *et al.* 2016). Moreover, the atmospheric CO₂ uptake into the ocean depends not only from its partial pressure, but also on the physical conditions of the air/sea interface, namely sea surface temperature, sea state (surface roughness) and ocean circulation. As a further example a simplified representation of the global

thermohaline circulation is shown in the figure below. Near-surface currents (red lines) flow towards three main deep-water formation regions at high latitudes — which act as atmospheric carbon sinks — (northern North Atlantic, the Ross Sea and the Weddell Sea) and recirculate at depth (deep currents shown in blue). This implies that there are several feedback loops between the hydrologic and carbon cycles, e.g., driven by the sea ice formation and melting, and sea surface temperature in the polar regions.



MRD-7.1. Global thermohaline circulation and carbon sinks by Robert Simmon, adapted from the *IPCC 2001* and *Rahmstorf (2002)*. CIMR will provide key information on the deep water formation through the freezing of seawater that releases dense cold brine water that sinks to the ocean floor driving the haline part of the thermohaline circulation. CIMR will monitor sea ice dynamics, the sea surface temperature (a surface expression of the thermos- part of the thermohaline circulation), and wind speed/vectors that force surface ocean circulation.

8 REFERENCES

8.1 Applicable Documents

Label	Identifier	Title	Published
[AD-1]	PEG-I	User requirements for a Copernicus polar mission, Step 1 report, Polar expert group.	12th June 2017
[AD-2]	PEG-II	Polar expert group, Phase 2 report on Users' requirements.	31st July 2017
[AD-3]	CMEMS-1	Copernicus Marine Environmental Monitoring System (CMEMS) requirements for the Evolution of the Copernicus Satellite Component	21th February 2017
[AD-4]	CLIMATE-1	Climate Change User Requirements Document Nextspace-SC3 Final v4	31st July 2017
[AD-5]	PEG-III	User Requirements for a Copernicus Polar Observing System–Phase 3 Report - Towards Operational Products and Services.	November 2021.

8.2 Reference Documents

Aaboe, S., Breivik, L.-A., Eastwood, S. (2016) Global Sea Ice Edge and Type Validation Report, v2.1, http://osisaf.met.no/docs/osisaf_cdop2_ss2_valrep_sea-ice-edge-type_v2p1.pdf

Aaboe, S., Breivik, L.-A., Sørensen, A., Eastwood, S. and Lavergne, T. (2018) Global Sea Ice Edge and Type Product User's Manual, v2.3, http://osisaf.met.no/docs/osisaf_cdop3_ss2_pum_sea-ice-edge-type_v2p3.pdf

Aires, F., Prigent, C., and Rossow, W.B., (2005), Soil moisture at a global scale. II – Global statistical relationships. *Journal of Geophysical Research*, Vol. 110, No. D11, D11103, 10.1029/2004JD005094.

Aires, F., Prigent, C., Rossow, W. B., & Rothstein, M. (2001). A new neural network approach including first guess for retrieval of atmospheric water vapor, cloud liquid water path, surface temperature, and emissivities over land from satellite microwave observations. *Journal of Geophysical Research: Atmospheres*, 106(D14), 14887-14907.

Albergel, C. C. Rüdiger, T. Pellarin, J. C. Calvet, N. Fritz, F. Froissard, D. Suquia, A. Petitpa, B. Piguet, E. Martin, (2008), From near-surface to root-zone soil moisture using an exponential filter: an assessment of the method based on in-situ observations and model simulations. *Hydrol. Earth Syst. Sci.*, vol.12, 1323-1337.

Andela, N., Liu, Y.Y., van Dijk, A.I.J.M., de Jeu, R.A.M., & McVicar, T.R. (2013). Global changes in dryland vegetation dynamics (1988–2008) assessed by satellite remote sensing: comparing a new passive microwave vegetation density record with reflective greenness data. *Biogeosciences*, 10, 6657-6676

Andersen, S., R. Tonboe, L. Kaleschke, G. Heygster, and L. T. Pedersen (2006), Intercomparison of passive microwave sea ice concentration retrievals over the high-concentration Arctic sea ice, *J. Geophys. Res.*, 112, C08004, doi:10.1029/2006JC003543.

- Andrews, M. J., J. T. Johnson, M. Brogioni, G.i Macelloni, and K. C. Jezek, (2002). Properties of the 500–2000-MHz RFI Environment Observed in High-Latitude Airborne Radiometer Measurements, IEEE Transactions on Geoscience and Remote Sensing, 60, 5301311-.
- Ashcroft, P. and F. J. Wentz, (2000), Algorithm Theoretical Basis Document for AMSR-E Level2A Algorithm. Revised Nov. 3, 2000, Santa Rosa, CA, Remote Sensing Systems, available from https://nsidc.org/sites/nsidc.org/files/technical-references/amsr_atbd_level2a.pdf
- Backus GE, Gilbert JF, (1967), Numerical applications of a formalism for geophysical inverse problems. Geophys. J. R. Astron. Soc. Jul; 1967 13(1–3):247–276.
- Backus GE, Gilbert JF, (1968), Resolving power of gross Earth data. Geophys. J. R. Astron. Soc. Oct; 1968 16(2):169–205.
- Balling, J. E., S. S. Kristensen, S. S. Sobjaerg and N. Skou, (2011). Surveys and Analysis of RFI in Preparation for SMOS: Results from Airborne Campaigns and First Impressions from Satellite Data, in IEEE Transactions on Geoscience and Remote Sensing, vol. 49, no. 12, pp. 4821-4831, doi: 10.1109/TGRS.2011.2172796.
- Bauer, P., and R. Bennartz, (1998), Tropical Rainfall Measuring Mission microwave imaging capabilities for the observation of rain clouds, Radio Sci., 33(2), 335–349, doi:10.1029/97RS02049.
- Baur, M.J., Jagdhuber, T., Feldman, A.F., Akbar, R., Entekhabi, D., (2019), Estimation of relative canopy absorption and scattering at L-, C- and X-bands, Remote Sensing of Environment, Volume 233, 111384, <https://doi.org/10.1016/j.rse.2019.111384>.
- Bell, S., (1999), Measurement Good Practice Guide No. 11 (Issue 2) A Beginner's Guide to Uncertainty of Measurement, National Physical Laboratory, UK, available from http://publications.npl.co.uk/npl_web/pdf/mgpg11.pdf
- Bender, M. A., T. P. Marchok, C. R. Sampson, J.A. Knaff, and M. J. Morin, 2017: Impact of Storm Size on Prediction of Storm Track and Intensity Using the 2016 Operational GFDL Hurricane Model. Wea. Forecasting, 32, 1491–1508, <https://doi.org/10.1175/WAF-D-16-0220.1>
- Bettenhausen, M., H, C. K. Smith, R. M. Bevilacqua, N-Y. Wang, P. W. Gaiser, and Stephen Cox, (2006) A Nonlinear Optimization Algorithm for WindSat Wind Vector Retrievals, IEEE Trans. Geosci. Rem. Sens., 44, 597-
- Bokhorst, S., Pedersen, S.H., Brucker, L. et al. (2016), Changing Arctic snow cover: A review of recent developments and assessment of future needs for observations, modelling, and impacts, Ambio, 45: 516. <https://doi.org/10.1007/s13280-016-0770-0>
- Bourassa, M. A et al, (2019), Remotely Sensed Winds and Wind Stresses for Marine Forecasting and Ocean Modeling, Front. Mar. Sci., 23 August 2019, <https://doi.org/10.3389/fmars.2019.00443>
- Brackmann-Folkmann, A. and C. Donlon, (2019), Estimating Snow Depth on Arctic Sea Ice using satellite Microwave Radiometry and a Neural Network, submitted to Cryosphere discussions, February 2019.
- Brocca, L., Tarpanelli, A., Filippucci, P., Dorigo, W., Zaussinger, F., Gruber, A., Prieto, D. (2018). How much water is used for irrigation? A new approach exploiting satellite soil moisture observations. International Journal of Applied Earth Observation and Geoinformation, 73, 752 - 766. doi: 10.1016/j.jag.2018.08.023
- Brodzik, M. J., B. Billingsley, T. Haran, B. Raup, M. H. Savoie, (2012), EASE-Grid 2.0: Incremental but Significant Improvements for Earth-Gridded Data Sets. ISPRS International Journal of

- Geo-Information, 1(1):32-45, doi:10.3390/ijgi1010032. <http://www.mdpi.com/2220-9964/1/1/32>.
- Brodzik, M. J., B. Billingsley, T. Haran, B. Raup, M. H. Savoie, (2014), Correction: Brodzik, M. J. et al. EASE-Grid 2.0: Incremental but Significant Improvements for Earth-Gridded Data Sets. ISPRS International Journal of Geo-Information 2012, 1, 32-45. ISPRS International Journal of Geo-Information, 3(3):1154-1156, doi:10.3390/ijgi3031154. <http://www.mdpi.com/2220-9964/3/3/1154>
- Brucker, L., and T. Markus, (2013), Arctic-scale assessment of satellite passive microwave-derived snow depth on sea ice using Operation IceBridge airborne data. Journal of Geophysical Research-Oceans 118: 2892–2905.
- Brucker, L., Dinnat, E.P. and Koenig, L.S. (2014). Weekly gridded Aquarius L-band radiometer/scatterometer observations and salinity retrievals over the polar regions-Part 1: Product description.
- Brun, E., Vionnet, V., Decharme, B., Peings, Y., Valette, R., Karbou, F., and Morin, S. (2013). Simulation of northern Eurasian local snow depth, mass and density using a detailed snowpack model and meteorological reanalyses. J. Hydrometeorol., 14, 203–219.
- Buongiorno Nardelli, B. (2012). A novel approach for the high-resolution interpolation of in situ sea surface salinity. J. Atmos. Ocean. Technol. 29, 867–879. doi: 10.1175/JTECH-D-11-00099.1
- Buongiorno Nardelli, B., Droghei, R., and Santoleri, R. (2016). Multi- dimensional interpolation of SMOS sea surface salinity with surface temperature and in situ salinity data. Remote Sens. Environ. 180, 392–402. doi: 10.1016/j.rse.2015.12.052
- Carrea, L., Embury, O. and Merchant, C. J. (2015) Datasets related to in-land water for limnology and remote sensing applications: distance-to-land, distance-to-water, water-body identifier and lake-centre co-ordinates. Geoscience Data Journal, 2 (2). pp. 83-97. ISSN 2049-6060 doi: <https://doi.org/10.1002/gdj3.32>
- Carrieres, T., Buehner, M., Lemieux, J., and Toudal Pedersen, L. (Eds.). (2017), *Sea Ice Analysis and Forecasting: Towards an Increased Reliance on Automated Prediction Systems*. Cambridge: Cambridge University Press. doi:10.1017/9781108277600
- Casella, D., Amaral, L., Dietrich, S., Marra, A., Sanò, P., and Panegrossi, G., 2017: The Cloud Dynamics and Radiation Database Algorithm for AMSR2: Exploitation of the GPM Observational Dataset for Operational Applications. IEEE Journal of Selected Topics in Applied Earth Observations and Remote Sensing. PP. 1-17. 10.1109/JSTARS.2017.2713485
- Cavalieri, D. and C. Parkinson, (2012), Antarctic sea ice variability and trends, 1979-2010, Cryosphere, vol. 6, p. 881, Jun. 2012.
- Cavalieri, D. J., J. P. Crawford, M. R. Drinkwater, D. T. Eppler, L. D. Farmer, R. R. Jentz, and C. C. Wackerman (1991), Aircraft active and passive microwave validation of the sea ice concentration from the Defence Meteorological Satellite Program Special Sensor Microwave Imager, J. Geophys. Res., 96(C12), 21,998– 22,008
- Cavalieri, D.J., T. Markus, A. Ivanoff, et al. (2012), A comparison of snow depth on sea ice retrievals using airborne altimeters and an AMSR-E simulator. IEEE Transactions on Geoscience and Remote Sensing 50: 3027–3040.
- Chelton, D. B. and F. J. Wentz, (2005), Global microwave satellite observations of sea surface temperature for numerical weather prediction and climate research, Amer. Meteorol. Soc., vol. 86, no. 8, pp. 1097–1115, Aug. 2005.

- Cho, E.; Tuttle, S.E.; Jacobs, J.M. (2017), Evaluating Consistency of Snow Water Equivalent Retrievals from Passive Microwave Sensors over the North Central U. S.: SSM/I vs. SSMIS and AMSR-E vs. AMSR2, *Remote Sens.*, 9, 465.
- Cohen, J., J. Lemmetyinen, J. Pullainen, K. Heinilä, F. Montomoli, J. Seppänen, and M. T. Hallikainen (2015). The effect of boreal forest canopy in satellite snow mapping – a multisensor analysis. *IEEE Trans Geosci Remote Sensing*, 52(6): 3275-3288.
- Comiso, J. C., and R. Kwok (1996), Surface and radiative characteristics of the summer Arctic sea ice cover from multisensor satellite observations, *J. Geophys. Res.*, 101(C12), 28397–28416, doi:10.1029/96JC02816.
- Comiso, J., (1995) SSM/I sea ice concentration using the bootstrap algorithm, NASA reference publication 1390, 57 pp, available from
https://www.geobotany.uaf.edu/library/pubs/ComisoJC1995_nasa_1380_53.pdf
- Comiso, J., D. Cavalieri, and T. Markus, (2003), Sea ice concentration, ice temperature and snow depth using AMSR-E data," *IEEE Trans. Geosci. Remote Sens.*, vol. 43, no. 2, pp. 243–252.
- De Jeu, R., Owe, M., (2003), Further validation of a new methodology for Surface soil moisture and vegetation optical depth retrieval. *Int. J. Remote Sens.* 24, 4559-4578.
- de Rosnay, P. and N. Rodríguez-Fernández, D. Fairbairn, J. Muñoz-Sabater , H. Lawrence, C. Baugh, F. Di Giuseppe , S. English, C. Prudhomme, M Drusch, S. Mecklenburg, oral (invited talk): "SMOS Soil Moisture Data Assimilation for Operational Numerical Weather Prediction", ESA living planet symposium, Milan, 13-17 May 2019
- de Rosnay, P., J. Muñoz-Sabater, C. Albergel, L. Isaksen, S. English, M. Drusch, J.-P. Wigneron: "SMOS brightness temperature forward modelling and long term monitoring at ECMWF", *Remote Sensing of Environment*, 237 (Feb 2020) <https://doi.org/10.1016/j.rse.2019.111424>
- Derkson C, Xu X, Scott Dunbar R et al. (2017) Retrieving landscape freeze/thaw state from Soil Moisture Active Passive (SMAP) radar and radiometer measurements. *Remote Sensing of Environment* 194:48-62
- Dinnat, E., D. LeVine, S. Abraham, and N. Flory (2018). Map of Sky background brightness temperature at L-band. Available online: <https://podaac-tools.jpl.nasa.gov/drive/files/allData/aquarius/L3/mapped/galaxy/2018>.
- Donlon, C. J., K. S. Casey, I. S. Robinson, C. L. Gentemann, R. W. Reynolds, I. Barton, O. Arino, J Stark, N. Rayner, P. LeBorgne, D. Poulter, J. Vazquez-Cuervo, E. Armstrong, H. Beggs, D. Llewellyn Jones, P. J. Minnett, C. J. Merchant, R. Evans, (20090, The GODAE High Resolution Sea Surface Temperature Pilot Project (GHRSST-PP), *Oceanography*, Volume 22, Number 3, 34-45.
- Donlon, C. J., M. Martin, J. D. Stark, J. Roberts-Jones, E. Fiedler and W. Wimmer, (2012), The Operational Sea Surface Temperature and Sea Ice analysis (OSTIA), *Remote Sensing of the Environment*, 116, 140-158, doi: 10.1016/j.rse.2010.10.017.
- Donlon, C. J., 2009. High Resolution Microwave Wind and Temperature (MICROWAT) Mission Concept Study, EOP-SM/1936, Issue: 1, Revision 1.9, available from the European Space Agency.
- Dorigo, W et al, (2017), ESA CCI Soil Moisture for improved Earth system understanding: State-of-the art and future directions, *Rem. Sens. of Env.*, 203, 185–215.

- Drinkwater, M.R., D.G. Long, D.S. Early, (1994), Enhanced Resolution Scatterometer Imaging of Southern Ocean Sea Ice, In Earth Observation Quarterly, 43, 4-6.
- Droghei, R. B. Buongiorno-Nardelli and R. Santolieri, (2018), A New Global Sea Surface Salinity and Density Dataset From Multivariate Observations (1993–2016), Front. Mar. Sci., 27, <https://doi.org/10.3389/fmars.2018.00084>
- Droghei, R., Nardelli, B. B., and Santolieri, R. (2016). Combining in situ and satellite observations to retrieve salinity and density at the ocean surface. J. Atmos. Ocean. Technol. 33, 1211–1223. doi: 10.1175/JTECH-D-15-0194.1
- Drüe, C. and G. Heinemann, (2004), High-resolution maps of the sea-ice concentration from MODIS satellite data," Geophys. Res. Lett., vol. 31, no. 20, pp. L20403-1–L20403.
- Du, J., J. S. Kimball and L. A. Jones, (2015), Satellite Microwave Retrieval of Total Precipitable Water Vapor and Surface Air Temperature Over Land From AMSR2, in IEEE Transactions on Geoscience and Remote Sensing, vol. 53, no. 5, pp. 2520-2531, doi: 10.1109/TGRS.2014.2361344
- Du, J., Kimball, J. S., Galantowicz, J., Kim, S. B., Chan, S. K., Reichle, R., and Watts, J. D. (2018). Assessing global surface water inundation dynamics using combined satellite information from SMAP, AMSR2 and Landsat. Remote sensing of environment, 213, 1-17.
- Duchossois G., P. Strobl, V. Toumazou, S. Antunes, A. Bartsch, T. Diehl, F. Dinessen, P. Eriksson, G. Garric, M-N. Houssais, M. Jindrova, J. Muñoz-Sabater, T. Nagler, O. Nordbeck, (2018a) User Requirements for a Copernicus Polar Mission - Phase 1 Report, EUR 29144 EN, Publications Office of the European Union, Luxembourg (2018) ISBN 978-92-79-80961-3,doi:10.2760/22832,JRC111067 <https://ec.europa.eu/jrc/en/publication/user-requirements-copernicus-polar-mission-0>
- Duchossois G., P. Strobl, V. Toumazou, S. Antunes, A. Bartsch, T. Diehl, F. Dinessen, P. Eriksson, G. Garric, K. Holmlund, M-N. Houssais, M. Jindrova, M. Kern, J. Muñoz-Sabater, T. Nagler, O. Nordbeck, E. de Witte, (2018b) User Requirements for a Copernicus Polar Mission - Phase 2 Report EUR 29144 EN, Publications Office of the European Union, Luxembourg (2018). ISBN 978-92-79-80960-6, doi:10.2760/44170, JRC111068. <https://ec.europa.eu/jrc/en/publication/user-requirements-copernicus-polar-mission>
- EC, (2022). Council conclusions on Copernicus by 2035, Brussels, 10 June 2022 (OR. en) 10070/22, ECOMP 2, CDP/FB/nj, 10 June 2022.
- Emery, W. J., Fowler, C. W. and Maslanik, J. A. (1997) Satellite-derived maps of Arctic and Antarctic sea ice motion: 1988–1994. Geophys. Res. Lett. 24, 897–900.
- Entekhabi, D. et al., (2008), The Soil Moisture Active/Passive Mission (SMAP), IGARSS 2008 - 2008 IEEE International Geoscience and Remote Sensing Symposium, Boston, MA, 2008, pp. III - 1-III - 4. doi: 10.1109/IGARSS.2008.4779267
- Entekhabi, D., Njoku, E. G., O'Neill, P. E., Kellogg, K. H., Crow, W. T., Edelstein, W. N., ... & Kimball, J. (2010). The soil moisture active passive (SMAP) mission. Proceedings of the IEEE, 98(5), 704-716.
- Eppler, D., L. Farmer, A. Lohanick, M. Anderson, D. Cavalieri, J. Comiso, P. Glorsen, C. Garrity, T. Grenfell, M. Hallikainen, et al. (1992), Passive microwave signatures of sea ice. In Microwave Remote Sensing of Sea Ice, in Carsey, F.D., Ed.; American Geophysical Union: Washington, DC, USA, 1992; doi:10.1029/GM068p0047.

- Ermida, S. L., Jiménez, C., Prigent, C., Trigo, I. F., & DaCamara, C. C. (2017). Inversion of AMSR-E observations for land surface temperature estimation: 2. Global comparison with infrared satellite temperature. *Journal of Geophysical Research Atmospheres*, 122 (6), 3348-3360.
- ESA, (20192022), CSC-4 Long Term Scenario (LTS), ESA/PB-EO(2019)10, 7 February 2019, ESA/PB-EO(2022)39, 5 May 2022, available from the European Space Agency.
- Escorihuela, M. J., & Quintana-Seguí, P. (2016). Comparison of remote sensing and simulated soil moisture datasets in Mediterranean landscapes. *Remote sensing of environment*, 180, 99-114.
- ESSB-HB-E-003 working group, (2011), ESA Pointing error engineering handbook, ESSB-HB-E-003, version 1, 19th July 2011.
- Farrar, S., D. Draper, L. Jones and F. Alquaied, (2016), Advantages of Calibration Attitude Maneuvers for spaceborne microwave radiometer missions, 2016 14th Specialist Meeting on Microwave Radiometry and Remote Sensing of the Environment (MicroRad), Espoo, 2016, pp. 186-190, doi: 10.1109/MICRORAD.2016.7530531.
- Fernandez-Moran, R.; Al-Yaari, A.; Mialon, A.; Mahmoodi, A.; Al Bitar, A.; De Lannoy, G.; Rodriguez-Fernandez, N.; Lopez-Baeza, E.; Kerr, Y.; Wigneron, J.-P. (2017) SMOS-IC: An Alternative SMOS Soil Moisture and Vegetation Optical Depth Product. *Remote Sens.*, 9, 457.
- Fowler, C., W. Emery, and M. Tschudi (2013), Polar Pathfinder Daily 25 km EASE-Grid Sea Ice Motion Vectors. Version 2. (daily and meangridded field), NASA DAAC at the Natl. Snow and Ice Data Cent., Boulder, Colo., USA.
- Freitas, S. C., I. Trigo, J. Macedo, C. Barroso, R. Silva, and R Perdigao, (2013), Land Surface Temperature from multiple geostationary satellites. *Int. J. Rem. Sens.*, Vol 34, 3051-3068.
- Gabarro, C., A. Turiel, P. Elosegui, J.A. Pla-Resina, and M. Portabella, (2017), New methodology to estimate Arctic sea ice concentration from SMOS combining brightness temperature differences in a maximum-likelihood estimator, *The Cryosphere*, 11, 1987–2002, 2017 <https://doi.org/10.5194/tc-11-1987-2017>
- Gaiser, P. W. et al., (2004), The WindSat spaceborne polarimetric microwave radiometer: sensor description and early orbit performance, in *IEEE Transactions on Geoscience and Remote Sensing*, vol. 42, no. 11, pp. 2347-2361, Nov. 2004. doi: 10.1109/TGRS.2004.836867
- Gao, H. N. Nie, W. Zhang, H. Chen, (2020). Monitoring the spatial distribution and changes in permafrost with passive microwave remote sensing, *ISPRS Journal of Photogrammetry and Remote Sensing*, 170, 142-155, ISSN 0924-2716, <https://doi.org/10.1016/j.isprsjprs.2020.10.011>.
- Garcia-Eidell, C., J. C. Comiso, E. Dinnat, and L. Brucker (2017), Satellite observed salinity distributions at high latitudes in the Northern Hemisphere: A comparison of four products, *J. Geophys. Res. Oceans*, 122, 7717–7736, doi:10.1002/2017JC013184.
- GCOS (2003), The Global Observing System for Climate: Climate Monitoring Principles, available from <https://gcos.wmo.int/en/essential-climate-variables/about/gcos-monitoring-principles>
- GCOS (2016). The Global Observing System for Climate: Implementation Needs, GCOS-200: available from https://library.wmo.int/opac/doc_num.php?explnum_id=3417
- Gentemann, C. L. ,T. Meissner, and F. J. Wentz, (2010), Accuracy of satellite sea surface temperatures at 7 and 11 GHz,” *IEEE Trans. Geosci. Remote Sens.*, vol. 48, no. 3, pp. 1009–1018.

- Gevaert, A. I., Parinussa, R. M., Renzullo, L. J., van Dijk, A. I., & de Jeu, R. A. (2016). Spatio-temporal evaluation of resolution enhancement for passive microwave soil moisture and vegetation optical depth. *International journal of applied earth observation and geoinformation*, 45, 235–244.
- GHRSST, Group for High Resolution Sea Surface Temperature Team (2012), The Recommended GHRSST Data Specification (GDS) 2.0, document revision 5, available from the GHRSST International Project Office, latest version available at <https://zenodo.org/record/4700466#.YrRVzOxByan>
- Girard-Ardhuin, F.; Ezraty, R. (2012), Enhanced Arctic Sea Ice Drift Estimation Merging Radiometer and Scatterometer Data. *IEEE Trans. Geosci. Remote Sens.*, 50, 2639–2648.
- Greenwald, T. J., Bennartz, R., Lebsack, M., and Teixeira, J. (2018). An uncertainty data set for passive microwave satellite observations of warm cloud liquid water path. *Journal of Geophysical Research: Atmospheres*, 123(7), 3668–3687.
- Grenfell, T. C., Barber, D. G., Fung, A. K., Gow, A. J., Jezek, K. C., Knapp, E. J., Nghiem, S. V., Onstott, R. G., Perovich, D. K., Roesler, C. S., Swift, C. T., and Tanis, F., (1998), Evolution of electromagnetic signatures of sea ice from initial formation to the establishment of thick first year ice, *IEEE T. Geosci. Remote*, 36, 1642–1654, 1998.
- Grenfell, T. C., Cavalieri, D. J., Comiso, J. C., Drinkwater, M. R., Onstott, R. G., Rubinstein, I., Steffen, K., and Winebrenner, D. P, (1992), Considerations for microwave remote sensing of thin sea ice, in: *Microwave Remote Sensing of Sea Ice*, edited by: Carsey, F. D., American Geophysical Union, Washington, D.C., doi:10.1029/GM068p0291.
- Gu, H and A. W. England, (2007), AMSR-E data resampling with near circular synthesized footprint shape and noise/reduction trade-off study, *IEEE Tras. GeoSci and Rem. Sens*, 45(10), pp. 3193–3203
- Guerreiro, K., Fleury, S., Zakharova, E., Kouraev, A., Rémy, F., and Maisongrande, P., (2017), Comparison of CryoSat-2 and ENVISAT radar freeboard over Arctic sea ice: toward an improved Envisat freeboard retrieval, *The Cryosphere*, 11, 2059–2073, <https://doi.org/10.5194/tc-11-2059-2017>, 2017.
- Hall, D., Kelly, R. E. J., Riggs, G. A., Chang, A. T. C., & Foster, J. L. (2002). Assessment of the relative accuracy of hemispheric-scale snow-cover maps. *Annals of Glaciology*, 34, 24–30.
- Hallikainen, M., and P. Jolma (1992), Comparison of algorithms for retrieval of snow water equivalent from Nimbus-7 SMMR data in Finland, *IEEE Trans. Geosci. Remote Sens.*, 30(1), 124–131, doi:10.1109/36.124222.
- Hanjsek, I., G. Parrella, H. Rott, T. Nagler, C. Derksen and J. Lemmetyinen, 2017. Identification of needs and requirements for a space mission on snow mass. Technical Note 1, v1.2. ESTEC Contract No. 4000118310/16/NL/FF/gp.
- Heil, P., Fowler, C. W. & Lake, S. E. (2006), Antarctic sea-ice velocity as derived from SSM/I imagery. *Ann. Glaciol. Ser.* 44, 361–366.
- Heygster, G., Huntemann, M., Ivanova, N., Saldo, R., and Pedersen, L. T. (2014), Response of passive microwave sea ice concentration algorithms to thin ice, *Proceedings Geoscience and Remote Sensing Symposium (IGARSS)*, 2014 IEEE International, 13–18 July, Quebec City, QC, 3618–3621, doi:10.1109/IGARSS.2014.6947266.
- Hilburn, K. A., Meissner, T., Wentz, F. J., and Brown, S. T. (2016). Ocean vector winds from WindSat two-look polarimetric radiances. *IEEE Trans. Geosci. Remote Sens.* 54, 918–931. doi: 10.1109/TGRS.2015.2469633

- Hilburton, H and F. J. Wentz, (2008), Inter-calibrated Passive Microwave Rain Products from the Unified Microwave Ocean Retrieval Algorithm (UMORA), *J. Applied Met. And Climatology*, 778-794, DOI: 10.1175/2007JAMC1635.1
- Hollinger, D. Y., S.M. Goltz, E.A. Davidson, J.T. Lee, K. Tu, H.T. (1999). Valentine Seasonal patterns and environmental control of carbon dioxide and water vapour exchange in an ecotonal boreal forest *Global Change Biology*, 5, pp. 891-902
- Hollinger, J., R. Lo, G. Poe, R. Savage, and J. Peirce, (1987), Special sensor microwave / imager user's guide, Naval Research Laboratory, Washington, DC, Dec. 14, 1987.
- Holmes, T. R. H., De Jeu, R. A. M., Owe, M., & Dolman, A. J. (2009). Land surface temperature from Ka band (37 GHz) passive microwave observations. *Journal of Geophysical Research: Atmospheres*, 114(D4).
- Hrbáček, F., Engel, Z., Kňažková, M., and Smolíková, J., (2021). Effect of ephemeral snow cover on the active layer thermal regime and thickness on CALM-S JGM site, James Ross Island, eastern Antarctic Peninsula, *The Cryosphere Discuss. [preprint]*, <https://doi.org/10.5194/tc-2021-5>, 2021.
- Huang, Y., S. Huang and J. Sun (2018), Experiments on navigating resistance of an icebreaker in snow covered level ice, *Cold Regions Science and Technology*, v152, 1-14, <https://doi.org/10.1016/j.coldregions.2018.04.007>.
- Huntemann, M., Heygster, G., Kaleschke, L., Krumpen, T., Mäkynen, M., and Drusch, M., (2014), Empirical sea ice thickness retrieval during the freeze-up period from SMOS high incident angle observations, *The Cryosphere*, 8, 439-451, <https://doi.org/10.5194/tc-8-439-2014>.
- Imaoka, K., M. KAchi, M. Kashara, N. Ito, K. Nakagawa and T. Oki, (2010), Instrument performance and calibrationof AMSR-E and AMSR2, *Int. Archive of Photorammetry, Rem. Sens. And spatial Information Science*, XXXVIII, part 8, Kyoto, Japan.
- IPCC, 2018, Global Warming of 1.5°C, SR15 available from <http://www.ipcc.ch/report/sr15/>
- ITU, 2016, Radio Regulations, Edition 2016, available from <https://www.itu.int>
- Ivanova, N., Johannessen, O. M., Pedersen, L. T., and Tonboe, R. T., (2014), Retrieval of Arctic sea ice parameters by satellite passive microwave sensors: a comparison of eleven sea ice algorithms, *IEEE T. Geosci. Remote*, 52, 7233–7246, 2014.
- Ivanova, N., Pedersen, L. T., Tonboe, R. T., Kern, S., Heygster, G., Lavergne, T., Sørensen, A., Saldo, R., Dybkjær, G., Brucker, L., and Shokr, M., (2015), Inter-comparison and evaluation of sea ice algorithms: towards further identification of challenges and optimal approach using passive microwave observations, *The Cryosphere*, 9, 1797-1817, <https://doi.org/10.5194/tc-9-1797-2015>.
- Jacob, M., Ament, F., Gutleben, M., Konow, H., Mech, M., Wirth, M., and Crewell, S.: Investigating the liquid water path over the tropical Atlantic with synergistic airborne measurements, *Atmos. Meas. Tech.*, 12, 3237–3254, <https://doi.org/10.5194/amt-12-3237-2019>, 2019.
- JAXA, Japan Aerospace Exploration Agency (2005), AMSR-E Data Users Hand- book, 3rd ed., Saitama, Japan.
- JAXA, Japan Aerospace Exploration Agency (2005), Aqua AMSR-E Level 1 Product Format Description Document, MAS-100045A
- JAXA, Japan Aerospace Exploration Agency (2020), Overview of the Advanced Microwave Scanning Radiometer 3 (AMSR-3), available from https://earth.jaxa.jp/files/research/ra/3rd_ra_eo/material/EORA3_APPENDIX8_AMSR3.pdf

- JCGM, 2008, Evaluation of measurement data — Guide to the expression of uncertainty in measurement JCGM 100:2008, GUM 1995 with minor corrections, First edition September 2008, available from
http://www.bipm.org/utils/common/documents/jcgm/JCGM_100_2008_E.pdf
- Jiménez, C., Prigent, C., Ermida, S. L., & Moncet, J. L. (2017). Inversion of AMSR-E observations for land surface temperature estimation: 1. Methodology and evaluation with station temperature. *Journal of Geophysical Research Atmospheres*, 122 (6), 3330-3347.
- Jiménez, C., Tenerelli, J., Prigent, C., Kilic, L., Lavergne, T., Skarpalezos, S., et al. (2021). Ocean and sea ice retrievals from an end-to-end simulation of the Copernicus Imaging Microwave Radiometer (CIMR) 1.4–36.5 GHz measurements. *Journal of Geophysical Research: Oceans*, 126, e2021JC017610. <https://doi.org/10.1029/2021JC017610>
- Johnson, J. T., et al., (2020). Real-Time Detection and Filtering of Radio Frequency Interference Onboard a Spaceborne Microwave Radiometer: The CubeRRT Mission," in IEEE Journal of Selected Topics in Applied Earth Observations and Remote Sensing, vol. 13, pp. 1610-1624, doi: 10.1109/JSTARS.2020.2978016.
- Johnson J. T. et al., (2021). Microwave Radiometry at Frequencies From 500 to 1400 MHz: An Emerging Technology for Earth Observations, in IEEE Journal of Selected Topics in Applied Earth Observations and Remote Sensing, vol. 14, pp. 4894-4914, doi: 10.1109/JSTARS.2021.3073286.
- Kaefer, L. S and R. F. Harrington (1983), Radiometer Requirements for Earth-Observation Systems Using Large Space Antennas, NASA reference publication, NASA-RP-1101 19830020139, available from
<https://ntrs.nasa.gov/archive/nasa/casi.ntrs.nasa.gov/19830020139.pdf>
- Kaleschke, L., Maaß, N., Haas, C., Hendricks, S., Heygster, G., and Tonboe, R. T., (2010), A sea-ice thickness retrieval model for 1.4 GHz radiometry and application to airborne measurements over low salinity sea-ice, *The Cryosphere*, 4, 583–592, doi:10.5194/tc-4-583-2010, 2010.
- Kaleschke, L., X. Tian-Kunze, N. Maaß, A. Beitsch, A. Wernecke, M. Miernecki, Gerd Müller, B. H. Fock, A. M.U. Gierisch, K. H. Schlünzen, T. Pohlmann, M. Dobrynin, S. Hendricks, J. Asseng, R. Gerdes, P. Jochmann, N. Reimer, J. Holtfort, C. Melsheimer, G. Heygster, G. Spreen, S. Gerland, J. King, N. Skou, S. Schmidl Søbjærg, C. Haas, F. Richter, and T. Casal, (2016), SMOS sea ice product: Operational application and validation in the Barents Sea marginal ice zone, *Rem. Sen. of Env.*, 180, 264-273,
<https://doi.org/10.1016/j.rse.2016.03.009>.
- Karvonen, J., (2014), Baltic Sea ice concentration estimation based on C-band dual-polarized SAR data, *IEEE Trans. Geosci. Remote Sens.*, vol. 52, no. 9, pp. 5558–5566, doi: 10.1109/TGRS.2013.2290331.
- Karvonen, J., (2017), Baltic Sea Ice Concentration Estimation Using SENTINEL-1 SAR and AMSR2 Microwave Radiometer Data, in *IEEE Transactions on Geoscience and Remote Sensing*, vol. 55, no. 5, pp. 2871-2883.
doi: 10.1109/TGRS.2017.2655567
- Kasahara, M., K. Imaoka, M. Kachi, H. Fujii, K. Naoki et al, (2012), Status of AMSR2 on GCOM-W1, Proc. SPIE 8533, Sensors, Systems and Next Generation Satellites XVI, 853307, doi: 10.1117/12.975810.
- Kazumori, M., (2012), A retrieval algorithm of atmospheric water vapor and cloud liquid water for AMSR-E, *Eur. J. Remote Sens.*, vol. 45 pp. 63–74, doi: 10.5721/EuJRS20124507.

- Kelly, R. E. J. (2009). The AMSR-E Snow Depth Algorithm: Description and Initial Results. *Journal of The Remote Sensing Society of Japan*, 29(1), 307-317.
- Kelly, R., A. Chang, L. Tsang, and J. Foster (2003). A prototype AMSR-E global snow area and snow depth algorithm. *IEEE Trans. Geosci. Remote Sens.*, 41(2), 230-242.
- Kelly, R.E.J., Chang, A.T.C, Tsang, L. and Foster, J.L. (2003) Development of a prototype AMSR-E global snow area and snow volume algorithm, *IEEE Transactions on Geoscience and Remote Sensing*, 41(2): 230-242.
- Kern, S., Khvorostovsky, K., Skourup, H., Rinne, E., Parsakhoo, Z. S., Djepa, V., Wadhams, P., and Sandven, S., (2015), The impact of snow depth, snow density and ice density on sea ice thickness retrieval from satellite radar altimetry: results from the ESA-CCI Sea Ice ECV Project Round Robin Exercise, *The Cryosphere*, 9, 37–52, doi:10.5194/tc-9-37-2015.
- Kern, S., Rösel, A., Pedersen, L. T., Ivanova, N., Saldo, R., and Tonboe, R. T.(2016). The impact of melt ponds on summertime microwave brightness temperatures and sea-ice concentrations, *The Cryosphere*, 10, 2217–2239, <https://doi.org/10.5194/tc-10-2217-2016>, 2016.
- Kerr, Y. H., Waldteufel, P., Richaume, P., Wigneron, J. P., Ferrazzoli, P., Mahmoodi, A., and Leroux, D. (2012). The SMOS soil moisture retrieval algorithm. *IEEE Transactions on Geoscience and Remote Sensing*, 50(5), 1384-1403.
- Kilic, L., Prigent, C., Jimenez, C., and Donlon, C. (2021). Technical note: A sensitivity analysis from 1 to 40 GHz for observing the Arctic Ocean with the Copernicus Imaging Microwave Radiometer, *Ocean Sci.*, 17, 455–461, <https://doi.org/10.5194/os-17-455-2021>, 2021.
- Kilic, L., C. Prigent, F. Aires, G. Heygster, V. Pellet, and C. Jimenez, (2020), Ice Concentration Retrieval from the Analysis of Microwaves: A New Methodology Designed for the Copernicus Imaging Microwave Radiometer. *Remote Sens.*, 12, 1060.
- Kilic, L., Prigent, C., Aires, F., Boutin, J., Heygster, G., Tonboe, R. T. et al. (2018a). Expected performances of the Copernicus Imaging Microwave Radiometer (CIMR) for an all-weather and high spatial resolution estimation of ocean and sea ice parameters. *Journal of Geophysical Research: Oceans*, 123. <https://doi.org/10.1029/2018JC014408>
- Kilic, L., Prigent, C., Boutin, J., Meissner, T., English, S., & Yueh, S. (2019). Comparisons of ocean radiative transfer models with SMAP and AMSR2 observations. *Journal of Geophysical Research: Oceans*, 124, 7683– 7699. <https://doi.org/10.1029/2019JC015493>
- Kilic, L., Tonboe, R. T., Prigent, C., and Heygster, G,(2018b), Estimating the snow depth, the snow-ice interface temperature, and the effective temperature of Arctic sea ice using Advanced Microwave Scanning Radiometer 2 and Ice Mass Balance buoys data, *The Cryosphere Discuss.*, <https://doi.org/10.5194/tc-2018-223>,
- Kim, Y., Kimball, J., McDonald. K. and Glassy, J. (2011). Developing a global data record of daily landscape freeze/thaw status using satellite passive microwave remote sensing. *IEEE Transactions on Geoscience and Remote Sensing*, 49(3), 949-960.
- Knaff, J. A., C. R. Sampson, and K. D. Musgrave, (2018). Statistical tropical cyclone wind radii prediction using climatology and persistence: Updates for the western North Pacific, *Wea. Forecasting*, doi: 10.1175/WAF-D-18-0027.1.
- Kolassa, J., Gentine, P., Prigent, C., Aires, F., and Alemohammad, S. H. (2017), Soil moisture retrieval from AMSR-E and ASCAT microwave observation synergy. Part 2: Product evaluation. *Remote Sensing of Environment*, 195, 202-217.

- Kolassa, J., P. Gentile, C. Prigent, and F. Aires, (2016), Remote sensing of soil moisture using AMSR-E and ASCAT observations, *Remote Sensing of Environment*, 1–73, 1–14.
- Konings, A.G., M. Piles, N. Das, D. Entekhabi (2017), L-Band Vegetation Optical Depth and Effective Scattering Albedo Estimation from SMAP, *Remote Sensing of the Environment*, Vol. 198, pp 460-470
- Konings, A.G., M. Piles; K. Rotzer; K.A. McColl; S. K. Chan; D. Entekhabi (2016), Vegetation optical depth and scattering albedo retrieval using time series of dual polarized L-band radiometer observations. *Remote Sensing of Environment*, Vol. 172, pp. 178 - 189.
- Kontu, A., J. Lemmettyinen, J. Pulliainen, J. Seppänen, and M. T. Hallikainen (2014). Observation and modeling of the microwave brightness temperature of snow-covered frozen lakes and wetlands. *IEEE Trans Geosci. Remote Sensing*, 52(6), 3275-3288.
- Kruopis, N., J. Praks, A. Arslan, H. Alasalmi, J. Koskinen and M. Hallikainen (1999). Passive microwave measurements of snow-covered forests in EMAC'95. *IEEE Trans Geosci Remote Sensing*, 37, 2699-2705.
- Kurtz, N.T., Farrell, S.L., Studinger, M., Galin, N., Harbeck, J.P., Lindsay, R., Onana, V.D., Panzer, B., Sonntag, J.G. (2013), Sea ice thickness, freeboard, and snow depth products from Operation IceBridge airborne data. *Cryosphere* 7:1035–1056. <http://dx.doi.org/10.5194/tc-7-1035-2013>.
- Kwok, R., G. F. Cunningham, M. Wensnahan, I. Rigor, H. J. Zwally, (2009), Thinning and volume loss of the Arctic ocean sea ice cover: 2003–2008, *J. Geophys. Res. Oceans*, vol. 114, 2009, Art. no. C07005. doi: 10.1029/2009JC005312.
- Kwok, R., Schweiger, A., Rothrock, D. A., Pang, S. & Kottmeier, C. (1998), Sea ice motion from satellite passive microwave imagery assessed with ERS SAR and buoy motions. *J. Geophys. Res.* 103, 8191–8214.
- Lahtinen., J. et al., (2019). Real-Time RFI Processor for Future Spaceborne Microwave Radiometers, in *IEEE Journal of Selected Topics in Applied Earth Observations and Remote Sensing*, vol. 12, no. 6, pp. 1658-1669, doi: 10.1109/JSTARS.2019.2910640.
- Langlois, A., A. Royer, F. Dupont, A. Roy, K. Goïta, and G. Pickard (2011). Improved corrections of forest effects on passive microwave satellite remote sensing of snow over boreal and subarctic regions. *IEEE Trans. Geosci. Remote Sens.*, 49(10), 3824-3836.
- Larue F., A. Royer, D. De Sève, A. Langlois, A. Roy and L. Brucker (2016). Validation analysis of the GlobSnow-2 database over an eco-climatic latitudinal gradient in Eastern Canada. *Remote Sensing of Environment*, 194, 264-277.
- Lavergne, T., (2016a), Low Resolution Sea Ice Drift Product User's Manual, Ocean & Sea Ice SAF GBL LR SID — OSI-405-c, Version 1.8 — July 2016 available from <http://osisaf.met.no/docs/>
- Lavergne, T., (2016b), Ocean & Sea Ice SAF Algorithm Theoretical Basis Document for the OSI SAF Low Resolution Sea Ice Drift Product GBL LR SID — OSI-405-c Version 1.3 — May 2016.
- Lavergne, T., Piñol Solé, M., Down, E., and Donlon, C.(2021). Towards a swath-to-swath sea-ice drift product for the Copernicus Imaging Microwave Radiometer mission, *The Cryosphere*, 15, 3681–3698, <https://doi.org/10.5194/tc-15-3681-2021>.
- Lavergne, T., R. Tonboe and L. Pendersen, (2020), CIMR Sea-Ice Concentration Algorithm Theoretical Basis Document (ATBD) v4 - January 2020, Deliverable D-60 from the CIMR

Mission Requirement Consolidation study (CIMR MRC), Contract 4000125290/18/NL/AI, available from the European Space Agency, Noordwijk, the Netherlands.

- Lavergne, T., Sørensen, A. M., Kern, S., Tonboe, R., Notz, D., Aaboe, S., Bell, L., Dybkjær, G., Eastwood, S., Gabarro, C., Heygster, G., Killie, M. A., Brandt Kreiner, M., Lavelle, J., Saldo, R., Sandven, S., and Pedersen, L. T. (2019), Version 2 of the EUMETSAT OSI SAF and ESA CCI sea-ice concentration climate data records, *The Cryosphere*, 13, 49-78, <https://doi.org/10.5194/tc-13-49-2019>.
- Lavergne, T.; Eastwood, S.; Teffah, Z.; Schyberg, H.; Breivik, L.A. (2010), Sea ice motion from low-resolution satellite sensors: An alternative method and its validation in the Arctic. *J. Geophys. Res. Oceans*, doi:10.1029/2009JC005958.
- Laxon, S.W.; Giles, K.A.; Ridout, A.L.; Wingham, D.J.; Willatt, R.; Cullen, R.; Kwok, R.; Schweiger, A.; Zhang, J.; Haas, C.; Hendricks, S.; Krishfield, R.; Kurtz, N.; Farrell S.; Davidson, M. (2013), CryoSat-2 estimates of Arctic sea ice thickness and volume. *Geophys. Res. Lett.*, 40, 1-6. doi:10.1002/grl.50193.
- Le Vine, D. M. and S. Abraham, (2000), Faraday Rotation and Passive Microwave Remote Sensing of Soil Moisture from Space, *Microw. Radiomet. Remote Sens. Earth's Surf. Atmosphere*, pp 89-96, Edited by P. Pampaloni and S. Paloscia, VSP., 2000.
- Ledley, T. S. (1991). Snow on sea ice: Competing effects in shaping climate. *Journal of Geophysical Research*, 96, 17,195–17,208. <https://doi.org/10.1029/91JD01439>.
- Lee, S.-M., B.-J. Sohn, and S.-J. Kim, (.2017) Differentiating between first-year and multiyear sea ice in the Arctic using microwave-retrieved ice emissivities. *J. Geophys. Res. Atmos.*, 122, 5097-5112, doi: 10.1002/2016JD026275.
- Lehner, B., and Döll, P. (2004). Development and validation of a global database of lakes, reservoirs and wetlands. *Journal of hydrology*, 296(1-4), 1-22.
- Lemmetyinen, J., A. Kontu, J-P. Kärnä, J. Vehviläinen, M. Takala, and J. Pulliainen (2011). Correcting for the influence of frozen lakes in satellite microwave radiometer observations through application of a microwave emission model. *Remote Sens. Environ.*, 115(12), 3695-3706.
- Leppäranta, M. (1983). A growth model for black ice, snow ice and snow thickness in subarctic basins. *Hydrology Research*, 14(2), 59–70.
- LeVine, D. and M. Abraham, (2004). Galactic Noise and Passive Microwave Remote Sensing From Space at L-Band, *IEEE TGRS* vo.42(1), pp. 119 - 129, doi: 10.1109/TGRS.2003.817977.
- Li, L., P. Gaiser, M. Albert, D. Long, and E. Twarog, (2008), WindSat passive microwave polarimetric signatures of the Greenland ice sheet, *IEEE Trans. Geosci. Remote Sens.*, vol. 46, no. 9, pp. 2622–2631.
- Li, Q, R. Kelly, L. Leppänen, J. Vehviläinen, A. Kontu, J. Lemmetyinen and J. Pulliainen, (2019). The Influence of Thermal Properties and Canopy-Intercepted Snow on Passive Microwave Transmissivity of a Scots Pine. *IEEE Trans Geosci Remote Sens.*, 57, 8, 54245433.
- Li, Q. and R.E.J. Kelly (2017) Correcting satellite passive microwave brightness temperatures in forested landscapes using satellite visible reflectance estimates of forest transmissivity, *IEEE Journal of Selected Topics in Applied Remote Sensing*; doi: 10.1109/JSTARS.2017.2707545
- Li, QH, Kelly, R; Lemmetyinen, J; De Roo, RD; Pan, JM; Qiu, YB (2021). The influence of tree transmissivity variations in winter on satellite snow parameter observations, *Int. J. Digital Earth*, 14, 10, 1337-1353, doi: 10.1080/17538947.2021.1950852.

- Liu, Y. and P. Minnett, (2016), Sampling errors in satellite-derived infrared sea-surface temperatures Part I: Global and Regional MODIS fields, *Rem. Sens. Env.*, 177, 48-64, <http://dx.doi.org/10.1016/j.rse.2016.02.026>
- Liu, Y.Y., van Dijk, A.I.J.M., de Jeu, R.A.M., Canadell, J.G., McCabe, M.F., Evans, J.P., & Wang, G. (2015). Recent reversal in loss of global terrestrial biomass. *Nature Clim. Change*, 5, 470-474
- Liu, Y.Y., van Dijk, A.I.J.M., McCabe, M.F., Evans, J.P., and de Jeu, R.A.M. (2013). Global vegetation biomass change (1988–2008) and attribution to environmental and human drivers. *Global Ecology and Biogeography*, 22, 692-705
- Long, D. G. and D. L. Daum, (1998), Spatial resolution enhancement of SSM/I data. *IEEE Trans. Geosci. Remote Sens. Mar*; 1998 36(2):407–417.
- Long, D. G. (2016), Optimum Image Formation for Spaceborne Microwave Radiometer Products, *IEEE, Tras. Geosci. Rem. Sens.*, 54(5), 2763-2779, doi:10.1109/TGRS.2015.2505677
- Long, D. G., (2017), Polar Applications of Spaceborne Scatterometers, in *IEEE Journal of Selected Topics in Applied Earth Observations and Remote Sensing*, vol. 10, no. 5, pp. 2307-2320. doi: 10.1109/JSTARS.2016.2629418.
- Lu, J., G. Heygster and G. Spreen, (2018), Atmospheric Correction of Sea Ice Concentration Retrieval for 89 GHz AMSR-E Observations, in *IEEE Journal of Selected Topics in Applied Earth Observations and Remote Sensing*, vol. 11, no. 5, pp. 1442-1457. doi: 10.1109/JSTARS.2018.2805193.
- Maass, N., Kaleschke, L., Tian-Kunze, X., Tonboe, R.T., (2015). Snow thickness retrieval from L-band brightness temperatures: a model comparison. *Ann. Glaciol.* 56 (69), 9–17.
- Maeda, K., A. Shibata and K. Imaoka, (2011), Protection of 6–7 GHz band spaceborne microwave radiometer from interferences to derive sea surface temperature and others, *IEEE International Geoscience and Remote Sensing Symposium*, Vancouver, BC, 2011, pp. 4217-4220. doi: 10.1109/IGARSS.2011.6050161
- Maeda, K., Y. Taniguchi and K. Imaoka, (2016), GCOM-W1 AMSR2 Level 1R Product: Dataset of Brightness Temperature Modified Using the Antenna Pattern Matching Technique, *IEEE Transactions on Geoscience and Remote Sensing*, VOL. 54, NO. 2.
- Maekynen, M., Cheng, B., and Similae, M. (2013), On the accuracy of thin-ice thickness retrieval using MODIS thermal imagery over Arctic first-year ice, *Ann. Glaciol.*, 62, 87–96, doi:10.3189/2013AoG62A166.
- Markus, T., D. Cavalieri, A. Gasiewski, M. Klein, J. Maslanik, D. Powell, B. Stankov, J. Stroeve and M. Sturm (2006). Microwave Signatures of Snow on Sea Ice: Observations. *IEEE Trans. Geosci. Remote Sens.*, 44, 3081-3090. doi:10.1109/TGRS.2006.883134
- Mätzler, C., E. Schanda, and W. Good (1982). Towards the definition of optimum sensor specifications for microwave remote sensing of snow. *IEEE Trans. Geosci. Remote Sens.*, GE-20, 57-66.
- Maykut, G. A. (1978). Energy exchange over young sea ice in the central Arctic. *Journal of Geophysical Research*, 83, 3646–3658. <https://doi.org/10.1029/JC083iC07p03646>
- Meier, W. N., J. S. Stewart, Y. Liu, J. Key and J. A. Miller, (2017), Operational Implementation of Sea Ice Concentration Estimates from the AMSR2 Sensor," in *IEEE Journal of Selected Topics in Applied Earth Observations and Remote Sensing*, vol. 10, no. 9, pp. 3904-3911. doi: 10.1109/JSTARS.2017.2693120

- Meier, W.N., Hovelsrud, G.K., van Oort, B.E., Key, J.R., Kovacs, K.M., Michel, C., Haas, C., Granskrog, M.A., Gerland, S., Perovich, D.K., Makshtas, A., Reist, J.D., (2014), Arctic sea ice in transformation: A review of recent observed changes and impacts on biology and human activity. *Rev. Geophys.* 52 (3), 185e217.
- Meissner, T. and F. J. Wentz, (2012), The emissivity of the ocean surface between 6 and 90 GHz over a large range of wind speeds and earth incidence angles," *IEEE Trans. Geosci. Remote Sens.*, vol. 50, no. 8, pp. 3004–3026.
- Meissner, T. and F. J. Wentz, (2016), Remote Sensing Systems SMAP Ocean Surface Salinities [Level 2C, Level 3 Running 8-day, Level 3 Monthly], Version 2.0 validated release. Remote Sensing Systems, Santa Rosa, CA, USA. Available online at www.remss.com/missions/smap
- Meissner, T. and F. Wentz, (2002), An updated analysis of the ocean surface wind direction signal in passive microwave brightness temperatures, *IEEE Trans. Geosci. Remote Sens.*, vol. 40, no. 6, pp. 1230–1240.
- Meissner, T., F. J. Wentz, and D. Draper, (2011), GMI calibration algorithm and analysis theoretical basis document, version F," *Remote Sens. Syst.*, Santa Rosa, CA, USA, Tech. Rep. 111311.
- Meissner, T., F. Wentz A. Manaster, R. Lindsley, M. Brewer, M. Densberger, 2022, NASA/RSS SMAP Salinity: Version 5.0 Validated Release, ATBD, RSS Technical Report 033122, Available online: www.remss.com/missions/smap.
- Meissner, T., F. Wentz, D. Le Vine (2017). Aquarius Salinity Retrieval Algorithm End of Mission ATBD, report number 120117, Remote Sensing Systems, Santa Rosa, CA, 113 pp. Available online: https://images.remss.com/papers/tech_reports/2017/Meissner_AQ_ATBD_EOM_final.pdf
- Meissner, T., L. Ricciardulli, and F.J. Wentz, (2017), Capability of the SMAP Mission to Measure Ocean Surface Winds in Storms. *Bull. Amer. Meteor. Soc.*, 98, 1660–1677,<https://doi.org/10.1175/BAMS-D-16-0052.1>
- Meissner, T.; Wentz, F.J.; Le Vine, D.M. (2018), The Salinity Retrieval Algorithms for the NASA Aquarius Version 5 and SMAP Version 3 Releases. *Remote Sens.*, 10, 1121. <https://doi.org/10.3390/rs10071121> .
- Melsheimer, C., Heygster, G. and Pedersen, L.T., (2008), Integrated retrieval of surface and atmospheric parameters over the Arctic from AMSR-E satellite microwave radiometer data using inverse methods. *IGARSS2008*, IEEE International Geoscience and Remote Sensing Symposium (Vol. 4, pp. IV-986).
- Meredith, M. , A. Sundfjord, S. Henson, A. Meijers, E. Murphy, R. Bellerby, M. Daase, F. Cottier, M. Belchier, M. Chierici, I. Ellingsen, S. Falk-Petersen, S. Hill, P. Holland, G. Tarling, P. Trathan, J. Turner, J. Wilkinson, L. Batchellier, L. Capper, J. Oliver, 2018, The State of the Polar Oceans 2018: Making Sense of Our Changing World, United Kingdom Foreign and Commonwealth Office as part of the UK-Norway Memorandum of Understanding on Polar Research and Cultural Heritage, available from www.gov.uk/government/publications/uk-norway-memorandum-of-understanding-on-polar-research-and-cultural-heritage
- Merkouriadi, I., B. Cheng, R. M. Graham, A. Rosel and M. A. Granskog, (2017), Critical role of snow on sea ice growth, *J. Geophys. Res. Lett.*, 44, 10,479–10,485. <https://doi.org/10.1002/2017GL075494>

- Moesinger, L., Dorigo, W., Jeu, R. de, Schalie, R. van der, Scanlon, T., Teubner, I., Forkel, M., 2019. The Global Long-term Microwave Vegetation Optical Depth Climate Archive VODCA. Earth System Science Data Discussions 1-26. <https://doi.org/10.5194/essd-2019-42>.
- Mohammed, P. N., M. Aksoy, J. R. Piepmeier, J. T. Johnson and A. Bringer, (2016), SMAP L-Band Microwave Radiometer: RFI Mitigation Prelaunch Analysis and First Year On-Orbit Observations, in IEEE Transactions on Geoscience and Remote Sensing, vol. 54, no. 10, pp. 6035-6047. doi: 10.1109/TGRS.2016.2580459.
- Momen, M., Wood, J. D., Novick, K. A., Pangle, R., Pockman, W. T., McDowell, N. G., & Konings, A. G. (2017). Interacting effects of leaf water potential and biomass on vegetation optical depth. Journal of Geophysical Research: Biogeosciences, 122, 3031–3046. <https://doi.org/10.1002/2017JG004145>
- Muñoz Sabater J., A. Fouilloux and P. de Rosnay, (2012), Technical implementation of SMOS data in the ECMWF Integrated Forecasting System, Geosci. Remote Sens. Let., vol 9(2), 2012 doi: [10.1109/LGRS.2011.2164777](https://doi.org/10.1109/LGRS.2011.2164777)
- Naoki, K., Ukita, J., Nishio, F., Nakayama, M., Comiso, J. C., and Gasiewski, A., (2008), Thin sea ice thickness as inferred from passive microwave and in situ observations, J. Geophys. Res., 113, C02S16, doi:10.1029/2007JC004270.
- Narvekar, G. Heygster, T. J. Jackson, G. Macelloni, R. Bindlish, and J. Notholt, (2010), Passive polarimetric microwave signatures observed over Antarctica, IEEE Trans. Geosci. Remote Sens., vol. 48, no. 3, pp. 1059–1075.
- Narvekar, P. S., G. Heygster, and R. Tonboe, (2020) Analysis of WindSat Measured Passive Fully Polarimetric Measurements Over Arctic Sea Ice, IUP, Univ. Bremen, Bremen, Germany, Final Rep. Danish Meteorol. Inst., Tech. Rep. [Online]. Available: <http://www.iup.uni-bremen.de/iuppage/psa/documents/WindSatArcticReplong.pdf>
- Narvekar, P. S., T. J. Jackson, R. Bindlish, L. Li, G. Heygster, and P. Gaiser, (2007), Observations of land surface passive polarimetry with the
- NASA, (2014), SMAP Handbook Soil Moisture Active Passive, Mapping Soil Moisture and freeze/Thaw from space, available from <https://smap.jpl.nasa.gov/mission/description/>
- Nielsen-Englyst, P. L., J. Høyer, L. Toudal Pedersen, C. Gentemann, E. Alerskans, T. Block, C. Donlon, (2018) Optimal Estimation of Sea Surface Temperature from AMSR-E., Remote Sens., 10, 229.
- Njoku, E. G., T. J. Jackson, V. Lakshmi, T. K. Chan and S. V. Nghiem, (2003), Soil moisture retrieval from AMSR-E, in IEEE Transactions on Geoscience and Remote Sensing, vol. 41, no. 2, pp. 215-229, doi: 10.1109/TGRS.2002.808243
- Nordbeck O., Duchossois G., Kohlhammer G., Andersson E., Diehl T., Dinessen F., Eriksson P., Flett D., Garric G., Gros J-C., Jacq F., Molch K., Nagler T., Nicolas J., Strobl P. (2021) User Requirements for a Copernicus Polar Observing System– Phase 3 Report - Towards Operational Products and Services. ISBN: 978-92-76-34378-3 DOI 10.2889/90647
- Olmedo, E., I. Taupier-Letage, A. Turiel, and A. Alvera-Azcárate, (2018), Improving SMOS Sea Surface Salinity in the Western Mediterranean Sea through Multivariate and Multifractal Analysis. Remote Sens., 10, 485.
- Olmedo, E., J. Martínez, A. Turiel, J. Ballabrera-Poy, M. Portabella, (2017), Debiased non-Bayesian retrieval: A novel approach to SMOS Sea Surface Salinity, In Remote Sensing of Environment, Volume 193, 2017, Pages 103-126, ISSN 0034-4257, <https://doi.org/10.1016/j.rse.2017.02.023>.

- OSI-SAF, (2017), Improving the effective temperature estimation over sea ice using low frequency microwave radiometer data and Arctic buoys.
- Owe, M., De Jeu, R., & Walker, J. (2001). A methodology for surface soil moisture and vegetation optical depth retrieval using the microwave polarization difference index. *IEEE Transactions on Geoscience and Remote Sensing*, 39, 1643-1654.
- Owe, M., De Jeu, R., Holmes, T. (2008). Multisensor Historical Climatology of Satellite-Derived Global Land Surface Moisture. *Journal of Geophysical Research*. 113. 10.1029/2007JF000769.
- Parrens, M., Al Bitar, A., Frappart, F., Papa, F., Calmant, S., Crétaux, J. F., and Kerr, Y. (2017). Mapping dynamic water fraction under the tropical rain forests of the amazonian basin from smos brightness temperatures. *Water*, 9(5), 350.
- Pațilea, C., Heygster, G., Huntemann, M., and Spreen, G.: Combined SMAP/SMOS Thin Sea Ice Thickness Retrieval, *The Cryosphere Discuss.*, <https://doi.org/10.5194/tc-2017-168>, in review, 2017.
- Pearson, K. J., C. J. Merchant, O. Embury and C. Donlon, (2018), The Role of Advanced Microwave Scanning Radiometer 2 Channels Within an Optimal Estimation Scheme for Climate Data Records of Sea Surface Temperature, *Remote Sens.* 2018, 10, 90; doi:10.3390/rs10010090
- Pedersen, L. T., Saldo, R., Ivanova, N., Kern, S., Heygster, G., Tonboe, R., Huntemann, M., Ozsoy, B., Arduuin, F., and Kaleschke, L. (2018), Reference dataset for sea ice concentration, <https://doi.org/10.6084/m9.figshare.6626549.v3>.
- Perovich, D. K. (1996). The optical properties of sea ice (no. MONO-96-1). Hanover, NH: Cold regions research and engineering lab.
- Picard, G., L. Brucker, A. Roy, F. Dupont, M. Fily, and A. Royer (2013). Simulation of the microwave emission of multi-layered snowpacks using the dense media radiative transfer theory: the DMRT-ML model. *Geosci Model Devel*, 6, 1061-1078.
- Picard, G., Sandells, M., and Löwe, H. (2018). SMRT: an active–passive microwave radiative transfer model for snow with multiple microstructure and scattering formulations (v1.0), *Geosci. Model Dev.*, 11, 2763–2788, <https://doi.org/10.5194/gmd-11-2763-2018>.
- Piepmeier et al., (2016), SMAP L-Band Microwave Radiometer: Instrument Design and First Year on Orbit, *IEEE Transactions On Geoscience And Remote Sensing*, Vol. 55, NO. 4.
- Poe, G. A., (1990), Optimum interpolation of imaging microwave radiometer data, *IEEE Trans. on Geoscience and Remote Sensing*, GE-28, pp. 800-810.
- Preston-Thomas, H, (1990), The International Temperature Scale of 1990 (ITS-90), *Metrologia* 27, 107 (1990).
- Prigent, C., C. Jimenez & P. Bousquet, J (2019), Satellite-derived global surface water extent and dynamics over the last 25 years (GIEMS-2), *Journal of Geophysical Research: Atmospheres*.
- Prigent, C., F. Aires, F. Bernardo, J.-C. Orlhac, J.-M. Goutoule, H. Roquet, and C. Donlon (2013), Analysis of the potential and limitations of microwave radiometry for the retrieval of sea surface temperature: Definition of MICROWAT, a new mission concept, *J. Geophys. Res. Oceans*, 118, 3074–3086, doi:10.1002/jgrc.20222.
- Prigent, C., Jimenez, C., & Aires, F. (2016). Toward “all weather,” long record, and real-time land surface temperature retrievals from microwave satellite observations. *Journal of Geophysical Research Atmospheres*, 121(10), 5699-5717.

- Prigent, C., Matthews, E., Aires, F., and Rossow, W. B. (2001). Remote sensing of global wetland dynamics with multiple satellite data sets. *Geophysical Research Letters*, 28(24), 4631-4634.
- Prigent, C., Papa, F., Aires, F., Jimenez, C., Rossow, W. B., and Matthews, E. (2012). Changes in land surface water dynamics since the 1990s and relation to population pressure. *Geophysical Research Letters*, 39(8).
- Pulliainen, J. (2006). Mapping of snow water equivalent and snow depth in boreal and sub-arctic zones by assimilating space-borne microwave radiometer data and ground-based observations. *Remote Sens. Environ.*, 101, 257-269.
- Pulliainen, J. and M. Hallikainen, (2001), Retrieval of Regional Snow Water Equivalent from Space-Borne Passive Microwave Observations, In *Remote Sensing of Environment*, Volume 75, Issue 1, Pages 76-85, ISSN 0034-4257, [https://doi.org/10.1016/S0034-4257\(00\)00157-7](https://doi.org/10.1016/S0034-4257(00)00157-7).
- Pulliainen, J. T., J. Grandell, and M. T. Hallikainen (1999). HUT Snow Emission Model and its Applicability to Snow Water Equivalent Retrieval. *IEEE Trans. Geosci. Remote Sens.*, 37(3), 1378-1390.
- Pulliainen, J., J.-P. Kärnä, and M. T. Hallikainen (1993). Development of geophysical retrieval algorithms for the MIMR. *IEEE Trans. Geosci. Remote Sens.*, 31, 268–277.
- Purdy, W., P. Gaiser, G. Poe E. Uliana, T. Meissner, and F. Wentz, (2006) Geolocation and pointing accuracy analysis for the WindSat sensor, *IEEE TGRS*, vol. 44(3), pp 496-505.
- Quilfen, Y., Prigent, C., Chapron, B., Mouche, A. A., and Houti, N. (2007), The potential of QuikSCAT and WindSat observations for the estimation of sea surface wind vector under severe weather conditions, *J. Geophys. Res.*, 112, C09023, doi:10.1029/2007JC004163.
- Rahmstorf S., (2002), Ocean circulation and climate during the past 120,000 years, *Nature* volume 419, pages 207–214.
- Rasmussen, E., and J. Turner, Eds., 2003: Polar Lows. Cambridge University Press, 612 pp.
- Rautiainen, K., Parkkinen, T., Lemmetyinen, J. et al. (2016), SMOS prototype algorithm for detecting autumn soil freezing. *Remote Sensing of Environment*, SMOS special issue 180:346-360.
- Reul, N., B. Chapron, E. Zabolotskikh, C. Donlon, A. Mouche, J. Tenerelli, F. Collard, J.F. Piolle, A. Fore, S. Yueh, J. Cotton, P. Francis, Y. Quilfen, and V. Kudryavtsev, (2017), A New Generation of Tropical Cyclone Size Measurements from Space. *Bull. Amer. Meteor. Soc.*, 98, 2367–2385, <https://doi.org/10.1175/BAMS-D-15-00291.1>
- Reul, N., B. Chapron, E. Zabolotskikh, C. Donlon, Y. Quilfen, S. Guimbard, and J. F. Piolle, (2016), A revised L-band radio-brightness sensitivity to extreme winds under tropical cyclones: The five year SMOS-storm database. *Remote Sens. Environ.*, 180, 274–291, doi:<https://doi.org/10.1016/j.rse.2016.03.011>.
- Reul, N., J. Tenerelli, B. Chapron, D. Vandemark, Y. Quilfen, and Y. Kerr (2012b), SMOS satellite L-band radiometer: A new capability for ocean surface remote sensing in hurricanes, *J. Geophys. Res.*, 117, C02006, doi:10.1029/2011JC007474.
- Reul, N., J. Tenerelli, J. Boutin, B. Chapron, F. Paul, E. Brion, F. Gaillard, and O. Archer (2012a), Overview of the first SMOS sea surface salinity products. Part I: Quality assessment for the second half of 2010, *IEEE Trans. Geosci. Remote Sens.*, 50(5), 1636–1647, doi:10.1109/TGRS.2012.2188408.

- Reul, N., J. Tenerelli, N. Flouri, and B. Chapron, (2008). Earth-Viewing L-Band Radiometer Sensing of Sea Surface Scattered Celestial Sky Radiation—Part II: Application to SMOS. *IEEE TGRS*, vol.46(3), pp. 1 – 14, doi: 10.1109/TGRS.2007.914804.
- Reul, N., Tenerelli, J., Chapron, B., & Waldteufel, P. (2007). Modeling sun glitter at L-band for sea surface salinity remote sensing with SMOS. *IEEE Transactions on Geoscience and Remote Sensing*, 45(7), 2073– 2087. <https://doi.org/10.1109/tgrs.2006.890421>
- Ricciardulli, L., Meissner, T., and Wentz, F. (2012), Towards a climate data record of satellite ocean vector winds, *Proceedings of the 2012 IEEE International Geoscience and Remote Sensing Symposium* (Munich: IEEE).
- Richter, F., M. Drusch, L. Kaleschke, N. Maaß, X. Tian-Kunze, and S. Mecklenburg, (2018), Arctic sea ice signatures: L-band brightness temperature sensitivity comparison using two radiation transfer models, *The Cryosphere*, 12, 921-933, <https://doi.org/10.5194/tc-12-921-2018>.
- Rio, M.-H., Santoleri R., (2018), Improved global surface currents from the merging of altimetry and Sea Surface Temperature data, *Remote Sensing of Environment*, ISSN 0034-4257, <https://doi.org/10.1016/j.rse.2018.06.003>.
- Roberts, J. et al. (2016), Evolution of South Atlantic density and chemical stratification across the last deglaciation, *PNAS* (2016). DOI: 10.1073/pnas.1511252113
- Robinson, W. D., C. Kummerow, and W. S. Olson, (1992), A technique for enhancing and matching the resolution of microwave measurements from the SSM/I instrument, *IEEE Trans. Geosci. Remote Sens.*, 30, 419-429, 1992.
- Rodríguez-Fernández, N., de Rosnay, P., Albergel, C., Richaume, P., Aires, F., Prigent, C., and Kerr, Y. (2019). SMOS Neural Network Soil Moisture Data Assimilation in a Land Surface Model and Atmospheric Impact. *Remote Sensing*, 11(11), 1334.
- Rodriguez-Fernandez, N.J., F. Aires, P. Richaume, F. Cabot, C. Jimenez, J. Kerr, J. Kolassa, A. Mahmoodi, C. Prigent, and M. Drush, (2015), Soil moisture retrieval from SMOS observations using neural networks, *IEEE TGRS*, doi:10.1109/TGRS.2015.2430845, 2015.
- Rodríguez-Fernández, N.J., Mialon, A., Mermoz, S., Bouvet, A., Richaume, P., Al Bitar, A., Al-Yaari, A., Brandt, M., Kaminski, T., Le Toan, T., Kerr, Y.H., and Wigneron, J.P. (2018). An evaluation of SMOS L-band vegetation optical depth (L-VOD) data sets: high sensitivity of L-VOD to above-ground biomass in Africa. *Biogeosciences*, 15, 4627-4645
- Rostan, T., D. Ulrich, S. Rieger and A. Østergaard, (2016), MetOp-SG SCA wind scatterometer design and performance, *IEEE International Geoscience and Remote Sensing Symposium (IGARSS)*, Beijing, 2016, pp. 7366-7369. doi: 10.1109/IGARSS.2016.7730921
- Rostosky, P., Spreen, G., Farrell, S. L., Frost, T., Heygster, G., & Melsheimer, C. (2018). Snow depth retrieval on Arctic sea ice from passive microwave Radiometers - Improvements and extensions to multiyear ice using lower frequencies. *Journal of Geophysical Research: Oceans*, 123. <https://doi.org/10.1029/2018JC014028>.
- Roy, A., A. Royer, J.-P. Wigneron, A. Langlois, J. Bergeron, and P. cliché, (2012), A simple parameterization for a boreal forest radiative transfer model at microwave frequencies. *Remote Sens. Environ.*, 124, 371-383.
- Rosenkranz, P. W. (2017). Line-by-line microwave radiative transfer (non-scattering). *Remote Sensing Code Library*, <https://doi.org/10.21982/M.81013>.
- Rubino, R.; Duffo, N.; González-Gambau, V.; Corbella, I.; Torres, F.; Durán, I.; Martín-Neira, M, (2020), Deriving VTEC Maps from SMOS Radiometric Data. *Remote Sens.*, 12, 1604.

- Ruf, C., (1998), Constraints on the polarization purity of a Stokes microwave radiometer, *Radio Science*, Volume 33, 6, Pages 1 617-1639.
- Sakov, P., Counillon, F., Bertino, L., Lisæter, K. A., Oke, P. R., and Koralev, A. (2012), TOPAZ4: an ocean-sea ice data assimilation system for the North Atlantic and Arctic, *Ocean Sci.*, 8, 633-656, <https://doi.org/10.5194/os-8-633-2012>.
- Sampson, C., and A. Schrader, (2000), The automated tropical cyclone forecasting system (Version 3.2). *Bull. Amer. Meteor. Soc.*, 81(6), 1231-1240, doi: 10.1175/1520-0477(2000)081
- Sanò, P.; Panegrossi, G.; Casella, D.; Marra, A.C.; D'Adderio, L.P.; Rysman, J.F.; Dietrich, S. (2018), The Passive Microwave Neural Network Precipitation Retrieval (PNPR) Algorithm for the CONICAL Scanning Global Microwave Imager (GMI) Radiometer. *Remote Sens.* , 10, 1122.
- Saunders, R., Hocking, J., Turner, E., Rayer, P., Rundle, D., Brunel, P., Vidot, J., Roquet, P., Matricardi, M., Geer, A., Bormann, N., and Lupu, C., (2018). An update on the RTTOV fast radiative transfer model (currently at version 12), *Geosci. Model Dev.*, 11, 2717-2737, <https://doi.org/10.5194/gmd-11-2717-2018>.
- Schmitt, A.U., L. Kaleschke, (2018), A Consistent Combination of Brightness Temperatures from SMOS and SMAP over Polar Oceans for Sea Ice Applications. *Remote Sens.*, 10, 553.
- Schwank, M; Kontu, A; Mialon, A; Naderpour, R; Houtz, D; Lemmetyinen, J; Rautiainen, K; Li, QH; Richaume, P; Kerr, Y; Matzler, C, (2021). Temperature effects on L-band vegetation optical depth of a boreal forest, *Remote Sens. Environ.*, 263, 112542, doi: 10.1016/j.rse.2021.112542.
- Scott, K. A., E. Li and A. Wong, (2014), Sea Ice Surface Temperature Estimation Using MODIS and AMSR-E Data Within a Guided Variational Model Along the Labrador Coast," in *IEEE Journal of Selected Topics in Applied Earth Observations and Remote Sensing*, vol. 7, no. 9, pp. 3685-3694, doi: 10.1109/JSTARS.2013.2292795
- Screen, J. A. and I. Simmonds, (2010), the central role of diminishing sea ice in recent Arctic temperature amplification, *Nature*, 464, 1334-
- Serreze, M. C. and Francis, J. A, (2006), The Arctic amplification debate. *Clim. Change* 76, 241–264.
- Seung-Bum, Kim, Frank J. Wentz, and Gary S. E. Lagerloef, (2011), Effects of Antenna Cross-Polarization Coupling on the Brightness Temperature Retrieval at L-Band, *IEEE Trans. Reosci. Re. Sens.*, 49, 5, 1637-
- Skoglund, T., Lomeland, S., & Goksoyr, J. (1988). Respiratory burst after freezing and thawing of soil: Experiments with soil bacteria. *Soil Biology and Biochemistry*, 20, 851–856.
- Smirnova, J.E., Zabolotskikh, E.V., Bobylev, L.P. et al. (2016), Statistical characteristics of polar lows over the Nordic Seas based on satellite passive microwave data, *Izv. Atmos. Ocean. Phys.* 52: 1128. <https://doi.org/10.1134/S001433816090255>
- Smith, D. M., (1996), Extraction of winter total sea-ice concentration in the Greenland and Barents Seas from SSM/I data, *International Journal of Remote Sensing*, 17:13, 2625-2646, DOI: 10.1080/01431169608949096
- Smith, S., and J. Brown, (2009). Permafrost. Permafrost and seasonally frozen ground. Assessment of the status of the development of standards for the terrestrial essential climate variables. *Global Terrestrial Observing System*, (22 pp., version 13, 8 May 2009, Rome, 2009).

- Soldo, Y., D. M. Le Vine and E. Dinnat, (2019), SMAP Observations of the Fourth Stokes Parameter At L-Band, IGARSS 2019 - 2019 IEEE International Geoscience and Remote Sensing Symposium, Yokohama, Japan, pp. 8407-8410, doi: 10.1109/IGARSS.2019.8900153.
- Soldo, Y., D. M. Le Vine, P. de Matthaeis and P. Richaume, (2017), L-Band RFI Detected by SMOS and Aquarius, in IEEE Transactions on Geoscience and Remote Sensing, vol. 55, no. 7, pp. 4220-4235, July 2017. doi: 10.1109/TGRS.2017.2690406
- Spreen, G., L. Kaleschke, and G. Heygster (2008), Sea ice remote sensing using AMSR-E 89-GHz channels, J. Geophys. Res., 113, C02S03, doi:10.1029/2005JC003384.
- Stephen, K, (2018), Societal Impacts of a rapidly changing Arctic, Current Climate Change Reports (2018) 4:223–237, <https://doi.org/10.1007/s40641-018-0106-1>
- Stogryn, A., (1978), Estimates of brightness temperatures from scanning radiometer data, IEEE Trans. on Antennas Propagation, AP-26, pp. 720-726.
- Stroeve, J. C., M. C. Serreze, M. M. Holland, J. E. Kay, J. Malanik, and A. P. Barrett, (2012), The Arctic's rapidly shrinking sea ice cover: A research synthesis, Climatic Change, vol. 110, nos. 3–4, pp. 1005–1027.
- Stroeve, J.C., T. Markus, J. A. Maslanik, D. J. Cavalieri, A. J. Gasiewski, J. F. Heinrichs, J. and M. Sturm, M., (2006), Impact of Surface Roughness on AMSR-E Sea Ice Products. IEEE Trans Geosci. Re, Sens., 44 (11), 3103-3117. doi:10.1109/TGRS.2006.880619
- Sturm, M., and R. Massom, (2010), Snow on sea ice. In D. Thomas and G. Dieckmann (Eds.), Sea ice (2nd ed), (pp. 153–204). Oxford, UK: Wiley-Blackwell.
- Sumata, H., T. Lavergne, F. Girard-Ardhuin, N. Kimura, M. A. Tschudi, F. Kauker, M. Karcher, and R. Gerdes (2014), An intercomparison of Arctic ice drift products to deduce uncertainty estimates, J. Geophys. Res. Oceans, 119, 4887–4921, doi:10.1002/2013JC009724
- Svendsen, E., K. Kloster, B. Farrelly, O. M. Johannessen, J. A. Johannessen, W. J. Campbell, P. Gloersen, D. Cavalieri, and C. Matzler, (1983), Norwegian remote sensing experiment: Evaluation of the NIMBUS 7 Scanning Multichannel Microwave Radiometer for sea ice research, J. Geophys. Res., 88(C5), 2781 – 2791.
- Svendsen, E., Matzler, C., and Grenfell, Th. (1987), A model for retrieving total sea ice concentration from a spaceborne dual-polarized passive microwave instrument operating near 90 GHz, Int. J. Remote Sens., 8, 1479–1487.
- Swift, C.T., D.J. Cavalieri, P. Gloersen, H.J. Zwally, N.M. Mognard, W.J. Campbell, L.S. Fedor, S. Peteherych, (1995), Observations of the Polar Regions from Satellites using Active and Passive Microwave Techniques, in Saltzman, B (Ed.), Advances in Geophysics, 27, 335-392, [https://doi.org/10.1016/S0065-2687\(08\)60409-4](https://doi.org/10.1016/S0065-2687(08)60409-4).
- Takala M., K. Luojus, J. Pulliainen, C. Derksen, J. Lemmetynen, J.-P. Kärnä, J. Koskinen and B. Bojkov, (2011), Estimating northern hemisphere snow water equivalent for climate research through assimilation of space-borne radiometer data and ground-based measurements. Remote Sensing of Environment, 115, 3517-3529.
- Takala, M., J. Pulliainen, S. Metsämäki and J. Koskinen, (2009), Detection of Snowmelt Using Spaceborne Microwave Radiometer Data in Eurasia From 1979 to 2007. IEEE Transactions on Geoscience and Remote Sensing, 47 (9), 2996-3007.
- Tedesco, M., and J. Jeyaratnam, (2016), A new operational snow retrieval algorithm applied to historical AMSR-E brightness temperatures. Remote Sens., 8, 1037; doi: 10.3390/ns8121037.

- Tenerelli, J., Reul, N., Mouche, A. A., and Chapron, B. (2008). Earth-viewing L-band radiometer sensing of sea surface scattered celestial sky radiation, Part I: General characteristics. *IEEE Transactions on Geoscience and Remote Sensing*, 46(3), 659– 674. <https://doi.org/10.1109/tgrs.2007.914803>
- Teubner, I.E., Forkel, M., Jung, M., Liu, Y.Y., Miralles, D.G., Parinussa, R., van der Schalie, R., Vreugdenhil, M., Schwalm, C.R., Tramontana, G., Camps-Valls, G., Dorigo, W., (2018), Assessing the relationship between microwave vegetation optical depth and gross primary production. *International Journal of Applied Earth Observation and Geoinformation* 65, 79– 91.<https://doi.org/10.1016/j.jag.2017.10.006>
- Tian-Kunze, X., Kaleschke, L., Maaß, N., Mäkynen, M., Serra, N., Drusch, M., and Krumpen, T. (2014), SMOS-derived thin sea ice thickness: algorithm baseline, product specifications and initial verification, *The Cryosphere*, 8, 997-1018, <https://doi.org/10.5194/tc-8-997-2014>.
- Tietsche S., M. A. Balmaseda, P. de Rosnay, H. Zuo, X. Tian-Kunze, and L. Kaleschke (2018), Thin sea ice in the Arctic: comparing L-band radiometry retrievals with an ocean reanalysis. *The Cryosphere*, 12, 2051-2072, doi: 10.5194/tc-2017-247
- Tonboe, R. T., Eastwood, S., Lavergne, T., Sørensen, A. M., Rathmann, N., Dybkjær, G., Pedersen, L. T., Høyer, J. L., and Kern, S., (2016), The EUMETSAT sea ice concentration climate data record, *The Cryosphere*, 10, 2275-2290, <https://doi.org/10.5194/tc-10-2275-2016>.
- Tonboe, R., G. Dybkjaer and J. L. Hoeyer, (2011), Simulations of the snow covered sea ice surface temperature and microwave effective temperature, *Tellus A: Dynamic Meteorology and Oceanography*, 63:5,1028-1037, DOI: 10.1111/j.1600-0870.2011.00530.x
- Tsang, L., C.-T. Chen, A. T. C. Chang, J. Guo, and K.-H. Ding, (2000), Dense media radiative transfer theory based on quasi-crystalline approximation with applications to microwave remote sensing of snow. *Radio Sci.*, 35(3), 731 - 749.
- Tsang, L., J. A. Kong, and R. T. Shin, (1985), *Theory of Microwave Remote Sensing*. New York: Wiley.
- Tsutsui, H.; Maeda, T. (2017), Possibility of Estimating Seasonal Snow Depth Based Solely on Passive Microwave Remote Sensing on the Greenland Ice Sheet in Spring. *Remote Sens.*, 9, 523.
- UNESCO, (1985), The international system of units (SI) in oceanography, UNESCO Technical Papers No. 45, IAPSO Pub. Sci. No. 32, Paris, France.
- Uranga, E., A. Llorente, R. Oliva, A. de la Fuente, E. Daganzo and Y. Kerr, "Monitoring of Smos Rfi Sources in the 1400-1427mhz Passive Band," IGARSS 2018 - 2018 IEEE International Geoscience and Remote Sensing Symposium, 2018, pp. 1241-1244, doi: 10.1109/IGARSS.2018.8517676.
- Vihma, T., (2014), Effects of Arctic sea ice decline on weather and climate: A review, *Surveys Geophys.*, vol. 35, no. 5, pp. 1175–1214.
- Wagner, W. G. Lemoine, and H. Rott, (1999), A Method for Estimating Soil Moisture from ERS Scatterometer and Soil Data. *Rem. Sens. of Env.*, vol.70, 191-207.
- Walker, N.; Partington, K.; Van Woert, M.; Street, T. (2006), Arctic sea ice type and concentration mapping using passive and active microwave sensors. *IEEE Trans. Geosci. Remote Sens.* 44, 3574–3584.
- Warren, S. G., Rigor, I. G., Untersteiner, N., Radionov, V. F., Bryazgin, N. N., Aleksandrov, Y. I., and Colony, R. (1999), Snow depth on Arctic sea ice, *J. Climate*, 12, 1814–1829.

- Watanabe, M., G. Kadosaki, Y. Kim, M. Ishikawa, K. Kushida, Y. Sawada, T. Tadono, M. Fukuda, M. Sato (2011), Analysis of the sources of variation in L-band backscatter from terrains with permafrost, IEEE Trans. Geosci. Remote Sens., 50 (1) , pp. 44-54
- Wentz F. J. and T. Meissner, (2007), Supplement 1: Algorithm theoretical basis document for AMSR-E ocean algorithms, Remote Sens. Syst., Santa Rosa, CA, USA, Tech. Rep. 051707.
- Wentz F. J. and T. Meissner, (2016), Atmospheric absorption model for dry air and water vapor at microwave frequencies below 100 GHz derived from spaceborne radiometer observations, Radio Sci., vol. 51, no. 5, pp. 381–391.
- Wentz, F. J. and T. Meissner, (2000), Algorithm theoretical basis document (ATBD) version 2 AMSR ocean algorithm, Remote Sens. Syst., Santa Rosa, CA, USA, Tech. Rep. 121599A-1.
- Wentz, F. J., (1997), A well-calibrated ocean algorithm for special sensor microwave/imager, J. Geophys. Res., vol. 102, no. C4, pp. 8703–8718.
- Wentz, F. J., C. Gentemann, D. Smith, and D. Chelton, (2000), Satellite measurements of sea surface temperature through clouds, Science, vol. 288, no. 5467, pp. 847–850, May 2000.
- Werner, K., M. Fritz, N. Morata, K. Keil, A. Pavlov, I. Peeken, A. Nikolopoulos, H. S. Findlay, M. Kędra, S. Majaneva, A. Renner, S. Hendricks, M. Jacquot, M. Nicolaus, M. O'Regan, M. Sampei, C. Wegner, (2016), Arctic in Rapid Transition: Priorities for the future of marine and coastal research in the Arctic, Polar Science, Volume 10, Issue 3, 364-373, <https://doi.org/10.1016/j.polar.2016.04.005>.
- Wiebe, H., G. Heygster and L. Meyer-Lerbs, (2008), Geolocation of AMSR-E Data. IEEE Trans. Geosci. and Remote Sensing 46(10), p. 3098-3103, doi:10.1109/TGRS.2008.919272.
- Wiesmann, A., and C. Mätzler, (1999), Microwave emission model of layered snowpacks. Remote Sens. Environ., 70(3) 307 - 316.
- Wilheit, T.T. and A. T. C. Chang, (1980), An algorithm for retrieval of ocean surface and atmospheric parameters from the observations of the scanning multichannel microwave radiometer. Radio Sci. 15, 525–544.
- WindSat instrument, IEEE Trans. Geosci. Remote Sens., vol. 45, no. 7, pp. 2019–2028,
- WMO, (2017), Sea-Ice Information Services in the World, Edition 2017 (last revision 2017-08-02), WMO-No. 574 available from http://www.jcomm.info/index.php?option=com_oe&task=viewDocumentRecord&docID=9607
- Xie, J., Counillon, F., Bertino, L., Tian-Kunze, X., and Kaleschke, L. (2016), Benefits of assimilating thin sea ice thickness from SMOS into the TOPAZ system, The Cryosphere, 10, 2745-2761, <https://doi.org/10.5194/tc-10-2745-2016>, 2016.
- Yamazaki D., D. Ikeshima, J. Sosa, P.D. Bates, G.H. Allen, T.M. Pavelsky, (2019). MERIT Hydro: A high-resolution global hydrography map based on latest topography datasets Water Resources Research, vol.55, pp.5053-5073, [doi:10.1029/2019WR024873](<https://doi.org/10.1029/2019WR024873>)
- Ye Y. and G. Heygster, (2016b), Arctic Multiyear Ice Concentration Retrieval from SSM/I Data Using the NASA Team Algorithm with Dynamic Tie Points. In: Lohmann G., Meggers H., Unnithan V., Wolf-Gladrow D., Notholt J., Bracher A. (eds) Towards an Interdisciplinary Approach in Earth System Science. Springer Earth System Sciences. Springer, Cham., https://doi.org/10.1007/978-3-319-13865-7_12

- Ye, Y., M. Shokr, G. Heygster, and G. Spreen, (2016a), Improving Multiyear Sea Ice Concentration Estimates with Sea Ice Drift. *Remote Sens.* 2016, 8, 397.
- Yueh, S. H., (1997), Modeling of wind direction signals in polarimetric sea surface brightness temperatures, *IEEE Trans. Geosci. Remote Sens.*, vol. 35, no. 6, pp. 1400–1418.
- Yueh, S. H., (2000), Estimates of Faraday rotation with passive microwave polarimetry for microwave remote sensing of Earth surfaces,” *IEEE Trans. Geosci. Remote Sens.*, vol. 38, no. 5, pp. 2434–2438.
- Yueh, S. H., R. West, W. J. Wilson, F. K. Li, E. G. Njoku and Y. Rahmat-Samii, (2001), Error sources and feasibility for microwave remote sensing of ocean surface salinity, in *IEEE Transactions on Geoscience and Remote Sensing*, vol. 39, no. 5, pp. 1049-1060,. doi: 10.1109/36.921423
- Yueh, S. H., W. J. Wilson, S. J. Dinardo, and S. V. Hsiao, (2006), Polarimetric microwave wind radiometer model function and retrieval testing for WindSat, *IEEE Trans. Geosci. Remote Sens.*, vol. 44, no. 3, pp. 584–596.
- Yueh, S., W. Tang, A. Fore, A. Hayashi, Y. T. Song, and G. Lagerloef (2014), Aquarius geophysical model function and combined active passive algorithm for ocean surface salinity and wind retrieval, *J. Geophys. Res. Oceans*, 119, 5360–5379, doi:10.1002/2014JC009939.
- Zabolotskikh, E. and B. Chapron, (2017), Improvements in Atmospheric Water Vapor Content Retrievals Over Open Oceans from Satellite Passive Microwave Radiometers, in *IEEE Journal of Selected Topics in Applied Earth Observations and Remote Sensing*, vol. 10, no. 7, pp. 3125-3133. doi: 10.1109/JSTARS.2017.2671920
- Zabolotskikh, E. V., (2019), Review of Methods to Retrieve Sea-Ice Parameters from Satellite Microwave Radiometer Data, *Izvestiya, Atmospheric and Oceanic Physics*, 2019, Vol. 55, No. 1, pp. 109–127.
- Zabolotskikh, E. V., Mitnik, L. M., and Chapron, B., (2013). New approach for severe marine weather study using satellite passive microwave sensing, *Geophys. Res. Lett.*, 40, 3347– 3350, doi:10.1002/grl.50664.
- Zabolotskikh, E., G. Irina, A. Myasoedov and B. Chapron, (2016), Detection and study of the polar lows over the arctic sea ice edge, *IEEE International Geoscience and Remote Sensing Symposium (IGARSS)*, Beijing, 2016, pp. 7705-7707. doi: 10.1109/IGARSS.2016.7731009
- Zaussinger, F., Dorigo, W., Gruber, A., Tarpanelli, A., Filippucci, P., Brocca, L. (2019). Estimating irrigation water use over the contiguous United States by combining satellite and reanalysis soil moisture data. *Hydrology and Earth System Sciences* 23, 897–923. <https://doi.org/10.5194/hess-23-897-2019>
- Zhang, Z., Y. Yu, X. Li, F. Hui, X. Cheng and Z. Chen, (2019), Arctic Sea Ice Classification Using Microwave Scatterometer and Radiometer Data During 2002–2017, *IEEE Transactions on Geoscience and Remote Sensing*, vol. 57, no. 8, pp. 5319-5328, Aug. doi: 10.1109/TGRS.2019.2898872
- Zhao, E. C. Gao, X. Jiang, and Z. Liu, (2017), Land surface temperature retrieval from AMSR-E passive microwave data, *Opt. Express*, 25, A940-A952.
- Zheng, J., T. Geldsetzer, and J. Yackel, (2017), Snow thickness estimation on first-year sea ice using microwave and optical remote sensing with melt modelling, In *Remote Sensing of Environment*, Volume 199, 2017, Pages 321-332, ISSN 0034-4257, <https://doi.org/10.1016/j.rse.2017.06.038>.

- Zhang, T., Barry, R. G., Knowles, K., Ling F., & Armstrong, R.L. (2003). Distribution of seasonally and perennially frozen ground in the Northern Hemisphere. In Phillips, M., S.M. Springman, and L.U. Arenson (Eds.), Proceedings of the 8th International Conference on Permafrost, 21-25. Zurich, Switzerland (pp 1289-1294). Lisse, the Netherlands: A.A. Balkema.
- Zhou, L., Xu, S., Liu, J., and Wang, B., (2018), On the retrieval of sea ice thickness and snow depth using concurrent laser altimetry and L-band remote sensing data, *The Cryosphere*, 12, 993-1012, <https://doi.org/10.5194/tc-12-993-2018>.

9 APPENDIX I. DEFINITION OF TERMS

Absolute Performance Error (APE): difference between the target (commanded) parameter (e.g., attitude, geolocation etc) and the actual parameter in a specified reference frame (ESSB-HB-E-003, 2011).

Absolute Knowledge Error (AKE): difference between an actual parameter (e.g., attitude, geolocation etc.) and the known (measured or estimated) parameter in a specified reference frame (ESSB-HB-E-003, 2011).

Absolute Radiometric Accuracy (ARA): see Total Standard Uncertainty.

Adjacent Seas: encompass all Seas and water bodies adjacent to the Arctic that are influenced by sea ice including Gulf of Bothnia, Gulf of Finland, Baltic Sea, Caspian Sea, Sea of Azov (Black Sea), Bering Sea, Sea of Okhotsk, northern Yellow Sea, Bohai Sea, Baikal Lake, Labrador Sea, Gulf of St Lawrence, American Great Lakes, Gulf of Alaska,

Along track direction: direction parallel to the projection of the spacecraft velocity on the tangent plane to the Earth at the geodetic sub-satellite position (See Observation Zenith Angle that shows a figure).

Along scan direction: direction parallel to the projection of the spacecraft velocity on the tangent plane to the Earth at the geodetic sub-satellite position

Altitude: the satellite altitude is the shortest distance from the satellite centre of mass to the Earth surface.

Note 1: The reference altitude is defined here as the difference between the mean semi-major axis of a circular orbit having the orbital period specified by the repeat cycle and the Earth's equatorial radius. The satellite altitude differs from the reference altitude, depending on the satellite's location along its orbit.

Ancillary Data: data acquired on-board in support of the observation data, both for the instrument and the platform, such as calibration and timing data.

Instrument Ancillary data: data generated on-board by the instrument in support of the observation data, such as calibration, timing for each line acquisition, compression ratio, data validity flag (e.g., nominal detector temperature), needed to process the measurement data on ground.

Platform Ancillary data: data acquired on-board by the platform in support of the observation data, such as orbit position, velocity and time, attitude (generated by the AOCS sensors) needed to process measurement data on ground. Depending on timing constraints (NRT1H, NRT3H product or not), these data will be post-processed on-ground to improve the accuracy of orbit and attitude restitution.

Ascending Node Crossing (ANX): the latest crossing of the equator by the satellite going from South to North.

Availability: Availability is defined as the probability that the space segment (including the link to the ground segment) provides all the required data with their nominal quality and within the specified timeliness.

All sources of unavailability after acquisition of the operational orbit and commissioning, validation and initial calibration shall be considered. Examples are planned and unplanned orbital excursions (e.g., manoeuvres required for orbit control and maintenance if incompatible with image

acquisition), atmospheric effects (e.g., leading to space-to-ground link outages), single event upsets due to cosmic ray effects, time spent in safe mode.

The space segment availability covers the instrument itself and all on-board elements needed to support the instrument, including the satellite data chain and the downlink transmission.

The availability of ground segment is assumed to be 100%.

Azimuth (angle): the angle in the xy plane from -y axis to the projection of the pointing direction in the xy plane; the angle direction is taken from -y axis to -x axis (see figure in definition of Elevation angle and also Figure MRD-4.2.4(b)).

Bandwidth: difference between the upper and lower frequencies in a continuous set of frequencies.

Beam Efficiency (η_{be}): the ratio between the received power (including co- and x-polar radiation) in the main beam and the total received power (including co- and x-polar radiation) over the full sphere:

$$\eta_{be} = \frac{\int_0^{2\pi} \int_0^{\theta_1} (|E_{co}(\theta, \varphi)|^2 + |E_x(\theta, \varphi)|^2) \sin\theta d\theta d\varphi}{\int_0^{2\pi} \int_0^{\pi} (|E_{co}(\theta, \varphi)|^2 + |E_x(\theta, \varphi)|^2) \sin\theta d\theta d\varphi}$$

where θ_1 equal to $2.5 \times \theta_{3dB}$ footprint are the electric field co-polar and cross-polar components.

Brightness temperature (Tb): a measurement of microwave radiation radiance traveling upward from the top of the atmosphere (TOA) to the satellite, expressed in units of the temperature of an equivalent black body. Tb is the fundamental parameter measured by the CIMR radiometer. TOA Tb is specific to a satellite implementation and refers to the measurement made in a specific frequency band, at a given polarization, with a specific instrument viewing the earth using a specific geometry. For clarity this includes all emission, reflection and scattering processes and Faraday rotation effects at the antenna.

Calibration Mode: mode of operation defined to support the in-flight characterisation of the payload.

Calibration key data: required for processing the Level-0 to Level-1b data. Since the characteristics of the instrument can (and will) change over the mission, the calibration key data will change along with it. At launch, the calibration key data will consist of the data that is derived from on-ground calibration. During the mission the calibration key data will be updated with in-flight calibration data and adapted to match new insights in the instrument's performance.

Calibration key data set: a set of data products that contains the calibration key data for a given orbit. The calibration key data set can consist of several files containing the actual data, for example in HDF or NetCDF format, and a descriptive file, for example in XML, that specifies, which parameter can be found in which data file.

Channel: polarised measurement (HH, VV, HV or VH) for a given band.

Note 1: Thus, there are a minimum of two CIMR instrument channels (HH and VV) for each CIMR instrument band e.g., 18.7V and 18.7H.

Characterisation: the direct measurement, or analytical derivation from measurement, of a set of technical and functional parameters, over a range of conditions (e.g., temperature) to provide data necessary for calibration, ground processor initialisation and verification.

Note 1: Characterisation can be performed either before launch on-ground and/or in-flight. In-flight, at least all those parameters have to be determined that may have varied since on-ground characterisation or which have not been measurable on-ground. In-flight characterisation may be based either on data derived from facilities built into the instrument (internal calibration) and/or on external sources (external calibration).

Coastal Zone: 370 km offshore of the coastline.

Note 1: The definition used here corresponds to the exclusive economic zone (EEZ), as prescribed by the 1982 United Nations Convention on the Law of the Sea, is an area of the sea in which a sovereign state has special rights regarding the exploration and use of marine resources, including energy production from water and wind. It stretches from the outer limit of the territorial sea (12 nautical miles from the baseline) out to 200 nautical miles, (~370 km) from the coast of the state in question.

Note 2: Considering the largest footprint of CIMR (60 km for L-band) this definition means that at least 4 measurements will be available at this frequency in a 300 km limit roughly corresponding to the definition of the Coastal Zone.

Coastal Region: (including all small islands): is defined by product type. It shall be 3 x **footprint_size** each side of the Coastal Boundary based on the dominant frequency for a given product.

Note 1: The coastal region is defined (a) to manage distance to coast aspects and (b) to facilitate processing of land data that requires access to ocean measurements in the coastal region and vice versa (side-lobes and grating lobes) (c) to monitor geolocation at coastal boundaries (defined in MRD-852) (d) to allow a focus of specific processing and retrievals in coastal regions. (e) to allow a sufficient number of L-band large footprint measurements to be available for all these aspects.

Note 2: Considering the largest footprint of CIMR (60 km for L-band) this definition means that at least 4 measurements will be available at this frequency in a 300 km limit roughly corresponding to the definition of the Coastal Zone.

Commissioning: verification and validation activities conducted after the launch and before the entry in operational service either on the space segment only or on the overall system (including the ground segment).

Coverage: geographical area systematically acquired, disregarding cloud cover, sun glint and OZA conditions

Cross-Polarisation: radiation orthogonal to the desired polarisation (e.g., the cross-polarisation of a vertically polarised antenna is the horizontally polarised field).

Note 1: Cross- polarisation power refers to the total power received in cross-polarisation in the main beam of the antenna, divided by the total power received by the antenna (in co- and cross- polarisations).

Cycle: one full completion of an orbit repeat period. A cycle starts at the equator when combined with orbit numbers, at the southern rollover point in when combined with pass numbers.

Data Latency: the time interval from data acquisition by the instrument to delivery as Level 1b data product at the user segment interface.

Dynamic range: range of brightness temperatures within which requirements are to be met.

Dwell Time: time period required to acquire a spectral channel for a given spatial sample.

Earth: ellipsoid as defined in the WGS-84 geodetic datum.

Effective Coverage time: the time required to perform systematic acquisition of a given area with precipitation below a specified threshold and possibly under different observation conditions (in particular varying OZA or SZA).

Effective Revisit time: represents the period for systematic acquisition of the same area with precipitation below a specified threshold and under the same observation conditions (in particular same OZA).

Effective field of View (EFOV): area swept by the antenna beam during the integration time for s L1b measurement.

Elevation (angle): the angle between the instrument boresight and the satellite velocity direction.

Note 1: the complementary angle to elevation, theta (θ), is defined as $\theta = 90 - \text{elevation}$

End Of Life (EOL): this event occurs at the end of the system in-orbit lifetime.

Fiducial Reference Measurement (FRM): the suite of independent ground measurements that provide the maximum Scientific Utility and Return On Investment for a satellite mission by delivering, to users, the required confidence in data products, in the form of independent validation results and satellite measurement uncertainty estimation, over the duration of the mission. The defining mandatory characteristics of an FRM are:

- Have documented evidence of SI traceability via inter-comparison of instruments under operational-like conditions.
- Are independent from the satellite retrieval process.
- Include an uncertainty budget for all FRM instruments and derived measurements is available and maintained, traceable where appropriate to SI ideally directly through an NMI
- Are collected using measurement protocols and community-wide management practices (measurement, processing, archive, documents etc.) are defined and adhered to.
- FRM uncertainties should be fit for purpose (ie. be of a magnitude that is relevant to the application e.g., “Validation of satellite derived TSCV 0.1 ms^{-1} or better”).

First Year Ice: floating ice of no more than one year's growth developing from young ice; thickness from 0.3 to 2 meters (1 to 6.6 feet); characteristically level where undisturbed by pressure, but where ridges occur, they are rough and sharply angular.

Floe: Any relatively flat piece of sea ice 20 m or more across. Floes are subdivided according to horizontal extent (giant, vast, big, medium, small).

Footprint: intersection of an instantaneous channel antenna pattern at half the maximum power level (-3dB) along the instrument bore sight with the Earth's surface represented by the WGS-84 ellipsoid. (See Full beam for schematic)

Note 1 For conically scanning radiometers, in the ideal case where the antenna pattern contour at half power level is circular, the 3dB footprint contour is elliptical. The ellipse representing the 3dB footprint contour is defined as in the following:

Note 2: The major axis is defined by the straight-line segment connecting the two points at maximum distance lying on the footprint contour;

Note 3: The minor axis is a segment, orthogonal to the major axis, and passing through the centre of the major axis. Its length is the maximum distance between any two points lying on the footprint contour along the direction orthogonal to the major axis.

Note 4: In the case of CIMR, Footprint is synonymous with the instantaneous field of view.

Footprint Centre: Intersection of the direction of maximum gain of a channel antenna pattern along the instrument bore sight with the Earth's surface represented by the WGS-84 ellipsoid.

footprint_size: arithmetic mean of the major and minor axes of a Footprint.

Full Beam: angular region described by the antenna pattern including all side lobes.

Gain: see System Gain.

Geo-location: worst-case pixel localisation (to zero mean 1-sigma knowledge error) knowledge expressed in geodetic coordinates within a Level 1B image product.

Geo-location Accuracy: difference between the estimated barycentre position of any spatial sample and its true position projected onto the WGS84 reference Earth ellipsoid.

Geometrical Coverage time: represents the time required to perform systematic acquisition of a given area disregarding precipitation and possibly under different observation conditions (in particular varying OZA or SZA).

Geometrical Revisit time: represents the period for systematic acquisition of the same area disregarding precipitation and under the same observation conditions (in particular same OZA).

Global Ocean: all saline water surfaces over the globe, including large lakes and internal seas (e.g., Caspian Sea). See *definitions of Polar Regions, Adjacent Seas and Coastal Zone*.

Goal: a non-mandatory but highly desirable requirement, the implementation of which shall be studied to allow for an assessment of the system impacts. The implementation or not of the goal requirements will be decided by the Agency after analysis of the implications.

Ground Segment (Copernicus GS): element of the system that perform the functions of data processing, archiving and distribution to the users. They normally also perform the long-term calibration and control the quality and status of the instrument(s) and data products.

Half Power Beam-width (HPBW): angle at which the antenna's power radiation pattern is at half its maximum value.

Horizontal Polarisation (H): electric field is perpendicular to the plane of incidence.

Housekeeping Telemetry: refers to all non-science TM that is generated on-board, either on a periodic basis (Periodic Housekeeping TM) or as on-board events, or on request (report of parameters and tables, dump of memories, dump of data, etc.)

Ice Cover: floating ice covering a water area regardless of its age, concentration, mobility, and other characteristics. This is the most general notion, usually requiring further specification. The ice cover boundaries are the ice edge and the coastline.

Image: ensemble of data acquired over a two-dimensional scene with equal number of spatial samples in the cross and along track direction. The number of spatial samples in cross track is defined by the instrument swath and spatial sampling interval.

Image Navigation: the knowledge of the relationship between a spatial sample in instrument coordinates and the corresponding point on the Earth, given by latitude and longitude coordinates. In general, Image navigation refers to the methods employed to obtain that knowledge. Image navigation accuracy is a measure of how well that relationship is known. Image registration is an indication as to how well that navigation knowledge is maintained and controlled over time.

Image swath: maximum distance on ground between the positions of two spatial samples belonging to the scan line or row.

In-Orbit Lifetime: period of time between the beginning of the in-orbit commissioning and the end of the delivery of data by the satellite.

Integration time: time it takes for the instrument scan mechanism to scan across the angular distance corresponding to the footprint ellipse minor axis.

Instrument Field of View (FOV): the angle subtended at the satellite nadir point between the most extreme position on the left-hand part of the instrument swath and the most extreme position on the right-hand part of the instrument swath. See Figure MRD-4.2.4(b)

Instantaneous Field of View (IFOV): see definition of footprint.

Inter-channel spatial co-registration: maximum equivalent ground distance between the positions of all pairs of spatial samples acquired in two channels and related to the same target on Earth.

Inter-channel temporal co-registration: maximum time interval between the acquisitions of channels related to the same target on Earth.

Inter-channel radiometric accuracy: unknown bias error (difference between measured value and true value) of the ratio of radiances measured in two channels and associated to the same target on Earth. The inter-channel radiometric accuracy shall be demonstrated by averaging a sufficiently large number of samples such that the residual temporal variation does not dominate the calculation.

Main Beam: angular region within 2.5 times the ellipse representing the 3dB angular contour of the antenna pattern (see Full Beam for schematic). This ellipse is referred to as the “3dB contour Ellipse”.

Note 1: The ellipse representing the 3dB angular contour of the antenna pattern is defined as in the following:

Note 2: The major axis is defined by the straight-line segment connecting the two points at maximum distance lying on the 3dB contour;

Note 3: The minor axis is a segment, orthogonal to the major axis, and passing through the centre of the major axis. Its length is the maximum distance between any two points lying on the 3dB contour along the direction orthogonal to the major axis.

Multi-Year Ice: Sea ice which has survived at least one summer's melt; typical thickness up to 3m or more. It is subdivided into residual first-year ice, second-year ice and multi-year ice.

Nadir: nadir direction is defined as the line from the centre of the satellite reference frame that is perpendicular to the reference ellipsoid tangent.

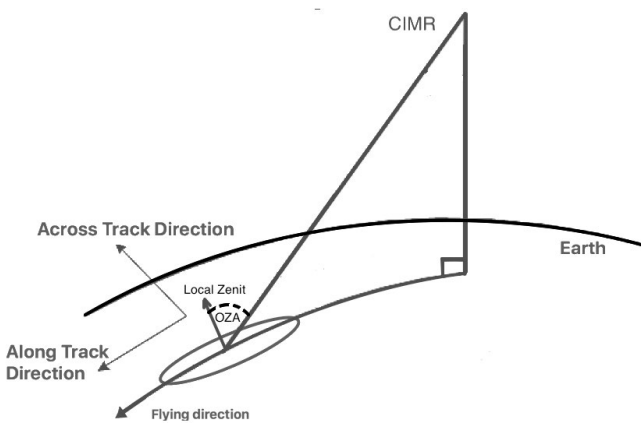
Near Real-Time (NRT): see near real time 3 hours.

Near-Real-Time-1-Hour (NRT1H): product delivered in ≤ 1 hour to the point of user pickup after data acquisition by the satellite. NRT1H products are used for nowcasting operational applications (e.g., navigation bulletins in the Arctic) from sea ice services, operational oceanography and meteorology.

Near-Real-Time-3-Hour (NTR3H): product delivered in ≤ 3 hour to the point of user pickup after data acquisition by the satellite. NRT3H products are used for operational applications such as sea ice services, operational oceanography, and meteorology.

Non-Time-Critical (NTC): product delivered in less than 30 days to the point of user pickup after data acquisition by the satellite. NTC target climate users rely on the availability of auxiliary of the highest quality. NTC products are consolidated products as they are generated using the most precise auxiliary information, orbit knowledge, uncertainty estimates, quality control and other parameter available.

Observation zenith angle (OZA): angle between the satellite viewing direction and the local zenith defined in the surface target reference frame (i.e., zenith – target – satellite) as shown in the figure below.



Old Ice: see Multi-Year Ice.

Orbit: one full revolution of the satellite starting and ending at an ascending node.

Note 1: a satellite orbit can be specified in two ways: absolute orbit and relative to a specific orbit cycle. The orbit numbers are specified at the sensing start time and sensing stop time of the product.

Out-of-band rejection: the minimum level of suppression of a signal outside of specified channel.

Pass: spans half an orbital revolution and is either ascending (South-North) or descending (North-South). This means that a pass always starts at the turnover point, i.e. the passing near the South or North Pole. The pass number represents the number of passes since the beginning of the mission (absolute) or since the beginning of the cycle (relative). Odd pass numbers are ascending, even are descending.

Payload: see instrument

Platform: parts of the satellite that provide the functionalities and resources required to operate the instrument and to control and monitor the satellite.

Polar Regions: encompass:

- The pan-Arctic domain ($>55^{\circ}\text{N}$ latitude, $0\text{-}360^{\circ}$ longitude) and,
- Antarctic ($>50^{\circ}\text{S}$ latitude, $0\text{-}360^{\circ}$ longitude).

Polarisation sensitivity: assuming measurement of a stable, spatially uniform, linearly polarized scene, the polarization sensitivity is defined as:

$$P = \frac{S_{\max} - S_{\min}}{S_{\max} + S_{\min}}$$

where S_{\max} and S_{\min} are the maximum and minimum sample values obtained when the polarization is gradually rotated over 180 deg.

Position of sample: geographic location of the barycentre of the footprint.

Precipitation threshold: the maximum acceptable precipitation rate (determined from CIMR measurements) to be considered for the computation of the effective revisit/coverage/accessibility time is 15% per elementary image.

Precision: difference between one result and the mean of several results obtained by the same method, i.e., reproducibility (includes random uncertainties only).

Note 1: Precision describes the spread of these measurements when repeated. A measurement that has high precision has good repeatability. The statistical standard deviation derived from a number of repeated measurements may serve as a measure of precision.

Product level definitions: the concept of product levels, and the definitions thereof, have been codified by CEOS (Committee on Earth Observation Satellites). The CEOS definitions are the basis for the product levels defined in these requirements, with appropriate modifications since the original definitions were formulated with imaging sensors in mind. Data downlinked from the satellite consist of a serial stream of data bits embedded within a framework of transfer frames appropriate for the purpose. This level of data, which may be temporarily archived at the reception station, is not readable by a general-purpose computer and not included in the set of product level definitions.

Level	Description
L0	Reconstructed, unprocessed instrument and payload data at full resolution, with any and all communications artefacts (e.g., synchronization frames, communications headers, duplicate data) removed.
L1a	L0 data reconstructed, unprocessed instrument data at full resolution, time-referenced, and annotated with ancillary information, including radiometric and geometric calibration coefficients and geo-referencing parameters (e.g., platform ephemeris) computed and appended but not applied to the data.
L1b	Level 1a data that have been quality controlled and reformatted but not re-sampled. All radiometric and spectral calibration have been applied to provide top-of-atmosphere spectral brightness temperatures (Tb) in units of Kelvin. Geometric information is computed, appended but not applied. Preliminary pixel classification is included in the product.
L2	Derived geophysical variables at the same resolution and location as Level 1 source data.
L3	Variables mapped on uniform space-time grid scales, usually with some completeness and consistency. L3U (Uncollated) product are from gridded individual satellite swath data. L3C (generally referred to as L3) collate several swaths from an instrument (e.g., daily composite).

L4	Results from analyses of lower-level data (e.g., variables derived from multiple measurements) typically using an analysis technique (e.g., optimal estimation) or a model.
----	---

Within these general definitions several distinct products may be defined at each level, containing different levels of detail in the parameters provided.

Radiometric accuracy: see Absolute radiometric accuracy.

Radiometric resolution: smallest change of radiometric sensitivity that can be measured.

Radiometric Sensitivity (NEΔT): smallest value of input brightness temperature or radiance that can be detected in the system output for an integration time that is compliant with each individual CIMR footprint along the conical scan direction.

Note 1: The sensitivity requirement applies to calibrated radiances and is applicable throughout the dynamic range. System noise, gain variations and calibration noise shall be taken into account when calculating the sensitivity. In case of multiple beams for single channel the definition and the associated requirements for NEΔT applies to each individual footprint and related integration time. The following formula shall be used:

$$NE\Delta T = (T_{sys} + T_{scene}) \sqrt{\left(\frac{1}{B\tau}\right) + \left(\frac{\Delta G}{G}\right)^2 + \left(\frac{1}{BN\tau_c}\right)}$$

where TSYS is the receiver noise temperature (including antenna losses), Tscene is the scene temperature, B is the bandwidth, τ is the integration time ΔG/G is the receiver gain variation, τc is the calibration target integration time and N is the number of calibration cycles averaged.

Radiometric Stability: degree to which radiometric accuracy remains constants over time.

Note 1: Changes in radiometric stability, also known as drift, can be due to components aging, decrease in sensitivity of components, and/or a change in the signal to noise ratio, etc. Radiometric stability is quantified as the standard deviation of measurement differences when viewing an invariant and homogeneous calibration target(s) over a defined period of time and of such magnitude that NEΔT is insignificant, with the system operating within its dynamic range.

Relative Pointing Error (RPE): angular separation between the instantaneous pointing direction and the short-time average pointing direction at a given period.

Revisit time: time between two consecutive possible observations of a same target within the specified incidence angle range.

Sample: measurement made during a fraction of the L1b integration time.

Satellite or Spacecraft: refers to each one of the independently flying elements of the space segment. It comprises all hardware to be placed into Earth orbit except for the launch vehicle. The satellite is composed of the platform and the instrument.

Sea Ice Concentration: the fraction of an area ocean that is covered by sea ice. Sea Ice concentration typically is reported as a percentage (0 to 100 percent ice), a fraction from 0 to 1, or sometimes in tenths (0/10 to 10/10).

Sea Ice Draft: thickness of sea ice extending below the water level. (See Sea Ice thickness)

Sea Ice Drift: displacement vector of a sea ice field from its place of origin. Sea ice may be highly dynamic and moves due to wind forcing, ocean currents, internal ice stress and other forces.

Sea Ice Edge: the boundary at any given time between open water and sea, lake ice of any kind, whether drifting or fast. Sea Ice Edge can take the form of a line, a polygon an ICE/NO_ICE mask;

Sea Ice Extent: the total area covered by some amount of ice, including open water between ice floes; ice extent is typically reported in square kilometres. Extent defines a region as either "ice-covered" or "not ice-covered." A threshold determines this labelling. A typical threshold is 15 percent, meaning that if the data cell has greater than 15 percent ice concentration, the cell is labelled as "ice-covered."

Sea Ice Freeboard: Sea ice freeboard is the distance between the interpolated local sea surface and the ice-air interface or, in the case of snow layer, to ice-snow interface. (See Sea Ice thickness)

Sea Ice Stage of Development: see sea ice type.

Sea Ice Thickness: vertical thickness of the floating ice, converted from freeboard assuming hydrostatic equilibrium, and excludes the snow layer on top. Sea Ice Freeboard and sea ice draft comprise total sea ice thickness.

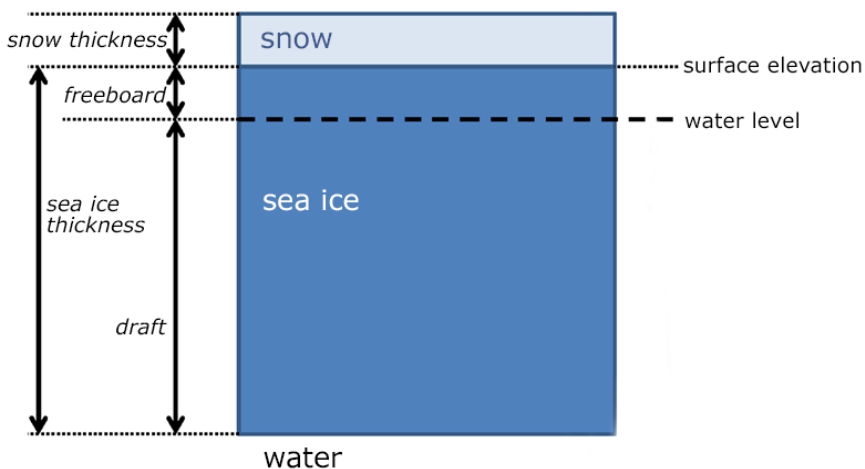


(Image courtesy Walt Meier, NSIDC)

Sea Ice Type: classification of sea ice according to ice age: new ice, young ice (grey/grey-white), first year ice, second year ice, and multi-year ice). New ice refers to ice less than 10 centimetres. As the ice thickens, it enters the young ice stage, defined as ice that is 10 to 30 centimetres thick. Young ice is sometimes split into two subcategories, based on colour: grey ice (10 to 15 centimetres) and grey-white ice (15 to 30 centimetres). First-year ice is thicker than 30 centimetres but has not survived a summer melt season. Second-year ice is up to 2.5 m thick (although sometimes more). Multiyear ice is ice that has survived a summer melt season and is much thicker than younger ice, typically ranging from 2 to 4 meters thick.

Sea Ice: ice, which has originated from the freezing of sea water. It presents the main kind of floating ice encountered at sea.

Seasonal Sea Ice (zone): an area of ocean that extends from the permanent ice zone to the boundary where winter sea ice extent is at a maximum; here, sea ice is present only part of the year; this area (zone) primarily consists of first-year ice.

Second-year Ice: Old ice which has survived only one summer's melt; typical thickness up to 2.5 m and sometimes more. Because it is thicker than first-year ice, it has a larger freeboard. Ridged features as a result of melting during the preceding summer attain a smoothed rounded shape. In summer, numerous melt ponds of extended irregular shape form on its surface. Bare ice patches and melt ponds are usually greenish-blue.

Snow Cover Extent: see terrestrial snow area.

Snow Cover: (1) in general, the accumulation of snow on the ground surface (2) the areal extent of snow-covered ground, usually expressed as percent of total area in a given region.

Snow Density: the mass of snow per unit volume which is equal to the water content of snow divided by its snow depth.

Snow Depth: the combined total depth of both old and new snow on the ground.

Snow Extent: the total land area covered by some amount of snow; typically reported in square kilometres.

Snow Water Equivalent: is the equivalent amount of liquid water stored in a snow pack. It indicates the water column that would theoretically result should the snow pack melt instantaneously and is defined as product between the snow layer's depth and snow density.

Terrestrial Snow Area: snow extent over land surfaces.

Sea Surface Salinity: Sea Surface Salinity (SSS) is expressed according to the Practical Salinity Scale (UNESCO, 1985) defined as conductivity ratio: a seawater sample of Practical Salinity 35 has a conductivity ratio of 1.0 at 15°C and 1 atmosphere pressure, using a potassium chloride (KCl) standard solution containing a mass of 32.4356 grams of KCl per Kg of solution. Thus SSS is ratio quantity and has no physical units. The use of PSU or PSS as a physical unit for SSS is incorrect. However, the use of PSS to indicate that the PSS scale has been used is appropriate.

Side Lobe: lobes of local maxima in the far field radiation pattern that are not the main beam (see Full beam for schematic).

Note 1: Multiple side lobes may exist in any given antenna gain pattern and the peak side lobe is the largest magnitude side lobe.

Sea Surface Temperature: temperature of the ocean surface derived from thermal emissions measured by a microwave radiometer within a specified frequency bandwidth. The SST derived from a microwave radiometer represents sub-skin temperature of the ocean surface over a e-folding depth (mm to cm) depending on the microwave frequencies used.

Signal to Noise Ratio: ratio of signal power to the noise power.

Spatial Resolution: see `footprint_size`.

Spatial Sampling Distance (SSD): distance between the centre of adjacent footprint samples on the Earth's surface.

Sub-Satellite Point (SSP): the point on the Earth's reference ellipsoid that intersects the nadir direction.

Swath width: the across-track ground which is imaged and over which the performance requirements are met.

System Gain: the overall gain of the instrument channel (from the antenna aperture to the instrument output).

Total Standard Uncertainty: For CIMR ARA is not used in the traditional manner but instead we calculate the Total Standard Uncertainty (which is a zero mean “1-sigma” total uncertainty). The strength of this approach is that each component of the total standard uncertainty can be validated (which is not the case for ARA which implies a reference of “truth”). It is noted that this approach, while consistent with international agreements on uncertainty specification (JCGM, 2008), it is different compared to other formulations (e.g., as for the MetOp-SG(B) MWI) that do not include NEΔT as part of the absolute radiometric accuracy definition. Four components of Total Standard Uncertainty are: NEΔT, Lifetime radiometric stability, orbital stability and beginning of life uncertainty. The total standard uncertainty for a single measurement (in one channel) is the combination of uncertainty from random and systematic effects. These correctly combine in quadrature:

$$u_{total} = \sqrt{u_{random}^2 + u_{systematic}^2} + 0 \quad (\text{Eqn. 4.2.10.1})$$

Channel NEΔT addresses the uncertainty from random effects in the instrument. Since in the case of CIMR NEΔT is specified at one reference temperature, it follows that TSU is also specified at that same temperature. As an ideal goal, TSU should be valid across the full dynamic range of the measurements although it is recognised that in practice this is normally unattainable.

The stability requirements limit the excursions of the calibration from “truth” on slower timescales: the orbit stability requirement constrains the drift of the calibration on orbital timescales; the lifetime stability constrains the degree of drift of calibration over the mission lifetime; and one further component is required to obtain the total standard uncertainty, namely the beginning of life uncertainty of pre-launch calibration knowledge (u_{pl-cal}) e.g., derived from ground characterisation). In particular, u_{pl-cal} implies a rigorous pre-launch characterisation of the CIMR instrument (and thus links to the CIMR calibration and validation plans). This is consistent with the definition of all quantities as zero mean 1-sigma standard deviations in the MRD requirements. Therefore, the requirements adhere to the formulation of Total Standard Uncertainty:

$$u_{total}^2 \cong u_{NE\Delta T}^2 + u_{orbit-stability}^2 + u_{lifetime-stability}^2 + u_{pl-cal}^2 + 0 \quad (\text{Eqn. 4.2.10.2})$$

Interpretation of total standard uncertainty, NEΔT, orbital stability and the lifetime stability as uncertainty components is consistent with the definition of all of them as zero mean **1-sigma** standard deviations in the MRD requirements.

Uncertainty: the closeness of agreement between the result of a measurement and a true value of a measurand as follows:

- **Uncertainty (of measurement):** parameter, associated with the result of a measurement, that characterizes the dispersion of the values that could reasonably be attributed to the measurand.
- **Standard Uncertainty:** uncertainty of the result of a measurement expressed as a standard deviation.
- **Type A evaluation (of uncertainty):** method of evaluation of uncertainty by the statistical analysis of series of observations
- **Type B evaluation (of uncertainty):** method of evaluation of uncertainty by means other than the statistical analysis of series of observations.
- **Combined standard uncertainty:** standard uncertainty of the result of a measurement when that result is obtained from the values of a number of other quantities, equal to the positive square root of a sum of terms, the terms being the variances or covariances of these other quantities.

Validation: confirmation, through the provision of objective evidence, that the requirements for a specific intended use or application have been fulfilled.

Note 1: CEOS definition is the process of assessing by independent means the quality of the data products (the results) derived from the system outputs.

Verification: confirmation, through the provision of objective evidence, that the specified requirements have been fulfilled.

Vertical Polarisation (V): electric field is parallel to the plane of incidence.

Wide Beam: angular region 3.0 times the ellipse representing the 3dB angular contour described by the antenna pattern (see Full Beam for schematic).

Wide Beam Efficiency: the ratio of total (cross- and co-polarised) power received by an antenna within its wide beam to the total power received from the full sphere.

10 APPENDIX II MAJOR POLICIES AND EO APPLICATIONS SUPPORTED BY THE CIMR MISSION

Table All-1: Summary major policies and EO applications supported by the CIMR mission.

Policies Directives	Applications	User Requirements	User entities
EU Integrated Policy on the Arctic	Climate Change and the Arctic Environment, sustainable development in the Arctic, International cooperation on Arctic matters,	Monitoring of floating sea ice and ocean surface parameters with high spatial resolution to support sustainable development and environmental security, cooperation and long-term monitoring of societal impacts in the Arctic Environment. Enhance the safety of navigation in the Arctic.	Arctic States, EC, ESIF ³⁵ , UN, UNCLOS ³⁶ , ECGFF ³⁷ , ACGF ³⁸ , TEN-T ³⁹ , OSPAR, GEORI.
EU Water Framework Directive	Water rights management, Water pricing, Ground water abstraction limits, Protection of inland and coastal water surfaces	Monitoring of water use from field scale to irrigation system level for enforcing sustainable water abstraction for agricultural production	EEA; national and river basin management authorities
UN Sustainable Development Goals	Water use efficiency and management, Sustainable agricultural production	Reporting on the SDG 6.4 for increase water-use efficiency across all sectors and ensure sustainable withdrawals.	National statistical offices, UNEP, UN Statistics
UN Framework Convention on Climate Change	Risk management and climate change adaptation	Mitigating water scarcity impacts related to climate change or extreme weather calamities	Insurance providers; farmers; national water authorities

³⁵ European Structural and Investment Funds³⁶ UN Convention on the Law of the Sea (UNCLOS)³⁷ European Coast Guard Functions Forum (ECGFF)³⁸ Arctic Coast Guard Forum (ACGF)³⁹ trans-European Network for Transport (TEN-T)

Marine Strategy Framework Directive (MSFD)	Integrated coastal zone management, Protection of marine biodiversity http://ec.europa.eu/environment/marine/eu-coast-and-marine-policy/marine-strategy-framework-directive/index_en.htm	Water thermal plume monitoring, aquaculture management	Coastal authorities; power plants OSPAR
Convention for the Protection of the Marine Environment of the North-East Atlantic (the 'OSPAR Convention')	OSPAR work areas: biological diversity & ecosystems, hazardous substances & eutrophication, human activities, offshore industry, radioactive substances, cross cutting issues. https://www.ospar.org/about	Marine biodiversity indicator remote sensing, need for higher accuracy of measurements and classification, continuity of data sources	OSPAR contracting parties, Users of nautical charts and sailing directions in high risk/ prohibited areas, more general users of the coastline, Fishermen etc.
Geo Cold Regions Initiative (GEOCRI)	Biodiversity and ecosystem sustainability, disaster resilience, energy and mineral resource management, food security and sustainable agriculture, infrastructure and transportation management, public health surveillance (weather extremes, water-related illness etc.) water resources management, The GEOCRI mission is to develop a user-driven approach for Cold Regions information services to complement the mainly current science-driven efforts, which will strengthen synergies between the environmental, climate, and cryosphere research efforts and foster the collaboration for improved earth observations and information on a global scale. https://www.earthobservations.org/activity.php?id=114	There is the need to provide coordinated Earth observations and information services across a range of stakeholders to facilitate well-informed decisions and support the sustainable development of the cold regions globally.	Users from both the public and private sectors, including managers and policy makers in the targeted societal benefit areas, scientific researchers and engineers, governmental and non-governmental organizations, and international bodies
EU-PolarNet initiative	Supports a EU-wide consortium of expertise and infrastructure for polar research to better assimilate Europe's scientific and operational capabilities in the Polar regions. http://www.eu-polar.net.eu/	Improved co-ordination of data and infrastructure between EU member polar research institutions.	EC, EU member polar research institutions, public, private organizations, universities and research centres
Northern Dimension policy framework	Thematic partnerships related to environment (NDEP), public health and social well-being	Arctic coastal zone monitoring, satellite hydrographic monitoring and	Regional and sub-regional organizations and commissions in the Baltic and Barents

	(NDPHS), transport and logistics (NDPTL), and culture (NDPC). The Northern Dimension policy aims at providing a common framework for the promotion of dialogue and cooperation, strengthening stability, well being and intensified economic cooperation, promotion of economic integration and competitiveness and sustainable development in Northern Europe. https://eeas.europa.eu/diplomatic-network/northern-dimension_en	assessment of environmental trends along the arctic coast.	area, the sub-national and local authorities, non-governmental organizations and other civil society organizations (including notably indigenous peoples' organizations), universities and research centres, business and trade union communities, etc.
European Maritime Transport Policy	Maritime Safety and Security; Digitalisation and Administrative Simplification; Environmental Sustainability and Decarbonisation; Raising the Profile and Qualifications of Seafarers and Maritime Professions and; EU Shipping: A stronger global player. https://ec.europa.eu/transport/themes/strategies/2018_maritime_transport_strategy_en	Floating sea ice and ocean surface parameters to be monitored with high spatial resolution.	Shipping operators, Maritime transport industry, CLIA ⁴⁰ , EBA ⁴¹ , ECSA ⁴² , EMPA ⁴³ , ETF ⁴⁴ , Interferry, and WSC ⁴⁵
IMO International Code for ships operating in polar waters (Polar Code)	The Polar Code is intended to cover the full range of shipping-related matters relevant to navigation in waters surrounding the two poles – ship design, construction and equipment; operational and training concerns; search and rescue; and, equally important, the protection of the unique environment and ecosystems of the polar regions. http://www.imo.org/en/MediaCentre/HotTopics/polar/Pages/default.aspx	Improved knowledge on sea ice and other hazards for polar navigation. In particular sea ice thickness and concentration forecasting.	European Community Ship owners' Association (ECSA), ship operators

⁴⁰ Cruise Lines International Association (CLIA)⁴¹ European Boatmen's Association (EBA)⁴² European Community Shipowners' Association (ECSA)⁴³ European Maritime Pilots Association (EMPA)⁴⁴ European Transport Workers' Federation (ETF)⁴⁵ World Shipping Council (WSC)

11 APPENDIX III CIMR REQUIREMENTS TRACEABILITY MATRIX.

Copernicus is a user-driven programme. User Requirements are critical to steer and to adjust the future evolution of the Copernicus programme in particular in the frame of the next Multi-annual Financial Framework of the European Union (2021-2028):

- The evolution of the Copernicus data and information products and the related services;
- The definition of the next generation of Sentinels (expected type of observation and performances);
- The requirements for additional data that could be complementary to the Sentinels and necessary for the purpose of services.

To prepare this evolution, the Commission has undertaken the collection of User Requirements, the establishment of possible Copernicus service evolution and the elaboration of Observation Requirements that should best fulfil both users' requirements with direct observations or enhanced Copernicus information services.

The following tables are taken from AD1, AD2 and AD3 and summarise the link of the user requirements to the mission requirements.

Some of the products cannot be satisfied with this mission.

Table AIII-1 Abbreviations used in parameter specification tables

THEMES (THM)		DOMAINS (DOM)	
AT	Atmosphere	ME	Meteorology
OC	Ocean	CL	Climatology
FW	Surface water (freshwater)	HY	Hydrology
SN	Snow (seasonal)	OC	Oceanography
GL	Glaciers, Caps	EC	Ecology
IS	Ice sheets	HZ	Natural and technical Hazards (preparedness)
SI	Sea Ice/Iceberg	EM	Emergency response (incl. Search and Rescue)
LA	Land surface and vegetation	EN	Energy
PF	Permafrost and soils	TR	Transport/Navigation
		OI	other Infrastructure
		SE	Security
		GEN	general – all domains

Table AIII-2 Parameter specification scheme used in PEG survey

AOI (coverage)	Area Of Interest to be covered, options are:
----------------	--

	[0] global, [1] high latitude (>60), [2] regional - in this case provide details (bounding box, shapefile) or map (raster mask at 10-100km resolution)
Spatial Resolution	the sampling distance of measurements in [m], equal spacing in x and y is assumed
TOY (seasonality)	Time Of Year for measurements, options are: [0] year round, [1] seasonal - in this case provide the time window for measurements (months)
Frequency	temporal frequency, options are: [0] 'on demand' acquisitions - estimate nr of acquisitions per year, [1] regular measurements - provide repetition rate in [mn, hr, dy, mo, yr]
Leadtime	in case of 'on demand', what should be the minimum lead time for an acquisition to be scheduled in [hr]
Timeliness	how long after acquisition should the product be available, options are: [0] non time critical, [1] within 6hr [2] within 1hr
Unit	how is the variable assessed: [0] as continuous scale, in this case give (physical) units (SI) [1] in different categorical classes - in this case provide reference
Range	dynamic range of measurements in physical units or number (and name) of categories
Accuracy	95% confidence interval for uncertainty (continuous scale variable) or commission and omission errors (categorical variable)
In-Situ (I)	availability of in-situ observations, options are: [0] hardly accessible, [1] irregular measurements available, [2] various sources exist and (non-harmonised) data are made available on a regular basis, [3] international standardised network
Status (S)	is variable currently monitored by means of EO: [0] no [1] experimental research ongoing, [2] operational service, (ATBDs available); for [1] and [2] provide references
Gaps	If variable is currently observed, give actual specs if different from requirements listed under 1-8 above
Continuity (C)	what are the expectations with respect to future availability of this variable: [0] current status of EO and IS ensured or likely to improve, [1] in-situ at risk, [2] EO not available or at risk [3] availability/quality of both IS and EO at risk to deteriorate
Priority (P)	[0] low, nice to have, dispensable, models and/or proxies available [1] low, but continuity must be guaranteed [2] high, improvements are essential for progress in the domain

11.1.1 Sea Ice Concentration (Sea Ice Fraction)

THM	DOM	Parameter	AOI	Resolution	TOY	Frequency	Leadtime	TL	Unit	Range	Accuracy	-	S	C	P	Mission Requirement	Compliance statement
SI	OC	Sea ice Fraction	0	T: 5km	0	6hr	n/a	2	0: [%]	[0,100]	5%	0	0	3	2	MRD-890, MRD-895, MRD-1110	F in Arctic
	CL		1	T: 10 km G: 1km	0	1dy	n/a	0	0: [%]	[0,100]	1%	0	2	2	2	MRD-890, MRD-895, MRD-1110	F
	TR		0	T: 20m G: 2m	0	T: 1dy G: 12hr	24h	1	0: [%]	[0,100]	5%	1	2	2	2	MRD-890, MRD-895, MRD-1110	

Parameter	CMEMS Recommendation	Mission Requirement MRD	Compliance statement
Sea Ice Concentration (Sea Ice Fraction)	[AD-3] recommends to fly a European microwave mission for high spatial resolution (< 10 km) ocean surface temperature and sea ice concentration and sustainable operation of multi-frequency and - polarization passive microwave observations of SST, sea ice lead fraction and sea ice concentration.	MRD-890, MRD-895, MRD-1110	F

11.1.2 Sea Surface Temperature (SST)

THM	DOM	Parameter	AOI	Resolution	TOY	Frequency	Leadtime	TL	Unit	Range	Accuracy	-	S	C	P	Mission Requirement	Compliance statement
																	Full F, Non Compliant NC, Partial P
OC	CL	SST	0	T: 10km G: 1km	0		n/a	0	0 : [°K]	[271,283]	0.1K	1		2	MRD-900, MRD-905	P (Accuracy 0.1 K not attainable)	
OC	OC			T: 5km	0	6hr	n/a	1	0 : [°K]			0	2	1	MRD-900, MRD-905	P (95% global coverage using 1 satellite)	

Parameter	CMEMS Recommendation	Mission Requirement MRD	Compliance statement
Sea Surface Temperature SST	[AD-3] states that sustainable passive microwave SST observations are also very important in the global ocean as well as in polar regions. Such observations are available in all weather conditions, while infra-red SST observations are available in cloud free conditions only. SST from PMW is a crucial contribution providing input to weather forecasting and CMEMS ocean and analysis and forecasting models. The future for PMW SSTs is very uncertain and as, of today, CMEMS cannot solely rely on USA or Japan contributing missions.	MRD-900, MRD-905	F

11.1.3 Sea Ice Thickness (SIT)

THM	DOM	Parameter	AOI	Resolution	TOY	Frequency	Leadtime	TL	Unit	Range	Accuracy	-	S	C	P	Mission Requirement	Compliance statement
SI	CL	Thin sea ice	1	T: 10km G: 1km	0	1dy	n/a	0	0: [m]	[0, 0.5]	5%	1	2	2	MRD-910	Partially compliant 10% instead of 5%, <60km instead of 10km	
SI	OC		0	T: 5km	0	T: 6hr	n/a	2	0: [%]	[0,100]	5%	0	0	2	2		
SI	TR		0	T: 20m G: 2m	0	T: 2d G: 1d	24h	1	0: [m]	[0, 0.3]	T: 0.03 G: 0.01	0	1	1			

11.1.4 Snow Depth on Sea Ice

THM	DOM	Parameter	AOI	Resolution	TOY	Frequency	Leadtime	TL	Unit	Range	Accuracy	-	S	C	P	Mission Requirement	Compliance statement
SI	OC	snow depth and density	0	< 5km	0	1dy	n/a	1	0: [m]	[0,10]		0	0	1	MRD-940	P, Resolution <15km, Uncertainty ≤10 cm	
SI	CL		1	1-10 km	0	1dy	n/a	0	0: [m]	[0,1]	0,01 m	1	1	2	MRD-940	P, Resolution <15km, Uncertainty ≤10 cm	
SI	TR		0	25m	0	T: 1dy G: 12hr	n/a	2	0: [m]	[0,10]	0,1m	0	2	2			

SI	OC, ME		0	T: 3 km G: 1 km	0	T: 12hr G: 6hr	n/a	2	0: [m]	[0,10]	horizontal: T: 10 % , G: 5% vertical: T: 0.1m	0	1	2	2		
SI	OC		0	T: 10km G: 1km	0	30dy	n/a	0	0: [m]	[0,0.5]	T: 0.05m , G: 0.02m	1	1	2	2	MRD-940	P, Resolution <15km, Uncertainty ≤10 cm
SN	ME EM TR OI		0	T: 1km G: 5m	snow covered period	T: 1dy G: 1hr	n/a	1	0: [m]	[0,4]	vertical: T: 0.1m G: 0.01m	3	1	2	2		

11.1.5 Ice type/Ice stage of development

THM	DOM	Parameter	AOI	Resolution	TOY	Frequency	Leadtime	TL	Unit	Range	Accuracy	I	S	C	P	Mission Requirement	Compliance statement Full F, Non Compliant NC, Partial P
SI	TR	Ice Type	0	T: 20m G: 2m	0	T: 2d G: 1d	24h	1	1	[New Ice, Nilas/Level Ice, Rafted Ice, Ridged Ice, Hummocked Ice, Brash Ice]	T: 85%, G: 95%	1	0	2	2		
SI	TR		0	T: 40m G: 25m	0	T: 1dy G: 6hr	n/a	2	1	FY/MY/ New Ice	T: 85%, G: 95%	0	2	0			
SI	ME, OC		0	T: 3 km G: 1 km	0	T: 1dy G: 12hr	1	0	1	FY/MY	T: 85%,				MRD-930	P: resolution 15 km	

										G: 95%					
--	--	--	--	--	--	--	--	--	--	-----------	--	--	--	--	--

11.1.6 Ice Surface Temperature (IST)

THM	DOM	Parameter	AOI	Resolution	TOY Frequency	Leadtime	TL	Unit	Range	Accuracy	I	S	C	P	Mission Requirement	Compliance statement
SI	OC	IST	0	T: 5km	0 6hr	n/a	2	0 : [°K]	[210,290]	0,5K	0	2	2	1	MRD-970	P: Uncertainty <1K Resolution ≤15 km
SI	TR		0	T: 150m G: 50m	0 T: 2dy G: 1dy	24h	1	0 : [°K]	[173,278]	T: 1K G: 0.25K	1	2	0	0		
IS	CL ME HY		2 Antarctica Greenland	10 km	0 T: 1 yr G: 1 mo	n/a	0	0 : [°K]	[178-278]	1 K	1	1	0	0	MRD-970	P: Uncertainty <1K Resolution ≤15 km

11.1.7 Snow Melt and Total Snow Area (dry) on Ice Sheets and Glaciers.

THM	DOM	Parameter	AOI	Resolution	TOY	Frequency	Lead time	TL	Unit	Range	Accuracy	I	S	C	P	Mission Requirement	Compliance statement Full F, Non Compliant NC, Partial P
SN	GEN CL ME	Snow Water Equivalent	T: Northern Hemisphere G: Global	T: 10km G: 1km	0	T: 5dy G: 1dy	n/a	1	[mm (kg/m ²)]	[0,500]	For SWE < 200 mm: T: 40 mm, G: 20 mm For SWE > 200 mm: T: 20%, G: 10%		2	2	2	MRD-950 MRD-960	P: Uncertainty 10%, Resolution ≤15 km
SN	GEN HY EN ME		2: T: North. Hemis. G: Global:	T: 1km G: 200m	0	T: 5dy G: 1dy	n/a	1	[mm (kg/m ²)]	[0,500]	For SWE < 200 mm: T: 40 mm, G: 20 mm For SWE > 200 mm: T: 20%, G: 10%		1	2	2		
SN	GEN PF		2: G: Mountain regions, permafrost regions;	T: 50m G: 10m	1 snow covered period	T: 5dy G: 1dy	n/a		[mm (kg/m ²)]	[0,500]		0	1	3	2		

SEASONAL SNOW	Status	Gaps	Mission Requirement MRD	Compliance statement
Total Snow Area	VIS, NIR & TIR imager, some problems with cloud / snow discrimination; available products show significant differences.	Higher resolution required for complex terrain (mountains); cloudiness / polar night; in some products filled with coarse IMWR.	MRD-950	F
Snow Mass (SWE) on land	Low spatial resolution SWE maps available from IMWR, but at comparatively large uncertainty. Operational products available (GlobSnow, etc.), continuity of PMW on METOP.	IMWR SWE: accuracy needs to be improved; problems with spatial resolution in complex terrain, forests, saturation over deep snow. High resolution product needed, not covered by current sensors.	MRD-960	F
Snow Melt Extent	C Band SAR (S1, ERS, ENVISAT) provide snapshot, algorithms mature for mountain regions.	Problems in forests. Melt extent depends on acquisition time;		

11.1.8 Sea Surface Salinity (SSS)

Parameter	CMEMS Recommendation	Mission Requirement MRD	Compliance statement
			Full F, Non Compliant NC, Partial P

Sea Surface Salinity SSS	[AD-3] requests that there is a further advance in Copernicus capabilities to observe sea surface salinity over the global ocean from space. During recent workshops (Cesbio, Nov 2017; ECMWF, Dec 2017) the need for L-band radiometer continuity was discussed. It was identified that any future sensor shall at least provide observations with the same spatial resolution than currently orbiting systems (SMOS and SMAP), i.e., ~40-50 km and an accuracy of ≤0.2 (TBC)	MRD-980, MRD-985	F
-------------------------------------	--	------------------	---

[AD-2] Climate Requirements:

Parameter	Existing products	Gaps	AOI / temporal and spatial resolution	Mission Requirement MRD	Compliance statement
Sea ice concentration	<p>Core resolution ~25km</p> <p>Resolution of 6km (12 km) are provided by AMSR (SSM/I) products in case they use radiometric measurements in the 89 GHz (85 GHz) channels</p> <p>Sea ice concentration is the most important sea ice variable for climate studies as it provides the longest satellite time series available to assess the sea ice variability. It is also the parameter now predicted by all climate models and routinely assimilated in ocean and atmosphere reanalyses</p>	<p>MWI on MetOp SG will eventually secure continuation of the SSMI(S) serie, but will not fulfil a requirement for medium resolution (<10km) as currently available on AMSR-2. A continuation of AMSR-2 like sensor is highly uncertain.</p> <p>Accuracy in the small concentration range (MIZ and near the ice edge) should be improved by an order of magnitude. This will require in-situ infrastructure as well as space infrastructure.</p> <p>A PMW with <10km resolution could have been an important contribution for an high resolution concentration product for operational navigation. (See separate table for operational needs)</p>	<p>Area: Pan Arctic</p> <p>Frequency: At least daily</p> <p>Resolution: 25km with a goal of < 5km (depending on the channel used).</p>	MRD-890, MRD-895,	F
Sea ice thickness (freeboard) (including	Cryosat-2 for thick ice (medium resolution, 25 km ?) and SMOS estimates of thin (<0.5 -1 m) sea ice	Cryosat estimates are too uncertain in the melt season (due to melt pond effects). Complete coverage of the Arctic is only available at the expense of the	The threshold requirements in terms of revisit, coverage and precision are the same as those specified for	MRD-910	P: 10% instead of 5%, <60km instead of 10km

summer ice and thin ice)		time resolution (monthly means). SMOS estimates are limited to small thickness ranges (< 1 m). Revisit and resolution should be similar as described by the climate community. Uncertainty due to snow cover in CS2 ice thickness estimates must be reduced	Cryosat-2. The goal requirements would also include to extend temporal coverage over the melt season, to reduce uncertainties due to snow loading and ice density by a TBD amount, and to be able to measure over the entire range of ice thicknesses.		
Sea Ice drift	Pan-Arctic coarse resolution (25-60 km) (combination of active and passive sensors) gridded datasets. High resolution lagrangian products deduced from processed SAR images (ex: RADARSAT GPS) are also extremely useful for process studies on sea ice mechanics as well as validation of drift/deformation fields produced by sea ice models	Resolution of gridded products is too low. Products deteriorate near the ice edge or in summer. SAR data do not provide global coverage : improve on the use of these data.	Area: Pan Arctic Frequency: daily Resolution: 10 km, as for SIC	MRD-920	F
Snow depth and density on sea ice	Empirical method exist based on PMW brightness temperatures measured at different frequencies for SSM/I or AMSR-E.	The current estimates of snow over ice are empirical and medium resolution. They do not work for thick snow cover	Snow depth measurements are needed to better assess snow loading and altimeter freeboard measurements, as well as the role of snow in the evolution of the sea ice cover. The specification should follow the ice thickness specifications in	MRD-940	F

			terms of resolution and time sampling.		
Ice type	Multiyear ice concentration are available from PMW. Distinction of deformed/leveled ice is available via scatterometer data.	Continuity of the PMW brightness temperature at different polarizations.	Accuracy: Fractions of deformed ice has to be measured with an accuracy of 10%. Coverage: pan-arctic Frequency: daily (for monitoring of ice kinematics) Spatial resolution: same as for ice drift (order 10 km), ultimate goal would be 1 km.	MRD-930	F
All weather SST/IST	All weather SST/IST are available at low resolution based on PMW . High resolution, weather dependent IR products are available at 1 km resolution	High resolution (1 km) IST are useful to estimate heat transfer through sea ice and sea ice growth rates but are hardly available in cloudy high latitudes.	Continuity of the PMW retrieved SST/IST is required together with high resolution weather dependent SST/IST as this parameter is crucial for climate studies and model validation	MRD-900, MRD-905, MRD-970	F

[AD-2] Operational Requirements:

Sea ice concentration	<p>Sea ice concentration is the most important variable for operational oceanography.</p> <p>Passive Microwave products are currently assimilated in CMEM's operational systems.</p> <p>High resolution concentration from the manually derived ice charts. These products are mainly based on Sentinel-1 in Extra Wide Swath Dual polarisation but also on corresponding data from Copernicus Contributing Missions.</p>	<p>The future availability of multifrequency microwave radiometry (AMSR-2) is uncertain and reason for concern. The future MWI in MetOp SG will eventually secure continuation of the SSMI(S) series of coarse resolution radiometry for climate monitoring, but will not fulfil the requirements for medium resolution (< 10 km).</p> <p>Reliable automated sea ice-chart-like products that can be delivered in NRT for navigational aid and for high-resolution input to numerical forecasting models are needed. Such product will probably need a multisensor approach where SAR will be the core input in combination with PMW.</p>	<p>Actual PMW data from CMEM's catalogue are available at coarse resolution. It will be likely that increase in resolution and time availability of products from operational systems will require sub-daily and resolution less than 10km in the future with at least a continuation of observations with a spatial resolution no less than those provided by the AMSR-2 instrument (threshold). Area: pan-Arctic, frequency: at least daily, threshold resolution < 10km/. SAR requirements: Area: Pan Arctic; Frequency: At least daily or 2-4 times in key areas. Resolution: 20m or at least no less than those provided by Sentinel-1</p>	MRD-890, MRD-895, MRD-1110	F for PMW references
All weather SST	SST is a key variable for short term forecasts but also seasonal forecast applications. These data also are likely the oldest variables being assimilated in oceanic systems.	MWI also lack the necessary frequencies to measure all weather SST. A potential future C-band microwave radiometer (EE-10 suggestion) could fulfil the SST requirements, but resolution better than 5km at frequencies below 40 GHz is not foreseen and still will be	<p>A continuity is at least required. Infrared ice surface temperature is also required.</p> <p>Area : Pan-Arctic</p> <p>Frequency: At least daily; Sub-daily sampling shall be monitored to sample diurnal cycle.</p>	MRD-900, MRD-905	F

	<p>Global daily ocean SST (L4) from Pathfinder AVHRR and (A)ASTR instrument is a CMEMS' product given at 1/20° horizontal resolution (~5km) in NRT and presently assimilated</p> <p>Ice surface temperature (IST) is a CMEMS' product .</p>	<p>needed. Other Status of Pathfinder instruments ?</p> <p>There is a gap in operational Sentinel-3 products where no SLSTR IST product is foreseen over sea ice.</p>	<p>Resolution: for gridded data : < 5km</p>		
Sea ice thickness (freeboard) (including summer ice and thin ice)	<p>Pan-Arctic data does not exist presently in the CMEM's catalogue.</p> <p>Assimilation of sea ice thickness data (SMOS-like one) is underway in operational systems.</p> <p>High resolution product for navigation purposes does not exist for the Arctic Ocean.</p>	<p>A need to solve the knowledge gap in snow depth estimation over sea ice.</p> <p>For operational navigation purposes it is difficult to utilize Cryosat data due to its temporal and spatial resolution and too large uncertainty.</p> <p>It is noted that the spatial and temporal resolution requirements needed may not be achievable with today's technology. However, some studies have shown a potential of using ice type as a proxy to derive ice thickness. This will need to be investigated further. Requirements related to ice type are included below.</p>	<p>Area: Pan Arctic</p> <p>Temporal resolution: 1 day (G), 2 days (T)</p> <p>Coverage: pan-arctic</p> <p>Spatial resolution: 20m (G), 80m (T)</p>	MRD-910	F (for SMOS like after re-gridding)
Sea Ice drift	CMEMS' operational systems assimilate pan-Arctic coarse resolution (60km) and 3 day-lag datasets.	It will be likely that increase in resolution and time availability of products from operational systems will require higher resolution and frequency.	<p>Coverage: Pan Arctic</p> <p>Temporal resolution: At least daily</p> <p>Spatial resolution: Corresponding to Sentinel-1</p>	MRD-920	F for PMW capability

	Currently CMEMS provide a pan Arctic high resolution ice drift product based on Sentinel-1 data in HH polarisation that meets the current high-priority requirements.	Higher resolution could be used to increase the drift resolution. For planning of a next generation of S1 this should be taken into consideration.			
Stage of development / Ice type	Ice services are making a visual interpretation based on the SAR backscatter values.	Automatic products should be available. Fully polarimetric SAR observations are required in order to enable automation of product generation. Dynamic topography products are required at high spatial and temporal resolutions. These can be provided by single pass interferometric SAR (bistatic SAR).	Accuracy: Fractions of deformed ice has to be measured with an accuracy of 10%. Coverage: pan-arctic (G), areas near shipping routes and marginal ice zone (T) Frequency: 1 day(G), 2 days (T) Spatial resolution: 20m(G), 80m (T)	MRD-930	F: 15 km resolution

12 APPENDIX IV ACRONYMS

AIV	Assembly, Integration and Verification
(A)ATSR	Advanced Along Track Scanning Radiometer [of ESA]
AMSR	Advanced Microwave Scanning Radiometer [of JAXA]
AMOC	Atlantic Meridional Overturning Circulation
APC	Antenna Pattern correction
APKE	Absolute Pointing Knowledge Error
ARA	Absolute Radiometric Accuracy
ASCAT	Advanced Scatterometer [of MetOp]
AOCS	Attitude and Orbit Control Subsystem
AVHRR	Advanced Very High Resolution Radiometer [of NOAA]
BEC	Barcelona Expert Center
BOL	Beginning Of Life
3CS	Copernicus Climate Change Service
CAMS	Copernicus Atmospheric Monitoring Service
CCDB	Characterisation and Calibration Database
CCI	Climate Change Initiative [of ESA]
CCSDS	Consultative Committee for Space Data Systems
CDR	Climate Data Record
CEMS	Copernicus Emergency Management Service
CEOS	Committee on Earth Observation Satellites
CFOV	Composite Field Of View [gridding scheme]
CGLS	Copernicus Global Land Service
CIMR	Copernicus Imaging Microwave Radiometer
LWP	Liquid Water Path
CMEMS	Copernicus Marine Environmental Monitoring System
COP	Conference of the Parties [of IPCC]
CSC	Copernicus Space Component
dB	deciBel [unit]
DIB	Drop In Bucket [processing scheme]
DMI	Danish Meteorological Institute
DMSP	Defense Meteorological Satellite Program
ECMWF	European Centre for Medium Range Weather Forecasting
ECSS	European Cooperation for Space Standardization
EEA	European Environment Agency

ENSO	El Nino Southern Oscillation
EOL	End Of Life
EU	European Union
ESA	European Space Agency
EUMETSAT	European Organisation for the Exploitation of Meteorological Satellites
FOS	Flight Operations Segment
FOV	Field Of View
FYI	First Year Ice
FWHM	Full Width at Half Maximum
G	Goal
GCOM	Global Climate Observation Mission [of JAXA]
GCOS	Global Climate Observing System
GMI	Global Monitoring Imager [of JAXA]
GNSS	Global Navigation Satellite System
GPP	Ground Processor Prototype
GS	[Copernicus] Ground Segment
HEO	Highly elliptic Orbit
HF	High Frequency
HKTM	House Keeping Telemetry
HPCM	High Priority Copernicus Mission
IFOV	Instantaneous Field Of View
IOD	Indian Ocean Dipole
IR	Infrared
IPCC	International Panel for Climate Change
IST	Ice Surface Temperature (also Sea Ice Surface Temperature SIST)
ITU	International Telecommunications Union
IWS	Interferometric Wide Swath [radar mode of Sentinel;-1]
JAXA	Japan Aerospace Exploration Agency
LEO	Low Earth Orbit
LEOP	Launch and Early Orbit Phase
LF	Low Frequency
LST	Land Surface Temperature
LTS	Long Term Scenario
MAG	Mission Advisory Group
MERIS	MEedium-spectral Resolution Imaging Spectrometer [of ESA]
MFC	Modelling and Forecast Centre [of CMEMS]

MIZ	Marginal Ice Zone
MLST	Mean Local Solar Time
MODIS	MODerate resolution Imaging Spectrometer [of NASA]
MRD	Mission Requirement Document
MYI	Multi Year Ice
MWI	Microwave Imager [of MetOp-SG(B)]
NASA	National Aeronautics and Space Administration [of the USA]
NEΔT	Noise Equivalent difference Temperature
NEMO	Nucleus for European Modelling of the Ocean
NIR	Near Infrared
NRT	Near Real Time, see more specific definitions of NRT1H and NRT3H
NSIDC	National Snow and Ice Data Center [of the USA]
OI	Optimal Interpolation
OPSI	Observation Performance Simulator
OSCAR	Observing Systems Capability analysis and Review Tool [of WMO]
OSISAF	Ocean and Sea Ice Satellite Applications Facility [of EUMETSAT]
OTS	Off-The-Shelf
OZA	Observation Zenith Angle
OW	Open Water
PBEO	Program Board for Earth Observations [of ESA]
PCP	Precipitation
PEG	Polar Expert Group [of the EC]
PL	Polar Low
PSF	Point Spread Function
QMS	Quality Management system
RF	Radio Frequency
RFC	Radio Frequency Compatibility
RFI	Radio Frequency Interference
RPKE	Relative Pointing Knowledge Error
SAR	Synthetic Aperture Radar
SD	1. Standard Deviation 2. Snow Depth
SI	1. Sea Ice 2. Systeme Internationale [of metrology units]
SIC	Sea Ice Concentration
SID	Sea Ice Drift

SIE	Sea Ice Extent
SIR	Scatterometer Image Reconstruction [algorithm]
SIST	Sea Ice Surface Temperature SIST
SIT	Sea Ice Thickness
SM	Soil Moisture
SMAP	Soil Moisture Active Passive [mission of NASA]
SMOS	Soil Moisture and Ocean Salinity [mission of ESA]
SNR	Signal to Noise Ratio
SPF	Single Point Failure
SRD	System Requirements Document
SSD	1. Spatial Sampling Distance 2. Sea Surface Density
SSM/I	Special Sensor Microwave Imager [of DMSP]
SSP	Sub Satellite Point
SSS	Sea Surface Salinity
SST	Sea Surface Temperature
SWE	Snow Water Equivalent
TBC	To Be Confirmed (by ESA)
TBD	To Be Defined (by ESA)
TBS	To Be Specified
TC	TeleCommand
TCWV	Total Column Water Vapour
TEC	Total Electron Content
TIR	Thermal Infrared
TM	TeleMetry
TMI	TRIMM Microwave Imager
TOA	Top Of Atmosphere
TRIMM	Tropical Rainfall Imaging Microwave Radiometer [of JAXA]
TRP	Temperature Reference Point
VIS	Visible wavelength
VEGA	Vettore Europeo di Generazione Avanzata
WMO	World Meteorological Organisation
WS	Wind Speed
WVC	Water Vapour Content

[End of Document]